

Methodology, Data Interpretation and Practical Transfer of Freeze-Dry Microscopy

Der Naturwissenschaftlichen Fakultät
der Friedrich-Alexander-Universität Erlangen-Nürnberg
zur
Erlangung des Doktorgrades

vorgelegt von

Eva Meister
aus Münchberg

Als Dissertation genehmigt von der Naturwissenschaftlichen Fakultät
der Universität Erlangen-Nürnberg

Tag der mündlichen Prüfung: 12. März 2009

Vorsitzender

der Prüfungskommission: Prof. Dr. Eberhard Bänsch

Erstberichterstatter: Prof. Dr. Geoffrey Lee

Zweitberichterstatter: Prof. Dr. Wolfgang Frieß

Es gibt auf der Welt einen einzigen Weg,
auf welchem niemand gehen kann,
außer dir: Wohin er führt?
Frage nicht, gehe ihn.

Friedrich Nietzsche

Acknowledgements

The work for the present thesis has been performed between February 2005 and September 2008 at the Department of Pharmaceutics, University of Erlangen-Nuremberg, Erlangen, Germany.

Prof. Dr. Geoffrey Lee is gratefully acknowledged for offering me the opportunity to work at his department and for being my doctoral advisor. Many thanks to Prof. Dr. Wolfgang Frieß, Department of Pharmaceutical Technology, University of Munich, for being co-referee for this thesis.

Dr. Henning Gieseler is greatly acknowledged for giving me the chance to work in his focus group freeze-drying and for being my supervisor. Thank you for your support during this period, for research projects of significant interest, for the extensive discussions, and your confidence in my work.

Special thanks go to Carsten Brenk for his encouragement and optimism, for highly sophisticated scientific discussions we shared and for distractions during our free time.

I would like to gratefully acknowledge Stefan Schneid and Dr. Jörg Kunze for proofreading this thesis. Your support was great!

Thanks to Prof. Dr. Michael Pikal, School of Pharmacy, University of Connecticut, Storrs, USA, and to Dr. Evgenyi Shalaev, Pfizer Global Research and Development, Groton, USA, for the discussions and helpful advice.

For their technical support during my thesis period, I would like to greatly acknowledge LAT Labor- und Analysen-Technik GmbH, Garbsen, Germany, especially Thomas Wichert, and Dr. Bernhard Dringenberg, as well as Dr. Thorsten Kern and Dr. Susanne Klerner from Carl Zeiss AG, Oberkochen, Germany. Thank you very much for providing me the high-end equipment, and for the great time we had at the tradeshow exhibitions! Stephan Wasser from LAT Labor- und Analysen-Technik GmbH is kindly thanked for his software solutions.

In the department of pharmaceuticals I would like to thank all my colleagues, who helped me with equipment or teaching issues, and with whom I shared a good time during my thesis period. Thanks to my students Marek Ellnain, Stefan Schuster, and Elisabeth Scheffel for supporting me during some of my experiments. I further thank Petra Neubarth for taking care of administrative issues, Josef Huber and Winfried Bauer for solving technical problems, Dr. Stefan Seyferth for his IT support, Luise Schedl for the SEM pictures, and Christiane Blaha for ordering excipients and lab equipment. Additionally, Dr. Christian Führling and Dr. Heiko Schiffter are kindly acknowledged for their support.

During the period of this thesis, I had the great pleasure to make a lot of new friends, and to share many magnificent moments and events. First of all, I want to thank Yolanda Philipps-Gomez for her wonderful friendship, and all my other friends for their support. Special thanks go to all my flamenco co-dancers. I enjoyed the dancing lessons and festivals with you very much! Further, I would like to thank all “co-Ms” with whom I had a lot of fun participating in our annual meetings and other events.

Last, but not least, my parents Irene and Erich Meister are kindly acknowledged for laying the foundation for the path I followed.

Publications

Parts of this thesis were subject to articles, posters and invited talks:

1. Articles:

- **E. Meister, S. Klerner, H. Gieseler.** *Gefriertrocknungsmikroskopie: Proteine und Peptide zwischen Kollaps und Kristallisation.* Deutsche Apotheker Zeitung: 146 (24): 2552-2557, **2006.**
- **E. Meister, B. Dringenberg, H. Gieseler.** *Die Schlüsselstellung der Gefriertrocknungsmikroskopie in der Entwicklung parenteraler Formulierungen.* GIT Laborfachzeitschrift: 51 (6): 476-478, **2007.**
- **E. Meister, H. Gieseler.** *Freeze-Dry Microscopy of Protein/Sugar Mixtures: Drying Behavior, Interpretation of Collapse Temperatures and a Comparison to Corresponding Glass Transition Data.* J. Pharm. Sci., in press, **2008.**
- **E. Meister, H. Gieseler.** *Evaluation of the Critical Formulation Temperature in Freeze-Drying: A Comparison Between Collapse and Glass Transition Temperatures.* European Pharmaceutical Review, in press, **2008.**

2. Poster presentations:

- **E. Meister, H. Gieseler.** *Evaluation of Collapse Temperatures by Freeze-Dry Microscopy: Impact of Excipient Concentration on Measured Transition and the Overall Dependence on Measurement Methodology.* Proc. 5th World Meeting on Pharmaceutics and Pharmaceutical Technology, Geneva (SWITZERLAND), March 27-30, **2006.**
- **E. Meister, H. Gieseler.** *Measurement of Collapse Temperature by Freeze-Dry Microscopy: Dependence of Collapse Temperatures on Total Solid Content and Correlation to Physical Properties of the Measured Excipient Solution.* Proc. CPPR Freeze-Drying of Pharmaceuticals and Biologicals, Garmisch-Partenkirchen (GERMANY), Oct. 3-6, **2006.**
- **E. Meister, M. Ellnain, H. Gieseler.** *Collapse Temperature Measurement by Freeze-Dry Microscopy and Transferability to Freeze Drying Processes: Influence of Solute Concentration on Collapse Behavior and Effect on Cycle Design.* Proc. AAPS Annual Meeting and Exposition, San Antonio (USA), Oct. 29 - Nov. 2, **2006.**
- **E. Meister, H. Gieseler.** *Freeze-Dry Microscopy: Correlation between Physical Properties and Collapse Behavior of Excipients Frequently Used for Freeze-Drying.* Proc. AAPS Annual Meeting and Exposition, San Diego (USA), Nov. 11-15, **2007.**
- **E. Meister, H. Gieseler.** *Freeze-Dry Microscopy: Drying and Collapse Behavior of Human Serum Albumine and Bovine Serum Albumine Based Formulations.* Proc. AAPS Annual Meeting and Exposition, San Diego (USA), Nov. 11-15, **2007.**

- **S. Schneid, E. Meister, H. Gieseler.** *Design Space in Freeze-Drying: A Robustness Testing Procedure in the Laboratory to Delineate the Impact of Product Temperature Variability on Product Quality Attributes.* Proc. CPPR Freeze-Drying of Pharmaceuticals and Biologicals, Breckenridge (USA), Aug. 6-9, **2008**.

3. Invited talks:

- **E. Meister.** *Freeze-Dry Microscopy – Investigation of Interplay between Physical Properties of a Formulation and Collapse Behaviour.* DPhG - Graduate Student Symposium, Heroldsberg (GERMANY), Sept. 6-8, **2006**
- **E. Meister.** *Freeze-Dry Microscopy - A powerful Tool to Develop Optimized Freeze-Drying Cycles.* Lyophilization of Pharmaceuticals, Informa Life Science Seminar, London (UK), Dec. 3-5, **2007**
- **E. Meister.** *Freeze-Dry Microscopy (FDM) – Measurement Methodology, Data Interpretation and Transfer to Cycle Development.* Pfizer Global Research and Development, Groton (USA), Mar. 3, **2008**
- **E. Meister.** *The critical formulation temperature in freeze-drying.* SP Industries, Stone Ridge (USA), Mar. 6, **2008**
- **E. Meister.** *Analytical Tools I: Evaluation of the Critical Formulation Temperature by DSC and Freeze-Dry Microscopy.* Seminar on Freeze-Drying (SP Industries), Mumbai, Ahmedabad, Delhi, Hyderabad (INDIA), Aug. 18-22, **2008**

List of abbreviations

API	active pharmaceutical ingredient
BSA	bovine serum albumin
Δc_p	change in heat capacity
DSC	differential scanning calorimetry
FD	freeze-drying
FDM	freeze-dry microscopy
HSA	human serum albumin
MDSC	modulated differential scanning calorimetry
MTM	manometric temperature measurement
P_c	chamber pressure
P_{ice}	vapor pressure of ice at the sublimation interface temperature
PVP	polyvinylpyrrolidone
rsdv	relative standard deviation
sdv	standard deviation
SEM	scanning electron microscopy
SSA	specific surface area
T_b	temperature at the vial bottom
T_c	collapse temperature
T_{c-50}	temperature of 50% collapse

T_{eu}	eutectic temperature
T_{fc}	temperature of full collapse
T_g	glass transition temperature
T_g'	glass transition temperature of the maximally freeze-concentrated solute
TM	(observation) time during measurement
T_n	nucleation temperature
T_{oc}	temperature of the onset of collapse
T_p	product temperature at sublimation interface
T_{pc}	temperature of partial collapse
T_s	temperature of shelf surface
ΔT_c	difference in temperature between the onset of collapse and full collapse
\bar{x}	mean value

Throughout this work, units consistent with those used on laboratory and commercial freeze-drying equipment in the USA are used. Thus, the pressure unit used is Torr (or mTorr), rather than the SI unit of Pascal (Pa). *The reader is reminded that 0.1 Torr is 100 mTorr and 13.3 Pa.*

Table of content

1	Introduction	1
1.1	General introduction.....	1
1.2	Freeze-drying process	4
1.2.1	Freezing	7
1.2.2	Primary drying.....	11
1.2.3	Secondary drying	17
1.3	Freeze-drying excipients.....	18
1.3.1	Stabilizers	20
1.3.2	Bulking agents	24
1.3.3	Others	25
1.4	Freeze-dry microscopy	26
1.4.1	Collapse	26
1.4.2	History of freeze-dry microscopy	35
1.4.3	Freeze-dry microscopy today.....	36
1.5	Differential scanning calorimetry.....	38
1.6	Critical formulation temperature in primary drying: collapse temperature vs. glass transition temperature.....	45
1.7	Objectives of this thesis	46
2	Materials and methods	51
2.1	Materials	51
2.1.1	Used proteins and their quality	51
2.1.2	Used excipients and their quality	51
2.1.3	Molecular weights of selected proteins and excipients	52
2.1.4	Quality of liquid nitrogen	53
2.2	Methods	53
2.2.1	Freeze-dry microscopy (FDM)	53
2.2.2	Dynamic viscosimetry	56
2.2.3	Bubble pressure tensiometry	58
2.2.4	Differential scanning calorimetry	59
2.2.5	Freeze-drying.....	60
2.2.6	Scanning electron microscopy (SEM).....	61
2.2.7	BET measurement of specific surface area (SSA)	61

3	Results and discussion	63
3.1	Methodology of FDM	63
3.1.1	Detection and definition of collapse	63
3.1.2	Theoretical overview and model on critical factors in FDM.....	67
3.1.3	Volume of sample and thickness of the frozen layer	74
3.1.4	Heating rate	77
3.1.5	Duration of holding time	84
3.1.6	Recooling and reheating cycles.....	89
3.1.7	Cooling rate and annealing.....	89
3.1.8	Pressure setting.....	97
3.2	Dependence of collapse temperatures on total solid content for excipient solutions.....	102
3.2.1	Concentration vs. collapse temperatures.....	103
3.2.2	Concentration vs. density.....	121
3.2.3	Concentration vs. surface tension.....	123
3.2.4	Concentration vs. viscosity	124
3.2.5	Impact of nucleation on concentration dependence of collapse temperatures	128
3.3	Collapse behavior of binary mixtures with model proteins.....	130
3.3.1	Composition of solutions.....	130
3.3.2	Dependence of collapse temperature on nucleation temperature	131
3.3.3	Dependence of collapse temperature on binary mixture composition	134
3.3.4	Dependence of collapse temperature of binary mixtures on sublimation velocity.....	140
3.4	Comparison of collapse temperatures (T_c) and glass transition temperatures (T_g') for excipient solutions and protein/disaccharide mixtures	144
3.4.1	T_c and T_g' data for excipient solutions	144
3.4.2	T_c and T_g' data for protein/disaccharide mixtures	145
3.5	Transferability of FDM results to freeze-drying cycles: preliminary experiments with sucrose	150
3.5.1	Run data	153
3.5.2	SEM and SSA for evaluation of product shrinkage.....	157
4	Summary and conclusion	162
5	Zusammenfassung	168
6	Suggestions for further research	174
7	References	176

1 Introduction

1.1 General introduction

In 2006, 29 new New Molecular Entities (New Chemical Entities as well as New Biological Entities) were launched to the pharmaceutical market. Fields of application of these new API (Active Pharmaceutical Ingredients) are given in Fig. 1-1. For the first time, a

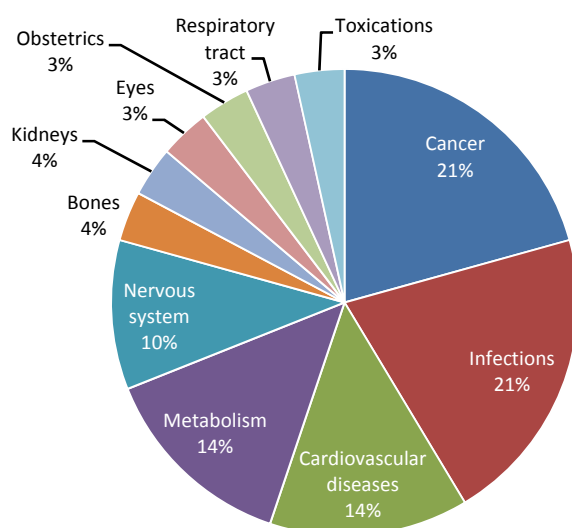


Fig. 1-1: Fields of application of new API in 2006 (adapted from [1])

vaccination against cervical cancer became available. New drugs for renal cancer or chronic hepatitis B make the treatment more efficient. One third of the medicaments are orphan drugs against e.g., morbus Pompe and mucopolysaccharidose VI. Research-based pharmaceutical companies in Germany (VFA) spent 4.37 billion € on research and development (R&D) while occupying 16,500 employees in R&D [1]. On

average, the R&D costs for a new drug were 800 million \$ during the 12 years of overall development. In Germany 1,301 bio-pharmaceutical patents (11% of all German patent registrations) were applied in 2006 (from a total of 10,919 patent applications): 40% came from the USA, 15% from Japan, 11% from German companies, 5% from the UK, 4% from France and 25% from other countries (only patents with an impact on the German market mentioned) [1]. The fraction of medications which are produced by bio-pharmaceutical processes is increasing continuously in Germany. In 2000, it was 7.6%

of a total turnover of 2.38 billion € (delivery charge of manufacturer), compared to 10.9% in 2006. Insulins and interferons amount for more than half of the turnover (cf. Fig. 1-2).

Other important fields of application are blood and rheumatic diseases, monoclonal antibodies against cancer, enzymes against metabolic diseases and vaccines [1]. Concerning the dosage forms Fig. 1-3 gives an overview on FDA-approved protein, peptide, vaccines, oligonucleotide, and cell-based products. The most common forms are lyophilized (from aqueous solution) and aqueous solutions, then aqueous suspensions. Depots include

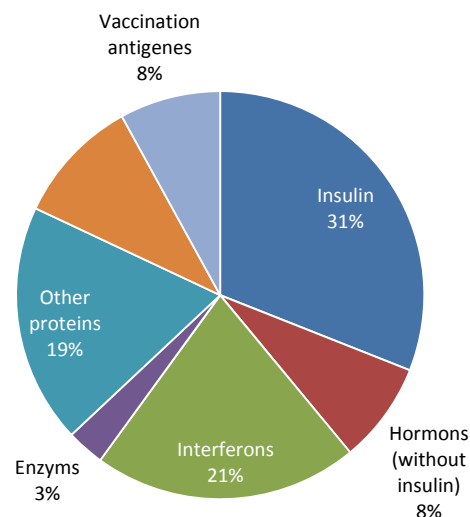


Fig. 1-2: Shares of biotechnologically produced drugs on turnover in 2006 (adapted from [1])

implants and biodegradable cylinders, microspheres, and *in situ* depots. Oral delivery forms include tablets and capsules. The category denoted “other” includes gels, emulsions, and ointments. In anticipation of points discussed later in this thesis, Fig. 1-4 shows storage conditions for these lyophilized FDA-approved products. The most common condition is refrigerated. Today, about 200 new antibody products are currently in development, many of them in a freeze-dried form [2, 3].

In economic and scientific fields described above, a detailed study on freeze-dry microscopy could not only gain new knowledge on procedure issues and the performance of this analytical tool, but also might have an impact on economical aspects. Usage of FDM for process optimization might increase turnover by decreasing process time. Lower in production are realizable for example by better knowledge on collapse behavior of formulations and single substances, by a better methodology for FDM experiments, by shorter freeze-drying cycles (higher temperatures in primary drying) and by producing

lyocakes of an appropriate appearance. The details behind these possibilities are explained in the next chapters.

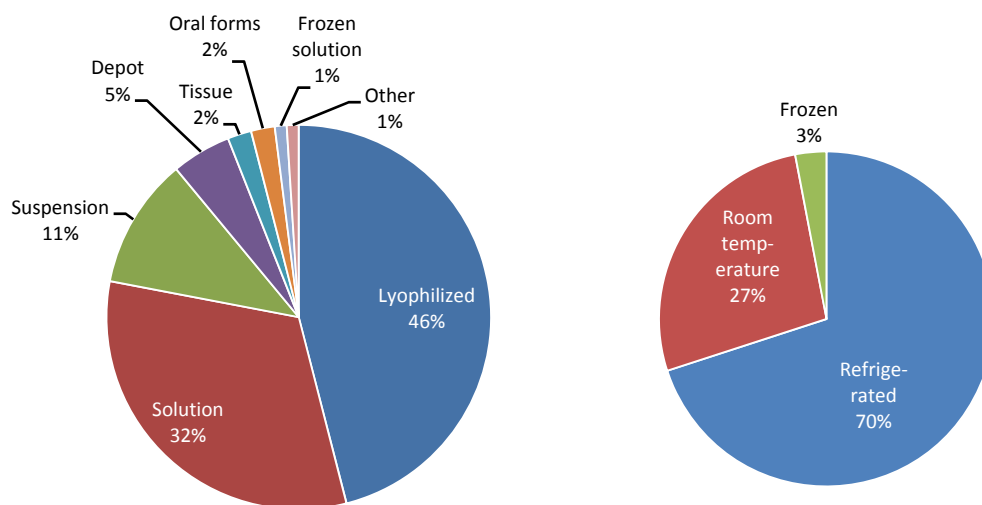


Fig. 1-3: Dosage forms of FDA-approved protein, peptide, vaccines, oligonucleotide, and cell-based products (330 total) (adapted from [4])

Fig. 1-4: Storage conditions of lyophilized, FDA-approved products (adapted from [4])

1.2 Freeze-drying process

Freeze-drying (also denoted “lyophilization”) may be defined as the drying of a substance by freezing it and removing a proportion of any associated solvent by direct sublimation from the solid phase to the gaseous phase, without passing through the intermediate liquid phase [5].

The drying of biological materials by sublimation was already known by the turn of the century. One of the first medicinal uses of the lyophilization process was by Greaves in 1944, who used it to dry serum for treating the victims of World War II. At this time, the first crude commercial apparatus became available [5].

Freeze-drying is a drying process often employed to convert solutions of unstable API into solids of sufficient stability for shipping and storage [6, 7]. Since in general, a formulation can be freeze-dried to 1% residual moisture content or less, without any of the product exceeding 30°C, it likely causes less thermal degradation than a high temperature process like spray-drying [6].

Usually, the desired attributes of a lyophilized product are [8]:

- (1) a consistent and high yield of API through freeze-drying,
- (2) appropriate crystallization or no crystallization of product and excipient(s),
- (3) glass transition temperature higher than the desired storage temperature¹ (related to the level of residual moisture),
- (4) pharmaceutically elegant, mechanically strong cake,
- (5) rapid and complete reconstitution,
- (6) fast and robust freeze-drying cycle, and
- (7) stability of all product quality attributes through the intended shelf-life.

¹ For common storage temperatures see chapter 1.1

In general, freeze-drying is an expensive process. It is highly time, energy and water consuming. If cycle conditions are designed far from optimum, unnecessarily long freezing times, secondary drying times and especially primary drying times can result [9-11]. Not only due to recent emphasis from the FDA on manufacturing sciences and PAT (process analytical technology) [12-14] the pharmaceutical industry has begun to further optimize and improve current lyophilization cycles and to design new processes that are

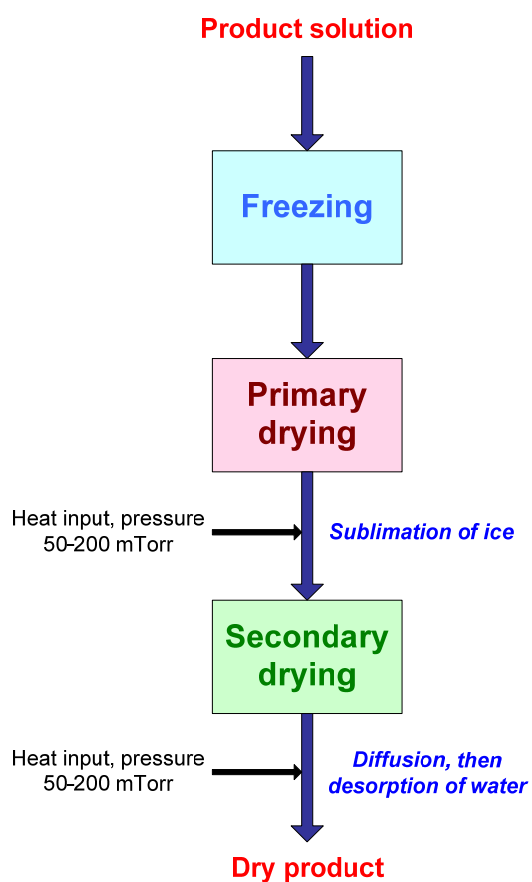


Fig. 1-5: Unit operations involved in freeze-drying

robust and economical from the very beginning. A freeze-dryer typically consists of a drying chamber with temperature-controlled shelves, and a condenser chamber with coils or plates connected to it via a duct. To achieve low pressures (0.03-0.3 Torr) during the process, one or several vacuum pumps are connected to the condenser chamber. A production freeze-dryer may have 10 to 20 shelves with a total load on the order of 50,000 vials [6]. Fig. 1-5 shows the unit operations of freeze-drying in an overview the details of which are discussed in the following paragraphs. Usually an aqueous solution containing the API and – if necessary – “excipients” is filled into a container system (e.g., serum tubing vials) which is loaded onto the shelves. During the freezing step (to a temperature of, e.g., -40°C) nearly all water is converted to ice. In the primary drying step, this frozen water is removed by sublimation.

robust and economical from the very beginning. A freeze-dryer typically consists of a drying chamber with temperature-controlled shelves, and a condenser chamber with coils or plates connected to it via a duct. To achieve low pressures (0.03-0.3 Torr) during the process, one or several vacuum pumps are connected to the condenser chamber. A production freeze-dryer may have 10 to 20 shelves with a total load on the order of 50,000 vials [6]. Fig. 1-5 shows the unit operations of freeze-drying in an overview the details of which are discussed in the following paragraphs. Usually an aqueous solution containing the API and – if necessary – “excipients” is filled into a container system (e.g., serum tubing vials) which is loaded onto the shelves. During the freezing step (to a temperature of, e.g., -40°C) nearly all water is converted to ice. In the primary drying step, this frozen water is removed by sublimation.

In the secondary drying stage, most of the unfrozen water is removed by diffusion and desorption. The water removed from the product is reconverted into ice on the condenser which must be cooled to temperatures below -50°C during operation [6].

MacKenzie first described a „supplemented phase diagram“, which simplifies the discussion of lyophilization, freezing and annealing. It is an equilibrium freezing point depression diagram supplemented with the glass transition curve [15].

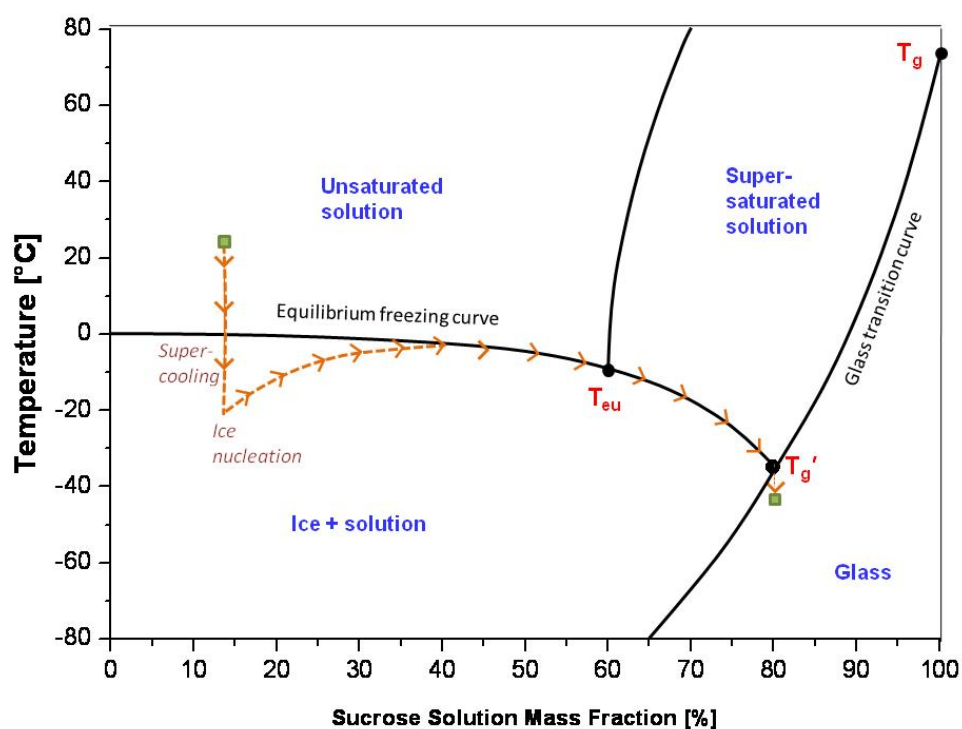


Fig. 1-6: Supplemented phase diagram for sucrose. Arrows show freeze-drying process for a 13% (w/w) sucrose solution; T_g' = glass transition of the maximally freeze-concentrated solute, C_q' = corresponding concentration (adapted from [9, 15])

Fig. 1-6 shows exemplarily a phase diagram for an aqueous solution of sucrose in combination with its freezing behavior. A 13% (w/w) sucrose solution is frozen beginning at room temperature. During the freezing step, the solution supercools until ice nucleation takes place (the temperature of which depends e.g., on cooling rate, nuclei in the solution and the surface of the container system).

Now ice crystals grow combined with simultaneous freeze-concentration of the solution following the equilibrium freezing curve until T_g' is reached [9]. The temperature of the glass is then lowered to the set shelf temperature. In the next step, the product is dried under the T_g' or T_c of the formulation (if known) by lowering the pressure and subliming the ice. In secondary drying, the unfrozen water is removed by diffusion and desorption with further heat input at low pressure. The cake gets more and more stable and its T_g increases until the desired moisture content is reached [15].

1.2.1 Freezing

The freezing step is of paramount importance. It is the principal dehydration step, and it determines the morphology and pore sizes of the ice and product phases [15]. The objective of freezing is to convert all solutes into solids, either crystalline solids or a glass. When cooling a solute with a slow or moderate cooling rate in the absence of seeding, the system remains liquid well below the equilibrium freezing point [16]. Sufficient supercooling leads to nucleation of ice and growing ice crystals [6]. During the initial nucleation event, only a fraction of freezable water crystallizes because crystallization is exothermic, and the supercooling is not sufficient to allow complete solidification [15]. In the regions between these ice crystals all solutes are concentrated. For a sample that nucleates at -15°C , about 20% of freezable water crystallizes before the supercooling is extinguished [17] and the temperature reaches the equilibrium freezing temperature for the freeze-concentrated solution [15]. Through the subsequent cooling, freeze concentration continues until the solutes crystallize or until the system increases in viscosity sufficiently to transform into a glass [6]. At this point (which is T_g')² any further thermodynamically favored freeze concentration is arrested by the high viscosity of the solute phase. The mobility of the water in this phase is too low to permit further migration of water to the ice

² cf. Fig. 1-6

interface by its high viscosity [15]. Accordingly, the obtained system is cooled to the final temperature of the freezing process.

The example presented in Fig. 1-7 is representative of a solute that does not crystallize during freezing. After supercooling to a temperature of -15°C , the ice nucleation becomes energetically favored enough to generate ice crystals. The sudden crystallization of ice increases the temperature in the solution to roughly the equilibrium freezing point (-5°C) which is reflected in a sharp decrease in the percentage of water in the solute

phase. Subsequently, water is continuously converted into ice while the solute in the remaining solution is concentrated. The final percentage of water of 24% (with a corresponding solute concentration of 76%) is reached when the system is cooled to T_g' at -24°C . Here, most of the water has been separated from the solute phase as ice. Even if the initial solute concentration would have been much lower (e.g., 1% instead of 30%) the final concentration would still be 76% (although the freezing profile would differ quantitatively from that shown in Fig. 1-7 [6].

For a sucrose solution (e.g., with a total solid content of 10%, cf. in Fig. 1-6) the sucrose concentration in the amorphous phase would be 81%, an eight-fold increase in concen-

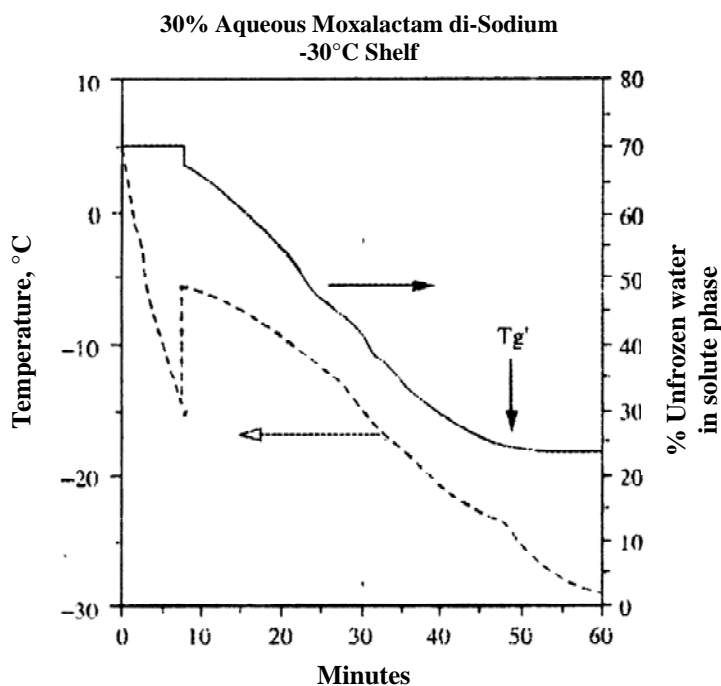


Fig. 1-7: Freeze concentration in an amorphous system. The product temperature is shown as a broken line whereas the percentage of unfrozen water is shown as a solid line [18]

tration. A material balance of the ice and amorphous phases reveals that at this point 88% of the water has been frozen [15].

In contrast, crystalline materials are characterized by a thermodynamically stable structure with a highly ordered lattice. Their “critical formulation temperature” is reflected in the eutectic temperature, T_{eu} . An aqueous solution of sodium chloride, for example, supercools until ice nucleation begins. Then, the crystallization of ice crystals is reflected in an energy release denoted as the equilibrium freeze point. Reaching the eutectic temperature, an equilibrium of pure solid ice, solid sodium chloride and solution can be found. Below T_{eu} , no more liquid is present, but only solid pure ice and solid sodium chloride. In more complex systems, hydrates may form during freezing. If in mixtures or formulations, one component does not fully crystallize, a T_g' can be determined at much lower temperatures [11].

Freeze concentration can lead to instability in partially frozen systems because the probability of bimolecular collisions is increased [6]. Here, the rate-enhancing effect of concentration far outweighs the rate-reducing effect of low temperature [19]. Increase of those second-order degradations has been observed in model systems (e.g., monoclonal antibodies) during freeze concentration [20]. Additionally, buffer salts may crystallize selectively during freeze concentration which can result in pH shifts and therefore destabilization of the native conformation of proteins.

Cooling rate has an impact on supercooling (Fig. 1-8) and consequently on product morphology. It is important to distinguish between “cooling rate” and “freezing rate”. The rate at which the vial (or sample in the FDM stage) is cooled, is called cooling rate ($^{\circ}\text{C}/\text{min}$). It affects the temperature at which ice nucleates. The freezing rate only applies to the post-nucleation freezing [15].

It is well known that the formation of ice crystals during cooling is a random event, even in a well controlled process [21]. In 1998, it was suggested that the stochastic nature of nucleation results in heterogeneity among samples [9] which could be confirmed in 2001

[17] with regard to an impact of nucleation temperature during shelf freezing on the freezing mechanism, product morphology, and primary drying rate. Sample particulate content, vial scoring, and ice nucleating agents were varied and primary drying was found to correlate inversely with the degree of supercooling. Nucleation temperature heterogeneity was reported to result in variation of other morphology-related parameters, such as surface area and secondary drying rate [15]. Fennema et al. found that ice crystal size is inversely correlated to the extent of supercooling [22]. Hence, a high degree of supercooling produces a large number of ice crystals, and as the total amount of water that freezes is fixed, the ice crystals produced after completion of freezing are small in size [6]. Consequently, the degree of supercooling and its effects on product morphology during a freeze-drying run are a scale-up issue in lyophilization [21].

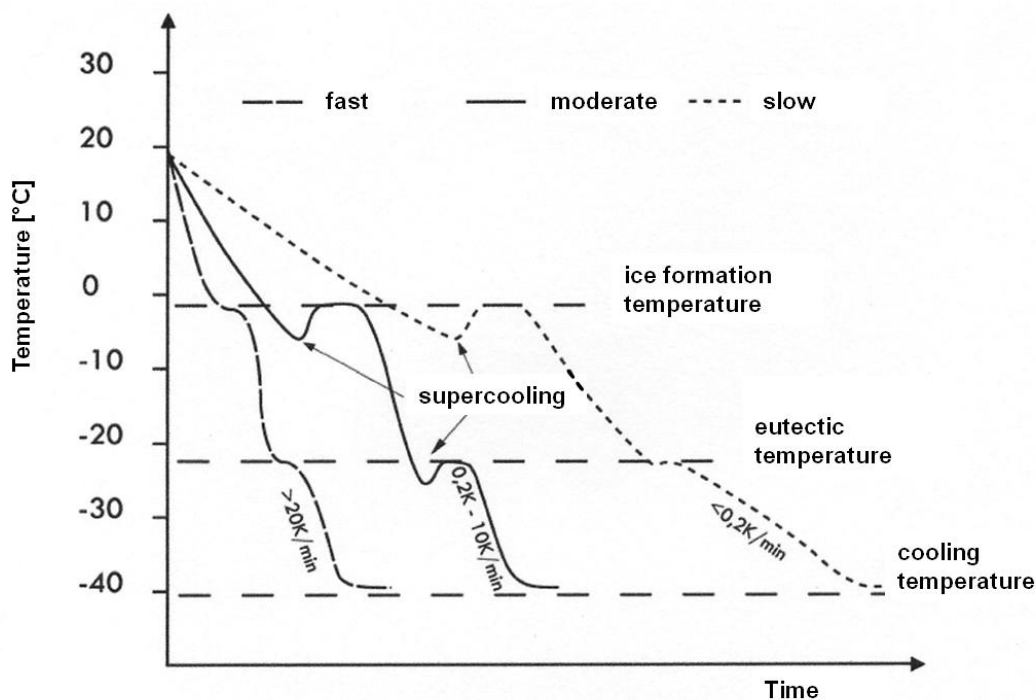


Fig. 1-8: Impact of cooling rate on supercooling, adapted from [23]

In the pharmaceutical industry „shelframp“ freezing is the most prevalent method, where the shelf temperature is reduced in the typical range of 0.1-2 °C/min [15].

Depending on the nature and concentration of formulation components and the details of the freezing process, crystallization may occur (cf. Fig. 1-8). High initial concentrations of the substance the crystallization of which is desired, low vial fill volume and slow freezing tend to favor crystallization [6].

Annealing is an equilibrium step at a temperature above the glass transition temperature. It can be carried out as a waypoint during the initial cooling, but more commonly it is a post-freezing warming and hold step, followed by recooling [15]. On the one hand, annealing is used for crystallization of solutes where the optimum annealing conditions are a compromise between crystallinity and crystallization rate. For mannitol or glycine, a temperature of -20 or -25°C and an annealing time of 2 h or longer are suggested if the fill depth in a vial is 1 cm or more [24]. On the other hand it can be applied to grow ice crystal size. The 10% sucrose solution in Fig. 1-6 for example could be held at an annealing temperature of -20°C . It would follow the equilibrium freezing curve and equilibrate at 70% sucrose in the solute (non-ice) phase. The ice fraction decreases to dilute the sucrose phase. Since the sample is now well above its T_g' , ice crystal maturation through Ostwald ripening, and possibly degradative reactions are free to take place. Recrystallization or Ostwald ripening is a phenomenon by which dispersed crystals smaller than a critical size decrease in size as those larger than the critical size grow, and can be either diffusion or surface attachment limited [15].

1.2.2 Primary drying

Primary drying is usually the longest part of the freeze-drying process. Drying times in the order of days are common. If a poor formulation and suboptimal process design are combined, it may take weeks [6].

During the freezing step, all water and solutes have been converted into solids. First, the condenser is cooled, and then, primary drying is started by evacuation of the system to a desired controlled pressure via the vacuum pump(s). Then, the shelf temperature is

slowly increased to supply energy for sublimation. During primary drying, a large heat flow is required (cooling by sublimation). Due to heat transfer barriers represented by the shelf, the vial, and the product, the product temperature hereby runs much lower than the shelf temperature. The removal of ice crystals by sublimation creates an open network of pores, which allows pathways for escape of water vapor from the product. The ice-vapor boundary (i.e., the boundary between frozen and “dried” regions) generally moves from the top of the product toward the bottom of the vial as primary drying proceeds, ideally in a horizontal way [6].

The product temperature at the sublimation interface (T_p) depends on the properties of the formulation (chemical structure and quantity of the solutes etc.), shelf temperature, chamber pressure, and container system. Therefore, it cannot be directly controlled during primary drying. Even if the collapse temperature, T_c , and T_g' are known, it is still difficult to optimize the freeze-drying process for a given formulation [24]. The concept of primary drying is to choose the optimum target T_p at the sublimation interface, bring the product to this target temperature quickly, and hold the product temperature constant at T_p target throughout primary drying. To obtain a dry product with acceptable appearance, T_p should always be several degrees below T_c . The temperature difference between T_p and T_c is called safety margin [24]. T_p target should be 2-5°C lower than T_p (temperature at ice sublimation interface), based on cycle duration and time in primary drying. For a slow process with therefore a low mass transfer, the safety margin may be 2°C, for an aggressive cycle (high mass flow), it should be 5°C.

High T_p yields a fast process, with each 1°C increase in T_p decreasing primary drying time by roughly 13% [25].

Primary drying is carried out at low pressures to improve the rate of sublimation. The chamber pressure (P_c) is an important parameter because it impacts heat and mass transfer. P_c should be well below the ice vapor pressure at the target T_p to allow a high sublimation rate [24].

The sublimation rate is defined by Eq. 1-1 [26]:

$$\frac{dm}{dt} = \frac{P_{ice} - P_c}{R_p + R_s} \quad \text{Eq. 1-1}$$

where, $\frac{dm}{dt}$ is the ice sublimation rate (g/hour per vial), P_{ice} is the equilibrium vapor pressure of ice at the sublimation interface temperature (Torr), P_c is the chamber pressure (Torr), and R_p and R_s are the dry layer and stopper resistance, respectively, to water vapor transport from the sublimation interface (Torr-h/g).

Very low chamber pressures (e.g., < 30 mTorr) may lead to problems, e.g., contamination of product with volatile stopper components or pump oil [27]. Additionally, they produce larger heterogeneity in heat transfer and T_p between vials [28]. In most applications of practical interest, the chamber pressure varies from 50 to 200 mTorr [24].

Temperature (°C)	Vapor Pressure (mTorr)				
	0	-2	-4	-6	-8
0	4579	3880	3280	2765	2326
-10	1950	1632	1361	1132	939
-20	776	640	526	440	351
-30	286	232	187	151	121
-40	96.6	76.8	60.9	48.1	37.8
-50	29.6	23.0	17.8	13.8	10.6
-60	8.08	6.14	4.64	3.49	2.61
-70	1.94	1.43	1.05	0.77	0.56

Tab. 1-1: Dependence of vapor pressure of ice from sub-zero temperatures [29], pressure unit adapted (vapor pressures given for the sum of the temperatures in the respective row and column).

The mentioned dependence of vapor pressure of ice on temperature is illustrated in Tab. 1-1. As P_{ice} increases exponentially with temperature, it is obvious that the driving force for sublimation, and, therefore, also the sublimation rate, increases dramatically as the product temperature increases [6].

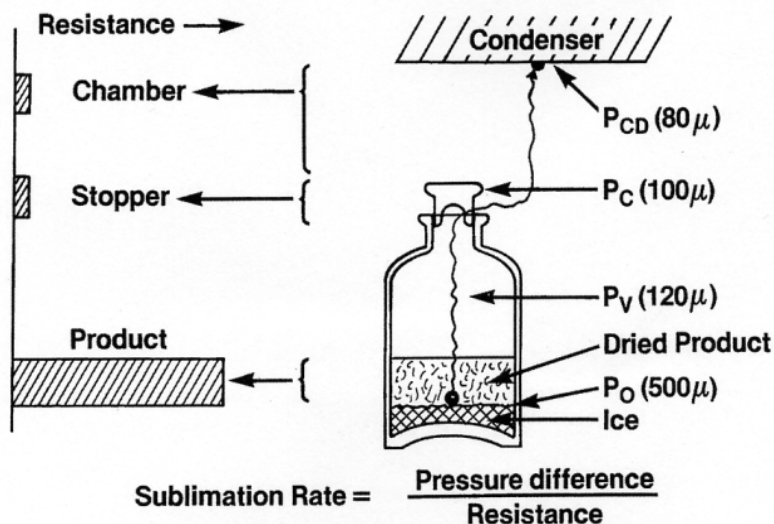


Fig. 1-9: Resistance to vapor flow during primary drying [32]

As mentioned in Eq. 1-1, mass transfer depends on the resistance to the flow of water vapor from the product through pathways in the dried layer, through the openings in the stopper, through the chamber to condenser pathway, and the resistance to re-

sublimation, cf. [30]. Fig. 1-9 is a schematic of various resistances to the flow of water vapor through the dried product. The sublimation front proceeds horizontally from the top toward the bottom, and water vapor created by the sublimation of ice must pass through the dried layer above, which was formed by removal of ice [30]. Within the dried layer, mass transfer occurs by two mechanisms: by bulk flow of material in the direction of a pressure gradient or by diffusive flow that occurs by the relative movement of molecules due to differences in concentration, mole fraction, partial pressure, and so on [31]. Bulk flow through the porous structure could be either free molecular flow or viscous flow. The range of pore diameters is generally 15-60 μm for freeze-drying in vials [30]. At typical product temperatures and pressures during freeze-drying and at typical average pore diameters (20 μm), the mean free path is much larger than the pore size. Therefore, during freeze-drying in a vial, the flow of vapor through the dried product is free molecular flow or Knudsen flow [30]. For the sublimation of ice a heat input of about 650-670 cal/g is required (depending on T_{ice}). This heat has to be transferred from the shelves to the frozen product over several barriers. The temperature gradient depends on the container system, the shelf design, chamber pressure, and sublimation rate.

Fig. 1-10 gives an idea of these factors. Today, bottomless trays or automatic loading systems are used instead of the shown tray which imposes a strong resistance to heat flow [30]. The vial heat transfer coefficient is defined as the ratio of the area-normalized heat flow to the difference

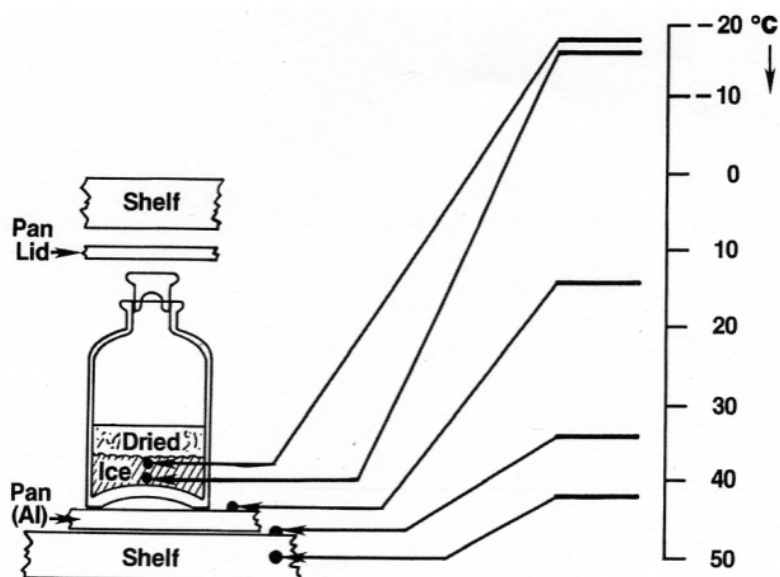


Fig. 1-10: Temperature profile (primary drying) of a vial placed in a flat aluminum tray containing a solution of dobutamine HCl-Mannitol (1:1) at a chamber pressure of 0.1 Torr [28]

between the temperature of the heat source (shelf surface, T_s) and the heat sink (product, T_p) as illustrated in Eq. 1-2,

$$K_v = \frac{dQ}{dt} \frac{1}{A_v(T_s - T_b)} \quad \text{Eq. 1-2}$$

where $\frac{dQ}{dt}$ is the heat flow (cal/s) from the shelf to the product in a given vial, and A_v is the outer cross-sectional area of the vial (cm^2). T_s ($^{\circ}\text{C}$) refers to the temperature of the shelf surface on which the vial rests, and T_b ($^{\circ}\text{C}$) is the product temperature at the vial bottom [30]. The vial heat transfer coefficient K_v receives contributions from three heat transfer mechanisms:

$$K_v = K_c + K_r + K_g \quad \text{Eq. 1-3}$$

K_c is the contribution from direct conduction from the shelf to the vial at the points of contact, K_r is the contribution from radiation heat transfer from the top, bottom, and sides to the vial, and K_g is the contribution from gas conduction in the vapor space between the shelf and the bottom of the vial [30].

Conventionally, T_b is monitored in a small number of vials by placing temperature sensors (e.g., thermocouples) at the bottom center of the vials. It is assumed that at least the average of the measured temperatures is representative for the rest of the vials, although a temperature and drying rate bias between the monitored vials and the rest of the batch has been reputed [6]. Monitored vials usually freeze sooner with less supercooling than the batch as a whole [33]. Nevertheless, the trend in product temperature measurement is often used to determine the end of primary drying by registering the sharp increase in T_p [6] which simply reflects that T_p has reached T_s . Atypical temperature profiles in front vials as well as drying differences between edge and center vials make this detection method not representative for the batch as a whole.

In contrast, it is both possible and practical to monitor T_p without placing temperature sensors in the product vials [34], for example using manometric temperature measurements (MTM). It is based on a non-linear regression analysis pressure rise in the chamber when the valve separating the drying chamber from the condenser chamber is periodically closed for a short period of time (25 s). It provides vapor pressure of ice which can then be correlated to T_p , which is the temperature relevant to collapse, and a representative temperature of the product vials without risk of sterility compromise [6]. The concept of MTM is the key feature of the SMARTTM Freeze Dryer technology, a commercially available software for process optimization. This technology has been used in the present work and has a “built in” expert algorithm, which controls all stages of freeze-drying [24]. Particularly interesting for our purposes is that in primary drying the system uses the feedback information from MTM, including current T_p and dry layer resistance, selects the target T_p , calculates the optimum chamber pressure for primary drying, predicts primary drying time at the target T_p , calculates the optimum shelf temperature to achieve the target T_p , and determines the end point of primary drying [35].

1.2.3 Secondary drying

Water removal during secondary drying involves diffusion of water in the amorphous glass, evaporation at the solid-vapor boundary, and water vapor flow through the pore structure of the dried product [6]. The rate-limiting mass transfer process for drying an amorphous solid is either diffusion in the solid or evaporation at the solid-vapor boundary, depending on the product [36]. Therefore, the chamber pressure in primary drying is also appropriate for secondary drying [24].

During primary drying some secondary drying occurs. To a limited extent water desorbs from the surface of the amorphous phase once the ice is removed from that region. Accordingly, water from the inner matrix diffuses to the surface by gradient compensation. However, in an operational sense the onset of secondary drying is normally defined once all ice has been removed. The judgment that all vials are free of ice is not always easy since not all vials dry equally due to edge vial effects etc. When switching to secondary drying, the shelf temperature is increased typically to a temperature in the range of 25-50°C [37]. Thereby, the energy required for efficient removal of the bound water is provided. Because desorption rate is relatively low, the shelf temperature and the product temperature at the vial bottom are nearly identical [6].

After primary drying, an amorphous product still contains a fair amount of residual moisture. Depending on the formulation, 5-20% water on a dried solids basis is still in the cake. The objective of secondary drying is to reduce the residual moisture content to a level for optimal stability, which is usually less than 1% [24]. As the water content of the amorphous phase decreases during drying, the glass transition temperature increases very sharply [6].

1.3 Freeze-drying excipients

Freeze-drying equipment is very expensive and process times are often long, so that a lyophilized drug is relatively expensive to produce. Indeed, the preferred option for a parenteral dosage is a ready-to-use solution. It is less costly to produce and easier in its application [6]. For small molecules, stability normally increases in the following order: solution < glassy solid < crystalline solid [38-40]. Hence, if an API does not have sufficient stability in an aqueous solution, it must be produced in solid form.

Some freeze-dried formulations contain API only (e.g., cephalosporins, vancomycin, antibodies), possibly because of the relatively high content of the active ingredient (typically 10 mg/mL or more) [41]. In many other cases, excipients are needed. According to the International Pharmaceutical Excipients Council, pharmaceutical excipients are substances other than the pharmacologically active drug or pro-drug which are included in the manufacturing process or are contained in a finished pharmaceutical product dosage form [42].

Tab. 1-2: Examples of commonly used excipients in freeze-drying of pharmaceutical products [44]

Type	Function	Substance
Bulking agents	Provide bulk to the formulation, especially when the concentration of product to freeze dry is very low	Hydroxyethyl starch, trehalose, mannitol, lactose, and glycine
Buffers	Adjust pH changes during freezing	Phosphate, tris HCl, citrate, and histidine
Stabilizers	Protect the product during freeze-drying against the freezing and the drying stresses	Sucrose, lactose, glucose, trehalose, glycerol, mannitol, sorbitol, glycine, alanine, lysine, polyethylene glycol, dextran, and PVP
Tonicity adjusters	Yield an isotonic solution and control osmotic pressure	Mannitol, sucrose, glycine, glycerol, and sodium chloride
Collapse temperature modifiers	Increase collapse temperature of the product to get higher drying temperatures	Dextran, hydroxypropyl- β -cyclodextrin, PEG, PVP

Excipients for lyophilization usually fit one of the following categories: bulking agents, stabilizers, buffering agents, tonicity modifiers, surface-active agents [43], or collapse temperature modifiers. Tab. 1-2 presents some examples of the excipients commonly used in freeze-drying process of pharmaceutical products with the presentation of their different role.

Tab. 1-3 shows some examples of lyophilized market products with their components, of which selected will be discussed in detail in this chapter.

Tab. 1-3: Examples of lyophilized market products stabilized with excipients introduced in the text [41]

Trade name	Generic name (indication)	Component	Concentration
BETASERON®	Interferon β -1B (multiple sclerosis)	Interferon β -1B	0.3 mg
		Human serum albumin	15 mg
		Mannitol	15 mg
HERCEPTIN®	Trastuzumab (breast cancer)	Trastuzumab	440 mg
		L-histidine HCl	9.9 mg
		L-histidine	6.4 mg
		Trehalose	400 mg
		Polysorbate 20	1.8 mg
NUTROPIN®	Somatropin (human growth hormone)	Somatropin	5 mg
		Mannitol	45 mg
		Sodium phosphate monobasic	0.4 mg
		Sodium phosphate dibasic	1.3 mg
		Glycine	1.7 mg
		Benzyl alcohol (diluent)	0.90%
XIGRIS™	Drotrecogin 2 Alfa (sepsis)	Drotrecogin alfa	5.3 or 20.8 mg
		Sodium chloride	40.3 or 158.1 mg
		Sodium citrate	10.9 or 42.9 mg
		Sucrose	31.8 or 124.9 mg

1.3.1 Stabilizers

The most important group of stabilizers used in freeze-drying is classified in cryo- and lyoprotectants. They protect the API (favorably a protein) from damage during freezing (cryoprotection) and/or dehydration (lyoprotection) induced denaturation [45].

In liquid state (during freezing) preferential interaction is the most important stabilization mechanism which means that a protein prefers to interact with either water or an excipient in an aqueous solution [46-52]. In the presence of a stabilizer, the protein prefers to interact with water (preferential hydration [53-55]) and the excipient is preferentially excluded from the domain of the protein (preferential exclusion). Therefore, proportionally more water molecules and fewer excipient molecules are found at the surface of the protein than in the bulk. Accordingly, preferential exclusion of an excipient is usually associated with an increase in the surface tension of water [56]. Examples for excluded solutes are saccharides, polyols and amino acids [6].

Other stabilization mechanisms include modification of the size of ice crystals, reduction (instead of elevation) of surface tension, increase of the viscosity of the solution (restricting diffusion of reactive molecules) [45] and suppression of pH changes [57].

During drying the hydration shell of proteins is removed. Therefore, the preferential interaction mechanism is no longer applicable. The most important mechanism for lyoprotection is known as the water replacement hypothesis [58-60]. This stabilization mechanism was subject to many publications [16, 61, 62]. The native structure of the protein is preserved by serving as a water substitute and intra- or interprotein hydrogen bonding may be prevented during dehydration by satisfying the hydrogen bonding requirement of polar groups on the protein surface [63, 64]. Carbohydrates, for example, are prominent lyoprotectants. Allison and co-workers [59] reported that hydrogen bonding between carbohydrate and protein is necessary to prevent dehydration induced protein damage. However, the failure of glucose to prevent lysozyme unfolding during freeze-drying shows that hydrogen bonding between carbohydrate and protein alone is not sufficient to pro-

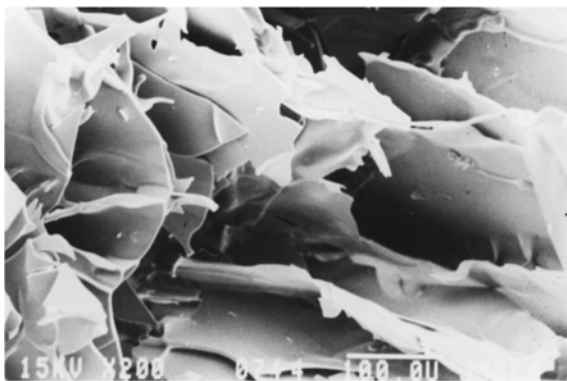
protect a protein during lyophilization, but that it must be protected against both freezing- and dehydration-induced unfolding. For sucrose and trehalose it was found that the degree of structural protection of lysozyme correlated with the extent of hydrogen bonding, and that sucrose forms hydrogen bonds to a greater extent than trehalose [60].

Another mechanism of lyoprotection is the formation of an amorphous glass [65]. Due to its extreme viscosity, the interconversion of conformational substrates and conformational relaxation of a protein are slowed down [66]. Here, it was reported that trehalose is more effective than sucrose, glucose, or fructose in its stabilizing effect because of its higher solution viscosity which limits diffusion [67].

Among stabilizers [41, 45, 68] and especially among disaccharides, sucrose and trehalose are most commonly used as excipients. They can be used as nonspecific protein stabilizers in solution, and during freeze-thawing and freeze-drying as effective cryoprotectants and remarkable lyoprotectants [45, 69, 70]. It was already in 1981, when Lee and Timasheff found that sucrose is preferentially excluded from the protein domain, increasing the free energy of the system. Thermodynamically this leads to protein stabilization since the unfolded state of the protein becomes thermodynamically even less favorable in the presence of sucrose [71].

In addition, both sucrose and trehalose were found to form fragile glasses [72]. In contrast to strong glasses, the viscosity of fragile glasses increases more rapidly for a given temperature which results in stabilizing advantages [45]. They effectively slow down the transformation of conformational substances and conformational relaxation of a protein by forming a highly viscous amorphous glass [73].

The relative stabilizing effect of sucrose and trehalose seems to be dependent on both the protein and sugar concentration [45].



Pic. 1-1: Scanning electron micrograph of a 10% freeze-dried sucrose solution. The temperature of the sample was not allowed to exceed T_g by a significant amount or for a significant period. Scale bar = 100 μm . [9]

Pic. 1-1 shows a well freeze-dried 10% solution of sucrose with its typical appearance of an amorphous solid [9]. Sucrose as well as trehalose needs to be added in a sufficient quantity for a satisfactory stabilizing effect. Recently a molar ratio of 300:1 up to 500:1 (disaccharide:protein) was suggested [74, 75]. In 1991 Tanaka et al. reported that the concentration of the tested saccharides must be high enough to form a mono-

molecular layer onto the catalase surface to ensure lyoprotection [76].

Both sucrose and trehalose are approved by the FDA (Food and Drug Administration, USA), and were reported to be equally effective in stabilizing proteins [77]. When comparing them, trehalose might have some advantages with regard less hygroscopicity, no internal hydrogen bonds (which results in more flexibility in protein bounding), and a reduced chemical reactivity [45]. In addition, its glass transition (and collapse) temperature is higher [78] due to a limited plasticizing effect of water to the amorphous phase [79]. However, trehalose might show a higher fragility of the lyophilized structure at lower temperatures which was explained by its complex dehydration behavior into the anhydrate [80].

To stabilize other proteins during freeze-thawing and freeze-drying, further the protein serum albumin was used as a cryoprotectant and lyoprotectant [45, 81, 82]. Many protein products on the market, such as Betaseron[®], Epogen[®], Kogenate[®], and Recombinate[™] contain albumin [83]. Additionally, serum albumin is sometimes used as a model protein in placebo formulations. However, the ever-increasing concern about the potential contamination of serum albumin with blood-borne pathogens limits its future applica-

tion in protein products [45]. Therefore, recombinant human albumin has been recommended recently to replace serum albumin as a protein stabilizer [84]. The molecular weight of bovine serum albumin (BSA) has frequently been cited as 66,120 [85] or 66,267 [86], but it was revised in 1990 to 66,430 [87]. All three values are based on amino acid sequence information available at the time of publication. BSA is a single polypeptide chain consisting of about 583 amino acid residues and no carbohydrates. At pH 5-7 it contains 17 intrachain disulfide bridges and one sulfhydryl group [85; 86]. BSA consists of about 54% of α -helix and 18% of β -form and its overall dimensions are 40 x 140 Å [85]. Human serum albumin (HSA) has a molecular weight of 66,248.3 [88] or 66,437 [89] (based on amino acid composition). Like BSA it is a single polypeptide chain with one free sulfhydryl group on residue #34 and 17 intrachain disulfide bonds [88]. Its structure was estimated 48% of α -helix and 15% of β -form. Its overall dimensions are 38 x 150 Å [88]. Albumins are readily soluble in water and can only be precipitated by high concentrations of salts such as ammonium sulfate [90].

Stabilization of proteins by polymers can generally be attributed to one or more of these polymer properties: preferential exclusion, surface activity, steric hindrance of protein–protein interactions, and/or increased solution viscosity limiting protein structural movement [45]. Additionally, it was reported that polymers like dextran stabilize proteins by raising the glass transition temperature of a protein formulation significantly (function of collapse temperature modifiers [91]), and by inhibiting crystallization of small stabilizing excipients such as sucrose [92]. In buffer systems they are able to inhibit a pH-drop by inhibiting the crystallization of disodium phosphate if the formulation contains a phosphate buffer [93].

PVP 40 kDa, e.g., increased both the freeze-thawing and freeze-drying recovery of lactate dehydrogenase in a concentration-dependent manner [57]. For rabbit muscle LDH, a combination of dextran, hydroxypropylmethylcellulose and gelatin had a stabilizing effect in dependence on their concentration [82].

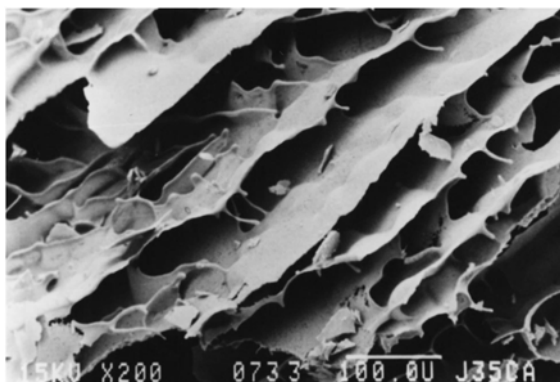
1.3.2 Bulking agents

Bulking agents are used to provide product elegance (i.e., satisfactory appearance) as well as sufficient cake mechanical strength to avoid product blow-out. When a very dilute solution is lyophilized, the flow of water vapor during primary drying may generate sufficient force on the cake to break it and carry some of it out of the vial. Here, bulking agents simply function as fillers to increase the density of the product cake [6].

Amorphous excipients can serve as bulking agents, but due to relatively low collapse temperatures most of them require long processing times, and are not favored.

Here, mannitol and glycine are preferred since they are crystallizing compounds.

Mannitol is by far the most commonly used bulking agent. A formulation based on mannitol is usually elegant, reconstitutes quickly, and is generally easy to freeze-dry without risk of product damages [6], except for the potential of vial breakage [94], which can be minimized



Pic. 1-2: Scanning electron micrograph of a 10% freeze-dried mannitol solution illustrating the typical directional appearance of a substance that crystallized from solution during freezing and/or drying. Scale bar = 100 μm . [9]

by small fill depths, slow freezing, avoiding freezing temperatures less than about -25°C until crystallization is complete [6], or annealing respectively. The typical crystalline appearance of a mannitol cake is illustrated by an SE micrograph in Pic. 1-2. Originally, mannitol shows three modifications which were investigated in detail [95], and its crystallization during freezing depends on the cooling rate. Cavatur and co-workers investigated the crystallization behavior of mannitol in dependence on cooling rate as well as the influence of phosphate buffers and PVP [96]. They found that rapid cooling ($20^{\circ}\text{C}/\text{min}$) inhibited mannitol crystallization, whereas slower cooling rates (10°C and $5^{\circ}\text{C}/\text{min}$) resulted in partial crystallization. For the amorphous freeze-concentrate they

reported two glass transitions (at -32°C and -25°C). The induction time for the crystallization of mannitol hydrate, which was observed when heating past the two glass transition temperatures, was increased by PVP. Concentrations of ≥ 100 mM of phosphate buffers significantly inhibited mannitol crystallization [96]. Mannitol (as well as glycine) does exhibit crystalline polymorphism in freeze-dried systems [97], and might form a hydrate under some conditions [98, 99]. The hydrate does not easily desolvate to an anhydrate during secondary drying which may compromise stability if secondary drying is performed below 50°C [6]. Previously, it was reported that amorphous mannitol provides some protection to β -galactosidase during freezing and thawing, but annealing and crystallization reduce the protein stabilizing effects. In addition, crystallization of mannitol resulted in protein inactivation of three different protein formulations to an extent proportional to the fraction of crystalline mannitol [100].

Another frequently used bulking agent is glycine. On the one hand, it crystallizes easily to form an elegant product that reconstitutes quickly and does not induce vial breakage. On the other hand, its cake is more fragile than a mannitol cake and is generally perceived as being somewhat less elegant than a mannitol cake [6]. Neutral glycine exists in three polymorphic forms. Hence, arising from different thermal history of freezing, reconstitution time can be affected by the polymorph of glycine in the freeze-dried solid [101, 102].

1.3.3 Others

To control pH buffering agents are often added. Yet, caution must be exercised when they are used. As discussed before, crystallization of either buffer component during freezing may cause a significant pH shift (due to freeze concentration effects) [6]. When a buffer is desired in an amorphous form in the freeze-dried product this may cause a drop in T_c of the formulation. Therefore, handling is difficult and the content of a buffer should be as low as possible or avoided.

Tonicity modifiers (e.g., NaCl or glycerol) are occasionally formulated in products for human use to make the reconstituted product isotonic (e.g., for subcutaneous or intramuscular injections). Since tonicity modifiers (like buffering agents) can lower the T_c significantly, isotonic adjustment is best accomplished by including them in the diluents rather than in the freeze-dried product [6].

At low levels ($\sim 0.05\%$ w/w) surface-active agents may be added. They aid reconstitution if the API does not wet well and minimize losses due to surface adsorption (e.g., in low dose products). Surfactants may also be effective as stabilizers in low dose protein systems [6].

1.4 Freeze-dry microscopy

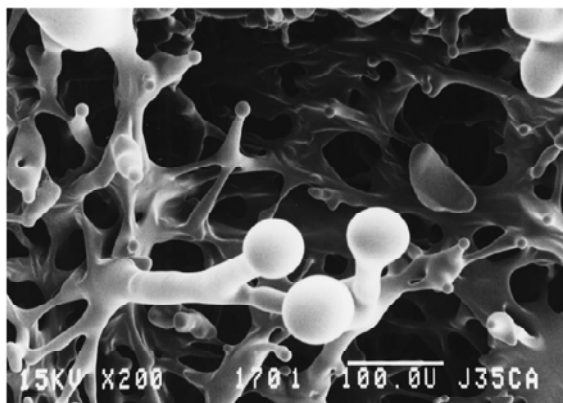
By attaching a cryo-stage and a controllable cooling and vacuum system, a light microscope can be used to directly observe the microstructures of the formulation solution sample under conditions of freezing and freeze-drying [103]. This technique is termed freeze-drying microscopy or freeze-dry microscopy (FDM).

1.4.1 Collapse

For a true optimization of a lyophilization cycle, the product temperature (T_p) at the sublimation interface is controlled close to or below the critical formulation temperature of the formulation. For crystalline systems, this critical formulation temperature is represented by the eutectic temperature (T_{eu}), for amorphous systems by the glass transition temperature of the maximally freeze-concentrated solution (T_g') or the collapse temperature (T_c), respectively. T_c and T_g' are generally much lower than T_{eu} for the corresponding crystalline structures [24]. In general, FDM has been accepted as the best technique for the determination of the critical formulation temperature of the product during primary drying, since the loss of structure (cake collapse) can be visually observed under experimental conditions which are controlled to simulate the real freeze-drying

process [103]. However, T_c is not a unique property of the solute material, but rather depends on the measurement methodology and the rate of water removal from the glassy state [104]. In very few cases limited collapse is intentionally induced during freeze-drying, but in general, collapse is cause for rejection of lyophilized pharmaceuticals [15]. Collapse is defined as the process by which the structure created during freeze-drying is annihilated after the passage of the sublimation interface [105]. Another definition proclaims collapse as the phenomenon when amorphous material undergoes viscous flow, resulting in loss of the pore structure, if T_p is higher than T_c during primary drying [104].

In contrast to collapse where the whole structure loses its form, a microcollapse of a product



Pic. 1-3: SEM of a freeze-dried 10% Ficoll solution, illustrating partial microcollapse. Scale bar = 100 μm [9].

is characterized by a viscous flow of only substructures or structure in a very limited area. Pic. 1-3 shows a partial microcollapse which is reflected in a droplet formation. Both, microcollapse and collapse may lead to shrinkage of the cake which results in a significantly smaller volume of the freeze-dried cake in comparison to the original volume of the frozen cake. Besides the unacceptable appearance, various undesirable properties

result from the collapse of the cake: The rate of sublimation can be significantly reduced because the paths where water can escape are clogged. Consequently, the product tends to have higher residual moisture content and the water may be distributed unevenly through the sample [106]. Additionally, due to the loss of porosity and the reduction in specific surface area, a slower reconstitution is generally experienced with a collapsed product which can pose a significant marketing challenge [29]. Incomplete reconstitution

can as be caused by small amounts of undissolved solids which remain in the solution

after reconstitution [104, 107] or instability (i.e., precipitation) of the active ingredient. Finally, collapse might, but does not necessarily, perturb protein structure and lead to degradation. Fig. 1-11 shows a SEM picture (microstructure) and a photo of a vial (macrostructure) containing collapsed sucrose. The effects of collapse on API activity were studied recently: For IgG and lactate dehydrogenase no significant impact on stability was found, even when the cake was completely collapsed [108],

whereas toxins A and B of *Clostridium difficile*, porcine pancreatic elastase and actin showed a significant loss of activity (during storage) when primary dried at a T_p above T_g' [60, 109, 110].

Since a small variation in product temperature at the sublimation front T_p can greatly modify the dried product structure as well as the primary drying time, an accurate determination of T_c is critical for the process optimization [111]. In other words: collapse in a given region results from surface tension induced viscous flow of the amorphous phase after the ice-vapor interface has moved past that region [104].

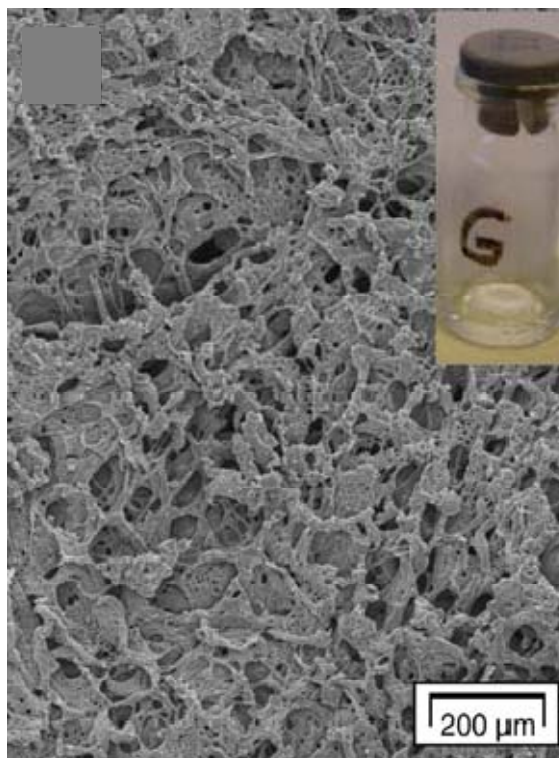


Fig. 1-11: Collapsed sucrose: SEM picture and cake in vial [44]

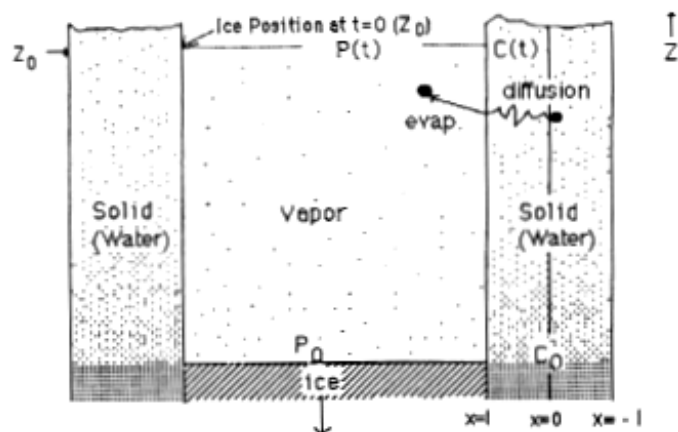


Fig. 1-12: Schematic of primary and secondary drying relevant for collapse [104]

At time zero ($t=0$), the ice position was at the top of the scheme as noted. The ice has moved down to a point near the bottom of the picture, i.e. sublimation has produced a pore. Since the original structure of the walls is maintained, this sample was dried below T_c . The solid walls have not undergone viscous flow. If the drying had been carried out above T_c , the walls would have begun to flow once the ice-vapor interface had moved below the initial position Z_0 . If flow had persisted over a sufficient period of time to cause the pore walls to flow over a distance on the order of the pore radius, r , collapse would have been obvious [104].

The simple Eq. 1-4 may be derived from energy balance between surface energy decrease and viscous dissipation for a single empty capillary in an infinite medium:

$$t = \frac{\mu r}{2\gamma} \quad \text{Eq. 1-4}$$

where t is the time for collapse (s), γ is the surface tension (dynes/cm), μ (mPa·s) is the viscosity of the pore walls (solid solute with unfrozen water), and r is the initial capillary radius (μm). It was assumed by Bellows and King that collapse will occur when the viscosity of the concentrated amorphous solution is of the order of 10^7 - 10^{10} mPa·s [113].

The viscosity of the concentrated amorphous solution tends to increase with decreasing temperature, increasing solute concentration and higher solute molecular weight. The

Fig. 1-12 depicts the primary and secondary drying during drying in a FDM stage. The channel or pore in the picture was initially filled with ice and bounded by walls of the amorphous solid (thickness $2l$).

At time zero ($t=0$), the ice position was at the top of the scheme as

concentration of the concentrated amorphous solution is uniquely determined thermodynamically by the temperature, the molecular weight and nonideality of the solutes. Pre-conditions for this statement are: (1) the chemical potential of water is equal between the ice and the concentrated amorphous solution phases, and (2) the ice crystals are large enough so that curvature effects may be ignored [113]. Accordingly, for a given solute or mix of solutes the concentrated amorphous solution has a unique viscosity-temperature relationship, which represents the effect of temperature, both directly and through changing solute concentration.

Fig. 1-13 shows the relationship between viscosity and temperature for various solutes.

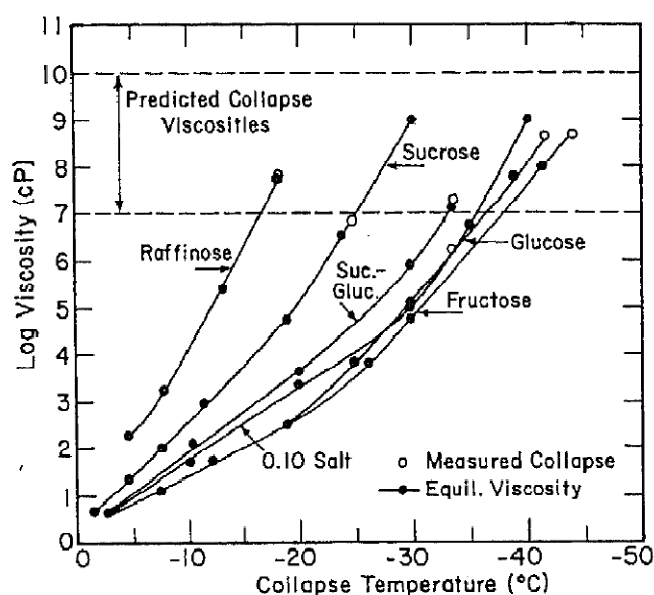


Fig. 1-13: Equilibrium viscosity curves for solutions of various sugars³ [113]

be changed to “temperature” for these equilibrium-viscosity curves.) They are strong functions of temperature, because lowering the temperature increases the concentration of the amorphous solution [113]. The authors conclude that “consequently” an order-of-magnitude viscosity analysis is sufficient for quantitative prediction of the collapse tem-

“Suc.-Gluc.” is a sucrose-glucose mixture with 50% (w/w) of each component. “0.10 Salt” represents a mixture of 10% (w/w) NaCl and 90% (w/w) sucrose. The open circles are collapse temperatures measured by the authors. The dark circles are derived from viscosity measurements dependent upon temperature. (For better understanding the term “collapse temperature” on the x-axis should

³ The reader is reminded that 1 cP = 1 mPa s.

perature. They ignore a fact described in the section about freezing: For a given solute (e.g., sucrose) during freezing freeze concentration takes place until the viscosity reaches a critical value which is characteristic for this solute (sucrose: 81% w/w). Here, further ice crystal growth is stopped and the remaining concentrated amorphous solute becomes a solid. For a given solute this means that dependent upon concentration the size and/or amount of ice crystals differs, but not the composition of the “walls” or the concentrated amorphous solute, respectively. Nevertheless, the authors give valuable hints for the comparison of T_c of different solutes: “Sugar solutions show markedly different equilibrium viscosity curves depending upon whether they are composed of mono-, di-, or trisaccharides, with higher molecular-weight solutes having higher viscosities, primarily because the concentrated amorphous solute concentration (% w/w) is higher at any given temperature”[113]. But as described later in chapter 3.2 (“Dependence on Concentration”, p. 102 ff.), for a prediction of T_c of different concentrated liquid solutions of a given solute, more parameters must be taken into account.

When assuming that surface tension γ is the driving force causing flow, Eq. 1-4 can be written as

$$v = \frac{2\gamma}{\mu} = \frac{r}{t} \quad \text{Eq. 1-5}$$

where r is the pore radius (or the size of the ice crystal before sublimation, respectively), t is the time for collapse, γ is the surface tension and μ is the viscosity of the concentrated amorphous solute (the “wall”). The “flow velocity” v ($\mu\text{m/s}$) is consequently a flow occurred over a distance in the order of r in the given collapse time t . As described above, the viscosity of the “wall” is a function of both temperature, T , and time, t . If surface tension is assumed to be only marginal dependent on temperature and time compared to the corresponding dependencies on viscosity, Eq. 1-5 may be written as:

$$r = \int_0^{TM} v \, dt = 2\gamma \int_0^{TM} \frac{dt}{\mu(T, t)} \quad \text{Eq. 1-6}$$

where TM is the time for observation, underlining that collapse has to occur in a given time frame to be observed under the microscope during a FDM measurement.

At low temperatures, the temperature dependence of viscosity for a concentrated aqueous solution is non-Arrhenius and may be written in the following form:

$$\mu(T, t) = A \exp\left(\frac{B}{T - k T_g}\right) \quad \text{Eq. 1-7}$$

where μ is the viscosity of the concentrated amorphous solution, T is the temperature, T_g is the glass transition temperature of the amorphous system as measured by DSC, and A , B and k are constants. This equation [104] is a combination of the Vogel-Tammann-Fulcher equation and the Williams-Landel-Ferry equation. Arrhenius kinetics describe the simplest type of temperature dependence:

$$\mu = A \exp\left(\frac{E_A}{RT}\right) \quad \text{Eq. 1-8}$$

where μ is the viscosity of the matrix, E_A is the activation energy (J), R is the gas constant ($8.314 \text{ J} \cdot \text{K}^{-1} \cdot \text{mol}^{-1}$), T is the temperature, and A is a constant [114]. Eq. 1-8 is valid for “strong network-formers” such as SiO_2 and BeF_2 [115] and for many liquids at temperatures far from their glass transition temperature.

Molecules in the investigated solutions are free to move, the Vogel-Tammann-Fulcher (VTF) equation describes the effect of temperature:

$$\mu = A \exp\left(\frac{B}{T - T_0}\right) \quad \text{Eq. 1-9}$$

where μ is the viscosity, T is the temperature, T_0 represents the temperature at which the free volume would vanish, and A and B are constants [114].

Williams, Landel, and Ferry (WLF) developed a related equation [116]:

$$\log\left(\frac{\mu}{\mu_0}\right) = -\frac{C_1(T - T_g)}{C_2 + (T - T_g)} \quad \text{Eq. 1-10}$$

where the viscosity μ is shown as a function of temperature T with respect to the μ_0 at the glass transition temperature T_g ; C_1 and C_2 are constants [114].

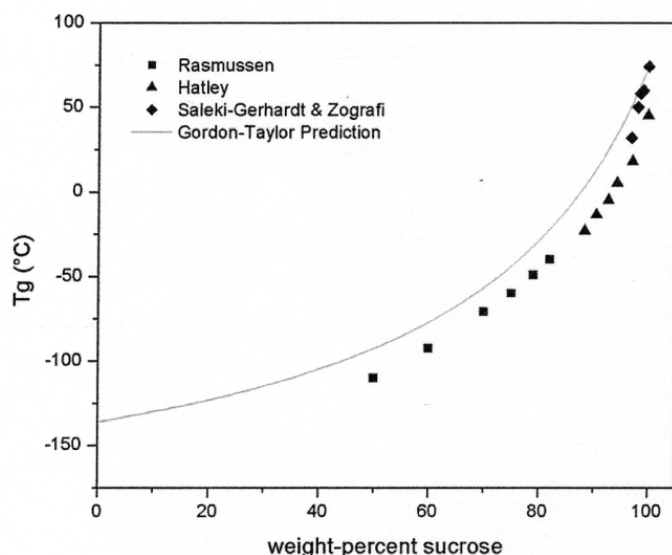


Fig. 1-14: Glass transition of sucrose-water mixtures as a function of water content [117]

The WLF equation has the advantage that the reference temperature T_g can be measured by thermoanalytical techniques, e.g., DSC (cf. Fig. 1-14). Fig. 1-15 illustrates that the fraction of matrix with unfrozen water (“wall” or concentrated amorphous solution, respectively) is

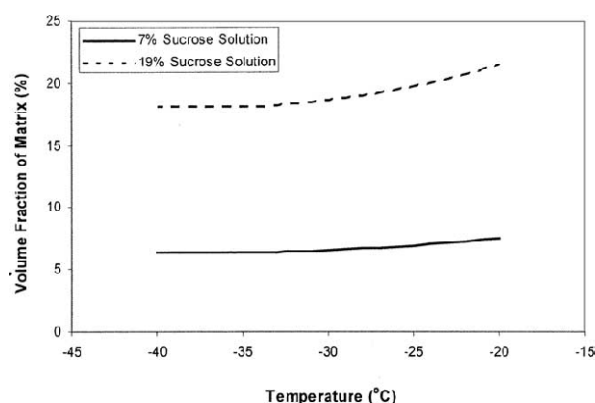


Fig. 1-15: Volume fraction of matrix in frozen sucrose as a function of temperature [118]

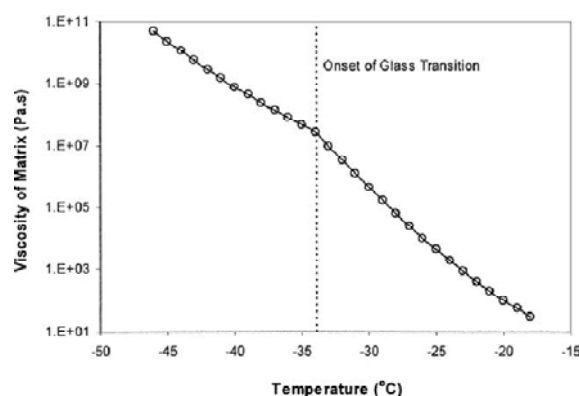


Fig. 1-16: Viscosity of matrix in frozen sucrose solutions as a function of temperature [118]

strongly affected by the initial concentration (in this case sucrose concentration) and slightly by the temperature. In contrast, the viscosity is related to the temperature and independent of the initial sucrose solution as shown in Fig. 1-16.

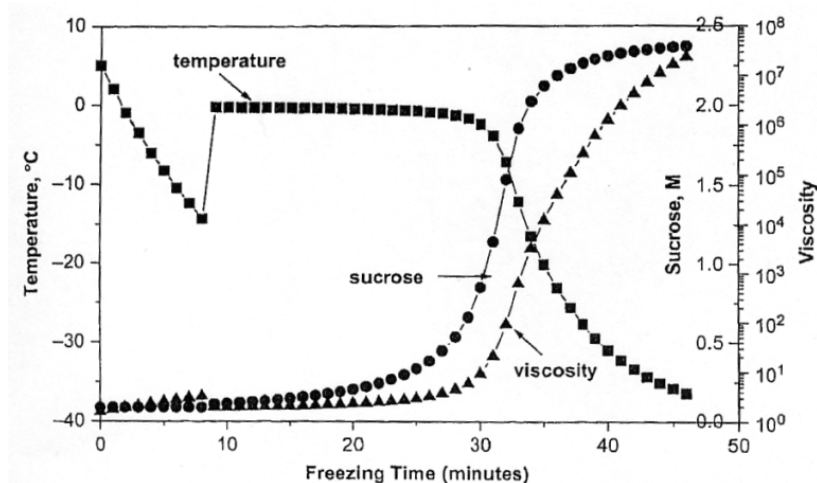


Fig. 1-17: Temperature, % solute concentration, and viscosity profiles as a function of temperature during freezing of 3% sucrose [16]

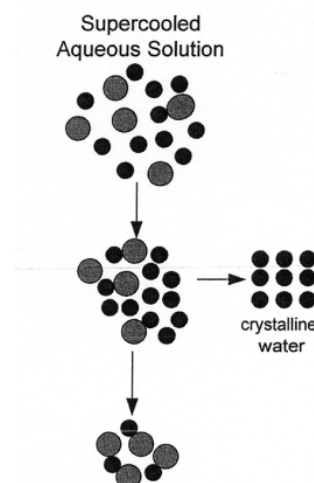


Fig. 1-18: Freeze concentration of a supercooled aqueous solution [117]

Combining the VTF equation (Eq. 1-9) with the phenomenon of freeze concentration (Fig. 1-18), the viscosity of e.g., a 3% sucrose solution can be calculated in the range relevant for freezing in freeze-drying. For the curves shown in Fig. 1-17 it was assumed that ice crystallization occurs at -15°C and that the solution composition follows the equilibrium freezing point depression curve. Since the heat removed from the solution is balanced by the heat of crystallization of ice in this example, the temperature of the solution remains nearly constant. Once ice formation is close to complete, the temperature decreases sharply, the sucrose concentration in the freeze-concentrate increases greatly, which in turn increases the viscosity of the freeze-concentrate [16].

During FDM measurements not only primary drying (= ice sublimation) occurs as described by the equations and findings above, but there are additional secondary drying effects which might influence T_c results. At time zero (cf. Fig. 1-12), the position of the ice-vapor interface is at Z_0 , and the water in the amorphous solid is assumed to be in equilibrium with ice having vapor pressure P_0 .

When sublimation occurs and ice crystals are being removed, the partial pressure of ice at Z_0 is less than the partial pressure of ice at the ice-vapor interface, P_0 . As soon as the ice-vapor interface recedes, the amorphous phase begins to dry. Water will evaporate at the surface, and Fickian diffusion from the interior of the solid will transport water to the surface. When this water is removed by sublimation, T_g of the remaining amorphous matrix increases in accordance with the water concentration dependence of T_g [104].

1.4.2 History of freeze-dry microscopy

In the early days of freeze-dry microscopy, FD microscopes were homemade by some pioneering scientists. The first known apparatus for microscopic observations was published in 1964 by MacKenzie [119], followed by new approaches from Flink and coworkers in 1978 [120] and Pikal et al. in 1983 [26].

The most critical part of the system is the cryo-stage the design of which varied widely. In most of the freeze-drying stages the temperature is nearly constant across the sample⁴. Yet, some were specially designed to achieve a temperature gradient across the sample to mimic the situation encountered in a real freeze-drying process [121-122].

Today, FDM systems are commercially available and increasingly used in pharmaceutical development laboratories. Only some scientist worked on further development of FDM. Nail and coworkers for example published in 1994 on a stage using thermoelectric (Peltier) heaters configured in two stages, with circulating fluid as a heat sink on the high temperature side [123]. The lowest attainable sample temperature was about -47°C . Hsu et al. improved the system in 1995 by using a cascade of four Peltier thermoelectric modules which enabled a freezing to -60°C [124].

⁴ All systems used in the publications discussed in section 3.1 (cf. p. 58 ff.) have a constant temperature across the sample (cf. references there).

Additionally, their system consisted of controllers to regulate temperature and pressure conditions, and a video camera to record the events under study.

Different publications on FDM, including the used systems and methodologies are discussed in the part “Methodology of FDM” (p. 63 ff.). Until today, the paper from Pikal and Shah from 1990 gives the most detailed theoretical background when using an FDM stage with a constant temperature across the sample [104].

1.4.3 Freeze-dry microscopy today

Fig. 1-19 illustrates the equipment commonly used today to perform FDM. The heart is a cryo-stage which is mounted on a light microscope equipped with a spectrum polarizer/analyzer system. A computer system, temperature controller, nitrogen controller, vacuum pump, nitrogen source and a Pirani gauge (for pressure measurement) are connected to this stage. Pressure is controlled by a valve. A PC system controls and monitors the whole system. Pictures can be recorded by a video system or a digital camera.

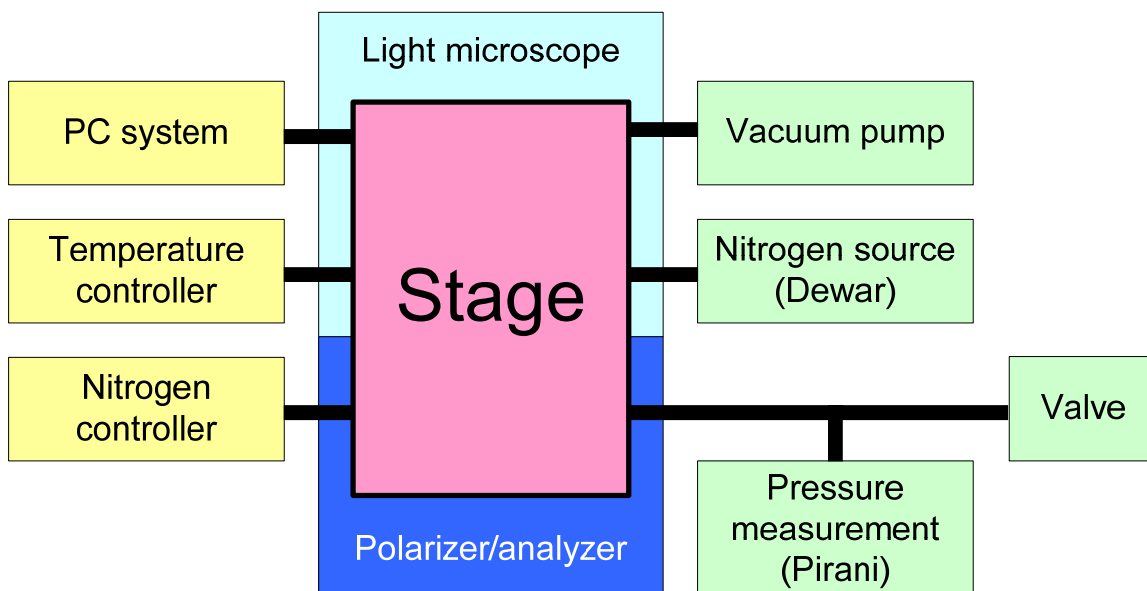


Fig. 1-19: Schematic of key equipment for freeze-dry microscopy

A picture of the commercially available FDM stage used for this work is presented in chapter 2.2.1 (p. 53 ff.).

In the last years, freeze-dry microscopy was often used for investigations on model proteins. In 1998, Jiang and co-workers used FDM on catalase, β -galactosidase and lactate dehydrogenase to gain a better understanding of the degree to which recovery of activity of model proteins after freeze-drying can be maximized by manipulation of freeze-dry process conditions in the absence of protective solutes [125]. One year before, Österberg et al. published on the development of a stable freeze-dried formulation of recombinant factor VIII-SQ without the addition of albumin [126]. The formulation strategy they describe may also be useful for other proteins which require a high ionic strength. Recombinant Factor VIII and α -amylase were used as model proteins to examine the effect of freeze-drying process conditions on the long-term stability of these proteins as freeze-dried solids in 2004 [127]. Three lyophilization protocols were used with an aggressive and a conservative cycle. Both produced pharmaceutically acceptable product. Additionally, a protocol resulting in a collapse matrix was used. The results support the conclusion that collapse is not necessarily detrimental to the long-term stability of freeze-dried proteins. In the same year reservoir-type microcapsules containing lysozyme as a model protein were produced by the solvent exchange method, and directly observed using FDM to characterize and optimize their properties [128]. Colandene and co-workers developed an efficient freeze-drying cycle for a high concentration monoclonal antibody formulation lacking a crystalline bulking agent in 2007 [129]. Characterization of the formulation was performed at multiple protein concentrations by DSC and FDM. At low protein concentrations T_g' (glass transition temperature of the maximally freeze-concentrated solution, see below) determined by DSC was similar to T_c determined by FDM. However, at higher protein concentrations, both the difference between T_c and T_g' and the difference between T_{oc} and T_{fc} became progressively larger.

It is important to note that in this study primary drying was shortened significantly by adjusting to conditions where the product temperature substantially exceeded T_g' without any apparent detrimental effect to the product [129].

In 2008, Kramer et al. published on a procedure to optimize scale-up for the primary drying phase of lyophilization [130]. Basis for the investigation was determination of the temperature at which lyophile collapse occurs by FDM. To facilitate scale-up for the primary drying phase of lyophilization the authors used a combination of empirical testing and numerical modeling. At both the laboratory and pilot scales, they found excellent agreement in both the sublimation interface temperature profiles and the time for completion of primary drying. Further, the computational model predicted the optimum operational settings of the pilot scale lyophilizer. Indeed, the presented combination of FDM, empirical testing and numerical modeling offers the potential (1) to reduce the time necessary to develop commercial freeze-drying cycles by eliminating experimentation, and (2) to minimize consumption of valuable API during process development [130].

1.5 Differential scanning calorimetry

Differential scanning calorimetry (DSC) is a commonly used thermal analysis technique which is for example often used in freeze-drying formulation development. It measures the heat flow change between a sample and a thermally inert reference material as a function of time or sample temperature [103].

Temperature conditions of the sample container (pan) can be controlled similar to a freeze-drying process. In recent years, for rational development or optimization, DSC has been extensively explored to characterize thermal properties of formulations in the frozen state. These properties include degree of supercooling, glass transition temperature of freeze concentrate (T_g'), eutectic temperature (T_{eu}), crystallization temperature, degree of crystallization, unfreezable water content and melting point [103].

To obtain DSC data, two types of methods are used. Power compensated DSC examines a pan containing the sample and the empty reference pan which were heated by separate heaters such that their temperatures are equal while they are linearly heated or cooled. In heat flux DSC, the difference in heat flow into the sample and reference is measured as the sample temperature is increased (or decreased) linearly. Although the two methods provide the same information, the instrumentation for the two is fundamentally different. Fig. 1-20 is a schematic showing the design of a power compensated calorimeter for performing DSC measurements.

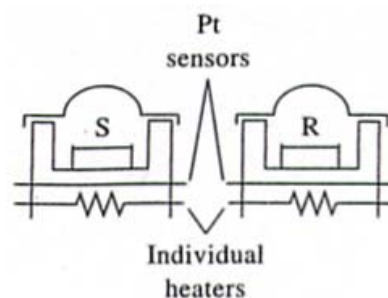


Fig. 1-20: Schematic of DSC sample holder and furnaces [131]

The instrument has two independent furnaces, one for heating the sample and the other for heating the reference. Fig. 1-21 shows a schematic of a commercial heat flux DSC cell. Here, heat flows into both the sample and the reference material via an electrically heated constantan thermoelectric disk [131].

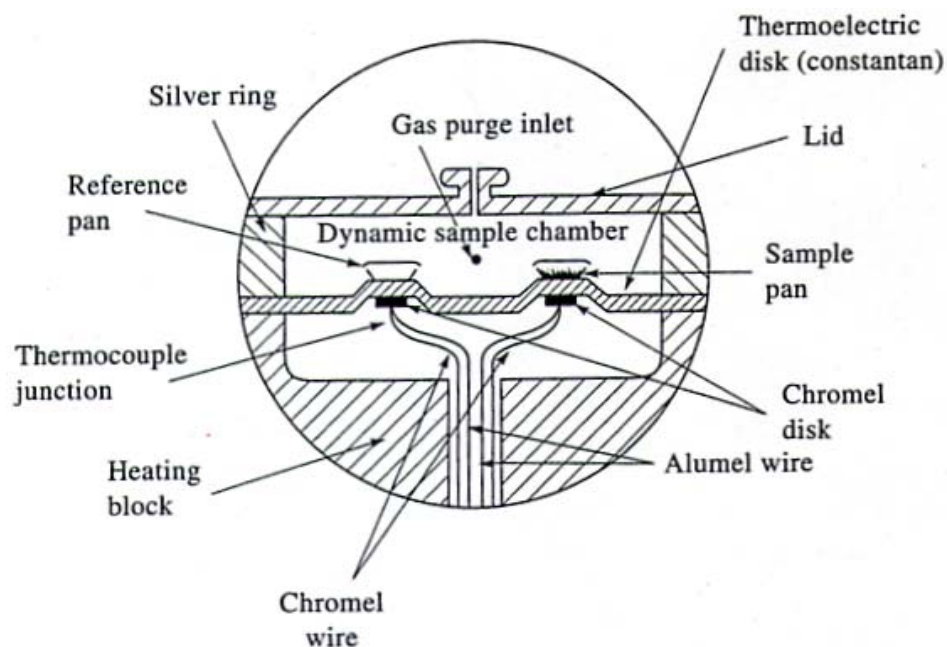


Fig. 1-21: Schematic of a heat flux DSC cell [131]

T_g' is the temperature at which a sharp increase in baseline occurs during a DSC scan of a frozen sample, suggesting a sharp increase in heat capacity (during heating, when plotting exothermic events upwards). Consequently, it is reported as the glass transition temperature of the maximally freeze-concentrated solute [10]. Additionally, a sharp decrease in electrical resistance of the frozen system can be determined (same conditions as before) [104].

DSC has played a key role in the measurement of T_g' of frozen aqueous solutions. Despite the focus of research in this area, there is little agreement in the literature regarding the T_g' and the corresponding solute concentration, C_g' , although differences are very important since the vapor pressure of ice increases exponentially with temperature (see above). Additionally, multiple T_g' values complicate the situation, e.g., for sucrose. T_g' values for sucrose are reported to be -46°C and -32°C . Controversy remains as to the physical significance of those measured thermal events, not only for sucrose, but for other simple saccharides as well [132].

In principle, T_g' and the related concentration, C_g' , are independent of the initial concentration of the solute in the initial, unfrozen aqueous solution. In one approach, the C_g' is determined from the amount of crystalline ice, which is calculated by integration of the ice-melting endotherm and the known latent heat of fusion of ice at 0°C . Ablett et al. found that the value of C_g' varied considerably with the initial solute concentration [133]. The described technique systematically underestimates C_g' because of the temperature dependence on the heat fusion of ice and, more important, because of the “background” signal contributed by the heat of dilution and the temperature-dependent heat capacities of the phases.

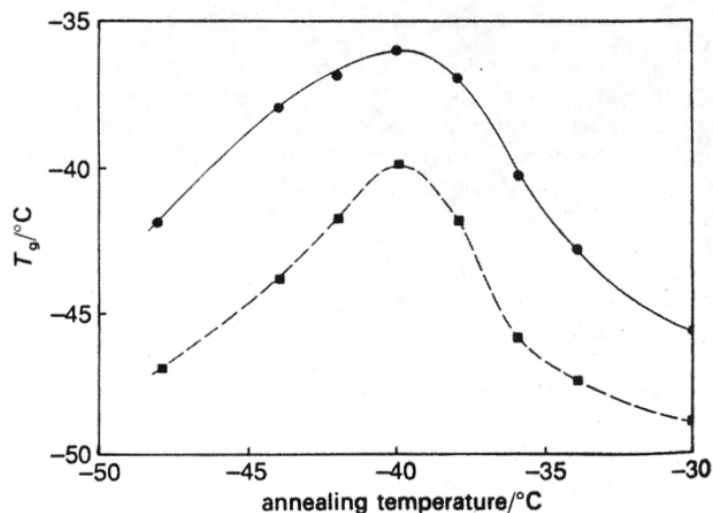


Fig. 1-22: Glass transition temperature measured using DSC, circles: T_g determined from peak position in derivative thermogram, squares: T_g determined from the onset of the transition [134]

With an annealing procedure of 16 hours at several temperatures in the vicinity of the estimated T_g' (see Fig. 1-22) a maximum in the measured T_g as a function of annealing temperature is found [134]. This temperature of the maximum is then defined T_g' . Annealing below T_g' leads to a submaximal amount of ice crystallization and a lower

concentration of the freeze-concentrated solute and a lower T_g . Annealing above T_g' results in dilution due to the onset of ice melting [132]. It is worth to mention that during annealing, the relaxation time increases (and molecular mobility decreases) in a glassy system [135]. To assess molecular mobility below T_g , enthalpy recovery experiments in

the DSC were performed [135-138]. The process of enthalpic relaxation is illustrated in Fig. 1-23 as well as the molecular level reorientation for a crystallizable material (line for crystal).

T_g' is usually reported as a single value although the transition

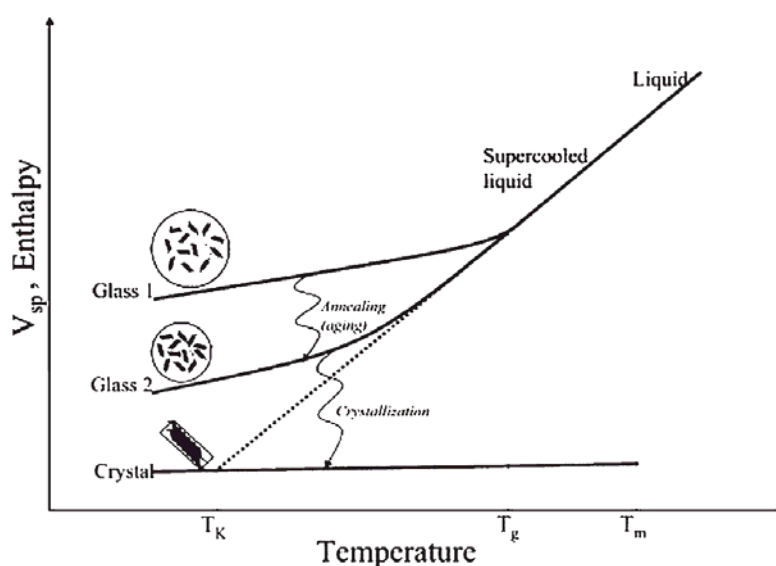


Fig. 1-23: Schematic representation of change in enthalpy and specific volume of a glass on annealing, and of behavior of crystallizing materials [139, 140]

always occurs in a temperature range. Commonly, the midpoint of the glass transition is reported as T_g' . It is often preferred since it tends to be a more reproducible value than the extrapolated onset temperature as long as the width of the glass transition is well defined. In general there are several possibilities of reporting T_g' as a midpoint: (1) half height of the step based on onset and endpoint ($\frac{1}{2} \Delta c_p$ = change in heat capacity), (2) half width of the step based on onset and endpoint, and (3) half extrapolated tangent (intersection point of the extrapolated straight line with the gradient which is defined by the initial point and end point of the tangent). If reported as inflection point, T_g' is equalized to the point of the curve with the maximum slope.

It is worth to mention that at the midpoint of T_g' , the frozen solution has already started to relax in physical terms [132]. Annealing studies performed at the temperature between the onset and midpoint of T_g' revealed that the ice dissolution started to occur at the onset of T_g' .

Apart from DSC, T_g' can be detected by using e.g., Electrical thermal analysis (ETA) [141] or dynamic mechanical analysis (DMA) [142].

A new approach to study samples with amorphous content is to use high ramp rate differential scanning calorimetry (HRR-DSC, where very high heating rates (from 50°C/min up to 500°C/min) are employed. The increased sensitivity from HRR-DSC is due to the fact that, as the heating rate is increased, the same heat flow occurs over a shorter time period, increasing the observable signal from the thermal event. This allows low-energy transitions (i.e., those with small Δc_p at T_g) to be detected and measured [143].

In solutions without ice formation, an exact calculation of T_g would be possible: In concentrated aqueous solutions water lowers (as a plasticizer) the glass transition temperature of any amorphous component with which it is intimately mixed at the molecular level [117]. This ability of water to act as a plasticizer for virtually any solute is due to its chemical affinity for many materials, low molecular weight, and extremely low glass transition temperature [144, 145]. Based on free volume theory a model originally developed by

Turnbull and Cohen [146, 147] was adapted by Gordon and Taylor [145]. It predicts the lowering of the glass transition temperature due to the plasticizing effects of water [79, 117]. According to the model of Gordon and Taylor, the glass transition temperature of a mixture is described by the equation:

$$T_{g \text{ mix}} = \frac{w_1 T_{g1} + K * w_2 T_{g2}}{w_1 + K * w_2} \quad \text{Eq. 1-11}$$

where w_1 and w_2 are the weight fractions (e.g., of the solute and water), and T_{g1} and T_{g2} are the T_g values (e.g., for water and for the solute with which it is mixed) and where

$$K = \frac{\Delta\alpha_1 \rho_1}{\Delta\alpha_2 \rho_2} \quad \text{Eq. 1-12}$$

The constant K is a physical parameter that is related to the ratio of the thermal expansivity coefficients, $\Delta\alpha$, at their respective glass transition temperatures, where ρ is the true density of the material [148].

The combination of Eq. 1-11 and Eq. 1-12 was used to describe the glass transition behavior of many compatible polymer blends and is identical to the one derived for polymer-plasticizer blends by Kelley and Bueche [149], based on viscosity and free volume effects [148]. Therefore it is often denoted as Gordon-Taylor/Kelley-Bueche equations.

The parameter K is often approximated using the densities of the two components, ρ , and the T_g values (e.g., for water and the solute) by employing the equation below [150]:

$$K = \frac{\Delta\alpha_1 \rho_1}{\Delta\alpha_2 \rho_2} \approx \frac{\rho_1 T_{g1}}{\rho_2 T_{g2}} \quad \text{Eq. 1-13}$$

This approximation of the constant K allows a prediction of the effect of water on the T_g to be predicted at any composition from values that are easy to obtain by experiment, assuming that the transition from a glass to a viscous liquid requires a certain degree of molecular mobility and hence free volume.

If the densities of the two components are equal, then the Gordon-Taylor/Kelley-Bueche equations simplify to the Fox equation [151]:

$$\frac{1}{T_{g \text{ mix}}} = w_1 T_{g1} + w_2 T_{g2} \quad \text{Eq. 1-14}$$

For most low molecular weight glass formers (e.g., drugs, sugars), the difference in densities will be significant and thus the Fox equation will not be satisfactory [148].

By systematically varying terms in the simplified Gordon-Taylor/Kelley-Bueche expression, it is possible to probe theoretically the effects of different substrate properties on the T_g of solid-water mixtures.

For two amorphous solids with the same T_g , the one with the higher density will be plasticized the most by any given amount of water, whereas for two materials with the same density, the one with the higher dry T_g should experience the greatest plasticization [148].

Tab. 1-4: Glass transition temperatures (T_g), densities and K values for selected amorphous materials [148]

Material	Dry T_g (°C)	True density (kg m ⁻³ ·10 ⁻³)	K value
Poly(vinylpyrrolidone)	177	1.25	0.2400
Hydroxypropylmethylcellulose	155	1.19	0.2660
Lactose	110	1.43	0.2452
Sucrose	74	1.43	0.2721
Indomethacin	57	1.32	0.3099
Water	-138	1.00	-

Her and Nail [152] performed detailed investigations on the thermal analysis (DSC) of aqueous solutions in which the solute does not crystallize immediately upon freezing. They aimed to define the effects of experimental parameters on thermograms in the glass transition region. The intensity of enthalpy relaxations in the glass transition region was related to the rate of cooling and the rate of heating: slow cooling or slow heating

increased the extent of structural relaxation in the glassy state and increased the intensity of the endotherm [152].

The investigation of Surana et al. published in 2004 shows some of the analytical possibilities of DSC in terms of freeze-drying, revealing interesting results on the effect of dif-

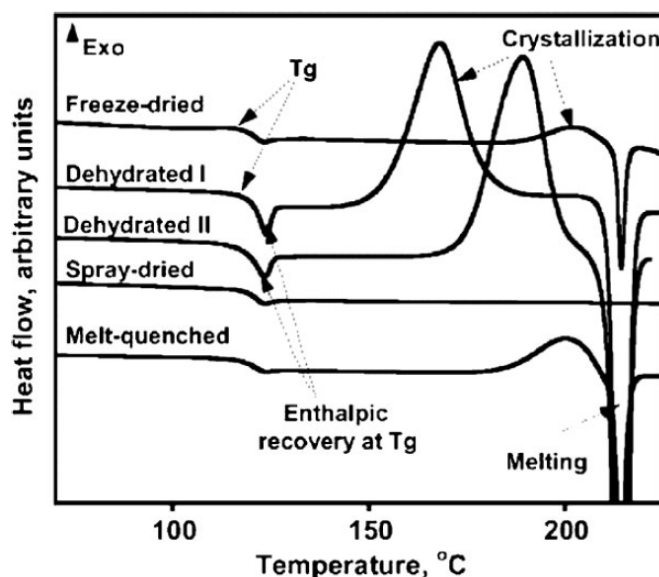


Fig. 1-24: DSC thermograms for amorphous trehalose prepared using different methods [153]

ferent processing conditions on the physical stability of amorphous trehalose [153]. Amorphous trehalose was prepared by freeze-drying, spray drying, dehydration, and melt quenching. Although glass transition temperature and fragility were not impacted by the processing conditions, properties like enthalpy relaxation, crystallization tendencies, and water sorption were

greatly altered.

Fig. 1-24 shows the DSC thermograms for the different sample types.

1.6 Critical formulation temperature in primary drying: collapse temperature vs. glass transition temperature

DSC has been used over several decades in the manner described above to measure thermal transitions like glass transitions (T_g), eutectic melting points (T_{eu}) or T_g' values [103]. In contrast, the visual observation of collapse behavior by FDM has been widely used only in more recent years [103, 104, 124, 154]. It is clear from the explanations given above that both technologies do not use the same experimental conditions to de-

scribe the maximally allowable product temperature for primary drying (“critical formulation temperature”).

The glass transition of the maximally freeze-concentrated solution, T_g' , appears as an endothermic shift in heat capacity which arises from a decrease of the viscosity of the amorphous matrix in a narrow temperature range.

This allows the system to access additional degrees of freedom. As already mentioned, new interpretations of this T_g' event were discussed recently as a combination of ice melting and T_g [155, 156] or ice melting alone [157]. By FDM, a decrease in viscosity of the glassy matrix is measured in the dynamic process of sublimation drying. The sample is frozen at atmospheric pressure and freeze-dried at a lower (controlled) pressure [104]. This ensures a more representative methodology of measuring the critical formulation temperature of a freeze-drying process. In contrast, during a T_g' measurement by DSC the matrix is in permanent direct contact with ice at atmospheric pressure without any drying procedure.

Probably due to the long-term usage of DSC equipment, freeze-drying literature still provides many T_g' values and only very few authors report both, T_c and T_g' values for excipients or even a final formulation [45, 158]. However, differences of 2-5°C between T_g' and T_c values were reported in the literature for a medium resistance product [104], which underlines the need to provide systematic data on T_c (and corresponding T_g').

1.7 Objectives of this thesis

The purpose of this thesis is (1) to provide theoretical background on methods (freeze-drying, freeze-dry microscopy, differential scanning calorimetry etc.), and (2) to perform, for the first time, a comprehensive investigation on appropriate freeze-dry microscopy measurement methodology for evaluation of collapse temperatures. Based on already published studies, it describes an improved classification procedure for observed col-

lapse behavior and delineates different collapse appearances found for various excipients and protein/disaccharide systems. In addition, it shows a detailed study of collapse temperature dependence on experimental conditions leading to a basic model which combines the understanding of collapse out of practical observations and theoretical background information.

Based on representative sets of data, this thesis also presents the dependence of collapse temperature on the total solid content for six excipients often used for freeze-drying. Background information and supportive data to explain these results are given. To deepen the discussion on critical formulation temperature measurement for the optimization of freeze-drying cycles, T_c (FDM) and T_g' (DSC) values are directly compared to calculations from the Gordon-Taylor equation [159]. A setup of freeze-drying runs in lab-scale give data on transferability of FDM results on freeze-drying processes and show a need for further detailed investigations in the future.

In the next chapters, the following questions (which are grouped in main questions and sub questions) will be answered:

- 1) What is a reasonable FDM methodology for day-by-day routine work?
- 2) What would be a most sophisticated “high-end” FDM methodology? Does it make sense to use this high-end methodology from practical or scientific point of view?
- 3) What are the important factors and parameters influencing collapse?
- 4) What is the typical temperature range of collapse temperatures for excipients often used in freeze-drying?
 - a) Is there really a dependence on total solid content?
 - b) If yes: How could it be explained?
 - c) Why can we see significant differences between the selected excipients?
 - d) Is there a general relationship derivable for the dependence of T_c on total solid content?
 - e) Is there a way of predicting collapse behavior of excipients and formulations?

- 5) What is the typical difference between T_c and T_g' ?
 - a) How can T_c and T_g' be compared in an easy way?
 - b) How should results be compared when a more detailed or sophisticated way is needed?
- 6) How can the drying and collapse behavior of a protein (model used: BSA) be characterized?
 - a) Is T_c detectable for proteins?
 - b) What is the collapse appearance of proteins (e.g., BSA or HSA)?
 - c) Are there differences between BSA and HSA reflected in FDM measurements?
- 7) How can the drying and collapse behavior of BSA or HSA in mixtures (with disaccharides like sucrose and trehalose) be characterized?
 - a) What T_c do the different mixtures have?
 - b) Does pressure applied during the measurement have an influence on T_c for these mixtures?
 - c) Are there measurable differences between BSA and HSA in the mixtures?
 - d) Does the difference in T_c between sucrose and trehalose impact the T_c of the mixtures?
 - e) How can the observed collapse behavior be explained?
 - f) Is there a way to predict the T_c for different ratios of BSA/disaccharide or HSA/disaccharide?
 - g) Are there differences between T_c and T_g' for the different mixtures?
 - h) Is it possible to predict T_g' of the mixtures by using the Gordon-Taylor equation?
- 8) How can T_c and T_g' be compared in a rational way?
 - a) Is it better to compare T_{c-50} to T_g' ?
 - b) Is it better to compare T_{oc} to T_g' (onset) / T_{fc} to T_g' (endset)?

- 9) Are T_c results directly transferable on FD runs for simple sucrose solutions?
- a) Are the differences deriving from the impact of total solid content transferable?
 - b) How do different product temperature over time profiles (T_p over t) influence the product characteristics, in particular the specific surface area (SSA)?
 - c) What are the temperature differences between
 - i) the shelf temperature, T_s , and the product temperature calculated from MTM measurements, T_{p-MTM} ?
 - ii) the product temperature calculated from MTM measurements and the temperature at the bottom of the vial calculated from MTM measurements, T_{b-MTM} ?
 - iii) the product temperature calculated from MTM measurements and the product temperature measured by thermocouples, T_{b-TC} ?

A detailed overview on materials and methods used to answer these questions is given in chapter 2. The results and discussion of the single points given are discussed in the same order in the chapters following the materials and methods section.

2 Materials and methods

2.1 Materials

2.1.1 Used proteins and their quality

Albumin from bovine serum (BSA) and albumin from human serum (HSA) were used as model proteins for FDM studies as well as density and viscosity measurements. Tab. 2-1 lists the qualities.

Tab. 2-1: Proteins used for this study

Protein	Used for	Supplier	Order No.	Lot No.
Albumin bovine serum	FDM	Sigma	A0281	075K7545
Albumin from bovine serum	Density and viscosity measurements	Sigma	A2153	103K1373
Albumin human	FDM	Sigma	A3782	085K7541
Albumin from human serum	Density and viscosity measurements	Sigma	A9511	044K7601

2.1.2 Used excipients and their quality

All excipients and reagents used for this study are listed in Tab. 2-2. Aqueous solutions were prepared with double distilled water from an all-glass apparatus (Destamat Bi 18 T, Heraeus) and filtered through a 0.22 μ L membrane (Millipore[®], Billerica, MA, USA) prior to use. For surface tension measurements, water for analysis (1.16754.5000, Lot: HC694073, Merck KGaA, Darmstadt, Germany) was used.

Tab. 2-2: Excipients used for this study

Excipient	Used for	Supplier	Order No.	Lot No.
(2-Hydroxypropyl)- β -cyclodextrin	FDM, density and viscosity measurements	Fluka	56332	454270/1 13404039
D-(+)-Glucose	FDM, density and viscosity measurements	Sigma	G8270	124K0018
D-Mannitol	FDM	Sigma	M9546	100K0129
PVP 10 kDa	FDM, density and viscosity measurements	Fluka	81390	1100082 44804041
PVP 40 kDa	FDM, density and viscosity measurements	Fluka	81420	1126884 33504234
Sucrose	FDM, density and viscosity measurements	Sigma	S7903	40K0201
Sucrose	Surface tension measurements	Sigma	S7903	016K01192
D-(+)-Trehalose dihydrate	FDM, density and viscosity measurements	Sigma	T5251	91K37901 096K3788
D-(+)-Trehalose dihydrate	Surface tension measurements	Sigma	T9531	115K7361
Potassium chloride	FDM calibration	Fluka	60129	1132011 31705270
Magnesium chloride	FDM calibration	Sigma	M8266	064K0195
Sodium chloride	FDM calibration	Sigma	S7653	074K0091

2.1.3 Molecular weights of selected proteins and excipients

For certain FDM studies the ratio of protein/disaccharide total solid content was varied to obtain a different sucrose or trehalose to protein mole ratio. For the calculations of these ratios the molecular weights presented in Tab. 2-3 which were obtained from the certificates of analysis (Sigma Chemical Company, St. Louis, MO, USA) were used.

Tab. 2-3: Molecular weights of selected molecules

Substance	Molecular weight M_r
BSA	66,430
HSA	66,437
Sucrose	342.3
Trehalose	342.3

2.1.4 Quality of liquid nitrogen

For the FDM cooling system, liquid nitrogen (quality 5.0) was obtained from Linde AG (Pullach, Germany).

2.2 Methods

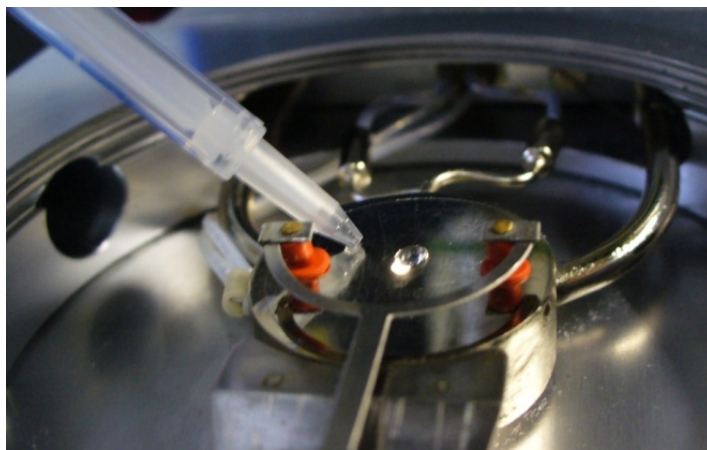
2.2.1 Freeze-dry microscopy (FDM)

The freeze-dry microscopy equipment used for the presented studies consisted of a microscope (Axiomager.A1 or Axiomager.Zm1, both Zeiss, Göttingen, Germany) with a lambda plate (polarizer D, 90° pivotable, disengageable) plus spectrum analyzer and a freeze-drying stage (FDCS 196, Linkam Scientific Instruments, Surrey, UK) with a liquid nitrogen cooling system. Pic. 2-1 gives an overview of the used equipment. The temperature controller (Linkam Scientific Instruments, Surrey, UK) was programmable via a PC system. A conventional vacuum pump (Ilmvac, Ilmenau, Germany) was used for evacuating the system. If not stated otherwise, magnification was 200-fold using the objective Zeiss LD Epiplan 20x. Self-made, precision cut spacers (brass platelets, height 0.025 mm) were used to assure a constant thickness of the sample layer. In the temperature range of interest pictures were recorded in a one second time interval using a digital firewire camera from Pixelink (resolution 1.3 mega pixels, Linkam Scientific Instruments, Surrey, UK) and were (after the measurement) analyzed using the LinkSys 32 software (Linkam Scientific Instruments, Surrey, UK). To support heat transfer from the oven to the sample, silicon oil provided together with the stage was used (Linkam Scientific Instruments, Surrey, UK).



Pic. 2-1: Freeze-dry microscopy equipment (Axiolmager.A1)

Regularly, a validation of the PT 100 (accuracy: ± 0.1 K) inserted in the stage beneath the surface of the silver block was performed by detecting the eutectic melting temperatures of 10% (w/w) solutions of KCl (-10.7°C), NaCl (-21.1°C) and MgCl_2 (-33.6°C)[160].



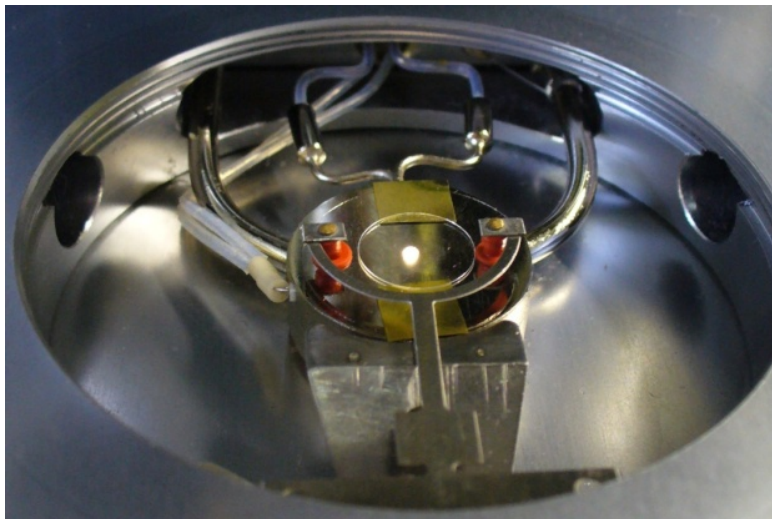
Pic. 2-2: Placement of sample drop

The freezing rate for this calibration procedure was $10^{\circ}\text{C}/\text{min}$ and the heating rate $1^{\circ}\text{C}/\text{min}$ in the temperature range of interest. Measurements were performed in triplicate. Deviations were within $\pm 0.1^{\circ}\text{C}$ and were not taken into account in discussion of results, or any calculations,

respectively. It was assumed that, due to the small deviations, the product temperature

in the sample was equal to the temperature measured by the PT 100 when using a heating rate of 1°C/min.

Sample preparation was as follows (cf. Pic. 2-2 and Pic. 2-3, respectively): A 5 µL drop of silicon oil was spread on the silver block oven near the observation hole by placing a 20 mm round glass cover slide (Linkam Scientific Instruments, Surrey, UK) onto it. The sample holder with two vacuum cups (Linkam Scientific Instruments, Surrey, UK) was inserted in the stage and fixed on the glass slide.



Pic. 2-3: Sample preparation in detail

Then, two of the spacer pieces were placed on opposite sides of the slide. A drop of 2 µL of the sample solution was pipetted in the middle of the slide near the hole by using an Eppendorf syringe (Combitip plus 0.5 mL, 0030 069.226, Eppendorf AG, Hamburg, Germany)-(cf. Pic. 2-2). Then a 10 mm round glass cover slide (Linkam Scientific Instruments, Surrey, UK) was placed on the two spacers spreading the solution (see Pic. 2-3). Only samples without contact between the solution and the edge of the small cover glass slide and with no contact between the solution and the spacers were measured.

If not stated otherwise, the freezing rate was 10°C/min. Standard lowest freezing temperature was -40°C. At 5°C a holding step for 1 min was implemented in the measurement routine to purge the system with dry nitrogen from the Dewar through the open valve. Before starting sublimation the sample was held at the lowest freezing temperature for equilibration for 8 to 10 min. After 5 to 8 min the vacuum pump was switched on so that sublimation could be observed a few seconds later. The sample was reheated at

a rate of 1.0°C/min (with isothermal intervals if necessary) through the point of collapse (if not stated otherwise).

Pressure was measured using a calibrated Pirani gauge (Linkam Scientific Instruments, Surrey, UK) and was controlled below 100 mTorr (unless otherwise stated, e.g., for the pressure setting experiments).

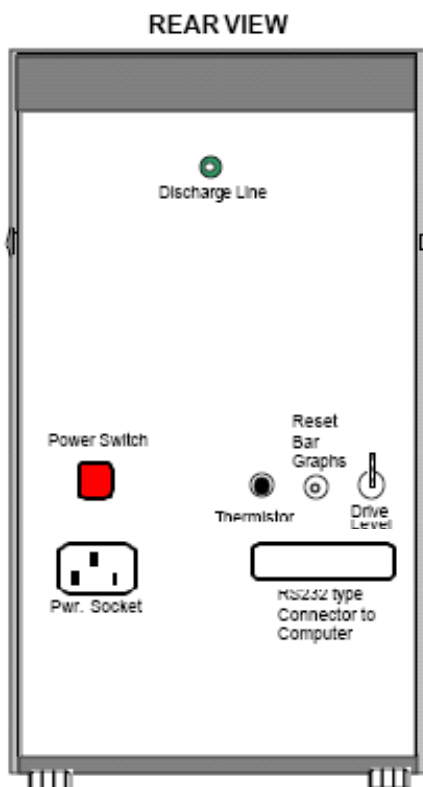
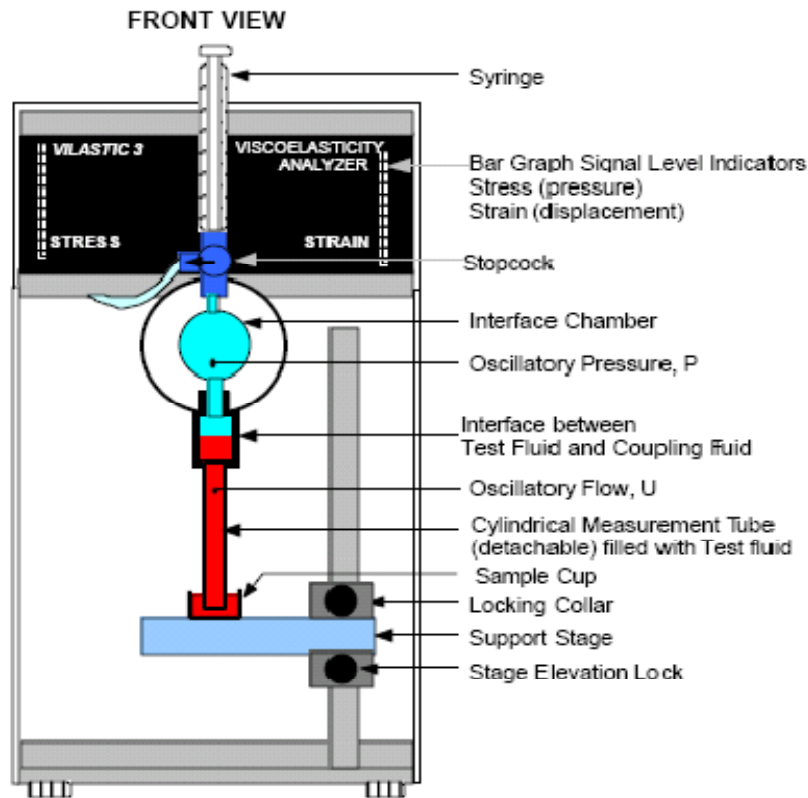
The velocity of sublimation (V_{sub}) was detected in a similar way as described previously [104]. For the detection of the velocity of the sublimation front (which reflects the drying rate and the resistance to water vapor flow) saved pictures were compared by a using custom-made supporting software.

A picture of a temperature of one degree Celsius below the desired temperature was compared to a picture at the desired temperature. The distance of the moving sublimation front between two equivalent points was measured by using the calibrated 200x objective and divided through the time difference. The objective was calibrated by a commercially available calibration slide (Zeiss, Göttingen, Germany), and the information saved in the software settings of the LinkSys 32 software.

2.2.2 Dynamic viscosimetry

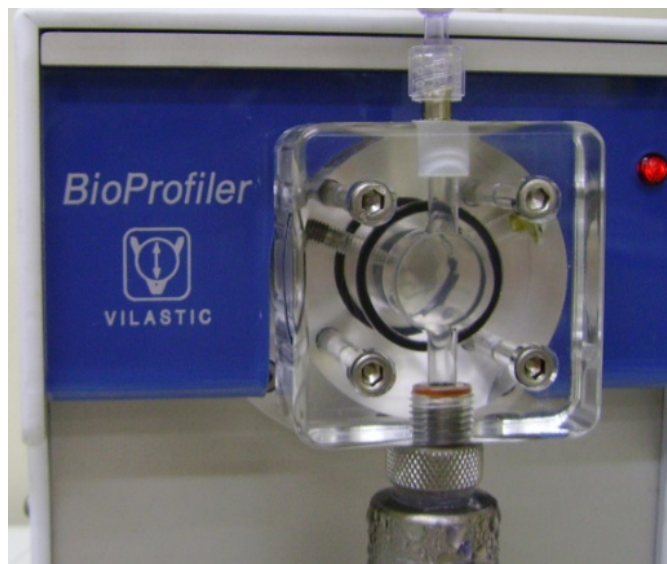
Density measurements were carried out at approximately 0°C by using a pycnometer (5 mL) and an ice-water bath. Density data were used for measurement of viscosity and of surface tension.

The measurement of viscosity was carried out using a VILASTIC Viscoelasticity Analyzer (Vilastic Scientific Inc., Austin, TX, USA), which is a capillary viscometer with oscillatory flow principle (see Pic. 2-4), connected to a chiller unit (HAAKE K + F4, kryo liquid Kryo 40, Lauda, Königshofen, Germany) with a temperature between 0.00°C and 1.00°C.



Pic. 2-4: Set-up of the VILASTIC Viscoelasticity Analyzer and of the connected chiller unit

To detect the shear rate dependence of viscosity the VMax software STRETCH protocol was used. As measurement frequency 10 Hz was chosen for standard solutions, and 5 Hz for PVP 10 kDa solutions with a high solid content. The drive level sweep was 10 to 30, the measurement sequence 10 with increasing drive level. The integration period was defined two seconds, pre-drive time 0 seconds. Density was entered as measured previously. Before every measurement the analyzer system was verified and reference values were used for the calculation of the results. The measurement system including the inter-



Pic. 2-5: Interface chamber

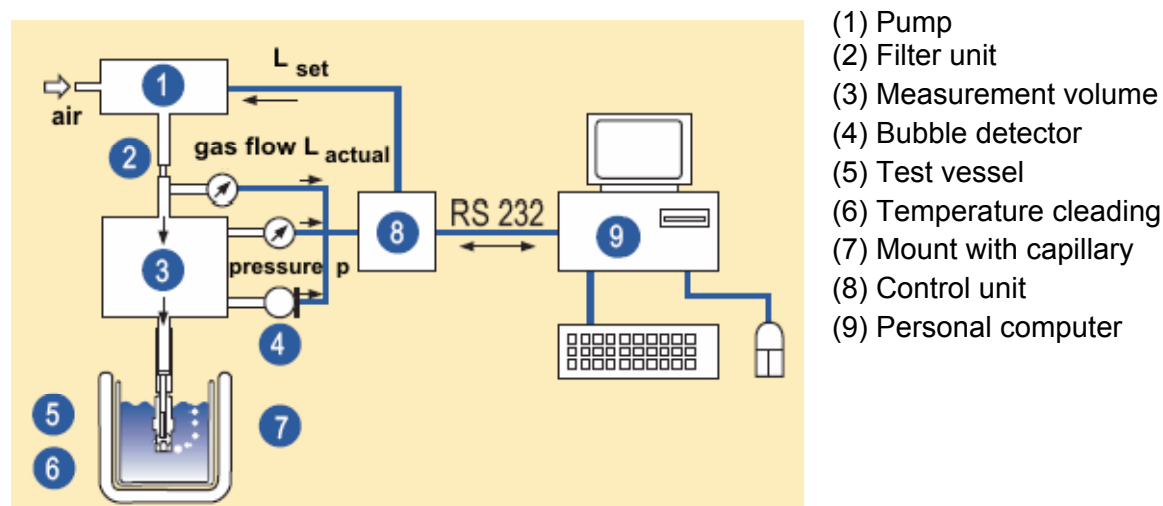
face chamber (see Pic. 2-5) was cleaned several times with double distilled water between experiments. Solutions were measured in duplicate performing each viscosity detection ten times for one measurement of a single solution and calculating the average value.

Based on viscosity data surface tension was measured by bubble pressure tensiometry.

2.2.3 Bubble pressure tensiometry

Time dependent dynamic interfacial tension was evaluated by a bubble pressure tensiometer (MPT 2, Lauda, Königshofen, Germany) connected to a chiller unit (HAAKE K + F4, kryo liquid Kryo 40, Lauda, Königshofen, Germany) with a temperature between 0.00°C and 1.00°C. The tensiometer had a dynamic time range of 0.0001 to 100 seconds. Its set-up is shown in Pic. 2-6. 10.0 mL aqueous solution of the desired concentration was investigated using capillary 41 with an immersion depth of 2.5 mm. The

flow rate was decreased stepwise from 100 mm³/s to 5 mm³/s (5% in each step). The adjustment time for each measurement point was 20 seconds. After about five measurements the resulting pressure values were relatively constant and the average value of at least ten of these measurements was used for calculation of the surface tension of the examined solution.



Pic. 2-6: Set-up of Lauda MPT 2 maximum bubble pressure tensiometer [161]

Surface tension measurements with the bubble point method were restricted to solutions with sucrose and trehalose.

2.2.4 Differential scanning calorimetry

The glass transition of the maximally freeze-concentrated solute (T_g') was determined using a Mettler Toledo DSC822^e (Mettler Scientific Instruments, Göttingen, Germany). 20-35 μ L of the sample were sealed in a 40 μ L Al pan at room temperature. To determine the value of T_g' the solution was cooled down to -60°C (10°C/min), equilibrated (10 min) and then heated at 10°C/min through the point of T_g' . The values for all transitions were analyzed as midpoints and points of inflection (Mettler STARe SW 9.01, Mettler Scientific Instruments, Göttingen, Germany). Dry nitrogen was used for cooling (100 mL/min) and purging the measuring cell (30 mL/min).

2.2.5 Freeze-drying

Freeze-drying was performed in a Lyostar II freeze-dryer (FTS, Stone Ridge, USA) with SMART™ software installed. The unit consists of three shelves, with a total shelf area of 0.5 m². Since the front door of the freeze-dryer is made of Plexiglas, aluminum foil was used as a radiation shield.

Solutions were prepared in flasks using a reference balance (LA 620S, Sartorius AG, Göttingen, Germany). The fill weight of every tenth vial was determined. The average fill weight as well as the calculated density was then inserted in the software.

Runs were performed using the SMART™ feature of the software with the parameters presented in Tab. 2-4, which included the performance of MTM measurements.

Tab. 2-4: SMART™ software parameters for freeze-drying cycles

SmartCycle Data	Parameter	Unit
Number of Vials	112	
Inner Area of Vials	5.64	cm ²
Fill Volume	3.00	cm ³
Primary Drying Option	Standard	
Secondary Drying Option	Fixed Time	
MTM Interval	60	min
Nature of Drug Product	Small Molecule	
Type of Vials	Tubing	
Type of Drug Product	Amorphous	
Type of Bulking Agent	Amorphous	
Endpoint Pressure	5	mTorr
Chamber Volume	104	L

The setpoint for $T_{eu} / T_c / T_g'$ was varied as stated in the text. Pressure settings were adjusted by the SMART™ software which resulted in 74 mTorr for all runs. Secondary drying was started by ramping with 0.3°C/min to 40°C and holding this temperature for 4 hours. After finishing secondary drying, ramping with 5°C/min to a final temperature of 15°C was performed.

One thermocouple (40 gauge, type T, Omega Engineering, Inc., Stamford, CT, USA) was placed on the shelf and three thermocouples were inserted into center vials at the back, in the middle and in the front of the shelf. The accuracy of the thermocouples was $\pm 0.5^{\circ}\text{C}$. Before freeze-drying the ports for the thermocouples were calibrated by using thermocouple calibrator CL300A (Omega Engineering, Inc., Stamford, CT, USA).

2.2.6 Scanning electron microscopy (SEM)

Lyophilized cakes were broken and fixed on Al stubs (Model G301, Plano) and then sputtered with gold at 20 mA / 5 kV (Hummer JR Technics) for 1.5 min. Cake morphology was examined using an Amray 1810 T Scanning Electron Microscope at 20 kV.

2.2.7 BET measurement of specific surface area (SSA)

Additionally, SSA (specific surface area) of lyophilized cakes was measured using an ASAP 2420 (Micromeritics, Mönchengladbach, Germany). The samples were held at 40°C for 14 hours under vacuum in an integrated heating unit, flashed with nitrogen and transferred to the analytical unit of the ASAP 2420. Krypton served as analysis adsorptive. The experiments were performed under automatic degas mode with an equilibration interval of 10 sec. A 10-point analysis at different pressure was carried out.

3 Results and discussion

3.1 Methodology of FDM

3.1.1 Detection and definition of collapse

Throughout this study the collapse behavior was determined by comparing individual pictures recorded in a time interval of one second. Three phases of collapse and the corresponding temperatures were defined:

- (1) the temperature of the onset of collapse (T_{oc}),
- (2) the temperature of full collapse (T_{fc}), and
- (3) the temperature of a 50% collapse (T_{c-50}).

Pictures of the onset of collapse were carefully compared to full collapse pictures to precisely define the onset of the observed collapse in a given experiment. This procedure assured that no holes in the dried non-collapsed structure were accidentally thought to be holes formed by collapse.



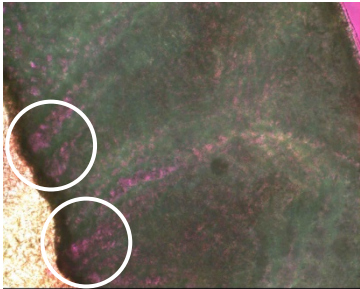
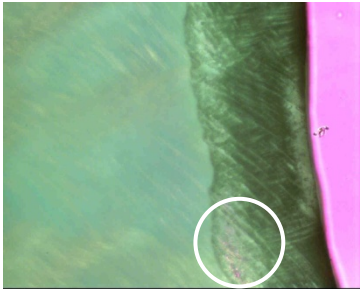
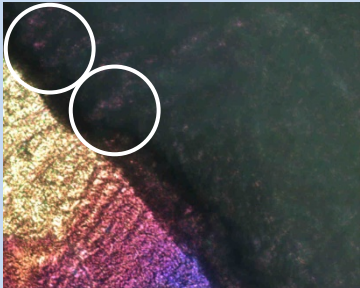
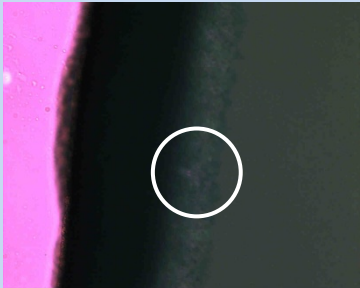
The onset of collapse was denoted when first structural alterations appeared in the dried structure adjacent to the sublimation interface. Dependent on the type of excipient, composition of the mixture, and/or its concentration, the structural changes were observed as holes, gaps or fissures. Using the pivotable lambda plate the light (without sample) was always adjusted to a pink color so that the collapsing areas were of pink color.

Tab. 3-1 gives examples for T_{oc} detection for excipients used in this thesis. For low concentrated solutions (here: 2% w/w) a distinction between non-collapse holes in the dried structure and collapse holes is mandatory as can be seen from the presented pictures in the middle column.

The column on the right hand side underlines the fact that observation of structural changes is more challenging for samples with a high total solid content (here: 20% w/w).

It is a common procedure to report T_c values in the literature as T_{oc} data [111].

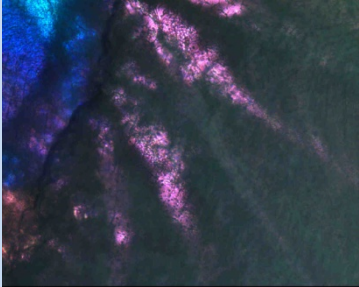
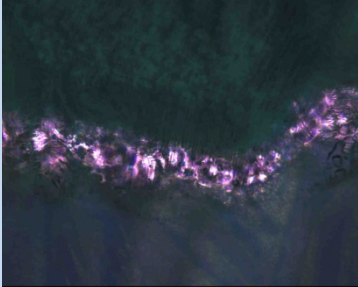
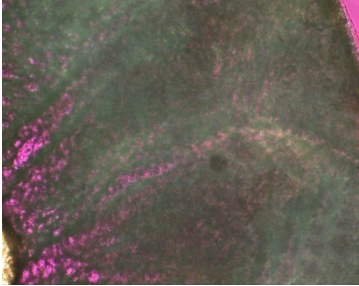


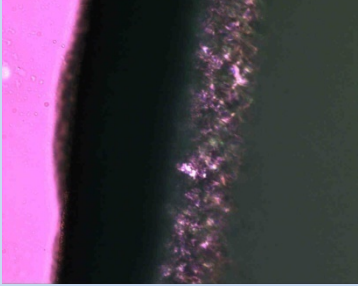
Tab. 3-1: Different types of onset of collapse for excipients frequently used for freeze-drying

Excipient	T_{oc} for 2% (w/w) total solid content	T_{oc} for 20% (w/w) total solid content
Trehalose	 -29.2°C	 -26.4°C
Sucrose	 -33.2°C	 -32.2°C
PVP 10 kDa	 -29.2°C	 -25.3°C

The temperature of full collapse was defined as the temperature where the dried structure close to the sublimation front degenerates and undergoes complete structural loss right after the sublimation process.

Here, no coherent product results from the drying, but with further heating after reaching T_{fc} there are fragments of dried material visible in the microscope. Tab. 3-2 presents some possibilities of visual appearance of full collapse in comparison to Tab. 3-1.



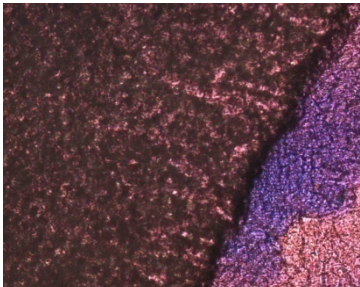
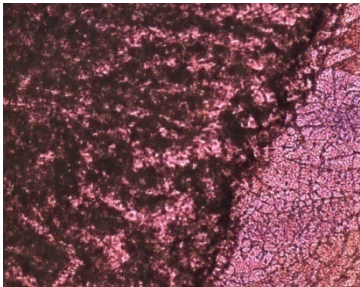
Tab. 3-2: Different types of full collapse for excipients frequently used for freeze-drying

Excipient	T_{fc} for 2% (w/w) total solid content	T_{fc} for 20% (w/w) total solid content
Trehalose	 -29.0°C	 -25.7°C
Sucrose	 -32.3°C	 -31.5°C
PVP 10 kDa	 -27.3°C	 -23.5°C

For pure aqueous protein solutions (containing BSA and HSA, see Tab. 3-3) a special collapse behavior was observed. Before reaching the point of collapse, such formulations dried with fissures in the matrix (restricted to subareas) which did not result in an overall loss of structure.

Onset of collapse was determined by color (change to dark pink) and following full collapse in the given area, whereas full collapse was delineated by a loss of structure of the chewing-gum like dried regions which resulted in thin, highly viscous and stretchy filaments connecting the sublimation interface and the product matrix dried before. Because of the observed vibrant behavior of the dried matrix close to the sublimation interface, a significant increase in elasticity served as an additional criterion for the indication of T_{fc} , especially when high protein concentrations were present. For a detailed description of changes in elasticity for proteins, the reader is referred to the literature [162].

Tab. 3-3: Collapse behavior of aqueous solutions of pure BSA 3% and 5% (w/w)

Total solid content [% w/w]	T_{oc}	T_{fc}
3	 -5.9°C	 -4.7°C
5	 -4.1°C	 -2.5°C

To facilitate a direct comparison with glass transition (T_g') data of the maximally freeze-concentrated solution, a 50% collapse temperature (T_{c-50}) was introduced for the first time in this work. According to the ASTM/IEC [163] it is the standard method [103] to report T_g' as midpoint temperatures, and not as an onset. Therefore T_{c-50} was calculated (not visually detected) as “midpoint” collapse i.e. the average value of the observed T_{oc} and T_{fc} .

From the explanations above it is clear that T_{c-50} and T_g' are based on different physical phenomena and cannot be directly compared [103], but “midpoint” T_c , T_{c-50} , might simplify discussions on “midpoint” T_g' . Yet, it is not assumed that T_{c-50} is generally reflected in 50% of structural loss. The correlation (e.g., possible linearity) between T_{oc} and T_{fc} with regard to the degree of structural loss has not been investigated.

3.1.2 Theoretical overview and model on critical factors in FDM

As a result of the author’s experimental experiences and theoretical investigations, a schematic was created which illustrates the factors impacting the FDM measurements. To give a better understanding on basic principles, the mentioned model is introduced in this section, while the theoretical background information and experiments providing evidence are explained in the following chapters.

Fig. 3-1 shows a flowchart of critical parameters and their impact on collapse during FDM measurements. As water is a strong plasticizer [79, 117], the interaction of water molecules with the product matrix plays a key role in collapse events. Due to the low pressure and transferred energy, the ice molecules sublime inside the matrix [104]. During this step they are in contact with the matrix (the amorphous freeze-concentrated solution). Collapse happens if the effective parameters in summary reach a critical point reflected in a critical decrease of rigidity of the product matrix which results in viscous flow and collapse [104]. The driving force for the viscous flow is the surface tension of the flowing plasticized product matrix [113].

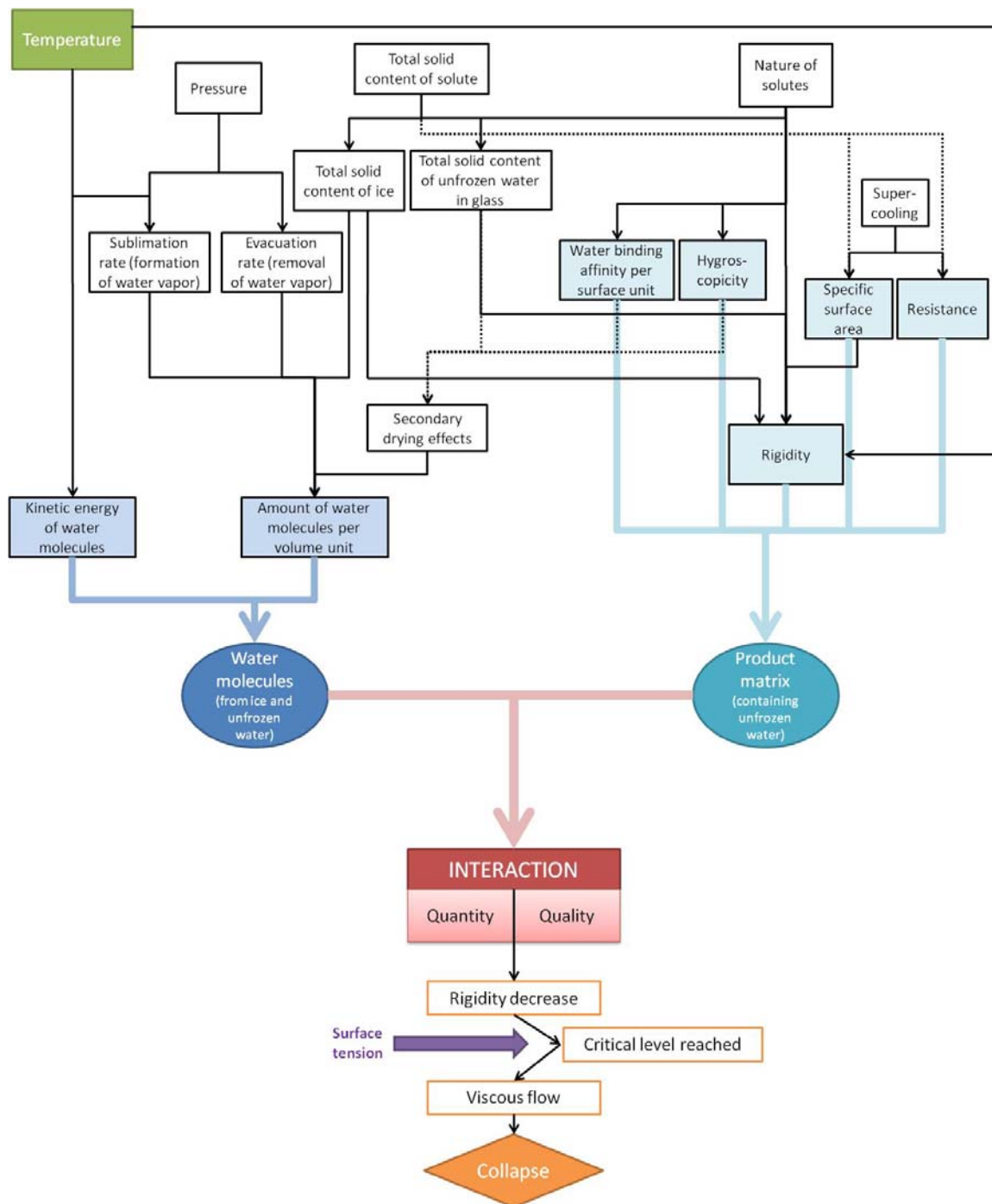


Fig. 3-1: Critical parameters and their impact on collapse during FDM measurements (emphasis is on influence of parameters with regard to collapse and NOT on dependences and/or interactions between parameters)

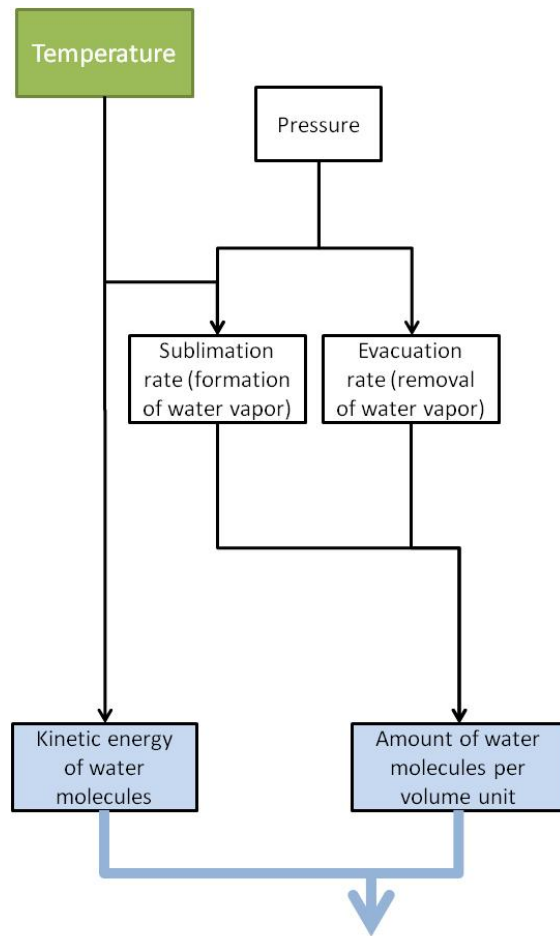


Fig. 3-2: Main effects on water molecules in the matrix during FDM experiments

effect, the kinetic energy of the water molecules is elevated with higher temperatures. More important is that as P_{ice} increases exponentially with temperature, the driving force for sublimation, and therefore the sublimation rate, increases dramatically as the product temperature increases [6].

In an FDM experiment the heat transferred to the sample should be the limiting parameter, and not the pressure [104].

The amount of water molecules is limited by the total solid content of ice on the one hand and by the sublimation⁵ and evacuation rate of the water vapor on the other hand (cf. Fig. 3-2) [104]. The sublimation rate depends on temperature and to a lesser extent on pressure, whereas the evacuation rate, which means the removal of water vapor out of the product matrix, is limited by the pressure setting alone [6].

As demonstrated the chamber pressure (P_c) impacts heat and mass transfer [26]. P_c should be well below the ice vapor pressure (P_{ice}) at the target T_p to allow a high sublimation rate. At the same time, the amount of subliming water molecules is highly dependent upon the momentary temperature in the sample [6]. In a side

⁵ Due to secondary drying effects discussed later, the water vapor in the product matrix is not only a result of sublimation, but desorption as well.

Nevertheless, the impact of pressure needs to be considered when performing FDM and was also investigated during this thesis work. A difference in pressure not only influences the amount of water molecules in the nitrogen/water atmosphere⁶ in the FDM stage, which is the driving force for sublimation, but also impacts the removal of water molecules from the product matrix [104]. If – as a theoretical consideration – e.g., the sublimation rate is constant and the evacuation rate is halved, the exposure time of the water molecules in the matrix is doubled which is equivalent to twice amount of water molecules in the matrix. It is clear that the movement of the water molecules is directed from the ice crystal surface to the outer regions of the product matrix in the direction of the vacuum pump [31].

To summarize, the probability of an interaction between a single water molecule and the product matrix is higher if more water molecules are present at the matrix surface (and the higher their kinetic energy).

The amount of subliming water molecules is higher the more ice is present between the walls of the freeze-concentrated solution focusing on a given area at the sublimation interface (cf. Fig. 3-3) [15]. In chapter 1.2.1 it was discussed in detail that dur-

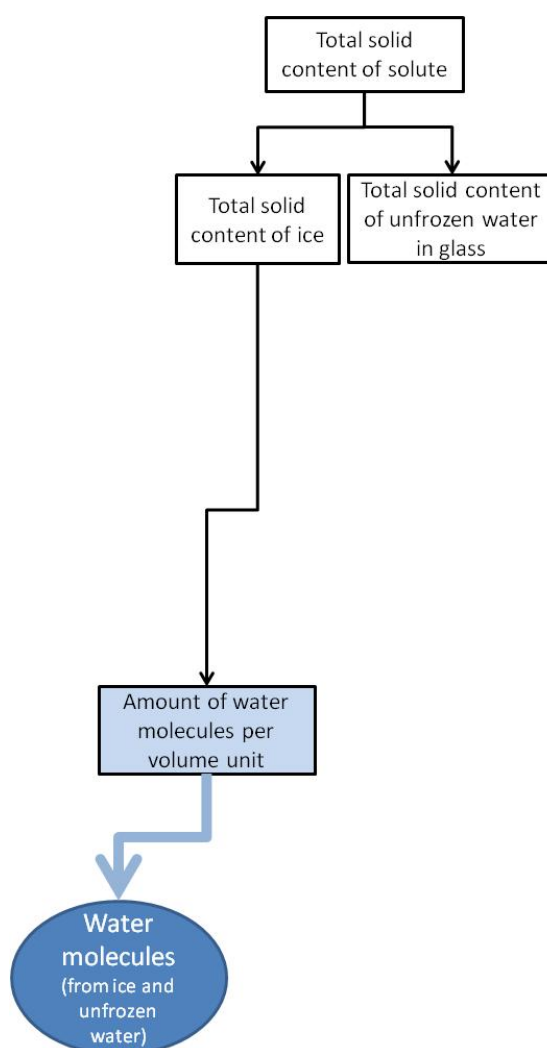


Fig. 3-3: Effects of total solid content of solutes during FDM measurements

⁶ The composition of the FDM stage atmosphere during measurements has not been investigated. It is assumed to consist mostly of nitrogen gas with some water vapor.

ing cooling freeze concentration takes place [17]. It continues until the solutes crystallize or until the system increases in viscosity sufficiently to transform into a glass. At this point any further thermodynamically favored freeze concentration is arrested by the high viscosity of the solute phase (for amorphous materials) [6]. The degree of viscosity is a function of the chemical structure of the solutes [6] and is reflected in the ratio of substance molecules to unfrozen water in the glass. In other words: The final concentration of solutes in the glass is identical for differently concentrated solutions of the same substance. In contrast, the ratio of glass (matrix including unfrozen water) to ice depends on the total solid content of the initial liquid solution [15]. Accordingly, different concentrations of dissolved substance lead to different total solid contents of ice.

The appearance of this ice fraction depends on the cooling method which results in different numbers and sizes of ice crystals [9, 17, 21]. But due to the freezing behavior discussed before, the overall amount of water molecules which are present in the form of ice (and not as unfrozen water) is in general a direct consequence of concentration [15].

This leads to the next point (cf. Fig. 3-4): When performing FDM experiments as described above (including the same cooling rate) the extent of supercooling cannot be controlled [30]. Thereby the size, shape and number of ice crystals change [9, 17]. Thus, the specific surface area of the product matrix and its resistance are (slightly) different in every experiment performed [15].

The statistical average of T_c measured from a single solution with

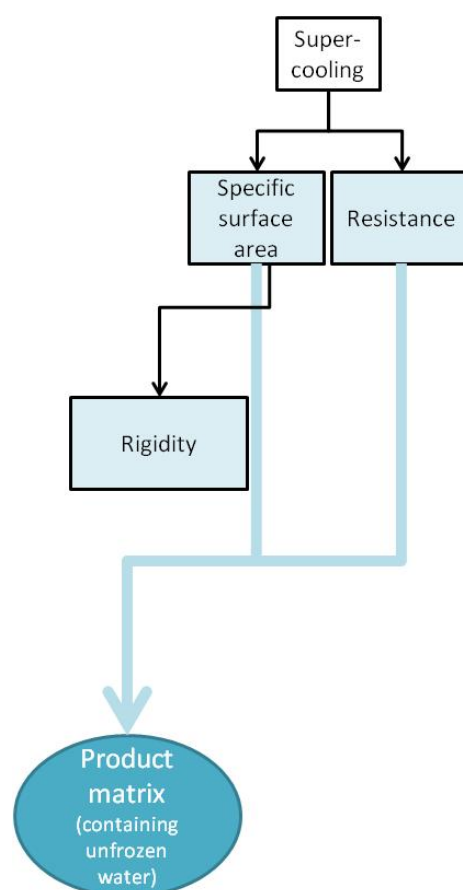


Fig. 3-4: Effects of supercooling on results of FDM experiments

regard to specific surface area and resistance is therefore a function of the total solid content (even more precise, of the total content of ice in the sample), but the SSA and resistance for a single experiment cannot be predicted due the random effect of supercooling [21]. On the one hand, a higher SSA influences the rigidity of the product matrix for a given solution and concentration, because it necessarily leads to thinner and less stable product walls. On the other hand, a higher SSA represents a greater platform for desorption during secondary drying effects (see below) [36].

But the cooling step does not only influence the surface area of the glass. It also has an impact on the resistance of the product matrix to water transport which represents a barrier to the water vapor flow directed toward the outside of the sample. If ice crystals are, for instance, large and directed to the outside of the sample (which can often be observed because many samples freeze from the edge of the cover glass towards the middle of the sample) the resistance of the amorphous glass is lower compared to a frozen structure with many small, undirected ice crystals [164].

Two more characteristics of the product matrix concerning possible interactions between matrix/water molecules as well as consequences for collapse behavior are hygroscopicity and water binding affinity, which are related. The term “hygroscopic” is commonly used to characterize the water binding potency of dry materials. In the model introduced here, hygroscopicity of the primary dried matrix is therefore important for the secondary drying of the sample walls and its effects on collapse [104]. For the physical potency of the glass to bind water molecules, the term “water binding affinity” is therefore used to emphasize that the glass itself contains a high amount of unfrozen water which influences contact and adsorption of water during the sublimation process. It is assumed that hygroscopicity and water binding affinity (as used in this context) are directly correlated as both are directly influenced by the chemical structure of the solved substance and describe similar properties [165, 166, 167]. The higher both parameters are the more is a

plasticization of the product matrix probable during primary (water binding affinity) or secondary drying (hygroscopicity) [25].

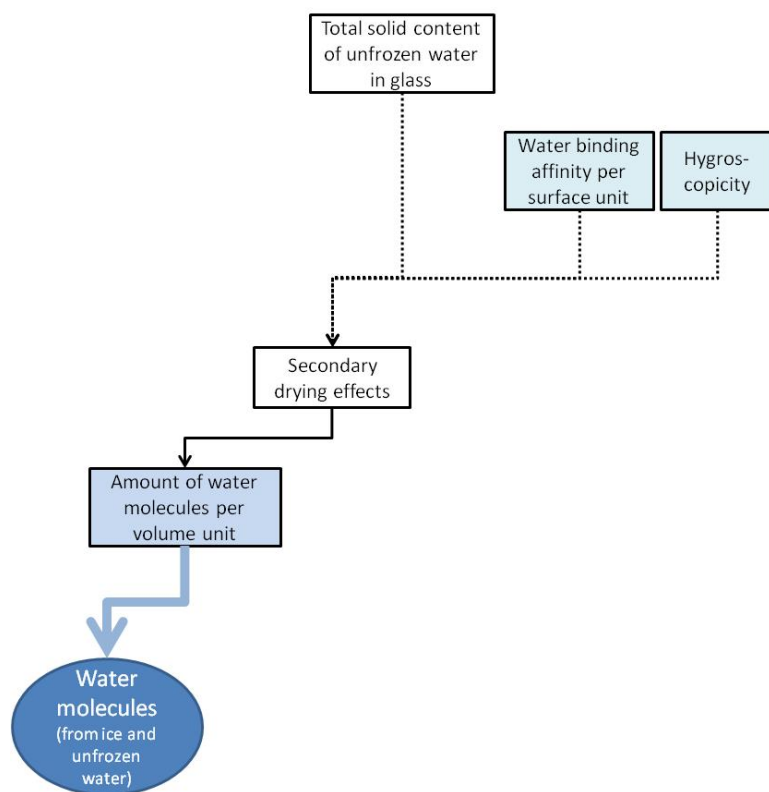


Fig. 3-5: Parameters influencing secondary drying during FDM experiments

molecules which move diffusion-controlled out of the product matrix, the amount of water molecules per volume unit which are reagents for plasticization [79, 117] is increased.

The rigidity of the product matrix wall is the most important and is directly influenced as follows: the stability of the walls increases with a low total content of unfrozen water in the glass (plasticizing effect of water) and with a low specific surface area (higher wall thickness).

As a summary, water molecules inside the matrix are characterized by their number, which is elementary, and their kinetic energy. The properties of the product matrix include its rigidity, its specific surface area, its resistance and its water binding affinity and hygroscopicity. The contact between water molecules and the product matrix is of quantitative and qualitative nature. Quantitative aspects include that in a given time frame the

Furthermore - as Pikal and Shah [104] underlined - secondary drying may occur in FDM experiments (cf. Fig. 3-5). The secondary drying of the primary dried matrix is reduced by a low total content of unfrozen water in the glass and by a high water binding affinity or hygroscopicity, respectively. Depending on the number of water

probability of collapse is increased by higher concentration of water molecules at the surface when focusing on a given area of the matrix or e.g., by having a higher surface area. The quality of this contact, i.e. the effect of a given water molecule (or a given number of water molecules) per given contact (limited time and product area) is in the first line influenced by the composition of the sample. If the effects in summary reach a critical level of rigidity decrease of the product matrix (which is different for every formulation), viscous flow of the product wall(s) into the pore occurs, a behavior which is commonly known as “collapse” [104].

In the next sections, experimental parameters like pressure and supercooling are discussed in detail. As discussed in chapter 3.5 FDM experiments cannot be transferred directly on freeze-drying runs. Therefore, the objective of FDM should be to investigate the main influence of temperature on the sample (shown in bright green color in the flow chart) and not to limit the sample behavior e.g., by pressure settings. However, for this purpose the magnitude of influence of all parameters mentioned in the model above must be known and was subject to investigation in this thesis.

3.1.3 Volume of sample and thickness of the frozen layer

When preparing a sample for measurement, one central question is how much sample solution should be used. A broad range of sample volumes can be found in the literature. For example, 1 μL of sample was used by Colandene and co-workers [129], 4 μL by Overcashier et al. [164], 5 μL were used in two studies [101, 128] and 10 μL as well [127, 165]. Knopp recognized that results were better reproducible when the sample volume was 3-5 μL compared to 8-10 μL .

The experiments performed with a higher volume resulted in higher variability and a 2-3°C higher collapse temperature onset than observed with smaller volumes [112]. He stated that this may be due to the inability to observe the onset of collapse in the material close to the bottom cover slip when the sample is relatively thick. Already in 1978, a uni-

form controlled thickness of approximately 170 μm (1 chip) or 340 μm (2 chip heights) was recommended by Flink for optical reasons using two self-constructed FDM stages [120]. In later publications, metallic spacers were used for that purpose [111, 166].

In the model presented on page 68, the thickness of the frozen layer is not mentioned. It is no key parameter that has an influence on the collapse behavior of the sample itself, but with regard to collapse observation by human eye of the user. The thickness does not change physical effects of collapse, but it limits detection possibilities.

As the small cover glass slide lying on the sample solution has approximately the same weight in every experiment, the thickness of the frozen layer depends on the viscosity of the measured solution if no spacers are used. The higher the volume used the thicker is the sample and the more difficult becomes the observation of the sample.

Tab. 3-4: Impact of different types of samples preparation on T_{oc} and T_{fc} results of 5% (w/w) sucrose solutions

Sample volume and usage of spacers [25 μm]	Experiment	T_{oc} [$^{\circ}\text{C}$]	T_{fc} [$^{\circ}\text{C}$]	ΔT_c [$^{\circ}\text{C}$]	Comment
Spacers, appr. 2 μL	#1	-31.9	-30.2	1.7	-
	#2	-33.0	-29.8	3.2	-
	#3	-31.5	-29.8	1.7	-
	$\bar{x} \pm \text{sdv}$	-32.1 ± 0.6	-29.9 ± 0.2	2.2 ± 0.7	
No spacers, exactly 2 μL	#1	-31.5	-30.3	1.2	-
	#2	-32.1	-30.8	1.3	-
	#3	-31.6	-30.5	1.1	-
	$\bar{x} \pm \text{sdv}$	-31.7 ± 0.3	-30.5 ± 0.2	1.2 ± 0.08	
No spacers, exactly 10 μL	#1	-32.2	-30.0	2.2	-
	#2	-29.4	-26.6	2.8	dark picture
	#3	-29.5	-28.2	1.3	dark picture
	$\bar{x} \pm \text{sdv}$	-30.4 ± 1.3	-28.3 ± 1.4	2.1 ± 0.6	

Tab. 3-4 shows results of different preparation methods for 5% (w/w) sucrose solutions.

Three experiments were performed as described in the materials and methods chapter,

using self-made metal spacers with a height of 25 μm and a sample volume of approximately 2 μL . As the thickness of the layer is controlled by the spacers the volume is no important parameter. However, as described before, the solution had no contact with the spacers (to avoid chemical reactions and disturbed thickness control by capillary effects) and no contact with the edge of the small cover slide (to exclude surface effects for formation of a barrier during freezing and sublimation). Three more experiments were performed by using an exact volume of 2 μL , and another three runs by using a volume of 10 μL without spacers. For the latter samples the thickness of the sample was therefore not controlled and depended on the viscosity of the 5% sucrose solution.

For two of the 10 μL samples the observation of collapse behavior was difficult due to the high thickness of the sample. This is reflected in the mean for T_{oc} and T_{fc} of the three experiments of 10 μL which are significantly higher than for the other six experiments.

Fig. 3-6 presents the mean values and standard deviations [167] in a diagram.

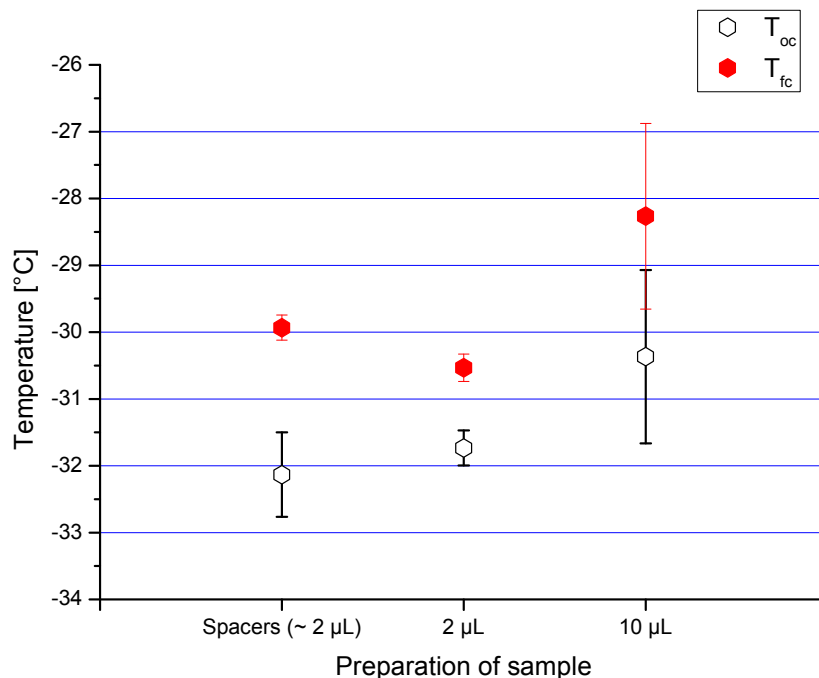


Fig. 3-6: Mean values of T_{oc} and T_{fc} and standard deviations in dependence on different types of sample preparation

For comparison between different types of solution and formulation (having different viscosities) the usage of spacers is highly recommended. If the viscosity of the measured solution is e.g., much higher than for 5% sucrose in water, the layer gets thicker than shown in this study and high variations might be expected. The kind of spacers used remains choice of the single user. To ensure an optimum thickness control they should be flat and of a defined constant height. Although not investigated explicitly, out of the author's experiences, the height of 25 μm used for all experiments discussed in this thesis was a good compromise giving very good observation possibilities for samples in the common range of concentrations (3-15% w/w in average).

3.1.4 Heating rate

The most variable parameter found in literature is the heating rate. Some authors like Adams and Ramsay [106] or Wang and co-workers [127] do not even mention the used heating rate in their publication or state that "heating rates were manually controlled" [165]. However, a user must be aware of the influence of this parameter on FDM results when considering the dependence of results of DSC experiments on different heating rates [101].

When characterizing microcapsules, Yeo and Park used a heating rate of 10°C/min [128]. Overcashier and co-workers used a sophisticated way of heating for their study on lyophilization of protein formulations: after the freezing step and an equilibration time they increased the temperature at 5°C/min and held it at the temperature of interest. Then it was increased stepwise in 2-5°C steps [164].

A rate of 1°C/min up to 30°C⁷ for heating is mentioned in the methods of an investigation on the lyophilization cycle development for a high-concentrated monoclonal antibody formulation done by Colandene et al. [129]. Fonseca and co-workers investigated the

⁷ The authors do not mention a reason for heating to 30°C in their publication.

influence of different heating rates on FDM results of aqueous sucrose solutions. They increased the temperature stepwise with holding periods every degree Celsius and studied “three levels” (1, 5 and 10°C/min) for the ramping rate in between these steps. They claim to have found that “whatever the warming rate applied, no sign of collapse was detected” (so collapse was always detected during one of the holding periods). Consequently, they used the heating rate of 10°C/min to reduce the experimental run time [111]. No data for the “three level” study are given in the paper nor a systematic study was found in literature which reports the optimal heating rate.

The model introduced in this thesis (cf. p. 68) presents the parameter “temperature” as the key parameter. The assumption that the temperature of the sample is the controlling factor to collapse behavior is only true, if heat transfer is sufficient to guarantee that the temperature measured by the thermocouple in the stage reflects the momentary temperature of the sample.

Of course a fast heating rate saves a lot of experimental run time. But apart from heat transfer issues, the user has to keep in mind that the frozen structure at the edge of the cover glass may be different from the structure which is located towards the middle of the sample. If there is no step with only sublimation and no heating at the beginning of the experiment in order to dry enough material at the edge, the collapse may happen in this unrepresentative region and the result obtained may be incorrect.

In first experiments, heating rates of 1°C/min and 10°C/min for aqueous sucrose solutions with a total solid content of 5% were compared. The results are shown in Tab. 3-5.

Tab. 3-5: Collapse temperatures for aqueous solution of sucrose 5% (w/w) dependent upon heating rate

Heating rate [°C/min]	Experiment	T _{oc} [°C]	T _{fc} [°C]	ΔT _c [°C]	T _{c-50} [°C]
1	#1	-31.3	-30.0	1.3	-30.7
	#2	-31.5	-29.9	1.6	-30.7
	#3	-31.1	-29.5	1.6	-30.3
	$\bar{x} \pm \text{sdv}$	-31.3 ± 0.2	-29.8 ± 0.2	1.5 ± 0.1	-30.6 ± 0.2
10	#1	-29.2	-27.4	1.8	-28.3
	#2	-29.4	-27.5	1.9	-28.5
	#3	-28.6	-26.1	2.5	-27.4
	$\bar{x} \pm \text{sdv}$	-29.1 ± 0.3	-27.0 ± 0.6	2.1 ± 0.3	-28.1 ± 0.5

The difference between the average values of the sucrose solution measured with 1°C/min and 10°C/min was 2.2°C for the onset of collapse, 2.8°C for full collapse and 2.5°C for T_{c-50}. Because of the geometry of the silver block, the thin sample layer and the usage of silicon oil, an excellent heat transfer from the silver block to the sample was ensured, but a heating rate of 10°C/min is obviously too fast. The sample cannot follow the heating profile and the collapse is detected at temperatures which are significantly higher than those measured with a low heating rate. Therefore cycle developments based on the results with a heating rate of 10°C/min might be too aggressive.

Additionally, the high heating rate led to higher standard deviations of the results and a higher difference between the onset of collapse and full collapse (1.5 ± 0.1 for 1°C/min vs. 2.1 ± 0.3 for 10°C/min).

From the view of the model on collapse factors (cf. p. 68) the momentary temperature which caused collapse should have been in the same narrow temperature range (taking standard deviations into account) for all experiments performed for this investigation of the influence of heating rate. This means that the differences in temperature between T_{oc}, T_{fc}, ΔT_c and T_{c-50} directly reflect the time-dependent heat transfer from the oven into the sample when using 10°C/min. The single sample begins to collapse most probably at

a momentary product temperature, T_p , (matrix temperature) of -31.3 ± 0.2 (T_{oc}) but at this very moment of collapse, the thermocouple in the silver block already measured a temperature of -29.1 ± 0.3 (T_{oc}). Therefore, a rough estimation reveals that the transfer of heat from the thermocouple into the product takes roughly 15 seconds (heating rate of $10^\circ\text{C}/\text{min}$ with a ΔT of 2.5°C for T_{c-50})⁸. Hence, an optimized heating rate should guarantee a real time and lag free heat transfer and ensure a short experimental run time at the same time.

Further experiments performed with HSA/sugar mixtures which were more difficult to interpret (cf. chapter 3.1.1 "Detection and definition of collapse", p. 63) seem to be in agreement with the statements discussed above. For a mixture of 2.5% (w/w) HSA + 2.5% (w/w) sucrose, a heating rate of $0.5^\circ\text{C}/\text{min}$ resulted in a T_{oc} of -25.8°C (T_{c-50} of -25.0°C), whereas a heating rate of $2^\circ\text{C}/\text{min}$ resulted in a T_{oc} of -24.6°C (T_{c-50} of -23.3°C , see Tab. 3-6).

Tab. 3-6: Collapse temperatures for aqueous solution of 2.5% (w/w) HSA + 2.5% (w/w) sucrose dependent upon heating rate

Heating rate [$^\circ\text{C}/\text{min}$]	T_{oc} [$^\circ\text{C}$]	T_{fc} [$^\circ\text{C}$]	ΔT_c [$^\circ\text{C}$]	T_{c-50} [$^\circ\text{C}$]
0.5	-25.8	-24.1	1.7	-25.0
2	-24.6	-22.0	2.6	-23.3

A more detailed investigation was performed with an aqueous solution of HSA 1% (w/w) + trehalose 4% (w/w) (Tab. 3-7). Here, the standard deviations for the values measured with a heating rate of $2^\circ\text{C}/\text{min}$ were lower, but the temperature data for the experiments performed with $0.5^\circ\text{C}/\text{min}$ were significantly lower in onset of collapse. Significant differences between the average onset of collapse (difference of 3.2°C), full collapse (3.5°C) and T_{c-50} (3.3°C) were found for different heating rates. The heating rate of $2^\circ\text{C}/\text{min}$ resulted in the detection of higher collapse temperatures which reflects the situation that

⁸ $\frac{2.5^\circ\text{C}}{0.16^\circ\text{C}/\text{s}} = 15\text{s}$

the sample could not follow the heating procedure and that the product temperature at the sublimation interface was lower than the temperature measured by the thermocouple installed in the silver block.

Tab. 3-7: Collapse temperatures for aqueous solution of HSA 1% (w/w) + trehalose 4% (w/w) dependent upon heating rate

Heating rate [°C/min]	Experiment	T _{oc} [°C]	T _{fc} [°C]	ΔT _c [°C]	T _{c-50} [°C]
0.5	#1	-26.9	-26.5	0.4	-26.7
	#2	-28.0	-26.3	1.7	-27.2
	#3	-30.8	-29.3	1.5	-30.1
	$\bar{x} \pm \text{sdv}$	-28.6 ± 1.6	-27.4 ± 1.4	1.2 ± 0.6	-28.0 ± 1.5
2	#1	-26.3	-24.2	2.1	-25.3
	#2	-24.3	-23.5	0.8	-23.9
	#3	-25.7	-23.9	1.8	-24.8
	$\bar{x} \pm \text{sdv}$	-25.4 ± 0.8	-23.9 ± 0.3	1.6 ± 0.6	-24.7 ± 0.6

Knopp et al. used a heating rate of 0.3°C/min for their investigation of sucrose solutions by FDM in comparison to MDSC curves [112]. The slowest rate found in the literature (0.1°C/min) was performed by Pikal and Shah [104]. Here, moxalactam di-sodium solutions formulated with mannitol were measured. The explanation for the chosen measurement procedure is based on observation time which is the most important parameter in their conclusion. This hypothesis is also discussed in section 3.1.5. From performed calibration experiments (cf. p. 53), a heating rate of 1°C/min was found to be sufficient for the sample to follow the temperature profile. The results of Tab. 3-7 indicate, that a rate of 2°C/min may be too high. Consequently, it might be questionable if a slow rate of 0.3 or even 0.1°C/min is really necessary to gain (more) accurate and reproducible FDM results as it extremely extends the experimental run time. The solutions used for calibration might be simple systems and one might claim that more difficult sample compositions need a slower heating rate or that observation time is the key parameter. Section 3.2 (p. 102 ff.) shows concentration effects of various excipients with regard to collapse

temperatures. Therefore, a study with sucrose solutions of 2, 10 and 30% (w/w) was performed with a ramp rate of 0.1 and 1°C/min to answer this question of a measurement procedure. The detailed results are presented in Tab. 3-8.

Tab. 3-8: Measured collapse temperatures for aqueous solutions of sucrose with constant heating rates of 0.1°C/min and 1°C/min

Total solid content	Heating rate [°C/min]	Experiment	T_{oc} [°C]	T_{fc} [°C]	ΔT_c [°C]	T_{c-50} [°C]		
2% (w/w)	0.1	#1	-34.2	-32.1	2.1	-33.2		
		#2	-35.0	-33.0	2.0	-34.0		
		#3	-35.3	-32.9	2.4	-34.1		
		$\bar{x} \pm \text{sdv}$	-34.8 ± 0.5	-32.7 ± 0.4	2.2 ± 0.2	-33.8 ± 0.4		
		1	#1	-34.2	-31.8	2.4	-33.0	
	1	#2	-33.9	-32.3	1.6	-33.1		
		#3	-34.4	-32.0	2.4	-33.2		
		$\bar{x} \pm \text{sdv}$	-34.2 ± 0.2	-32.0 ± 0.2	2.1 ± 0.4	-33.1 ± 0.1		
		10% (w/w)	0.1	#1	-32.1	-29.4	2.7	-30.8
				#2	-30.8	-30.4	0.4	-30.6
#3	-31.6			-29.8	1.8	-30.7		
$\bar{x} \pm \text{sdv}$	-31.5 ± 0.5			-29.9 ± 0.4	1.6 ± 1.0	-30.7 ± 0.1		
1	#1			-31.7	-29.3	2.4	-30.5	
1	#2	-30.4	-29.1	1.3	-29.8			
	#3	-30.9	-29.0	1.9	-30.0			
	$\bar{x} \pm \text{sdv}$	-31.0 ± 0.5	-29.1 ± 0.1	1.9 ± 0.5	-30.1 ± 0.3			
	30% (w/w)	0.1	#1	-31.8	-31.4	0.4	-31.6	
			#2	-32.0	-31.3	0.7	-31.7	
#3			-32.2	-31.3	0.9	-31.8		
$\bar{x} \pm \text{sdv}$			-32.0 ± 0.2	-31.3 ± 0.1	0.7 ± 0.2	-31.7 ± 0.1		
1			#1	-31.2	-29.8	1.4	-30.5	
1		#2	-32.1	-30.9	1.2	-31.5		
		#3	-31.7	-29.4	2.3	-30.6		
		$\bar{x} \pm \text{sdv}$	-31.7 ± 0.4	-30.0 ± 0.6	1.6 ± 0.5	-30.9 ± 0.5		

Considering the onset of collapse as well as full collapse for a given concentration, all measured values were in the same temperature range.

For the 30% (w/w) solutions, the averaged full collapse measured with a heating rate of 1°C/min ($-30.0 \pm 0.6^\circ\text{C}$) tends to be a bit higher than the one with a rate of 0.1°C/min ($-31.3 \pm 0.1^\circ\text{C}$). Accordingly, ΔT_c for 0.1°C/min was $0.7 \pm 0.2^\circ\text{C}$ and for 1°C/min $1.6 \pm 0.5^\circ\text{C}$. With regard to standard deviations there was no clear trend. For the onset of collapse, the rate of 0.1°C/min resulted in one case in a better sdv (for 30% w/w) while the rate of 1°C/min was superior in another (2% w/w). For full collapse in two cases (2% and 10% w/w) sdv was lower for 1°C/min and in one case (30% w/w) for 0.1°C/min. Those differences in sdv might probably be coincidental findings.

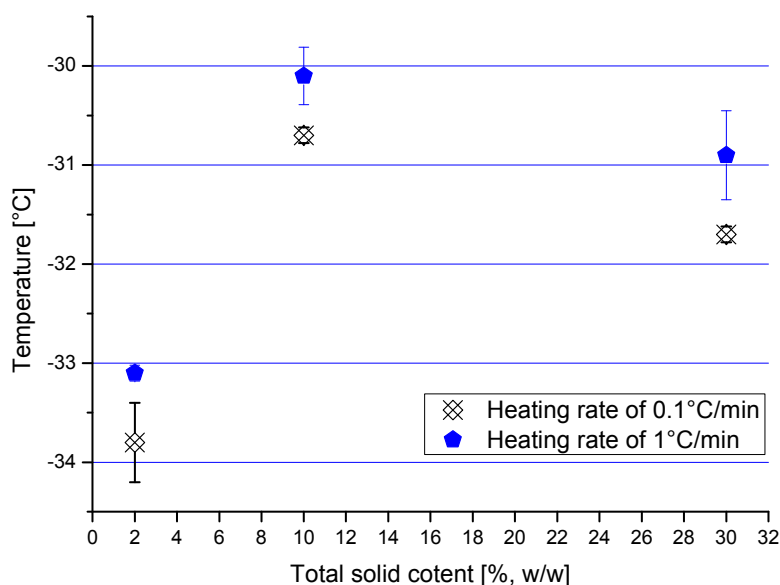


Fig. 3-7: Means of T_{c-50} with standard deviations, comparison of heating rates for differently concentrated sucrose solutions

Fig. 3-7 underlines the small differences in T_{c-50} values between the two heating rates which were only 0.2°C up to 0.8°C when taking standard deviations (sdv) into account.

These differences might probably not be great enough to justify an extension of experimental run time by a factor of about 5 to 10⁹.

Out of three reasons a standard heating rate of 1°C/min was chosen for all further experiments of this thesis: (1) Calibration runs (see above) showed good heat transfer when using this ramp rate. (2) No significant difference between ramp rates of 0.1 and 1°C/min could be found for sucrose solutions of 2, 10 and 30% (w/w) (Tab. 3-8). (3) This heating rate was claimed to be a good compromise between accuracy and experimental run times. It has no disadvantages with regard to accuracy and reproducibility (see 1 and 2 and 3.1.5) and enables the user to perform FDM measurements in a reasonable time frame (which provides the possibility e.g., to repeat measurements in a given working time).

3.1.5 Duration of holding time

As already mentioned before, Fonseca and co-workers used for their study in 2004 [111] a stepwise temperature rise of 1°C at a time with a ramp rate of 10°C/min in between the holding steps¹⁰. In the section “warming profile” they refer to Knopp’s paper with a constant heating rate of 0.3°C/min [112] where the authors say that collapse is a time-dependent phenomenon and claim that their stepwise method is adequate. The chapter about “time for measurement” is based on Pikal’s and Shah’s statements that the collapse temperature measurement is dependent on the time of observation [104]. To evaluate this effect Fonseca et al. dried various sucrose solutions 1°C below T_{oc} for one hour (time of observation longer than usual). As no sample showed signs of collapse they concluded that their measurement methodology is independent of the time of observation.

⁹ E.g., the heating step for a 10% sucrose solution would last 100 min (0.1°C/min) instead of 10 min (1°C/min).

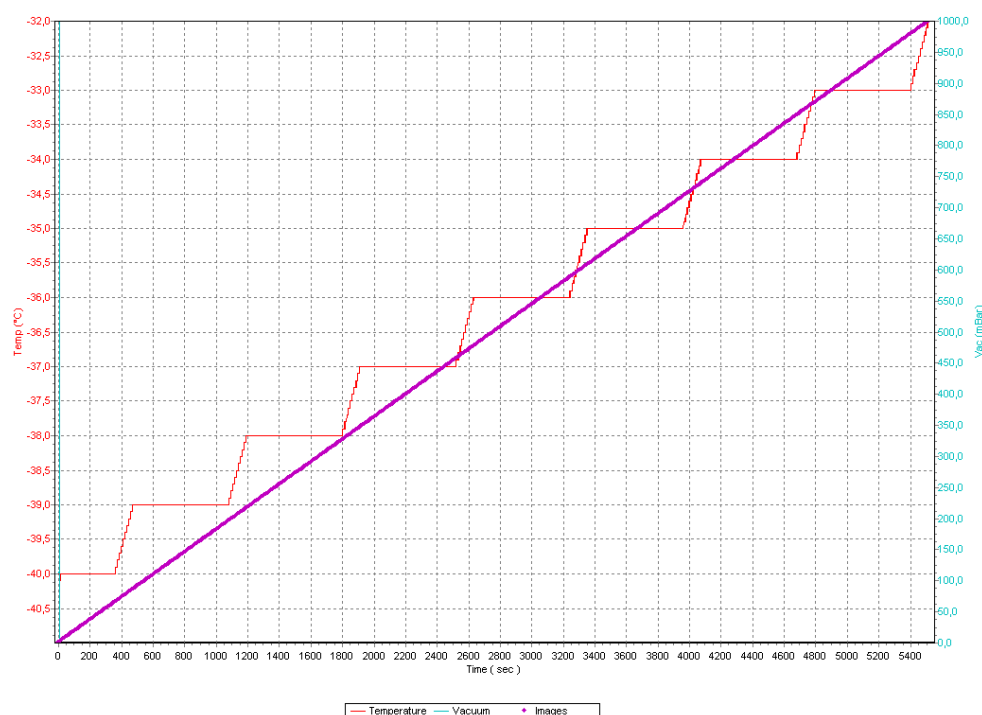
¹⁰ The length of the holding steps is not mentioned by the authors.

According to [104], the collapse temperature is defined by

$$\frac{2\gamma}{rA} \int_0^{TM} \exp\left(\frac{-B}{T_c - k * T_g}\right) dt - 1 = 0 \quad \text{Eq. 3-1}$$

where γ is the surface tension, r the pore radius, A , B and k are constants (which were evaluated by the authors from a fit of viscosity data for moxalactam di-sodium to equation Eq. 1-6 (p. 32) and an adjustment in k_2 made by a fit of collapse temperature data to Eq. 3-1), TM the observation time, T_c the collapse temperature and T_g the glass transition temperature of the amorphous system as measured by DSC¹¹. Eq. 3-1 is based on two equations discussed in section 2.2.1 (p. 53 ff.) and based on several publications [113; 168; 169; 170]. The publication [104] underlines that the freezing rate in FDM is very fast relative to the freezing rate normally encountered in vial freeze-drying. Product resistance and TM are mentioned as important parameters. In case that sublimation is very rapid, as in a system of low solids content, the effect of variation in TM is negligible [104]. Consequently, the authors wanted to ensure TM to be long enough in order to give the sample enough time for viscous flow phenomena. For their study and calculations they used a TM of 0.2 h or 12 min. This derives from their constant heating rate of 0.1°C/min which results in the fact that the time between each degree Celsius of heating is 10 min. As already shown in 3.1.4, no significant differences in results performed with ramp rates of 0.1 and 1°C/min could be found in this study. In order to further investigate the influence of TM and holding steps on T_{oc} and T_{fc} , an additional experimental setup was used implementing holding steps of 10 min at each full degree Celsius beginning at -40°C, and a heating rate of 1°C/min in between (cf. Pic. 3-1) for a 10% (w/w) aqueous sucrose solution.

¹¹ Units not given by the authors.



Pic. 3-1: Heating setting for experiments (Tab. 3-9) with aqueous solution of 10% (w/w) sucrose

When comparing the results in Tab. 3-9 (step procedure) to those from Tab. 3-8 (constant rate of 1°C/min), significant differences were found.

Tab. 3-9: Measured temperatures for aqueous solution of 10% (w/w) sucrose with 10 min holds every degree Celsius of heating

Experiment	T_{oc} [°C]	T_{fc} [°C]	ΔT_c [°C]	T_{c-50} [°C]
#1	-33.2	-31.0	2.2	-31.1
#2	-33.0	-32.0	1.0	-32.5
#3	-33.0	-32.0	1.0	-32.5
$\bar{x} \pm s_{dv}$	-33.1 ± 0.1	-31.7 ± 0.5	1.4 ± 0.6	-32.0 ± 0.7

T_{oc} for the step procedure was on average 2.1°C lower than for the linear procedure and T_{fc} was 2.6°C lower whereas ΔT_c was similar (stepwise: 1.4 ± 0.6 °C, constant: 1.9 ± 0.5 °C). Surprisingly, in five out of the six collapse detections, the collapse (T_{oc} and T_{fc}) was determined in an area not directly adjacent to the sublimation front, but in the dried structure in some distance from it and after at least 5 minutes of holding time at the same temperature. Obviously, time really matters during an FDM measurement although the

immanent importance of T_M in Eq. 3-1. is doubted. Observation time, T_M , reflects the time the walls of the product matrix need to flow into the pore. When using a holding time at a certain temperature and observing a collapse after five minutes of holding the temperature at this level, the factor T_M cannot serve as a good explanation. Here, the introduced model of influencing factors (cf. p. 68) helps to understand the experimental situation. For both measurement setups, the standard procedure and the method with the long holding steps, parameters are (approximately) the same with regard to composition, resistance and speed of sublimation. During the experiment, the water vapor flows through the dried matrix which underwent sublimation before. When focusing on this dried matrix, the probability of a “negative” interaction of water molecules with the matrix is increased by using a very long holding time at a given temperature. With a faster heating rate, worse-case conditions result in a collapse at the sublimation front, but with a temperature hold, the probability that a critical decrease in the rigidity of the product matrix is reached in the already primary dried area is increased because there is still a high amount of unfrozen water bound in the matrix. The temperature hold slows down secondary drying driven by diffusion and interactions leading to collapse become more probable. Additionally, a re-adsorption of water molecules from the vapor flowing through the matrix might be taken into consideration, although this effect might be negligible. As explained before, the collapse which was observed during the performed experiments with the long holding time did therefore not happen in the dried area adjacent to the sublimation interface but in the dried area nearby.

When comparing the described situation with the freeze-drying process in a freeze-dryer the experimental setup with the long holding steps represents the situation in a freeze-dryer in a better way than the standard procedure. Usually freeze-drying is carried out at a certain shelf temperature for hours or days, which results in a relatively constant T_p over a long period of time.

Hence, from a scientific view the holding step procedure is claimed to be more representative. At the same time, it is clear that the setpoint of holding steps has a great influence on measurement results. In the experiments shown above, a holding step was programmed every full °C. Therefore, the accuracy concerning the collapse after a holding time which lasted for longer than five minutes can only be $\pm 1^\circ\text{C}$. If the user wants to have a better accuracy, even more holding steps (e.g., every 0.5 or 0.2°C) must be performed, and resulting measurement procedures would not be applicable for day-to-day work routines.

Transferability of FDM results on FD cycles is discussed in section 3.5. However, it should be already clear at this point of the investigation that there cannot be a one to one transfer of T_c results on FD cycles because the two systems, FDM stage (25 μm frozen layer) and product vials with a given fill depth, have significant differences in geometry, heat transfer, drying behavior, etc. FDM measurements should give as accurate and representative T_c results as possible while being a routine measurement method at the same time. Regarding to the results given in Tab. 3-9, one has to keep in mind that to reach a temperature of e.g., 33.0°C (where T_{oc} was detected) a heating period time of 67 min was needed (without the freezing and equilibration steps). Dependent upon the freezing rate a single measurement could take 1.5 to 2 hours, and the user must observe and move the sample during the 67 min of heating regularly.

As pointed out before, the holding step method was claimed to possibly be closer to transfer conditions and it is therefore recommended to remember the results of Tab. 3-9. At the same time, this time consuming measurement procedure is not appropriate for routine measurements. In each case, an experimental “transferability factor” for FDM results to FD processes needs to be determined. Accordingly, a combination with a routine measurement procedure (1°C/min) makes more sense than a combination with a time consuming measurement methodology which results in a more conservative collapse temperature (which is not transferable 1:1 to a freeze-dryer set-up as well).

3.1.6 Recooling and reheating cycles

Additionally, Fonseca and co-workers [111] recooled the sample at a rate of 10°C/min (the freezing rate for the samples was 10°C/min) and reheated it with the procedure mentioned above in order to confirm the measured collapse temperatures. Experiences from DSC experiments and theory revealed that the sample thermal history has an impact on measurement results. A cooling phase in a MDSC cycle may influence melting and crystallization processes, compared to a conventional (linear heating) experiment [171]. The freezing step and any post-freezing temperature deviations to temperatures above T_g' will determine the texture, or morphology of the product [15]. For example, it was shown for glycine that thermal history affects the formation of different polymorphs and reconstitution times (compare section 3.1.7).

Therefore, no recooling and reheating methodology was performed in this study. Instead, solutions were investigated with two up to five re-runs with a completely fresh experimental preparation.

3.1.7 Cooling rate and annealing

3.1.7.1 Cooling rate

As already stated in the introduction chapter, cooling and freezing are a critical stage in a freeze-drying process. When reaching the ice nucleation temperature during the cooling process, the solution starts forming ice crystals [103]. The degree of supercooling is the temperature difference between the thermodynamic or equilibrium ice/freezing formation temperature and the actual temperature at which ice begins to form, which is usually around 10 to 25°C lower but varies with cooling rate and other factors [24]. Usually supercooling in production freeze-drying is much higher due to sterile conditions compared to FD/FDM experiments in a laboratory (without sterile conditions).

Small sized ice crystals result from a low ice nucleation temperature, which causes smaller pore sizes, a larger specific surface area, a longer primary drying and shorter secondary drying time [172]. The highest supercooling effect can be commonly reached by liquid nitrogen freezing of small volumes [125].

In DSC experiments, the cooling protocol shows a large impact on the sample microstructure and the thermal behavior in frozen sucrose solutions. Solute inclusions within the ice crystals resulted from high supercooling, rapid nucleation and a continually lowered temperature. Therefore a double glass transition was observed because of a complex relaxation in which the bulk phase and the plasticized solute underwent a glass transition. In contrast, a single glass transition was observed, when a homogeneous bulk phase with pure ice crystals was produced at a high temperature (low supercooling) and slow growth of a small number of ice nuclei [173].

It was recently shown that for 5% (w/w) aqueous solutions of sucrose no difference in collapse temperature measured by FDM was found when using a cooling rate of 1°C/min and of 10°C/min [111]. However, a study of Kochs et al. showed an effect of cooling rate on 10% hydroxyethyl starch solutions investigated with FDM. Cooling was applied at one end of the sample, and columnar ice crystals grew in the direction of heat transfer. When using faster cooling rates, the authors observed a decrease in column spacing, which led to greater resistance and slower drying. Additionally, they found a linear relationship between the diffusion coefficient for vapor transport through the dried layer, the lamellar spacing, and in turn the primary drying rate [174].

In this study the importance of the cooling rate was exemplarily examined by using glycine and mannitol. Glycine is a relatively common excipient used in freeze-drying formulations because of its favorable characteristics when it crystallizes. Its physico-chemical state has a striking effect on its characteristics during freeze-drying. Additionally, changes in the formulation or FD conditions may have a high impact on the acceptability of the freeze-dried product.

A different thermal history, based on different freezing procedures and on formation of different polymorphs, can affect reconstitution times [101]. When quench-cooling a glycine solution in liquid nitrogen, it forms an amorphous freeze concentrate, but crystallized as the β -form when frozen with a rate of 20 or 2°C/min in a DSC [175]. During freeze-drying the quench-cooled solutions formed γ -glycine during primary drying, and at the end of secondary drying β - and γ -glycine were found. Furthermore, it was determined that the amount of γ -glycine increased when primary drying was performed at higher temperatures and that the composition depended on the glycine concentration. In contrast, a cooling at 2 and 20°C/min resulted only in β -crystals of glycine after freeze-drying, independent of the primary drying temperature. These results are reflected in measurements performed with aqueous solutions of glycine with a total solid content of 2% (w/w) presented in Tab. 3-10. The high amount of amorphous glycine in the sample which was quench-cooled with an approximate rate of 100°C/s led to a T_{oc} of -63.3°C and a T_{fc} of -62.0°C. For detection of these collapse temperatures the silver block of the stage was precooled to -70°C and the prepared sample (two cover slide glasses, two spacers, sample drop) was placed on top of it. After immediate freezing the stage was closed rapidly and the sample was held at -70°C for 8 min. After 5 min maximum vacuum was pulled, the ice crystals inside the stage resulting from air humidity sublimed and the drying behavior was observed by using a heating rate of 1°C/min. The samples cooled at a rate of 1 or 10°C/min, respectively, showed a different drying behavior caused by the amount of β -glycine in the freeze-concentrated solute. A partial collapse at -15.1°C in one of those samples gave a hint that there was a significant amount of amorphous material in the frozen structure. No full collapse was determinable, but a eutectic melt at -2.9°C which was in agreement to literature [176].

The partial collapse was not an onset of collapse because the overall structure was still rigid and stable, but some collapse holes were observed in the dried structure adjacent to the sublimation interface.¹²

Tab. 3-10: Dependence of FDM measurement on cooling rate for aqueous solutions of glycine 2% (w/w)

Freezing rate [°C/s]	T _{oc} [°C]	T _{fc} [°C]	T _{c-50} [°C]	T _{pc} [°C]	T _{eu} [°C]
0.017 ¹³	none	none	none	-15.1	-2.9
0.17	none	none	none	none	-3.1
100	-63.3	-62.0	-62.7	none	none

Surprisingly, there was no partial collapse detected for the quench-cooled sample, and for the measurement with a cooling rate of 0.17°C/s. DSC measurements revealed, e.g., a complex low-temperature thermal behavior for quench-frozen solutions. A complex glass transition region was observed on the DSC thermogram, with midpoint temperatures at about -73°C and -60°C, as well as two separate crystallization exotherms [101].

Tab. 3-11 shows the impact of the cooling rate of 1% (w/w) mannitol solutions. Quench-cooling with an approximate cooling rate of 100°C/s (procedure as described for glycine) led to a highly amorphous structure of the freeze-concentrated solute. An onset of collapse could be detected at -29.1°C and a full collapse at -27.8°C. When cooling with a rate of 10°C/min, no collapse was observed at this low temperature. Instead, a partial collapse of the amorphous substructure comparable to the one observed for glycine began at -18.2°C and was followed by a eutectic melt at -3.0°C. Here, the cooling rate of 10°C/min obviously led to a structure containing a significantly higher amount of crystalline mannitol. At a rate of 1°C/min, no collapse was detectable which obviously reflects the fact that there was no amorphous mannitol in the freeze-concentrated solute.

¹² In all FDM experiments described here, crystallinity could not be judged based on visual appearance of the frozen sample.

¹³ 0.017°C/s = 1°C/min

Tab. 3-11: Dependence of FDM measurement on cooling rate for aqueous solutions of mannitol 1% (w/w)

Freezing rate [°C/s]	T _{oc} [°C]	T _{fc} [°C]	T _{c-50} [°C]	T _{pc} [°C]	T _{eu} [°C]
0.017	none	none	none	none	-2.7
0.17	none	none	none	-18.2	-3.0
100	-29.1	-27.8	-28.5	none	none

Experiments performed with mannitol as well as glycine using different cooling rates show the importance of this parameter for FDM methodology, and the possibility to utilize FDM for detailed studies on collapse behavior and melting characteristics.

3.1.7.2 Annealing

In previous studies annealing was used rarely when performing FDM measurements. In one example, annealing was performed for one hour at -20°C in contrast to a freezing step with no annealing by Wang et al. for investigating formulations containing recombinant Factor VIII and α -amylase by FDM [127].

The main purpose of annealing is to crystallize potentially crystallizing components (e.g., glycine or mannitol) in a formulation during the freezing stage [24]. To avoid vial breakage during primary drying, mannitol should be fully crystallized during freezing when using high concentrations and high fill depths [177]. Usually annealing is performed between T_g' of the amorphous phase and T_{eu} of the bulking agent. This procedure results in a high crystallization rate and a complete crystallization. For mannitol or glycine, a temperature of -20 or -25°C and an annealing time of two hours or longer are suggested if the fill depth is 1 cm or more [178].

In turn, annealing can also be used to improve the drying behavior of formulations by facilitating growth of ice crystals at a temperature above T_g' . Larger ice crystals decrease the product resistance to water vapor flow and result in shorter primary drying time [178].

In a set of experiments, the effect of different annealing times on 5% (w/w) sucrose solution at -15°C ¹⁴ was studied. The ramping rate to this annealing temperature was $1^{\circ}\text{C}/\text{min}$ and following the annealing step the samples were frozen to -40°C and treated in the standard procedure as reported before. Tab. 3-12 illustrates no significant differences in collapse temperature measurements (if sublimation took place). Surprisingly, sample #2 and #3 (annealing time of 60 min) did not undergo sublimation. The annealing step led to a growth of sucrose crystals, visible at the edge of the sample which imposed a barrier to the water vapor flow. For these samples a eutectic melting could be detected.

Tab. 3-12: Collapse or eutectic temperatures for sucrose 5% (w/w) solutions with annealing step at -15°C for various annealing times

Annealing time	Experiment	T_{oc} [$^{\circ}\text{C}$]	T_{fc} [$^{\circ}\text{C}$]	ΔT_c [$^{\circ}\text{C}$]	T_{c-50} [$^{\circ}\text{C}$]	T_{eu} [$^{\circ}\text{C}$]
15 min	#1	-32.4	-30.6	1.8	-31.5	not detected
	#2	-34.0	-31.7	2.3	-32.9	not detected
	#3	-32.1	-31.1	1.0	-31.7	not detected
	$\bar{x} \pm \text{sdv}$	-32.8 ± 0.8	-31.1 ± 0.5	1.7 ± 0.5	-32.0 ± 0.6	-
	30 min	#1	-34.3	-33.7	0.6	-34.0
#2		-32.3	-31.8	0.5	-32.1	not detected
#3		-32.4	-32.1	0.3	-32.3	not detected
$\bar{x} \pm \text{sdv}$		-33.0 ± 0.9	-32.5 ± 0.8	0.5 ± 0.1	-32.8 ± 0.9	-
60 min		#1	-32.5	-31.5	1.0	-32.0
	#2	no sublimation	no sublimation	-	-	-3.5
	#3	no sublimation	no sublimation	-	-	-3.2
	\bar{x}	-32.5	-31.5	1.0	-32.0	-3.4

¹⁴ T_g' of sucrose was reported to be -32°C [147]. The high annealing temperature of -15°C was chosen in order to detect maximum effects of the annealing procedure in terms of ice crystal growth.

A hint towards the hypothesis that ice crystals grow during annealing is the observation that the mean ΔT_c (which signifies the difference between T_{oc} and corresponding T_{fc} values) for the 30 min samples is lower than for the 15 min samples.

Tab. 3-13 gives an overview of sublimation rates measured as velocities of the sublimation front. The values varied highly, but in average the 15 min and the 30 min samples showed the same velocity of the sublimation front at -35.0°C and at T_{oc} . Therefore, no postulated difference in ice crystal size and resistance to water vapor flow could be confirmed.

Tab. 3-13: Velocities of sublimation front for sucrose 5% (w/w) solutions with an annealing step at -15°C (for 15 and 30 min)

Annealing time	Experiment	Velocity of sublimation front at -35.0°C [$\mu\text{m/s}$]	Velocity of sublimation front at T_{oc} (given in brackets) [$\mu\text{m/s}$]
15 min	#1	0.46	1.1 (-32.4°C)
	#2	0.25	0.24 (-34.0°C)
	#3	0.75	0.85 (-32.1°C)
	$\bar{x} \pm \text{sdv}$	0.49 ± 0.20	0.73 (-32.8°C)
	rsdv	42%	-
	30 min	#1	0.46
#2		0.21	0.24 (-32.3°C)
#3		0.56	1.0 (-32.4°C)
$\bar{x} \pm \text{sdv}$		0.41 ± 0.15	0.60 (-33.0°C)
rsdv		36%	-

Passot and co-workers investigated 13 formulations to stabilize toxin A and B e.g., by FDM measurements. For the formulations containing a crystalline bulking agent (mannitol or glycine), an annealing step at -20°C for 20 min was added after the freezing step in order to ensure the bulking agent crystallization [166].

Accordingly, collapse temperatures with and without annealing for various mixtures of sucrose and mannitol were investigated in this thesis to get an insight if FDM is a useful tool to optimize annealing steps for mixtures containing a crystallizing and a non-crystallizing component.

Tab. 3-14: Detection of collapse or eutectic temperatures for various aqueous mixtures of sucrose and mannitol with and without annealing

Mixture	Annealing step (30min)	T _{pc} [°C]	T _{oc} [°C]	T _{fc} [°C]
1%Sucrose + 4%mannitol (w/w)	none, #1	-26.8	-7.5	-3.3
	none, #2	-28.3	-9.5	-5.7
	at -20°C	none	-9.5	-4.3
	at -10°C	none	-15.9	-7.1
2.5% Sucrose + 2.5% mannitol (w/w)	none	none	-39.7	-36.5
	at -20°C	none	-38.1	-36.0
	at -10°C	none	-38.8	-36.4
4%Sucrose + 1% mannitol (w/w)	none	none	-36.9	-34.7
	at -20°C	none	-42.6	-39.5

In Tab. 3-14 the results of these experiments are illustrated. The solutions were measured without annealing, with an annealing step at -10°C for 30 min and/or an annealing at -20°C for 30 min. The mixtures of 2.5% sucrose with 2.5% mannitol and of 4% sucrose with 1% mannitol were frozen to -45.0°C before heating. The other measurement parameters can be found in the section 2.2.1.

The mixture with 1% sucrose and 4% mannitol showed a reproducible partial collapse at around -27°C. This observation of single holes which looked like an onset of collapse might be due to a collapse effect of amorphous mannitol substructures. Annealing of the solution led to a disappearance of this partial collapse phenomenon.

For the experiment with an annealing at -10°C mannitol crystallized probably to a higher extent, relative to annealing at -20°C. Accordingly, the amorphous sucrose had a greater

impact on T_{oc} and T_{fc} in the mixture annealed at -10°C which led to a lower T_{oc} and T_{fc} . In contrast, no significant differences in T_{oc} and T_{fc} were found for the 50:50 mixture of sucrose and mannitol. For the mixture with 4% sucrose and 1% mannitol annealing at -20°C resulted in a lower T_{oc} and T_{fc} (difference of 5.7 and 4.8°C). It is assumed that the growth of sucrose crystals shifted the T_c temperatures so that the amorphous mannitol substructures had a greater impact on T_c compared to the non-annealed solution.

3.1.8 Pressure setting

In almost all cases, pressure settings during FDM studies are not given in publications. An exception is a study by Overcashier et al. in 1999 on formulations with recombinant humanized antibody HER2, trehalose and sucrose [164], where the authors use a pressure of 100 mTorr.

Two FDM papers could be found containing studies on this parameter. Knopp et al. did some investigation on pressures settings in FDM measurements [112]. They used a pressure of 25 mTorr and 100 mTorr in order to examine the pressure dependence of collapse, but found no difference for sucrose solutions of 5 and 10% (w/w) total solid content. Referring to [104], they concluded that the drying rate was low enough for these samples to be in a region of little dependence of collapse temperature on drying rate. On the basis of [112] and [104] Fonseca and co-workers used a pressure of 7.5 mTorr in order to achieve a fast sublimation rate and a short experimental time frame. Pikal and Shah presented in 1990 measurements which are illustrated in an adapted form in Tab. 3-15 [104]. The authors reported that the collapse temperatures as the average value of at least two independent replicates and claimed that replication was usually within $\pm 0.5^{\circ}\text{C}$. Here, measurements were performed with a moxolactam di-sodium solution containing 12% mannitol.

Tab. 3-15: Impact of pressure on drying rate and collapse temperature for moxalactam di-sodium (with 12% mannitol), adapted from [104]

Total solid content [% w/w]	Pressure [Torr]	Drying rate at -30°C [μm/s]	Collapse temperature [°C]
2	0.0	0.52	-20.7
	0.2	0.21	-22.0
	1.0	0.14	-22.0
	$\bar{x} \pm \text{sdv}$	0.29 ± 0.17	-21.6 ± 0.4
20	0.0	0.056	-21.4
	0.2	0.089	-21.7
	1.0	0.081	-22.7
	$\bar{x} \pm \text{sdv}$	0.075 ± 0.075	-21.9 ± 0.0
30	0.0	0.14	-23.3
	0.2	0.10	-23.6
	1.0	0.04	-23.0
	760.0	0.00	-23.1
	$\bar{x} \pm \text{sdv}$	0.07 ± 0.05	-23.2 ± 0.1

Because of the restricted possibilities of pressure control described in the publication and the very special sample composition¹⁵, a series of experiments was performed to study the dependence of collapse temperatures on the pressure setting for a simple one component system (sucrose 5 and 10% w/w).

Using different pressure settings the pressure gradient between the sublimation interface (P_0) and the drying chamber (P_c) of the stage was altered. Due to technical restrictions of older FDM equipment, a much lower pressure than 0.5 Torr could not be applied. In contrast, pressures during freeze-drying are usually in the range of 0.05 to 0.2 Torr.

The parameter of the sublimation velocity (V_{sub}) may be taken as a qualitative indicator for the resistance of the product matrix to vapor flow during FDM measurements, making

¹⁵ A formulation of moxalactam di-sodium was measured. It contained 12% mannitol which might easily crystallize during FDM measurements as described before.

relative comparisons of V_{sub} data for different formulations during formulation development easier. Furthermore, a user could compare V_{sub} results with the time dependence of the receding ice layer thickness in a vial during a laboratory scale freeze-drying run [179, 180]. For such a comparison the gas composition in the FDM stage and in the freeze-drying chamber should be of minor importance although differences might be expected: In a freeze-dryer the vapor composition during the early phase of primary drying is mainly water [6] whereas the vapor in the FDM stage might be assumed to be a mixture of water and nitrogen where the share of nitrogen is higher relative to a freeze-drying run. Thus, the sublimation rate at a given temperature and for a given pore size might be expected to be slightly higher during an FDM experiment compared to the situation in a vial.

Tab. 3-6 and Tab. 3-7 underline that for 5 and 10% (w/w) sucrose solutions T_{oc} seems to be independent of the pressure setpoint. The standard deviations were well to very well acceptable for FDM experiments¹⁶. As already stated by Pikal and Shah, the velocity of the sublimation front (or drying rate, respectively) has a high relative standard deviation (rsdv) [104]. Here, a rsdv of 31% at -35°C for 5% sucrose, and of 40% at -35°C for 10% sucrose. For the velocity at T_{oc} rsdv values were better (16% and 29%). Compared to rsdv values in Tab. 3-15 the velocity rsdv for the sucrose solutions were lower which might be a result of the constant layer thickness of the frozen sample ensured by the custom-made spacers and of the improved detection methodology (calibrated distance measurement and software support).

¹⁶ For FDM measurements standard deviations of $\pm 0.5^{\circ}\text{C}$ were regarded as very well acceptable.

Tab. 3-16: Sucrose 5% (w/w) measured with different pressure settings

Pressure [Torr]	T _{oc} [°C]	T _{fc} [°C]	ΔT [°C]	T _{c-50} [°C]	Velocity at -35°C [μm/s]	Velocity at T _{oc} [μm/s]	MF	VT _{oc} [μm°C/s]
0.07	-31.5	-29.9	1.6	-30.7	0.22	0.40	1.8	-12.6
0.37	-32.8	-30.9	1.9	-31.9	0.23	0.30	1.3	-9.84
0.75	-31.3	-29.3	2.0	-30.3	0.29	0.43	1.5	-13.5
1.50	-31.7	-29.7	2.0	-30.7	0.45	0.47	1.0	-14.9
\bar{x} ± sdv	-31.8 ± 0.6	-30.0 ± 0.6	1.9 ± 0.2	-30.9 ± 0.6	0.30 ± 0.1	0.40 ± 0.1	1.4 ± 0.3	-12.7 ± 1.8
rsdv	1.8%	2.0%	8.7%	1.9%	31%	16%	21%	14%

Tab. 3-17: Sucrose 10% (w/w) measured with different pressure settings

Pressure [Torr]	T _{oc} [°C]	T _{fc} [°C]	ΔT _c [°C]	T _{c-50} [°C]	Velocity at -35°C [μm/s]	Velocity at T _{oc} [μm/s]	MF	VT _{oc} [μm°C/s]
0.07	-30.9	-29.0	1.9	-30.0	0.29	0.45	1.6	-13.9
0.37	-31.2	-30.4	0.8	-30.8	0.30	0.44	1.5	-13.7
0.75	-31.9	-30.2	1.7	-31.1	0.16	0.48	3.0	-15.3
1.50	-31.9	-29.8	2.1	-30.9	0.10	0.20	2.0	-6.38
\bar{x} ± sdv	-31.5 ± 0.4	-29.9 ± 0.5	1.6 ± 0.5	-30.7 ± 0.4	0.21 ± 0.1	0.39 ± 0.1	2.0 ± 0.6	-12.3 ± 3.5
rsdv	1.4%	1.8%	31%	1.4%	40%	29%	29%	28%

The multiplication factor (MF)

$$MF = \frac{V(T_{oc})}{V(-35^{\circ}C)} \quad \text{Eq. 3-2}$$

(where V is the velocity of the sublimation front at T_{oc}, or at a temperature of -35°C, respectively [μm/s]) is higher (2.0) for the 10% solution than for the 5% solution (1.4). At the same time, the factor VT_{oc} which is defined as the product of V(T_{oc}) and T_{oc} is roughly the same for both concentrations (-12.7 ± 1.84 μm°C/s for 5% vs. -12.3 ± 3.49 μm°C/s for 10%). For both total solid contents the velocity of the sublimation front is higher for

higher temperatures (T_{fc} compared to T_{oc}), which is expected. Additionally, V_{sub} was in average higher for the 5% solution which is obviously a result of the lower resistance of its product matrix compared to the 10% solution.

A discussion of the impact of concentration on T_{oc} and T_{fc} will follow in section 3.2. It is worth to mention at this point that the result of Pikal and Shah - lower T_c with higher total solid content - [104] could not be confirmed in these and other experiments, but the opposite impact could be determined.

If the schematic introduced in this thesis (p. 68) is taken into account, a theoretically based discussion on pressure influence is possible. The pressure setting has two main effects on the FDM. First, a decrease in pressure results in a higher amount of subliming water molecules, which is a result of a higher pressure difference between P_c and P_{ice} [6]. Second, a lower pressure leads to a higher velocity of the subliming water molecules in the water vapor flowing through the dried matrix [9]. These two effects have a contrary consequence on the probability of a contact between water molecules and the product matrix. Low pressure results in more water molecules with a higher average speed. In turn, high pressure results in less molecules with less kinetic energy. Therefore, it is a matter of the formulation and particularly of the temperature (which influences both parameters as well) which out of these two effects has the higher relevance. One may conclude e.g., that for the 5% sucrose solution in Tab. 3-16 the maximal “negative” effect (leading to the lowest collapse temperature) was found for the setting of 0.375 Torr, and for the 10% sucrose solution for a pressure setting of 0.75 and 1.5 Torr, respectively. However, these findings can most probably not be generalized.

3.2 Dependence of collapse temperatures on total solid content for excipient solutions

Already in 1972, a dependence of the collapse temperature on total solid content was observed by Bellows and King. They reported the following T_c data on sucrose: -22.5°C (15% initial wt %), -24°C (25%), -27°C (35%), -29°C (45%), and -29.5°C (55%) [113]. From the measurement experiences gained during the laboratory work for this thesis, the measurement of solutions with a total solid content higher than 30% is claimed to be very difficult – even when using the best equipment commercially on the market available at the moment. It is clear from the year of publication that Bellows and King must have had much worse equipment. They themselves seemed not to have expected this finding as well when they claim that “increasing the initial concentration of solutes before freezing decreases the collapse temperature *somewhat*, because the volumetric ratio of concentrated amorphous solution to ice increases and the concentrated amorphous solution dries more slowly. This allows more time for collapse and requires a *somewhat* higher equilibrium viscosity to prevent collapse [...]” [113].¹⁷ Based on the just mentioned arguments, the data reported by Bellows and King are questionable.

Pikal and Shah quote the results of the mentioned paper and complemented the data by investigating that a 2% solution of povidone collapses about 2.5°C higher than a 10% solution. They explain that primary drying in the 2% solution is much faster (1.4 mm/h at -30°C) than in the 10% solution (0.13 mm/h at -30°C) and that the observed concentration effect may well be a drying rate effect [104]. As already mentioned before, they also found a dependence of a special moxalactam di-sodium formulation (containing 12% mannitol) with a T_c of $-21.6 \pm 0.4^\circ\text{C}$ for 2% API, of $-21.9 \pm 0.04^\circ\text{C}$ for 20%, and of $-23.2 \pm 0.1^\circ\text{C}$ for 30%.

¹⁷ Accentuations inserted by the author of the thesis.

Fonseca and co-workers agreed to these results in their measurements on aqueous sucrose solutions ranging from 5% to 25% (w/w). They found the collapse temperatures were equivalent for all concentrations (between -34 and -33°C) [111].

In contrast, it was published in 1998, that sucrose showed a higher temperature for the “end” of collapse for a 10% (w/w) solution (-35.5°C) compared to a 5% (w/w) solution (-36.2°C). Onset of collapse was reported to be the same for both solutions (-37.7°C) [112].

A paper from 1996 showed the relationship between concentration and T_c in a formulation development study where the content of sodium chloride in a formulation of *Erwinia carotovora* L-asparaginase highly influences T_c ranging from roughly -54 to -31°C [106].

The highest differences due to different concentrations were found in a study of monoclonal antibody formulations [129]. The authors defined an onset collapse temperature, $T_{c,on}$ (which refers to T_{oc}) and a complete collapse temperature, $T_{c,com}$ (referring to T_{fc}). $T_{c,on}$ values ranged from -33°C (0 mg/mL protein) over -27°C for 40 mg/mL and -19°C for 60 mg/mL to -21°C for 100 mg/mL. Corresponding $T_{c,com}$ results were -31°C for 0 mg/mL protein, -23°C for 40 mg/mL, -12°C for 80 mg/mL, and, e.g., -13°C for 100 mg/mL. As the protein concentration increased, the collapse temperature increased and the difference between $T_{c,on}$ and $T_{c,com}$ increased [129].

3.2.1 Concentration vs. collapse temperatures

Because of inconsistent results mentioned above, a detailed study on the impact of the total solid content of the used excipient on T_c (T_{oc}/T_{fc} etc.) was performed with six different substances: sucrose, trehalose, glucose, (2-hydroxypropyl)- β -cyclodextrin, PVP 10 kDa and PVP 40 kDa.

To analyze the deviations in measured value sets, 90% confidence intervals were calculated based on known standard deviations using the following equation:

$$P(\bar{X} - z \left(\frac{\alpha}{2}\right) \sigma_{\bar{X}}) \leq \mu \leq P(\bar{X} + z \left(\frac{\alpha}{2}\right) \sigma_{\bar{X}}) \approx 1 - \alpha \quad \text{Eq. 3-3}$$

where P means probability, \bar{X} is the sample mean, z is a fixed number, $1 - \alpha$ is the coverage probability, $\sigma_{\bar{X}}$ is the standard deviation of the sample mean and μ is the confidence interval (here: 0.9) [181].

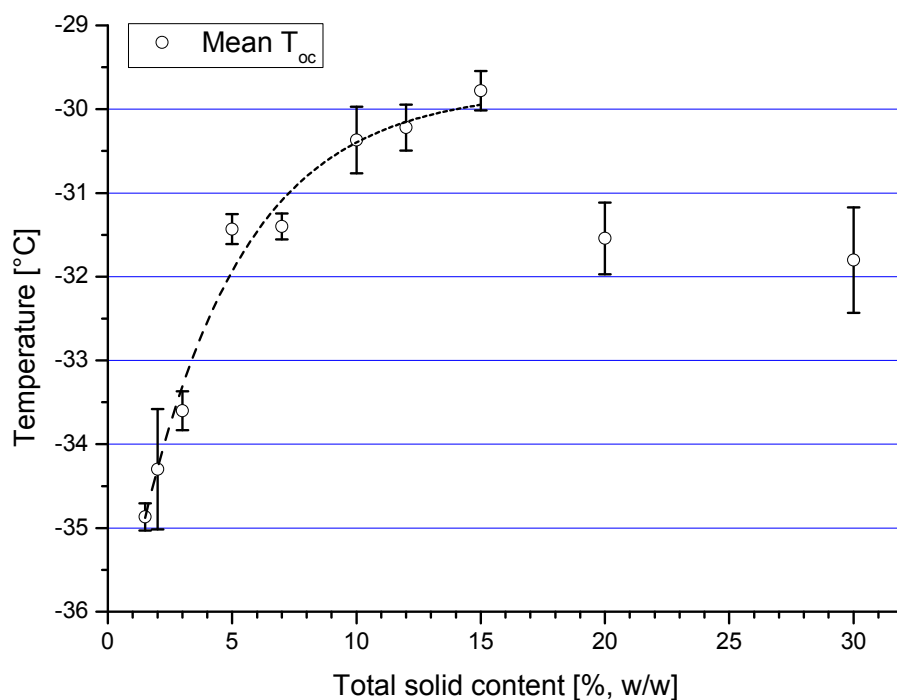
The squared multiple correlation coefficient, or coefficient of determination, was used as a crude measure of the strength of the relationship that has been fit by least squares. This coefficient is defined as the squared correlation of the dependent variable and the fitted values and can be expressed as

$$R^2 = \frac{s_y^2 - s_{\hat{e}}^2}{s_y^2} \quad \text{Eq. 3-4}$$

where R^2 is the squared multiple correlation coefficient, s_y^2 is the variance of the dependent variable and $s_{\hat{e}}^2$ is the variance of the residuals from the fit [181].

Additionally, reduced chi-square values were calculated by dividing the residual sum by the degrees of freedom. If Z is a standard normal random variable, the distribution of $U = Z^2$ is called the chi-square distribution with 1 degree of freedom. If U_1, U_2, \dots, U_n are independent chi-square random variables with 1 degree of freedom, the distribution of $V = U_1 + U_2 + \dots + U_n$ is called the chi-square distribution with n degrees of freedom as is denoted by X_n^2 [181].

3.2.1.1 Sucrose solutions



Equation	$y = A \cdot \exp(-x/t) + y_0$ ¹⁸			
<i>Parameter</i>	<i>Value</i>	<i>sdv</i>	R^2	0.964
A	-7.39	0.574	<i>Reduced X^2</i>	2.80
t	4.09	0.894		
y_0	-29.8	0.434		

Fig. 3-8: Dependence of T_{oc} on total solid content for sucrose solutions, exponential fit, mean values with 90% confidence intervals, T_{fc} were approximately 0.5 to 1°C higher than T_{oc} values.

Onset of collapse temperatures were measured for aqueous sucrose solutions with the following total solid contents: 1.5, 2, 3, 5, 7, 10, 12, 15, 20, 30% (w/w). The results are presented in Fig. 3-8.

¹⁸ For all data series presented in this chapter a linear fit was used in order to ensure a good comparability of curves. Other fits (e.g., polynomials) might be possible as well to show trends of the data series.

T_{oc} was found to highly depend on concentration ranging from about -35°C for a 1.5% solution to about -30°C for a 15% solution. For this interval an exponential dependence of T_{oc} on total solid content was found, the equation of which is given in Fig. 3-8. The values for the 20 and 30% solutions did not follow this pattern, but had a relatively low T_{oc} of around -31.5°C . Interestingly, the collapse event was not located directly at the sublimation interface, but in a dried area in some distance towards the edge of the used cover glass slide.

The model introduced in chapter 3.1.2 (p. 67 ff.) helps to understand the found dependence, the deviations determined for single solutions and the mentioned effect of a relatively low T_{oc} for 20 and 30% sucrose:

Different amounts of solved substance in the initial aqueous solution have effects on water molecules and on product matrix which have to get in contact in a certain quantity and quality to result in a rigidity decrease reaching a critical level (cf. Fig. 3-9) [25]. This critical rigidity decrease of the product matrix then leads to viscous flow and collapse [104].

On the side of the water molecules, a change in total solid content of solved substance results in a different total solid content of ice [9]. As described above (cf. chapter 1.2.1), the ratio of substance molecules to water molecules is the same (quench-cooling not included) for different concentrated solutions [15]. Therefore, the total solid content of ice outside the matrix is different and leads to more water molecules per volume unit for lower concentrated solutions. This higher amount of reactive water decreases the collapse temperature for low total solid contents.

Additionally, the secondary drying effect [104] is negatively influenced by a higher amount of unfrozen water in the glass when considering a given volume of sample of a high concentrated solution (lower extent of secondary drying due to more water molecules), as well as the rigidity of the product matrix walls. A higher total solid content leads probably to a higher resistance of the product matrix [15].

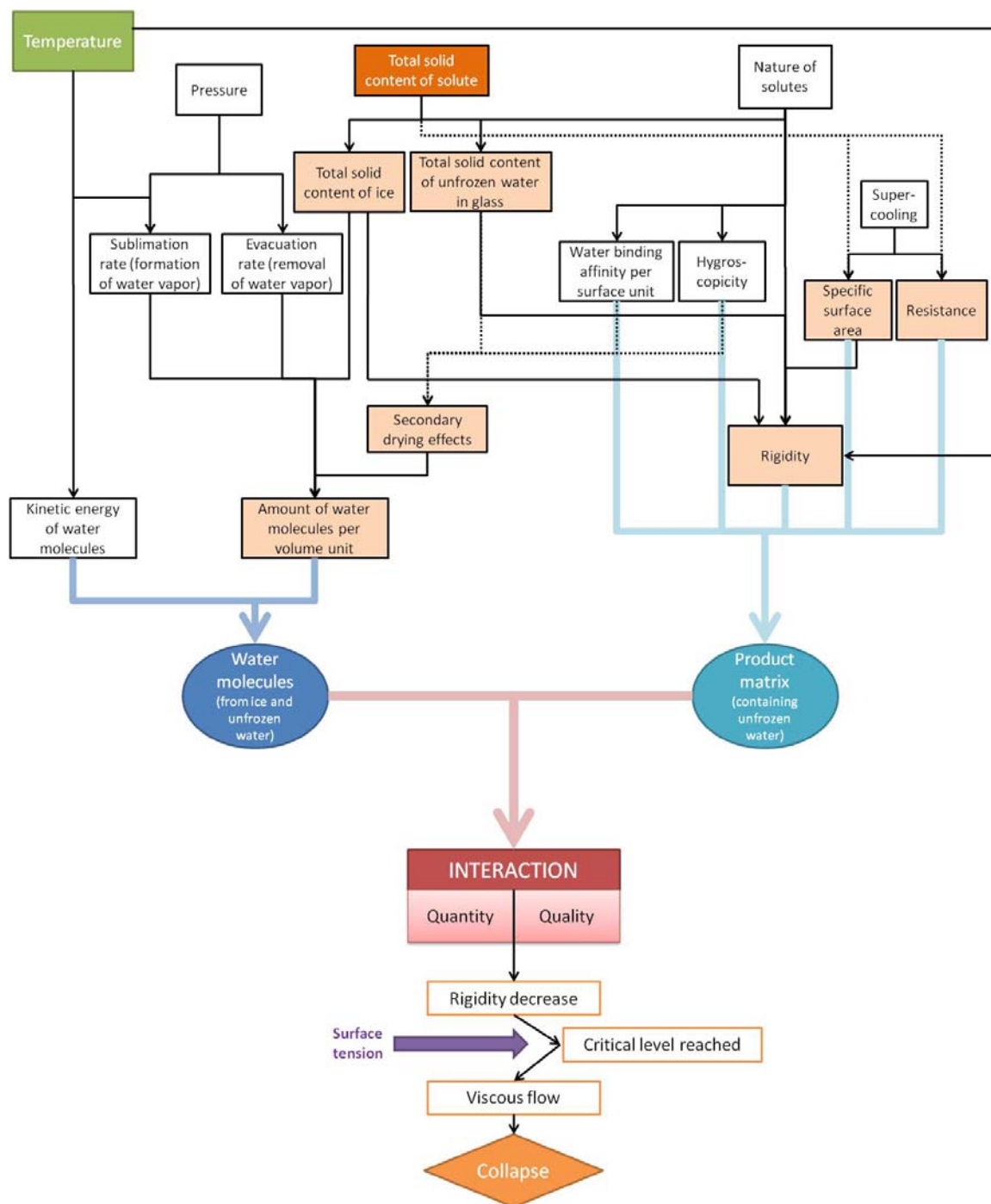


Fig. 3-9: Effects of changes in total solid content of excipient in the initial solution concerning collapse behavior

Taking the last two points into account, a solution with a very high concentration (20 or 30%) of a hygroscopic molecule (like sucrose) shows a lower T_{oc} than a solution with e.g., 15% solved substance. The hygroscopicity of dry sucrose is reflected in a high water binding affinity per surface area during the sublimation process [182-184] which eas-

es the probability of a contact between a water molecule and the product matrix (compared to non-hygroscopic substances). Together with the high specific surface area and high resistance of the product matrix (depending on cooling), which increase the probability of a contact for a water molecule passing the product matrix, collapse happens in the dried area near (but not directly at) the sublimation front (see collapse description before).

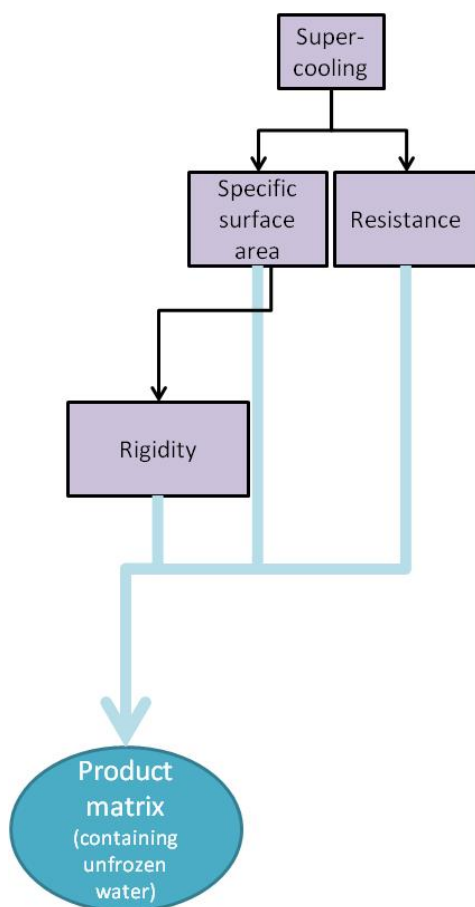


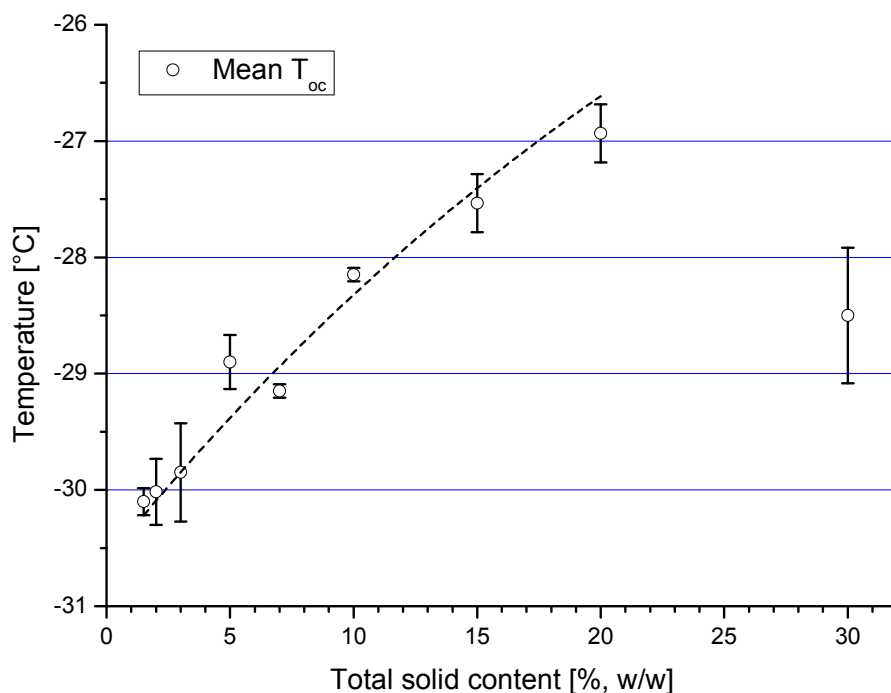
Fig. 3-10: Effect of supercooling differences on collapse behavior

Concluding the discussed effects, the main reason for the low T_{oc} of low concentrated sucrose solutions is the high amount of ice in the structure [15] which leads to a higher amount of water molecules per volume unit of product matrix and to product matrix with a low rigidity and a low specific surface area. For solutions with total solid contents of 10-15%, T_{oc} values reach a maximum. Here the single influencing parameters are in a good balance compared to other constellations. The high concentrated solutions (20 and 30%) result in a very high specific surface area and resistance¹⁹ [17], which exceeds the “positive” effect of less water molecules per given volume. It is assumed that (compared to non-hygroscopic substances) sucrose has a high affinity to bind water molecules [182-184] so that the influence of surface area and resistance has such a great impact on T_{oc} values, which are much lower than T_{oc} for 10-15% solutions. In Fig. 3-10 effects of different extents of supercooling are visualized. The high

¹⁹ For SSA the area itself is relevant, whereas resistance depends on the shape of the pores and their direction relative to the water vapor flow.

deviations of measured T_{oc} data result from this influencing parameter. Different nucleation temperatures lead to differences in the amount, size and shape of ice crystals [164, 177] which is reflected in different specific surface areas and resistance values of the product matrix [9]. Further, the SSA has an influence on the rigidity of the product matrix, leading to a higher rigidity for lower SSA (for a fixed total solid content of solved substance) [15]. As nucleation can not be controlled during FDM measurements [21], there are slight differences in supercooling and therefore in the described physical properties of the product matrix resulting in slightly different T_{oc} values for one and the same initial solution. The overall difference between the lowest (1.5% w/w) and the highest T_{oc} (15% w/w), ΔT_{oc} , is 5.1°C.

3.2.1.2 Trehalose solutions



Equation	$y = A \cdot \exp(-x/t) + y_0$			
<i>Parameter</i>	<i>Value</i>	<i>sdv</i>	R^2	0.896
A	-9.08	9.64	<i>Reduced X^2</i>	5.85
t	34.5	47.03		
y_0	-21.5	9.86		

Fig. 3-11: Dependence of T_{oc} on total solid content for trehalose solutions, exponential fit, mean values with 90% confidence intervals, T_{fc} were approximately 0.5 to 1°C higher than T_{oc} values.

For trehalose T_{oc} was detected for the following solutions (% w/w): 1.5, 2, 3, 5, 7, 10, 15, 20, and 30. Fig. 3-11 presents a diagram with the results including a trend line.

The dependence of T_{oc} on concentration for trehalose is found similar to the one for sucrose. The correlation was found to be exponential. In addition, the adsorption effect of water for high concentrated solutions could be verified. However, there are differences in the course of the curves for the two disaccharides.

For trehalose, the course of the curve is more linear. In addition, ΔT_{oc} was found to be only 3.2°C (compared to 5.1°C for sucrose) between the different concentrations. The effect that T_{oc} is lower for higher concentrations was shifted to 30% so that the maximum T_{oc} for trehalose was determined for 20% (about -27°C).

The most outstanding difference refers to the collapse temperature interval which ranges from about -30°C to -27°C for trehalose compared to about -35°C to -30°C for sucrose. One of the reasons for all those differences might be the different chemical structure of the substances although they both represent disaccharides.

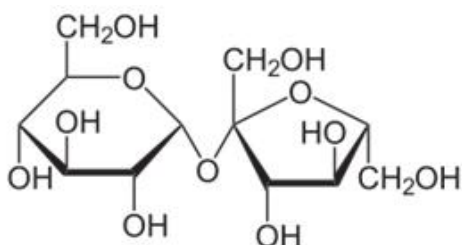


Fig. 3-12: Chemical structure of sucrose

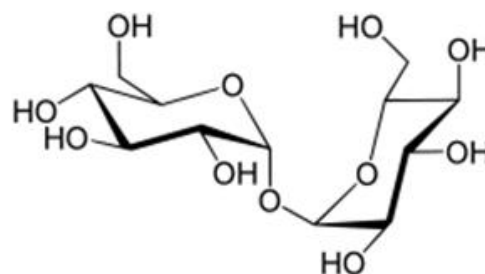
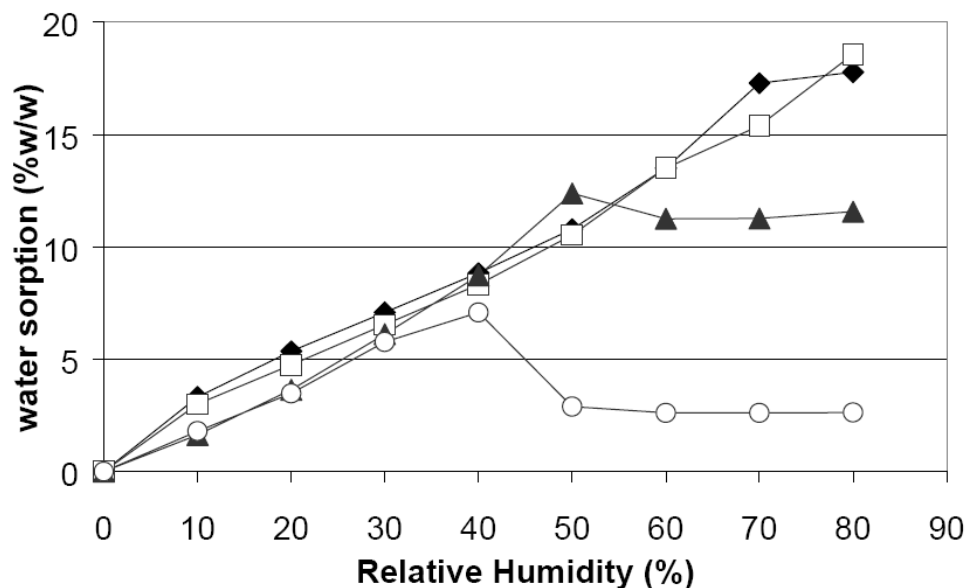


Fig. 3-13: Chemical structure of trehalose

As presented in Fig. 3-12 and Fig. 3-13 both disaccharides have eight polar OH groups. Sucrose is not stable to acid hydrolysis because of its acetal structure, whereas trehalose is stable to this kind of chemical reaction [45]. Concerning residual water after freeze-drying, sucrose requires a good control of residual moisture of the product due to its higher hygroscopicity [182]. In contrast, trehalose shows a good stability even at elevated residual moisture content [45].

The key factor for influencing collapse behavior is probably the hygroscopicity (for the dry substances) or water binding affinity (for the molecules in the glass) of the two sugars. It was found recently, that trehalose shows a higher hygroscopicity than sucrose for a relative humidity higher than 30% [184]. Fig. 3-14 shows the water vapor isotherm of lyophilized sugars including sucrose and trehalose at 25°C in comparison.

From 40% onwards, sucrose adsorbs significantly more water than trehalose, both having an adsorption level between a relative humidity of 50 to 80%.



Water vapour sorption isotherms of lyophilised sugars at 25°C (Key: ◆: inulin DP23, □: inulin DP11, ▲: trehalose, ○: sucrose)

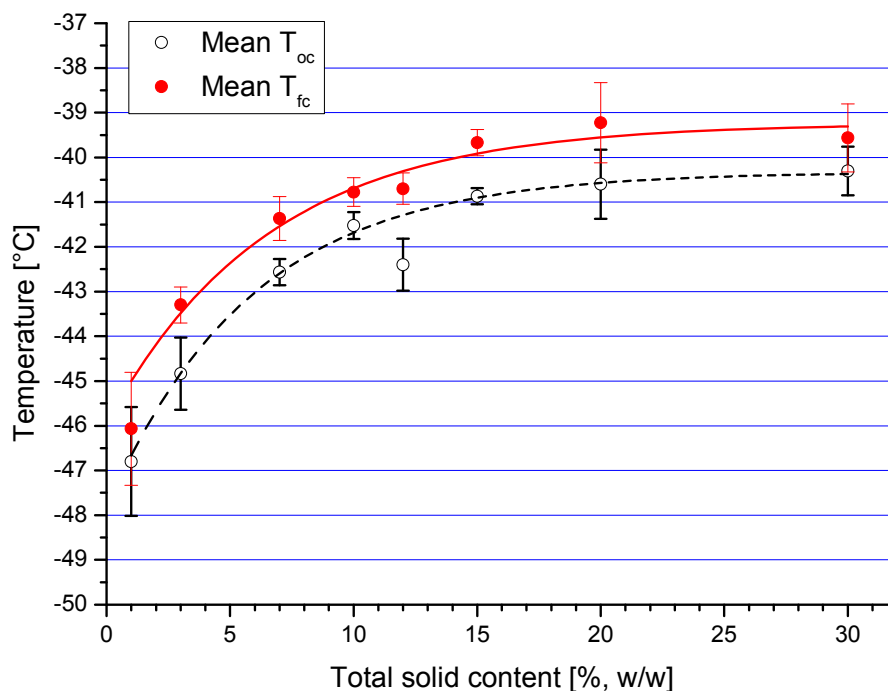
Fig. 3-14: Hygroscopicity of sucrose and trehalose in comparison [184]

A similar investigation was published in 2000 by Fakes and co-workers [183]. Both publications are relevant for FDM experiments since the relative humidity in the sample is thought to be $\geq 30\%$ during sublimation due to the very low layer thickness of the sample (25 μm), the small sublimation interface ($3 \cdot 10^{-3} \text{ cm}^2$), and the high resistance to water vapor flow.

As explained in detail before, water binding strongly affects the temperature at which the rigidity of the product walls is plasticized by water [79, 117] and leads to viscous flow. This effect and the slight differences in chemical structure seem to be so strong that the T_{oc} interval of sucrose (-35 to -30°C) is shifted to a much higher temperature interval for trehalose (-30 to -27°C).

In the next chapters, differences in the physical properties of the initial solutions were measured in order to investigate collapse parameters in more detail and to correlate them to T_c values.

3.2.1.3 Glucose solutions



T_{oc}

Equation $y = A \cdot \exp(-x/t) + y_0$

Parameter	Value	sdv	R^2	0.920
A	-7.53	1.06	Reduced X^2	0.799
t	5.84	1.29		
y_0	-40.3	0.343		

T_{fc}

Equation $y = A \cdot \exp(-x/t) + y_0$

Parameter	Value	sdv	R^2	0.940
A	-6.72	0.669	Reduced X^2	0.666
t	6.54	1.80		
y_0	-39.2	0.498		

Fig. 3-15: Dependence of T_{oc} and T_{fc} on total solid content for glucose solutions, exponential fit, mean values with 90% confidence intervals

In contrast to sucrose and trehalose, glucose does not show the effect of lower T_c values for higher concentrated solutions in its T_c vs. total solid content curves which are shown in Fig. 3-15. This is due to the fact that glucose (cf. Fig. 3-16) is significantly less hygroscopic than sucrose or trehalose [185]. For both T_{oc} and T_{fc} values, exponential trends of their correlation to concentration were found.

T_{oc} values ranged from about -47 to -40.5°C , and T_{fc} values from about -46°C to -39.9°C . The difference ΔT_c between both was determined relatively constant at 1°C .

The explanation of the impact of total solid content on T_c follows the discussion of effects for trehalose and sucrose given before.

In comparison to the disaccharides discussed before, the amorphous product matrix built by glucose during cooling appears to be significantly less stable against water binding during sublimation, which would explain its very low T_c values. This is probably due to the small size of the molecule [185].

The overall difference on T_{oc} or T_{fc} values, respectively, was detected to be about 6.5°C . This means that for glucose the product matrix gets significantly more stable when more molecules are present so that the importance of the small size of the molecule is decreased.

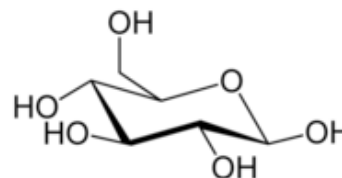
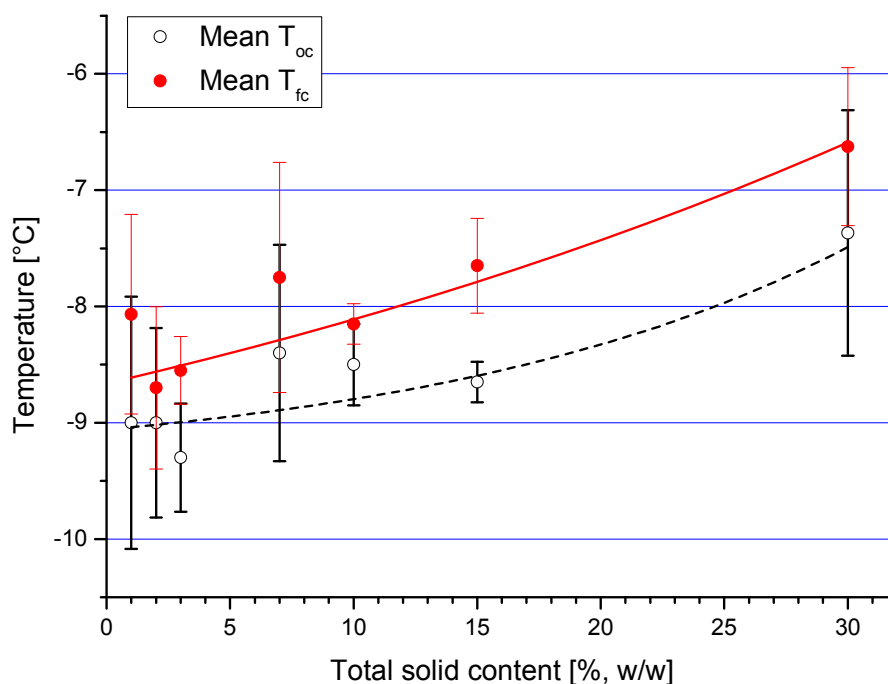


Fig. 3-16: Chemical structure of glucose

3.2.1.4 (2-Hydroxypropyl)- β -cyclodextrin solutions T_{oc}

Equation		$y = A \cdot \exp(-x/t) + y_0$		
Parameter	Value	sdv	R^2	0.414
A	0.333	0.729	Reduced X^2	0.385
t	-17.2	18.8		
y_0	-9.39	0.958		

 T_{fc}

Equation		$y = A \cdot \exp(-x/t) + y_0$		
Parameter	Value	sdv	R^2	0.849
A	2.34	4.30	Reduced X^2	0.232
t	-47.3	64.9		
y_0	-11.0	4.44		

Fig. 3-17: Dependence of T_{oc} and T_{fc} on total solid content for (2-hydroxy-propyl)- β -cyclodextrin solutions, exponential fit, mean values with 90% confidence intervals

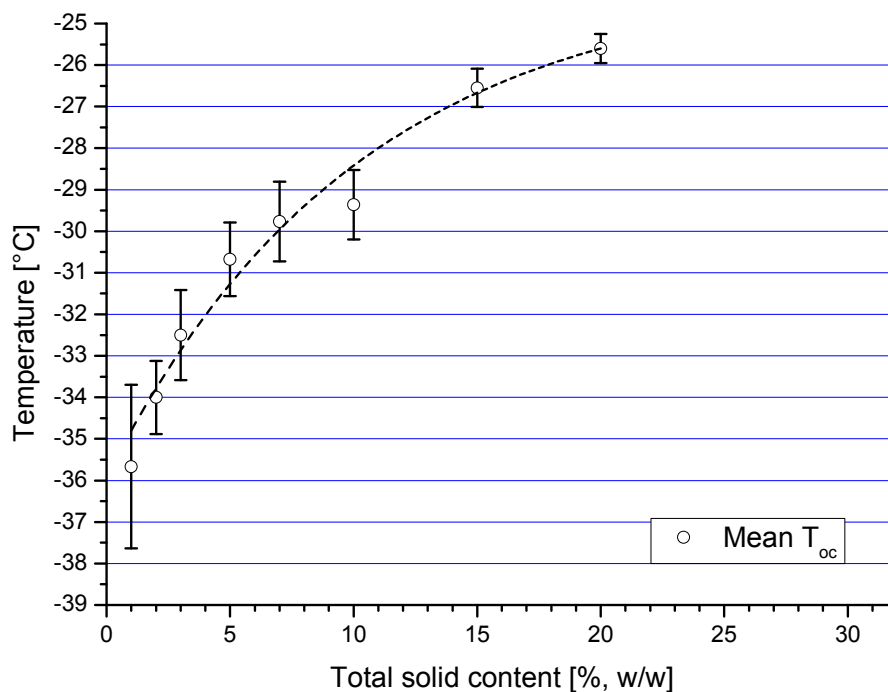
Fig. 3-17 presents the results for (2-hydroxy-propyl)- β -cyclodextrin. In contrast to glucose (as well as sucrose/trehalose) this excipient showed very high T_c values.

T_{oc} was found between about -9 and -7.5°C , T_{fc} between about -8.5 and -6.5°C which might be explained by the very different structure of this substance. Cyclodextrins are cyclic oligosaccharides consisting of 6, 7, or 8 glucopyranose units with hydrophobic interiors, usually referred to as α -, β -, or λ -cyclodextrins, respectively. The cavity diameter of β -cyclodextrins or 7-glucopyranose unit compounds is 7.5 \AA , and they are therefore most commonly used as complexing agents [62]. Because of its very high T_c values, (2-hydroxy-propyl)- β -cyclodextrin is frequently used as a “collapse temperature modifier” in formulations [44].

The amorphous product matrix formed by (2-hydroxy-propyl)- β -cyclodextrin during cooling seems to be quite rigid and resistant to collapse. This is reflected in the following observations: (1) T_c (T_{oc} and T_{fc}) values are extremely high. (2) The difference ΔT_c between T_{oc} and T_{fc} is only about 0.5°C in average. (3) The overall difference between lowest and highest values for T_{oc} and T_{fc} is only about 1.5 to 2°C .

In contrast to all other excipients measured in this study, (2-hydroxy-propyl)- β -cyclodextrin showed a contrary curvature of the trend-line for T_{oc} and T_{fc} values which is reflected in a positive value of A in the relevant equations. Because of the small differences in T_c values, this observation is not further discussed and is assumed to be not important for collapse behavior determination.

3.2.1.5 Polyvinylpyrrolidone 10 kDa solutions



Equation	$y = A \cdot \exp(-x/t) + y_0$			
Parameter	Value	sdv	R^2	0.979
A	-12.0	0.748	Reduced X^2	0.440
t	10.2	2.60		
y_0	-23.9	1.04		

Fig. 3-18: Dependence of T_{oc} on total solid content for PVP 10 kDa solutions, exponential fit, mean values with 90% confidence intervals, T_{fc} were approximately 0.5 to 1°C higher than T_{oc} values.

Polyvinylpyrrolidone (PVP) 10 kDa solutions (cf. Fig. 3-18) showed a very strong dependence of T_c values on concentration. The overall difference for T_{oc} was found to be about 10°C, ranging from ~ -35.5°C to ~ -25.5°C.

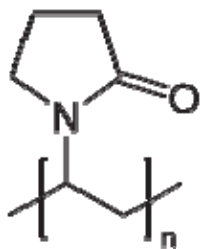


Fig. 3-19: Structure of PVP

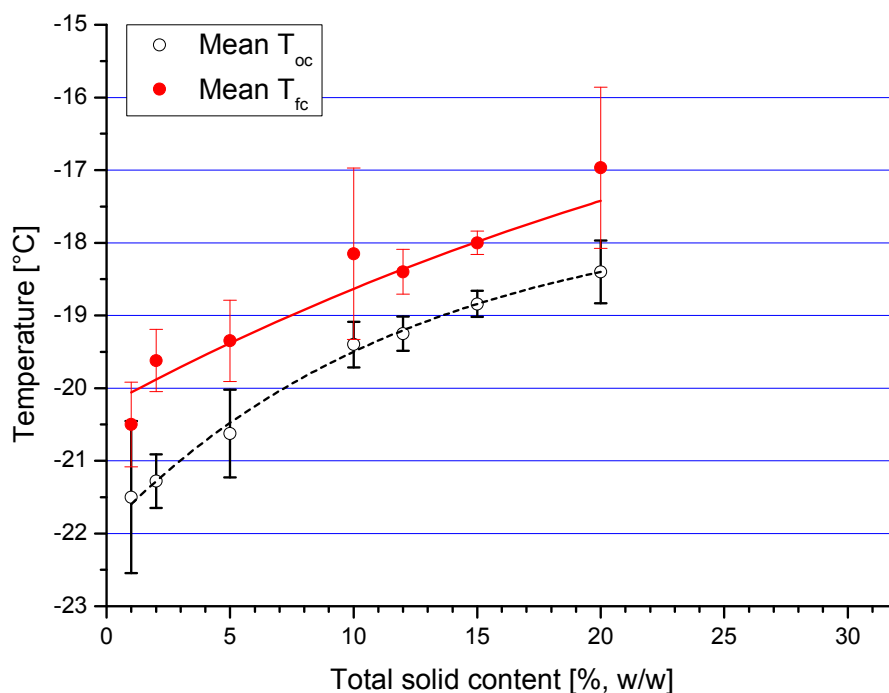
PVP is a hygroscopic polymer [183] the structure of which is outlined in Fig. 3-19. Because of experimental difficulties only PVP solutions of up to a total solid content of 20% could be measured. Higher concentrations had a very high density so that sublimation was very low or not observable and collapse was not determinable.

Therefore, the high dependence of PVP 10 kDa on concentration is on the one hand explained by the hygroscopicity of the substance [183], although the effect of a lower T_{oc} for higher concentrations could not be observed (in comparison to sucrose and trehalose) due to the measurement difficulties explained before. On the other hand, the size of the 10 kDa polymer is limited (compared to e.g., PVP 40 kDa) so that concentration has a higher impact on T_c .

The curvature of the T_{oc} vs. total solid content trend-line was found to be exponential.

If stabilizing functions of PVP 10 kDa are proven in a concentration range for a given formulation, the found T_{oc} vs. concentration curve suggests to slightly increase the total solid content of PVP 10 kDa in the formulation in order to increase T_c , or alternatively to exchange it by PVP 40 kDa (see below).

3.2.1.6 Polyvinylpyrrolidone 40 kDa solutions



T_{oc}	Equation $y = A \cdot \exp(-x/t) + y_0$				
	<i>Parameter</i>	<i>Value</i>	<i>sdv</i>	R^2	0.994
	A	-4.43	0.312	<i>Reduced X^2</i>	0.0513
	t	12.5	2.17		
	y_0	-17.5	0.373		
T_{fc}	Equation $y = A \cdot \exp(-x/t) + y_0$				
	<i>Parameter</i>	<i>Value</i>	<i>sdv</i>	R^2	0.938
	A	-6.52	11.1	<i>Reduced X^2</i>	0.327
	t	35.3	78.4		
	y_0	-13.7	11.3		

Fig. 3-20: Dependence of T_{oc} and T_{fc} on total solid content for PVP 40 kDa solutions, exponential fit, mean values with 90% confidence intervals

Compared to PVP 10 kDa, PVP 40 kDa has much higher T_{oc} and T_{fc} values (see Fig. 3-20). Here, the importance or impact of the chain length of PVP molecules can be studied. T_{oc} values range from about -21.5 to -18.5°C which means a difference of only 3°C.

T_{fc} values are in the temperature range starting from -20.5°C to -17°C (difference: 3.5°C).

This results in a ΔT_c of about 1.5 to 2°C .

Although the only difference between PVP 10 kDa and PVP 40 kDa (which are both mixtures of molecules with different chain lengths resulting in 10 or 40 kDa in average, respectively) is the length of the chains, the collapse behavior is highly influenced. The amorphous PVP 40 kDa product matrix is characterized by a much stronger resistance to collapse and by a higher rigidity concerning viscous flow [104]. This observation might also be transferable to other types of polymers. The 4-fold chain length leads to an increase of T_{oc} of about 14°C (lowest concentration) to 8.5°C (highest concentration) and a change in ΔT_{oc} from about 10 to about 3°C .

As already described for PVP 10 kDa, high concentrations of PVP 40 kDa could not be measured. Therefore, the impact of hygroscopicity on secondary drying of solutions with a high total solid content could not be determined.

With regard to curvature of the trend-lines, the PVP 40 kDa solutions are only slightly exponentially correlated (almost linear), whereas the PVP 10 kDa experiments show a significant exponential curve.

3.2.1.7 Summary: dependence of T_c on total solid content for all excipients

Comparing the results of all excipients used for T_c vs. concentration measurements (cf. Tab. 1-1) some trends become obvious: (1) In a given excipient class (e.g., saccharides), T_c increases with a higher molecular weight or chain length and the difference ΔT_{oc} or ΔT_{fc} decreases. (2) Hygroscopic substances show a decrease of T_c values for high (about 20 or 30%) total solid contents. (3) For all excipients an exponential correlation could be determined.

Tab. 3-18: Comparison of dependence of T_c on total solid content for all excipients used

Excipient	T_c interval [°C]	ΔT_{oc} [°C]	ΔT_{fc} [°C]	Fit/trend	Peculiarities
Sucrose	-35 to -30	5.1	-	exponential	adsorption effect for high concentrations
Trehalose	-30 to -27	3.2	-	exponential	adsorption effect for high concentrations
Glucose	-47 to -39.5	6.5	6.5	exponential	none
(2-Hydroxy-propyl)- β -cyclodextrin	-9 to -6.5	1.6	1.4	exponential	curve shape exception
PVP 10 kDa	-35.5 to -25.5	10.1	-	exponential	none
PVP 40 kDa	-21.5 to -17	3.1	3.5	exponential	none

With regard to R^2 values, all excipient curve fits showed acceptable values (>0.8), only for the T_{oc} vs. concentration curve of 2-(hydroxy-propyl)- β -cyclodextrin it was not (0.414).

3.2.2 Concentration vs. density

In order to measure surface tension and viscosity of the excipient solutions, density was measured by using a pycnometer and solutions of 1.5, 2, 3, 5, 7, 10, 12, 15, 20 and 30% total solid content. For sucrose and trehalose Fig. 3-21 and Fig. 3-22 present density data determined at 0°C and 20°C. Both disaccharides show a linear correlation which is parallel for both concentrations.

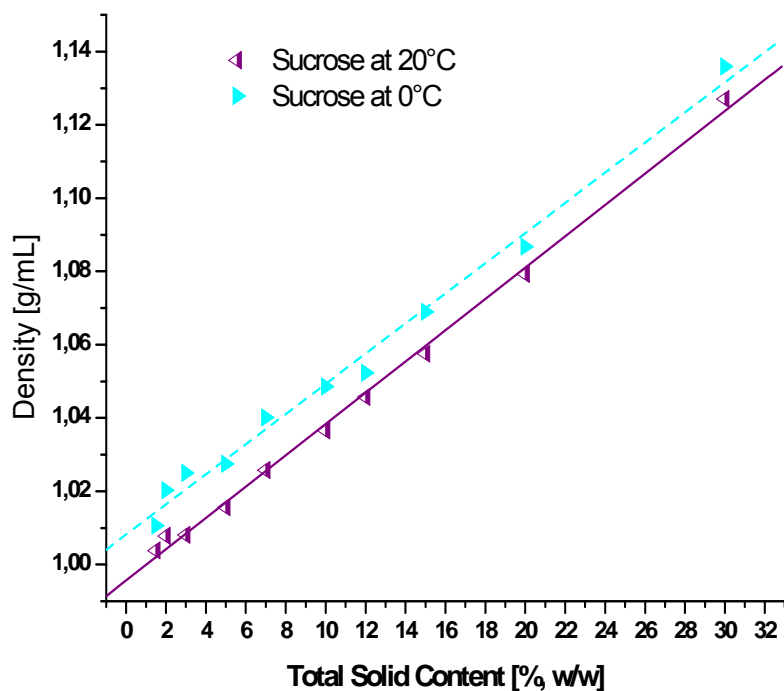


Fig. 3-21: Density of sucrose solutions in dependence on total solid content at 0°C and 20°C

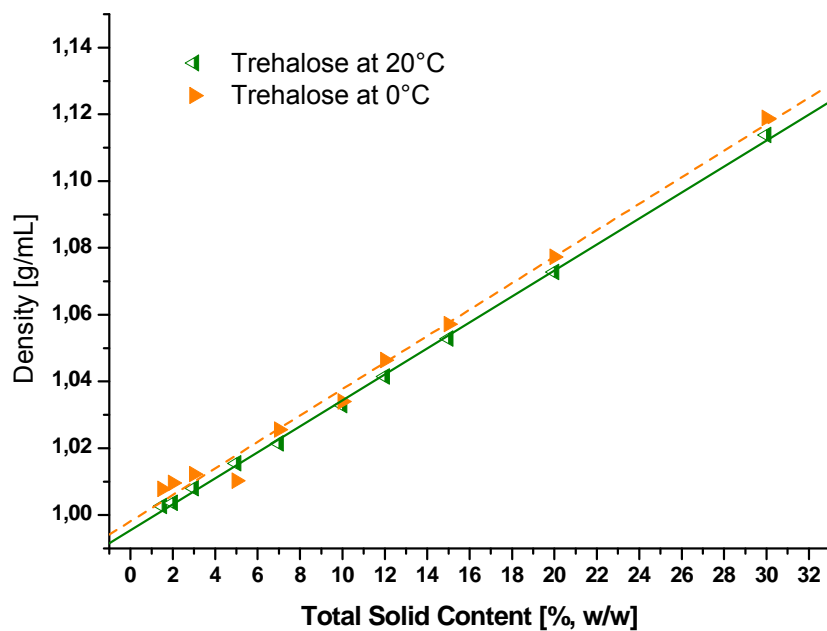


Fig. 3-22: Density of trehalose solutions in dependence on total solid content at 0°C and 20°C

Sucrose was found to have the highest density, followed by glucose, trehalose and 2-(hydroxypropyl)- β -cyclodextrin. The curves of all the mentioned substances are mainly parallel, whereas PVP 40 kDa showed the lowest density (between ~ 1.00 and 1.07 g/mL) which increased to a less degree with increasing concentration.

3.2.3 Concentration vs. surface tension

As mentioned earlier, surface tension is the driving force for the plasticized product wall to flow into the pore [113] which is illustrated in the variables of Eq. 1-5.

To get an impression of this driving parameter, the dynamic interfacial tension (which is here equivalent to surface tension) of sucrose and trehalose was measured at 0°C (the lowest possible temperature for this type of measurement) in dependence on total solid content. Solutions were concentrated as follows: 3, 5, 10, 20 and 30% w/w.

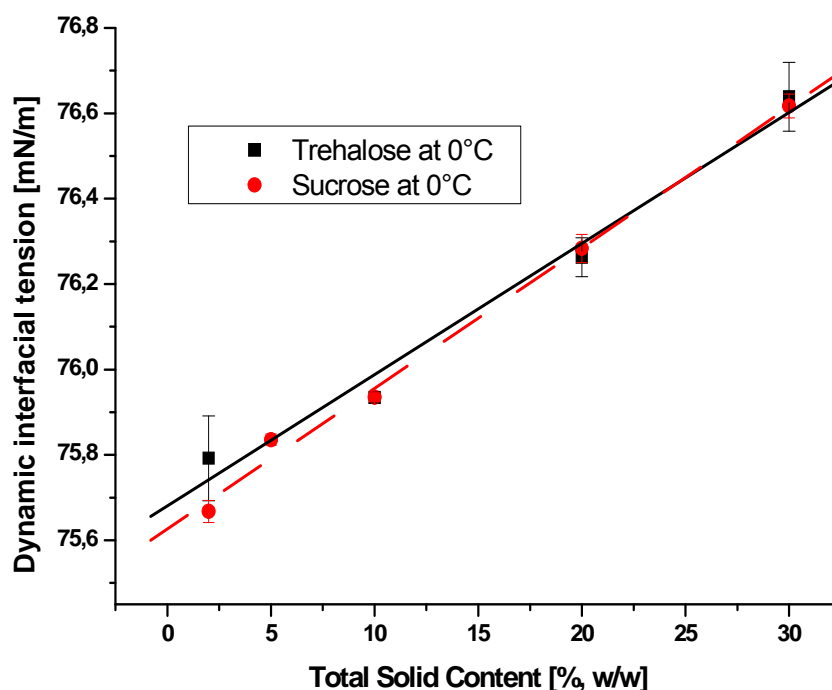


Fig. 3-23: Dynamic interfacial tension of sucrose and trehalose at 0°C

It is well known that the sugars used in this study cause an increase of surface tension in water [186]. As expected, surface tension for both disaccharides was determined to be approximately the same, i.e. in the range from about 75.7 to 76.6 mN/m. This means that surface tension increases by only 1.1% if comparing a 3% to a 30% solution. In contrast, the increase of T_{oc} was 14% for sucrose (-35 to -30°C) and about 10% for trehalose (-30 to -27°C).

It is obvious from the introduced parameter model on p. 68 that surface tension does not influence collapse behavior directly, but that viscosity is much more important concerning freezing and freeze concentration processes during freezing. Indeed, surface tension measurements strengthen the hypothesis of surface tension being the driving force. For 3% solution of sucrose, for instance, which is freeze-concentrated to 81% sucrose (cf. p. 8) an increase of surface tension by only ~3.2% would be expected (calculation by values measured at 0°C). When water is adsorbed during primary drying and temperature increases, surface tension is lowered again, but is still in the same range. Collapse therefore is limited by the rigidity of the product walls with surface tension as a “background” force “acting” as soon as viscosity of the walls has reached a critical level.

3.2.4 Concentration vs. viscosity

Viscosity – which represents the inner friction of solutions – is the vital parameter influencing the process of freeze concentration during cooling [6; 17] (cf. chapter 1.2.1). It governs the total solid content of ice for a given concentration of solved substance [15]. In addition, it is related to the ratio of water molecules to excipient molecules in the glass because it stops further ice crystal growth when reaching a critical limit [9].

To deepen the understanding of Eq. 1-6 to Eq. 1-10, and of the differences in collapse behavior for different excipients and different concentrations of one and the same excipient, viscosities of various solutions were measured. Concentrations were varied as follows: 1.5, 2, 3, 5, 7, 10, 12, 15, 20 and 30% (w/w).

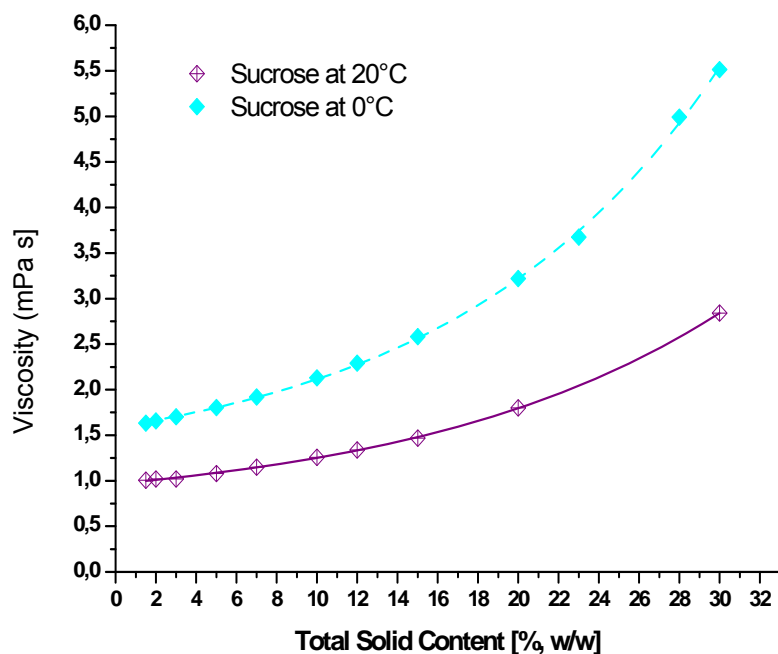


Fig. 3-24: Viscosity of sucrose solutions in dependence on total solid content measured at 0°C and 20°C

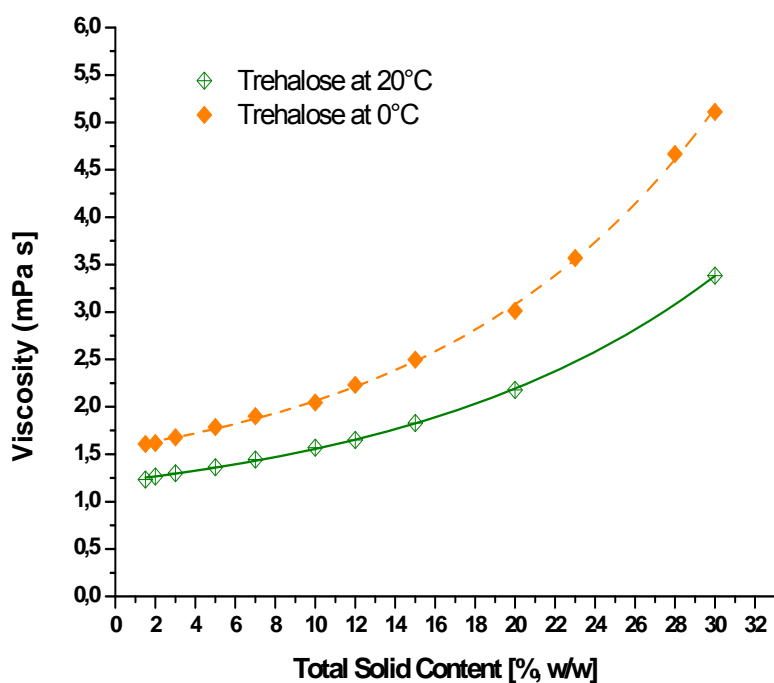


Fig. 3-25: Viscosity of trehalose solutions in dependence on total solid content measured at 0°C and 20°C

Fig. 3-24 and Fig. 3-25 show viscosity values of sucrose and trehalose vs. concentration, measured at 20°C and 0°C solution temperature. Both excipients show approximately similar curves for viscosity measured at 0°C, although values for 20°C are slightly higher for the trehalose solutions. The average increase in viscosity for sucrose is about 3.6% per 1°C and for trehalose about 1.7% every 1°C (in average over the entire concentration range).

For sucrose as well as for trehalose the dependence of viscosity on temperature is not linear. Sucrose solutions have an increase of viscosity of about 3.1%/°C for the 1.5% ranging to about 4.7%/°C for the 30% solution (difference of 1.6%/°C), compared to trehalose with about 1.5%/°C for 1.5% total solid content and a maximal increase of 2.6%/°C for 30% (difference of 1.1%/°C). Both correlations follow exponential functions which can be clearly seen in Fig. 3-24 or Fig. 3-25, respectively. Interestingly, T_{oc} vs. concentration curves showed as well a higher impact of concentration for sucrose compared to trehalose curves (cf. Tab. 3-18).

When comparing viscosity vs. concentration curves measured at 20°C for all excipients used for the FDM experiments described before (Fig. 3-26), PVP 10 kDa and 40 kDa showed a very strong dependence on total solid content with similar curves and curvatures (viscosity range from 2 to 159 mPa s), whereas the other excipients showed values in a totally different range of 1.6 to 8.4 mPa s (cf. Fig. 3-27).

For T_{oc} values big differences between PVP 10 kDa and 40 kDa were revealed which were not reflected in measured viscosity values. Similar results were found for the other excipients: 2-(hydroxypropyl)- β -cyclodextrin showed the highest dependence of viscosity on concentration, but a lower dependence of T_{oc} on concentration (ΔT_c 2.5°C) compared to e.g., glucose with a ΔT_c of 7.5°C.

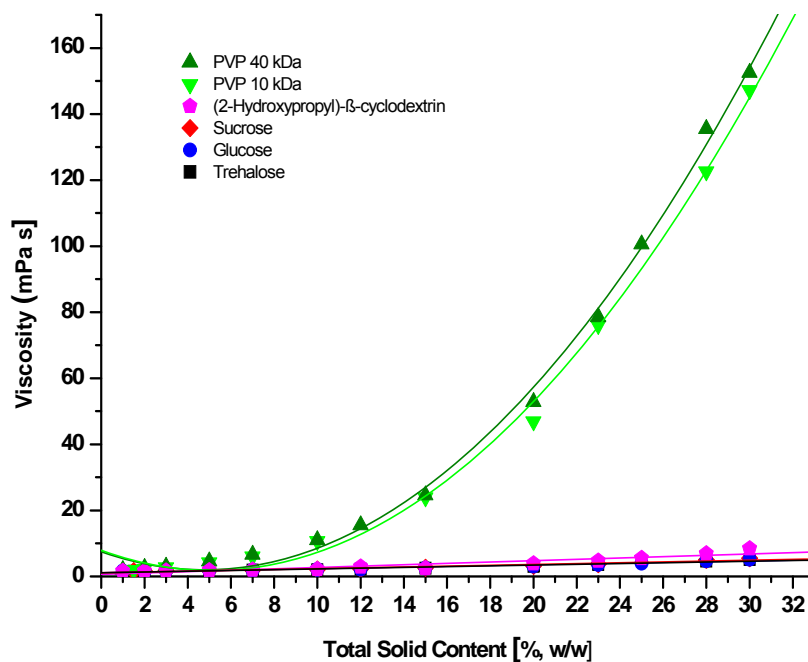


Fig. 3-26: Viscosities of various excipients in dependence on total solid content measured at 20°C

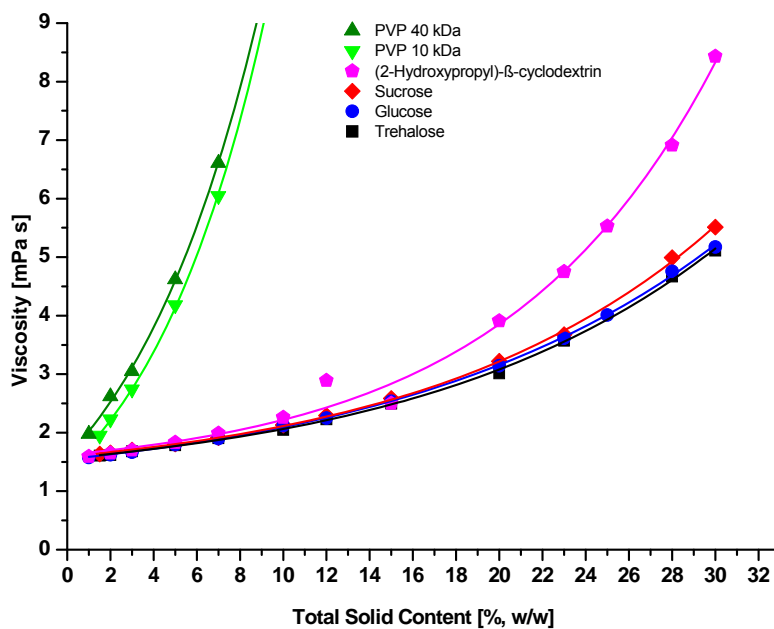


Fig. 3-27: Viscosities of various excipients in dependence on total solid content measured at 20°C, detailed view

Based on these data, one may conclude that in general the measurement of viscosity of the initial solutions used for FDM experiments does not allow a prediction of collapse behavior impacted by total solid content. Instead, chemical structures of the substances (including their size) and in particular hygroscopicity of the dried initial substance seem to have an important influence on collapse behavior.

3.2.5 Impact of nucleation on concentration dependence of collapse temperatures

For selected excipients (glucose, 2-(hydroxypropyl)- β -cyclodextrin, and PVP 40 kDa), nucleation temperatures (T_n) were correlated with measured T_{oc} values. Fig. 3-28 to Fig. 3-30 show measured T_n values for different solution concentrations of the single excipient measurement rows. Supercooling could not be controlled and no correlation between T_n and concentration could be determined.

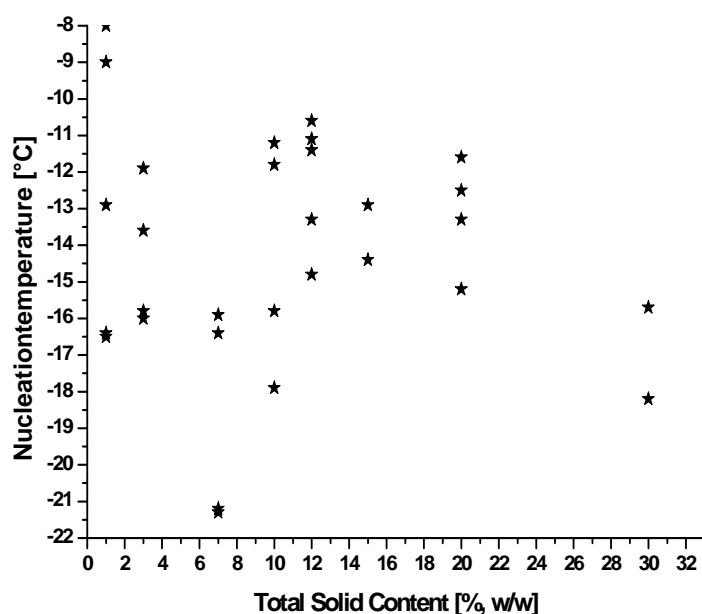


Fig. 3-28: Nucleation temperature of glucose solutions vs. total solid content

For 2-(hydroxypropyl)- β -cyclodextrin e.g., a correlation coefficient of 0.48 was calculated for T_{oc} vs. concentration values. In turn, this means that if all measured values are used for calculation no correlation was found. Calculations for glucose and PVP 40 kDa were similar.

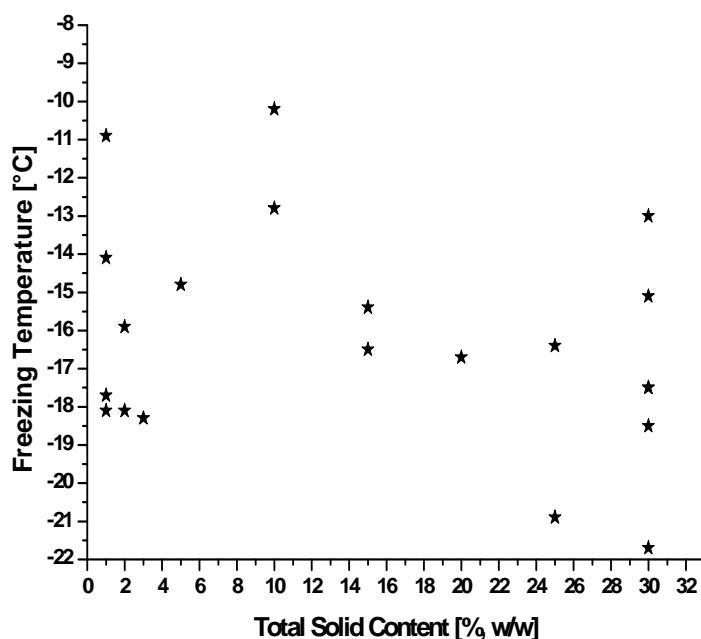


Fig. 3-29: Nucleation temperature of 2-(hydroxypropyl)-β-cyclodextrin solutions vs. total solid content

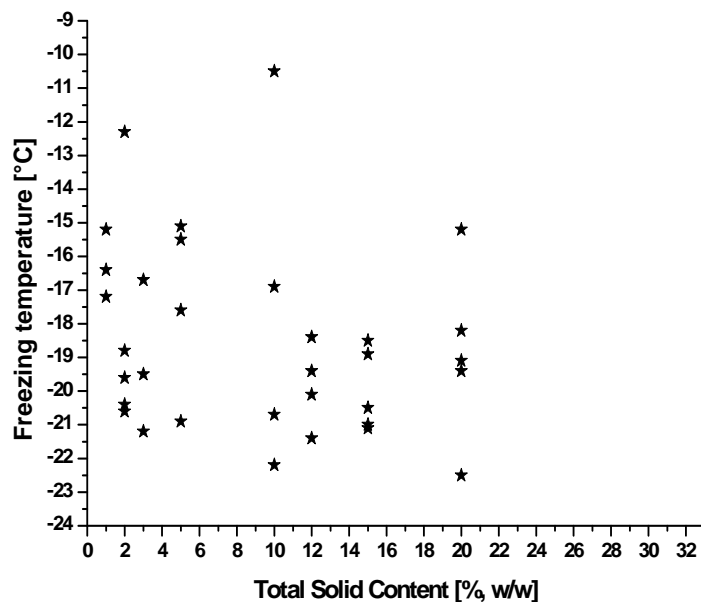


Fig. 3-30: Nucleation temperature of PVP 40 kDa solutions vs. total solid content

This finding was surprising because deviations in T_c values should be at least in part a result of differences in T_n (or supercooling, respectively) [21].

It is very likely that random circumstances (e.g., the surface of the glass cover slides) influence the frozen structure in addition so that the impact of T_n is not significant strong [21]. Moreover, T_c detection is difficult for very low (1.5 to 3%) and high concentrated solutions. For example, FDM measurements for 20% solutions of PVP 40 kDa are tricky due to the high density of the frozen material and the limited

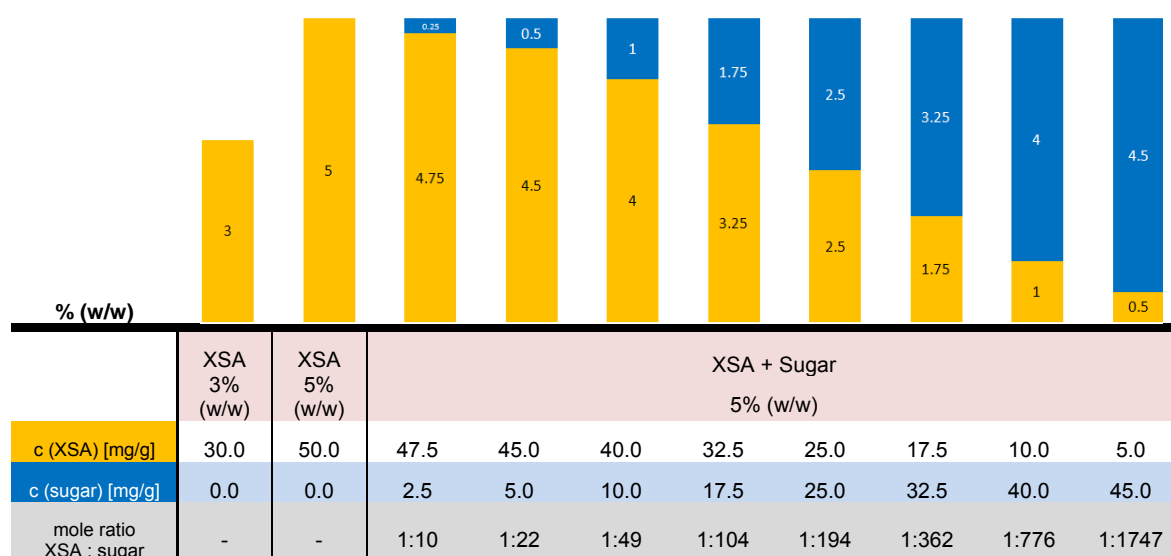
light source capabilities. These observations may contribute to the unfavorable correlation coefficients.

3.3 Collapse behavior of binary mixtures with model proteins

3.3.1 Composition of solutions

Tab. 3-19 shows the composition of single aqueous solutions used in this section of the study. BSA and HSA, introduced in the materials and methods section were used as model proteins. They were prepared as pure solutions (3% and 5% w/w) and in mixtures with sucrose or trehalose, all with a total solid content of 5% (50 mg/g).

Tab. 3-19: Composition of solutions for investigation on collapse behavior of binary mixtures with BSA and HSA as model proteins



To obtain a different stabilizer to protein mole ratio, the ratio of the BSA/HSA to disaccharide concentration was varied. Ratios were calculated using the molecular weights given in the section 2.1.3. In the following text the composition of the mixture is further reported as “sugar/protein mole ratio” following Cleland, et al. [74]. Results were compared with means of pure sucrose and trehalose solution results from chapter 3.2.1.

3.3.2 Dependence of collapse temperature on nucleation temperature

For every measured sample nucleation temperature (T_n) was determined. Fig. 3-31 and Fig. 3-32 provide the single values for the pure solutions and the binary mixtures. For

both measurement rows, T_n was found in a range from approximately -9 to -20°C which is in good agreement with the degree of supercooling found for laboratory scale freeze-drying runs [6, 7].

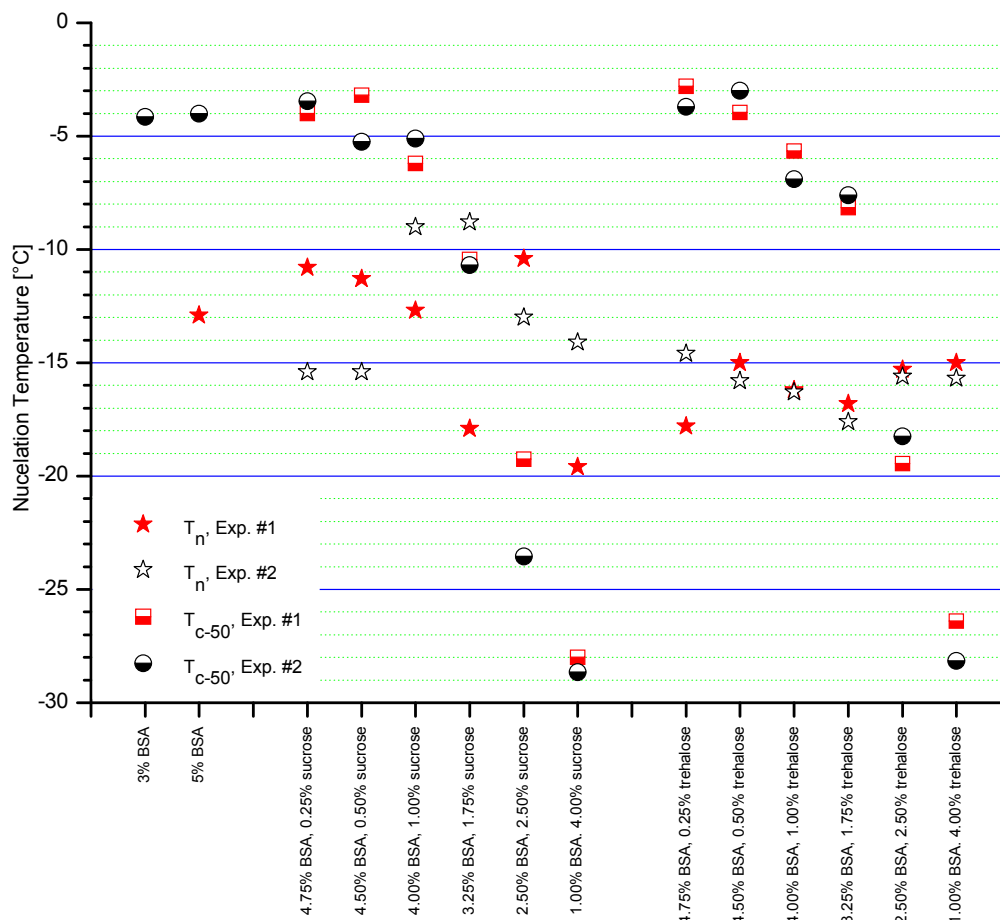


Fig. 3-31: T_n and T_{c-50} vs. composition of samples for pure BSA and BSA + sugar mixtures

As already mentioned in the section on freeze-drying, T_n can not be controlled during freeze-drying runs. This is also true for FDM experiments. The presented results underline this statement:

For example, a difference of up to 9°C was found for duplicate measurements for a mixture of 3.25% BSA with 1.75% (w/w) sucrose (cf. Fig. 3-31) and of up to 8°C for a mixture of 1% HSA with 4% sucrose (cf. Fig. 3-32).

There are hints given in the literature that T_n affects T_c . Here, it was found that differences in cooling rate produced differences in pore size in the order of a factor of two [26, 104]. A product with a higher T_n tends to form larger ice crystals during the cooling step which leads to a lower resistance to water vapor flow during primary drying and maybe a higher mass flow rate [21]. This might impact the T_c of a given structure during FDM measurements.

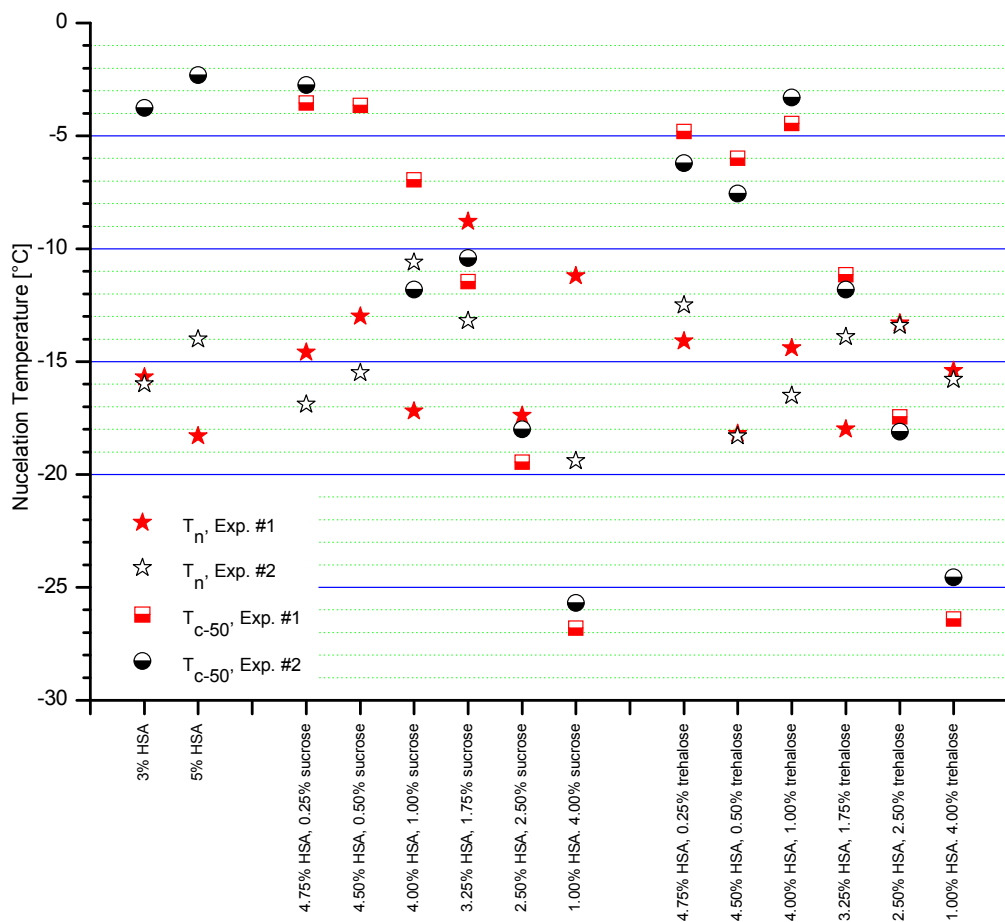


Fig. 3-32: T_n and T_{c-50} vs. composition of samples for pure HSA and HSA + sugar mixtures

For the measured values, no correlation between T_n and T_{c-50} could be revealed. Having a critical look at Fig. 3-31, the mixture of 1% BSA with 4% (w/w) sucrose showed a difference of 5.5°C between nucleation temperatures of identical measurements, but T_{c-50} was -28.0 and -28.7°C, respectively. In contrast, the solution with 4% BSA and 1% trehalose had a practically identical T_n showing a ΔT_{c-50} of 1.2°C. Fig. 3-32 presents similar results for HSA binary mixtures: 3.25% (w/w) HSA with 1.75% (w/w) trehalose resulted in ΔT_n of 4.1°C with a ΔT_{c-50} of only 0.6°C, whereas the 1% (w/w) HSA + 4% (w/w) trehalose solution showed a ΔT_n of only 0.4°C, but a ΔT_{c-50} of 1.8°C.

3.3.3 Dependence of collapse temperature on binary mixture composition

It is common knowledge that T_p during primary drying should not exceed T_c [24, 104]. Some recent reports however showed that drying above T_c might not have negative effects on the product. For example, Johnson and co-workers found that freeze-drying of cytokine plus sucrose systems with increasing protein concentration (total solid content of sucrose matrix constantly 25 mg/mL) below and well above T_{micro} (which corresponds to T_{oc}) during primary drying had no negative effects concerning shrinkage, water content and stability [158]. For the authors, the interpretation of T_{macro} (equivalent to T_{fc}) was additionally difficult, especially for high cytokine content.

Therefore, the impact of the ratio of stabilizer (sucrose or trehalose) to protein (BSA or HSA) on T_c (T_{oc} , T_{c-50} and T_{fc}) was investigated in detail. Measurements were performed in duplicate using the same experimental procedure. The results of these studies are visualized in Fig. 3-33 and Fig. 3-34.

First, no significant differences in T_{oc} , T_{fc} and T_{c-50} were found between BSA and HSA + disaccharide mixtures fulfilling the expectations about the similarity of the two proteins concerning their collapse behavior. Although it was found that between sucrose and trehalose there is a significant difference in T_{oc} , their contribution to the T_c in the binary mix-

tures is similar. At a given mole ratio, both rows of mixtures (with either sucrose or trehalose) were found in the same temperature range ($\pm 2^\circ\text{C}$).

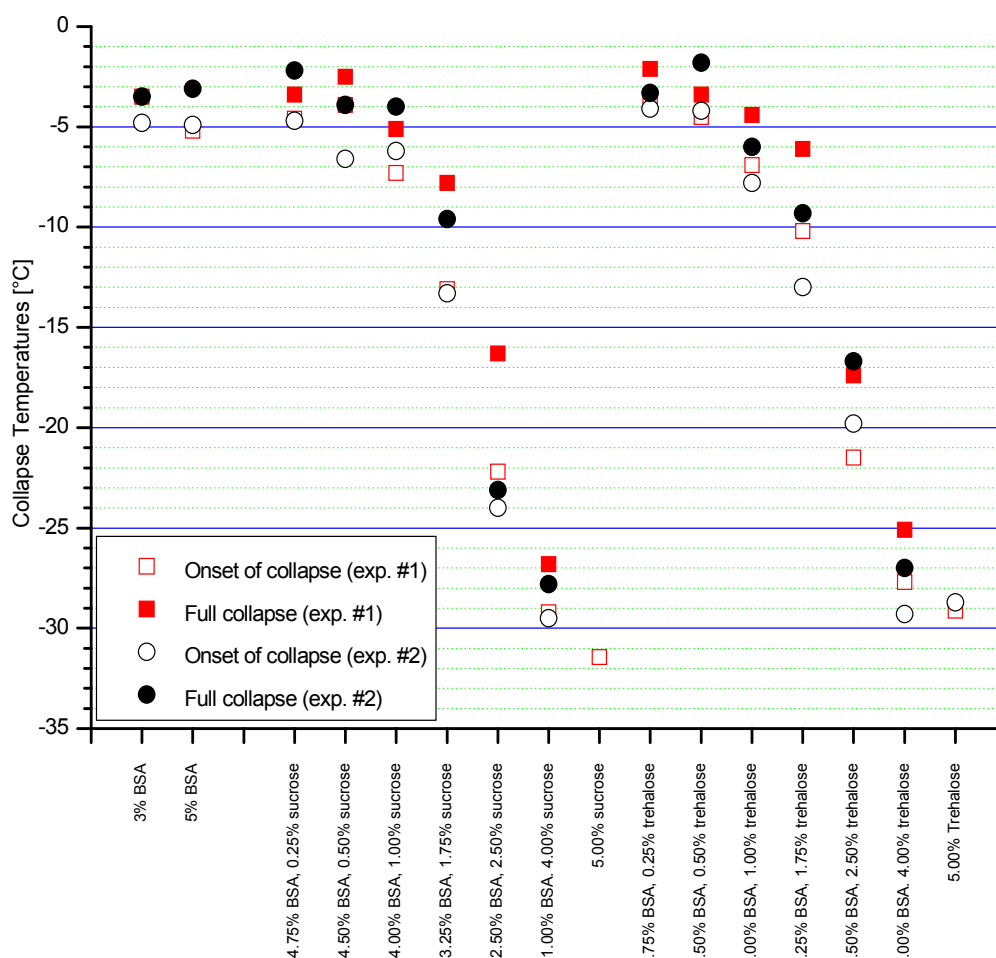


Fig. 3-33: Dependence of collapse temperatures on composition of samples for pure BSA, BSA + sugar mixtures and pure sugar

One of the questions to be answered in this thesis was whether a T_c detection for pure proteins like BSA and HSA is possible. For all measurements of both pure solutions with total solid contents of 3 and 5% (w/w) a T_{oc} could be clearly measured.

Although ice melting was observed in the temperature range of -3°C , the structural alterations of this melting event were significantly different from those of the collapse event. T_{fc} could not be determined for all measurements since the ice melt overlapped with the collapse.

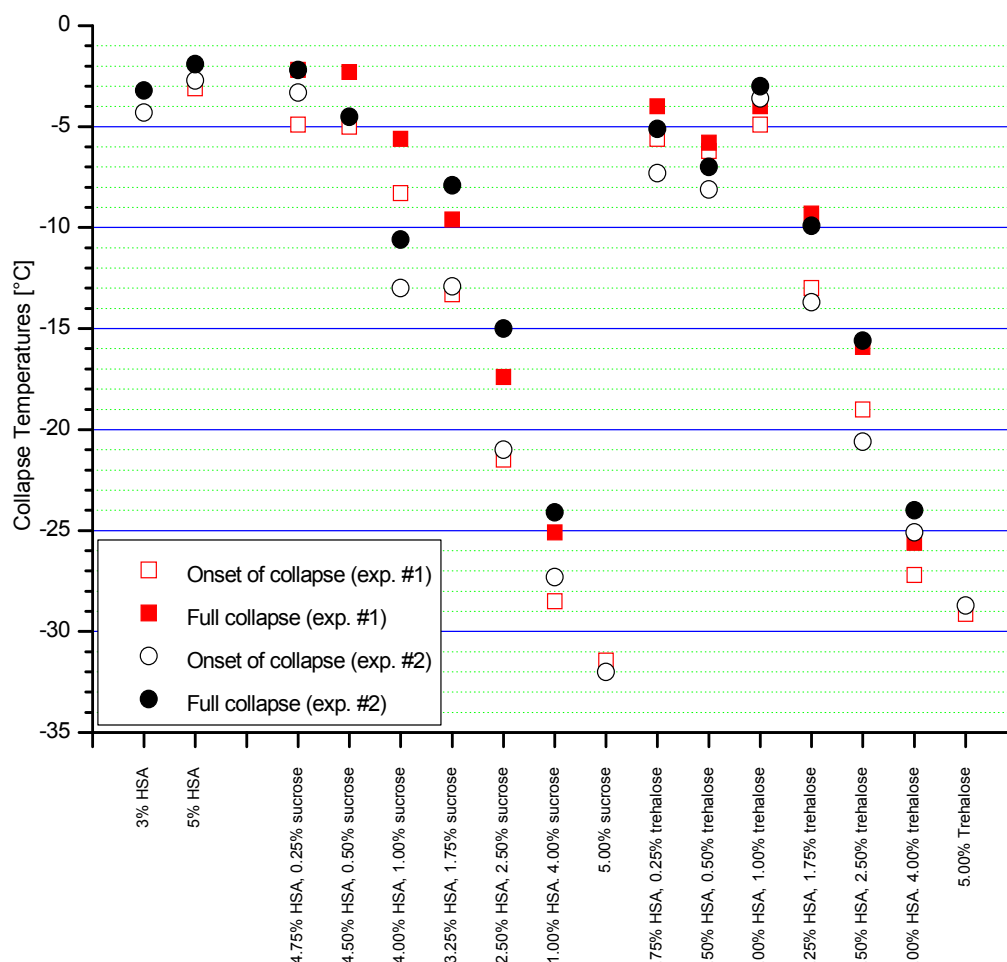


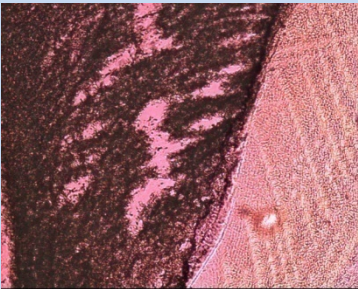
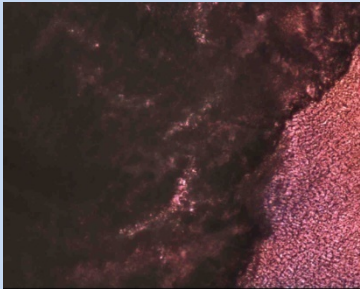
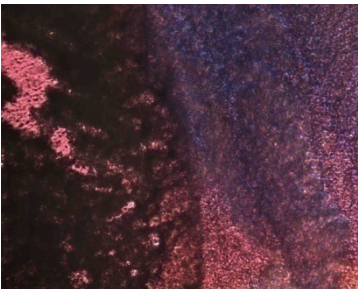
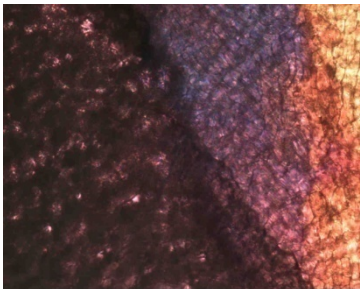
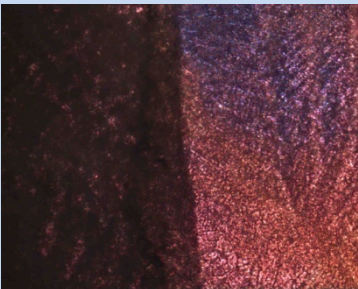

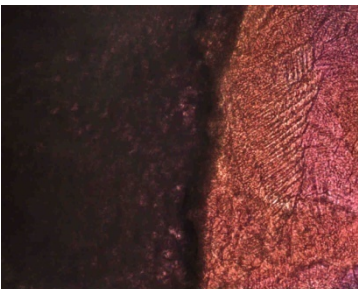
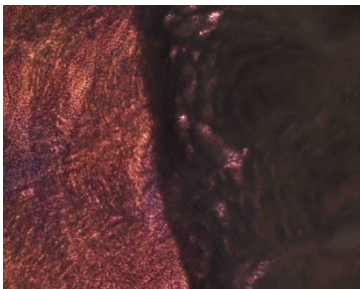
Fig. 3-34: Dependence of collapse temperatures on composition of samples for pure HSA, HSA + sugar mixtures and pure sugar

Surprisingly, the difference between T_{oc} and T_{fc} was found smaller ($\sim 3^{\circ}\text{C}$) when one of the two components was dominant and higher ($\sim 6^{\circ}\text{C}$) for the intermediate mixing ratios.

For mixtures with a high content of protein (4% to 5% w/w) no significant difference in T_c was found. When the content of sucrose or trehalose was e.g., increased to 10 mg/g (total solid content 50 mg/g) T_{oc} was only lowered by 2°C (for BSA mixtures). In contrast, the mole ratio of sugar to protein becomes critical concerning T_c for higher sugar contents (mole ratio of 49:1 to 104:1 of sugar:protein).

Tab. 3-20 presents example pictures for mixtures with BSA and HSA and different contents of sucrose.

Tab. 3-20: Pictures of onset of collapse for pure protein solutions (XSA) and different mixtures with sucrose, X signifies bovine or human

Sample	BSA	HSA
XSA 5% (w/w)	 $T_{oc}: -4.9^{\circ}\text{C}$	 $T_{oc}: -2.7^{\circ}\text{C}$
4.5% XSA, 0.5% sucrose	 $T_{oc}: -3.9^{\circ}\text{C}$	 $T_{oc}: -5.0^{\circ}\text{C}$
2.5% XSA, 2.5% sucrose	 $T_{oc}: -22.2^{\circ}\text{C}$	 $T_{oc}: -21.5^{\circ}\text{C}$
1% XSA, 4% sucrose	 $T_{oc}: -29.5^{\circ}\text{C}$	 $T_{oc}: -27.3^{\circ}\text{C}$

As underlined before, a clear definition of collapse and knowledge on freeze-drying behavior and/or experience on lyophilization characteristics of substances used are very important for data interpretation in FDM measurements.

In this study, clear differences in the visual appearance of freeze-drying and of collapse behavior could be revealed for increasing concentrations of sucrose or trehalose, respectively. Tab. 3-21 summarizes the appearance of drying and collapse for the different systems used in this study.

Tab. 3-21: FD microscopic appearance of drying and collapse for different types of solutions

Structural behavior	Pure BSA/HSA solution	Mixture of BSA/HSA and sugar in solution	Pure sugar solution
Below T_{oc}	Drying with well-defined fissures and cavities, no overall loss of structure	Drying with reduced number of fissures and gaps compared to pure BSA/HSA	Drying with no fissures and gaps
At T_{oc}/T_{fc}	Formation of thin, highly viscous and stretchy filaments with relative sharp edges, elastic behavior	Collapsing structure with smoother edges compared to pure BSA/HSA	Bright and distinct holes

Pure solutions of BSA and HSA or solutions with little sugar content dry with fissures and cavities. The development of these structural changes starts in a temperature region of 10 to 15°C below T_{oc} . As already described in the section 3.1.1 those fissures in the matrix were well-defined and did at no point result in an overall loss of structure. Collapse itself was recognized by the formation of thin, highly viscous and stretchy filaments with relative sharp edges. Concerning overall elasticity, this collapse behavior could be compared to the elasticity of a chewing gum when it is stretched in length. The more sugar was present in the sample solution the stronger the collapse behavior was impacted by the sugar. The pictures from Tab. 3-20 suggest that the fissures and gaps were reduced in number and had smoother edges for the mixtures with low amounts of sugar (up to 50:50 w/w mixtures). For higher sugar contents, a typical sugar collapse behavior with bright and distinct holes was observed and collapse temperatures were detected at much lower temperatures (cf. Fig. 3-33 and Fig. 3-34).

It is hypothesized that this discrepancy in freeze-drying and collapse behavior appearance in the different mixtures arises from the difference in molecular weight of the protein

(BSA/HSA) and the sugar (sucrose/trehalose). On the one hand, the product morphology which is formed from small disaccharide molecules undergoes viscous flow in a focused region close to the sublimation interface when its collapse temperature is reached. This local structural degradation of only a few pores (with a size of a few microns) is observed microscopically based on the increased transmission of light. On the other hand, the collapse behavior becomes more representative for the “chewing gum” behavior of the protein for increasing protein content.

For high protein concentrations (i.e. sugar:protein mole ratio lower than 49:1), a minimum sugar concentration is necessary to obtain a distinct plasticizing effect in the protein/sugar mixture and for the observation of a disaccharide typical collapse behavior. At low sugar contents, the smaller sugar molecules might act as “gap fillers” between the protein molecules and may interact closely with the protein structure [187; 64]. Accordingly, the fissures and disruptions (cf. Fig. 3-20) might result from a disaccharide content which is too low. In turn, this hypothesis would suggest that at a given mole ratio of sugar to protein the molecular interaction between a protein and a given number of disaccharides is depleted.

The number of sugar molecules which can maximally interact with the protein surface structure depending on protein size was estimated 50:1 in several publications and theories: Recently, a quantitative evaluation of the hydration state of BSA in a freeze-dried sugar matrix was followed by an investigation of the amount of sugar which is required to embed BSA [188]. If residual moisture was high within the cake structure (which would also be the case for FDM measurements), the hydration water of the BSA molecule was substituted by the sugar – both sucrose and trehalose – corresponding to ~ 20 to 25% of the hydration water for BSA alone.

The authors explained this phenomenon to the about 20-fold volume of the sugar molecule relative to a water molecule (steric hindrance) [188]. Both BSA and HSA tend to form hydrogen bonds to sugar molecules rather than to water molecules [188-190]. Addi-

tionally, the monolayer water substitution (M_0) for a protein structure can be determined according to the Pauling-Green Theory [190, 191] where moieties in the protein sequence are categorized into weak and strong binders for water adsorption. Based on this data M_0 can be estimated in the absence of sorption data. Using the actual Swiss Prot data base sequence [192], a total of 187 strong polar groups was calculated for BSA or HSA, respectively. Taking the 187 strong binding sites and the 25% of effective interaction between BSA/HSA and a sugar into account, the boundary for the mole ratio sugar/protein at which the sugar is expected to become more dominant for the drying and collapse behavior was roughly estimated to be 50:1 which is equivalent to a weight ratio of 1:4. This assumption is in excellent agreement with the results given in Fig. 3-33 and Fig. 3-34.

3.3.4 Dependence of collapse temperature of binary mixtures on sublimation velocity

As described before the velocity of sublimation was measured for BSA + sucrose mixtures (4.75% (w/w) BSA + 0.25% (w/w) sucrose and 2.5% (w/w) BSA and 2.5% (w/w) sucrose). The single results including T_n , T_{oc} , T_{fc} , ΔT_c , T_{c-50} , $V_{sub}(T_{oc})$ and $V(T_{oc}) \cdot T_{oc}$ are presented in Tab. 3-22 and illustrated in Fig. 3-35 and Fig. 3-36, respectively. The reader is referred to chapter 3.1.8 for a basic discussion on pressure setting during FDM experiments.

The results summarized in the figures and tables suggest that in this special case of binary mixtures of a protein and a disaccharide, the pressure setting is important for the collapse behavior if protein and sugar are mixed in a 50:50 weight ratio.

As indicated by the single values as well as by the term $V(T_{oc}) \cdot T_{oc}$, the sublimation velocity is higher for the mixture with 4.75% BSA + 0.25% sucrose ($\sim 2 \mu\text{m/s}$, $T_p = -6^\circ\text{C}$) compared to the 2.5% BSA + 2.5% sucrose mixture ($1.5 \mu\text{m/s}$ for $T_p = -17.5^\circ\text{C}$ at 0.075

Torr and 0.5 $\mu\text{m/s}$ at $T_p = -22^\circ\text{C}$ at 1.5 Torr). This was expected due to the much higher T_p , but the difference in V_{sub} is not (directly) proportional to the difference in T_p ($V(T_{\text{oc}}) \cdot T_{\text{oc}}$ is $-10 \pm 0.74 \mu\text{m}^\circ\text{C/s}$ for 4.75% BSA + 0.25% sucrose and $-16 \pm 5.3 \mu\text{m}^\circ\text{C/s}$ for 2.5% BSA + 2.5% sucrose).

Tab. 3-22: Nucleation temperature, collapse temperatures and velocity of the sublimation in dependence on pressure setting including ΔT_c , T_{c-50} and the ratio $V(T_{\text{oc}}) \cdot T_{\text{oc}}$ for BSA 4.75% + sucrose 0.25%

Pressure [Torr]	T_n [$^\circ\text{C}$]	T_{oc} [$^\circ\text{C}$]	T_{fc} [$^\circ\text{C}$]	ΔT_c [$^\circ\text{C}$]	T_{c-50} [$^\circ\text{C}$]	Velocity at T_{oc} [$\mu\text{m/s}$]	$V(T_{\text{oc}}) \cdot T_{\text{oc}}$ [$\mu\text{m}^\circ\text{C/s}$]
0.075	-21.6	-5.1	-4.4	0.7	-4.8	2.10	-11
0.375	-19.8	-5.5	-3.8	1.7	-4.7	1.83	-10
0.750	-21.0	-4.9	-3.1	1.8	-4.0	2.23	-11
1.50	-18.4	-4.1	-2.8	1.3	-3.5	2.20	-9
$\bar{x} \pm \text{sdv}$	-20.2 ± 1.2	-4.9 ± 0.5	-3.5 ± 0.6	1.4 ± 0.4	-4.2 ± 0.5	2.09 ± 0.2	-10 ± 0.7
rsdv	5.9%	10%	17%	29%	12%	7.7%	7.4%

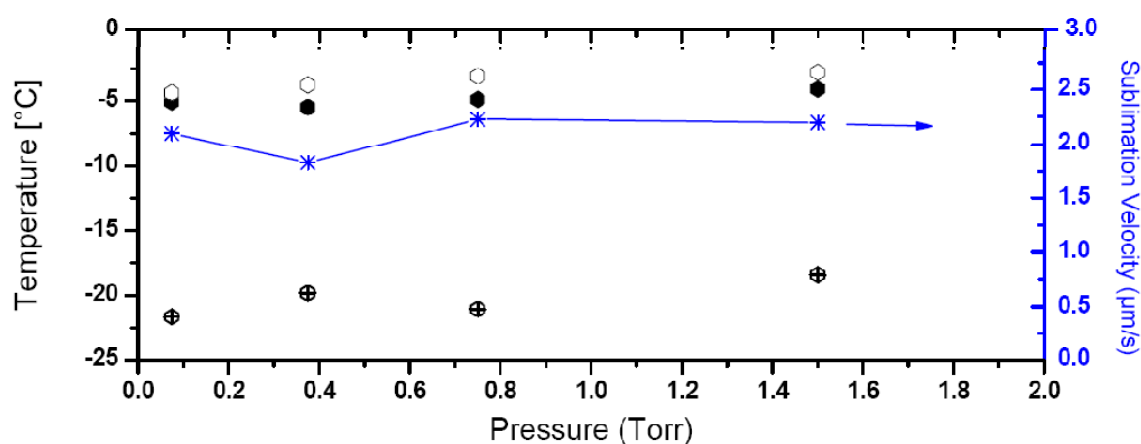


Fig. 3-35: Interrelationship between T_c and V_{sub} for BSA 4.75% + sucrose 0.25% using different pressure settings; crossed hexagons = T_n , filled hexagons = T_{oc} , open hexagons = T_{fc} , stars = speed of sublimation

Tab. 3-23: Nucleation temperature, collapse temperatures and velocity of the sublimation in dependence on pressure setting including ΔT_c , T_{c-50} and the ratio $V(T_{oc}) \cdot T_{oc}$ for BSA 2.5% + sucrose 2.5%

Pressure [Torr]	T_n [°C]	T_{oc} [°C]	T_{fc} [°C]	ΔT_c [°C]	T_{c-50} [°C]	Velocity at T_{oc} [$\mu\text{m/s}$]	$V(T_{oc}) \cdot T_{oc}$ [$\mu\text{m}^\circ\text{C/s}$]
0.075	-22.0	-16.7	-15.7	1.0	-16.2	1.46	-24
0.375	-10.1	-20.7	-18.6	2.1	-19.7	0.83	-17
0.750	-20.0	-20.7	-18.5	2.2	-19.6	0.47	-9.7
1.50	-21.1	-18.7	-16.2	2.5	-17.5	0.77	-14
$\bar{x} \pm \text{sdv}$	-18.3 ± 4.8	-19.2 ± 1.7	-17.3 ± 1.3	2.0 ± 0.6	-18.2 ± 1.5	0.88 ± 0.4	-16 ± 5.3
rsdv	26%	8.9%	1.8%	30%	8.2%	41%	33%

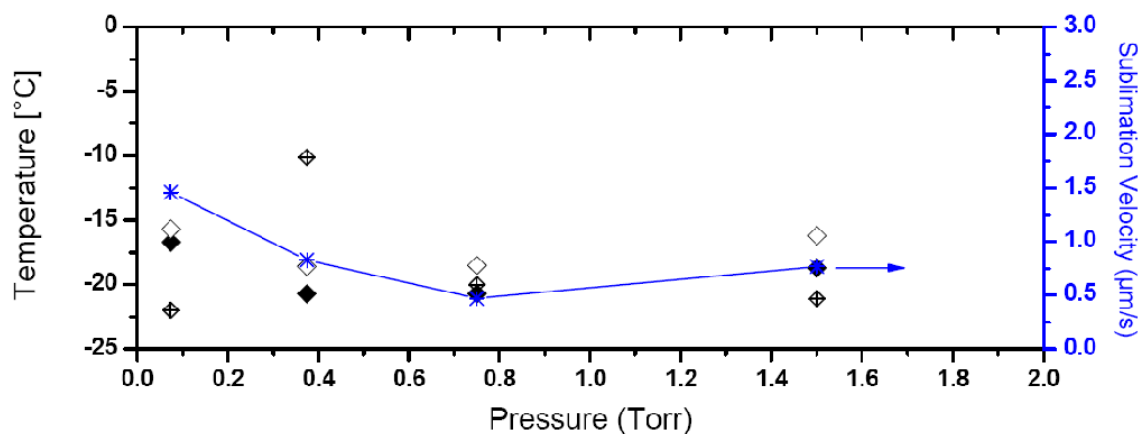


Fig. 3-36: Interrelationship between T_c and V_{sub} for BSA 2.5% + sucrose 2.5% using different pressure settings; crossed diamonds = T_n , filled diamonds = T_{oc} , open diamonds = T_{fc} , stars = speed of sublimation

There are several possibilities to explain the high difference in T_p combined with a relatively small difference in V_{sub} . (1) As explained in the introduction chapter, the driving force for sublimation is the pressure differential $P_0 - P_c$.

For a given pressure setting of P_c and a change in T_p from e.g., -19.2°C (BSA 2.5% + sucrose 2.5%) to -4.9°C (BSA 4.75% + sucrose 0.25%) which is a factor of about 4 there should be a difference in V_{sub} of a factor of 4 as well if resistance of both cakes would be equal. It was shown that V_{sub} is directly proportional to the pressure differential $P_0 - P_c$ and inversely proportional to product resistance [6, 24]. Additionally, T_n was found in the same temperature range for all experiments performed during this sub-study. With regard to $V(T_{\text{oc}}) \cdot T_{\text{oc}}$ values there is only a difference in average by a factor of 1.6. This observation would lead to the conclusion that the resistance of a mixture with a high protein content is higher than for the 50:50 mixture. A similar observation was made recently for resistance data for a freeze-drying run in vials using 100 mg/mL sucrose and a mixture of 25 mg/mL BSA with 75 mg/mL sucrose at chamber pressures < 0.1 Torr [180]. (2) Referring to the theoretical model presented in chapter 3.1.2, not only the composition of the solution is involved in differences in resistance and the amount of subliming water molecules, but the pressure setting itself impacts the amount of subliming water molecules per time and the velocity of subliming water molecules. As already pointed out before, all three parameters (amount of subliming water molecules, velocity of subliming water molecules and resistance of the product matrix) affect the contact between water molecules and the product matrix with regard to its quality (contact per time) leading to a critical viscosity decrease which results in a collapse of the structure. When summarizing the average situation for both mixtures, resistance data from freeze-drying runs could serve as an explanation, but all the other factors should as well play a role in the overall balance of impacting parameters. A more detailed investigation of the data for the 50:50 mixture shows an impact of pressure setting on V_{sub} **and** T_{oc} . For this composition a higher sensitivity to pressure could be explained by the assumption that for a pressure setting of 0.75 Torr P_c approaches P_0 [26] which would mean that pressure is the limiting factor in this constellation, and hence affecting the measured T_{oc} result.

Due to a higher T_p this is not the case for the mixture with the high protein content which is therefore insensitive to this pressure change. (3) Referring to the paper from Pikal and Shah [104] a third possibility for the explanation of the observed effects might be a difference in observation time (TM). However, this might not be the most relevant factor when comparing the results given before in the chapters on methodology of FDM. If one follows this line of argumentation, a higher V_{sub} has an effect on T_{oc} results for the 50:50 mixture (but not for the second mixture) by decreasing TM and shifting T_{oc} to higher T_p . This hypothesized effect might then be higher for lower pressures.

3.4 Comparison of collapse temperatures (T_c) and glass transition temperatures (T_g') for excipient solutions and protein/disaccharide mixtures

It is frequently reported that T_g' data are 2-5°C lower than corresponding T_c data [24, 104, 111]. This difference was explained by different heating rates during DSC and FDM measurements [104, 152, 193]. However, there are obviously differences in the measurement principle (as described before). At this point, no literature reference is available reporting T_c and T_g' data for a given formulation composition, and providing a detailed investigation or discussion.

3.4.1 T_c and T_g' data for excipient solutions

Tab. 3-24 provides an overview of T_{oc} , T_{c-50} and T_g' values and of the differences between the data for the excipients used in this study. Due to the dependence of T_c (including T_{oc} and T_{c-50}) on total solid content of the measured excipient, differences between T_c and T_g' values may vary significantly. For example, for glucose a difference between T_{oc} and T_g' of -0.5°C for the 5% solution and of +2.1°C for the 15% solution was calculated.

Tab. 3-24: Comparison of T_g' and T_{oc}/T_{c-50} values for various excipients and total solid contents of 5 and 15% (w/w)

Excipient	Total solid content (w/w)	$\bar{x}_{T_{oc}}$ [°C]	$\bar{x}_{T_{c-50}}$ [°C]	T_g' [°C]	$T_{oc}-T_g'$ [°C]	$T_{c-50}-T_g'$ [°C]
Sucrose	5%	-31.4	-	-32 [194]	0.6	-
	15%	-29.8	-	-32 [194]	2.2	-
Trehalose	5%	-28.9	-	-29 [152]	0.1	-
	15%	-27.5	-	-29 [152]	1.5	-
Glucose	5%	-43.5	-42.9	-43 [10]	-0.5	0.1
	15%	-40.9	-40.4	-43 [10]	2.1	2.6
(2-Hydroxypropyl)- β -cyclodextrin	5%	-8.9	-8.7	-9 ²⁰	0.1	0.3
	15%	-8.6	-8.2	-9 ²⁰	0.4	0.8
PVP 40 kDa	5%	-20.6	-20.0	-20.5 [195]	-0.1	0.5
	15%	-18.8	-18.4	-20.5 [195]	1.7	2.1

Except for the 5% solution of glucose and the 5% solution of PVP 40 kDa, all T_{oc} values were higher than the corresponding T_g' values. The lowest difference between T_{oc} and T_g' (which was only 0.1°C), was found for 5% (2-hydroxypropyl)- β -cyclodextrin, 5% PVP 40 kDa, and 5% trehalose. In contrast, the highest difference (2.2 °C) was determined for 15% sucrose. When comparing T_{c-50} and T_g' values, T_{c-50} was always higher than T_g' . As mentioned above, many authors postulated that T_c values are 2-5°C higher than T_g' values.

Therefore, a comparison of T_{c-50} and T_g' values is not only recommended because of the similarity concerning the representation of “midpoint values”, but as well due to the fact that T_{c-50} was always higher than T_g' for the results presented here.

3.4.2 T_c and T_g' data for protein/disaccharide mixtures

To gain a deeper insight into the comparability and the differences between FDM measurements and resulting T_c data and DSC measurements and resulting T_g' values, T_g'

²⁰ Measured as described in chapter 2.2.4 (“Materials and methods“, p. 56 ff.)

was measured as described in the materials and methods section and calculated by using the Gordon-Taylor/Kelley Bueche estimation [145, 149]. In a second step the width of the collapse transition ($T_{oc} - T_{fc}$) and of the glass transition ($T_{onset} - T_{end}$) were compared. The experiments were focused on BSA + sucrose as well as BSA + trehalose mixtures.

3.4.2.1 Comparison of T_{oc} , T_g' and Gordon-Taylor calculation

As described before, the equation published by Gordon and Taylor can be used to calculate T_g' of (binary) mixtures (given an ideal mixture behavior) [145, 149]. For exact calculations the water content in the three component freeze-concentrated solution is required. Since this content is not known for the given systems, it was assumed that the water content in this system is simply a weighted average of the water contents in the individual two component systems. By using T_g' of the pure components, T_g' of the mixture was then predicted and termed "Gordon-Taylor prediction". $K = 0.25$ was calculated from the densities of the two components [148]. T_g' data were taken from literature: T_g' (BSA) = -11°C [103], [194], T_g' (sucrose) = -32°C [111], and T_g' (trehalose) = -29°C [103].

T_g' for protein/sugar mixtures could only be identified up to a protein concentration of 32.5 mg/g using a $10^\circ\text{C}/\text{min}$ heating rate. Even with higher heating rates during the DSC experiment ($> 30^\circ\text{C}/\text{min}$), the step change in heat flow signaling the change in heat capacity at T_g' was not sufficiently large to detect the protein T_g' [7].

In contrast, (as described before), T_{oc} data could be determined clearly for high concentrated protein mixtures and for pure protein solutions.

Results of T_{oc} , as well as T_g' measured by DSC and predicted by using the Gordon-Taylor equation are given in Fig. 3-37 for mixtures of BSA with sucrose and in Fig. 3-38 for mixtures of BSA with trehalose.

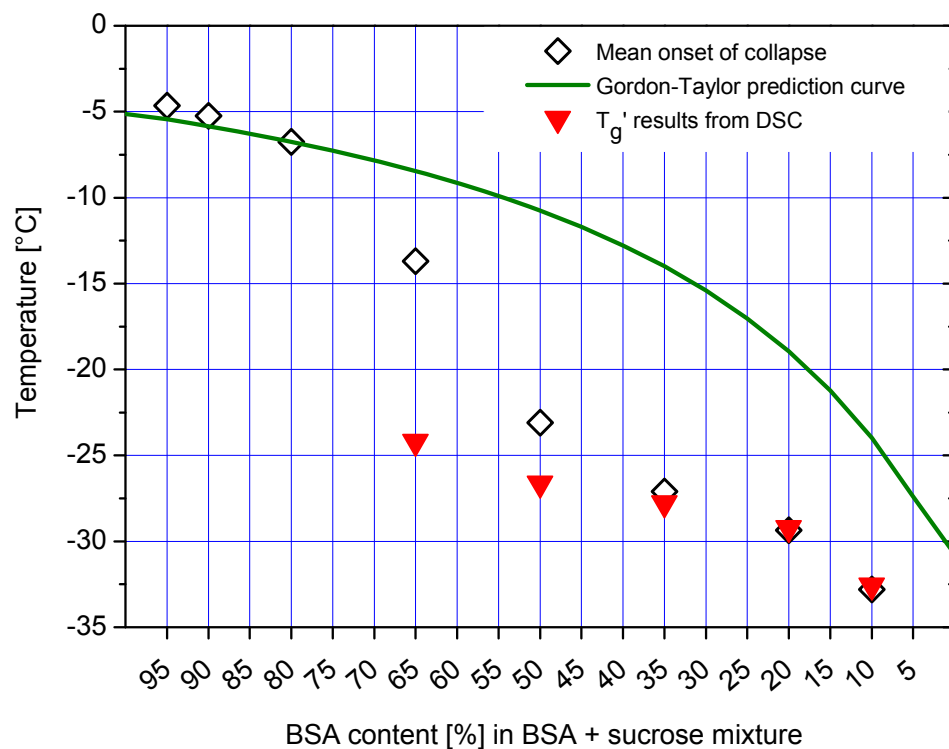


Fig. 3-37: T_{oc} , T_g' (measured by DSC) and T_g' predicted by Gordon-Taylor in dependence of the composition of various BSA + sucrose mixtures

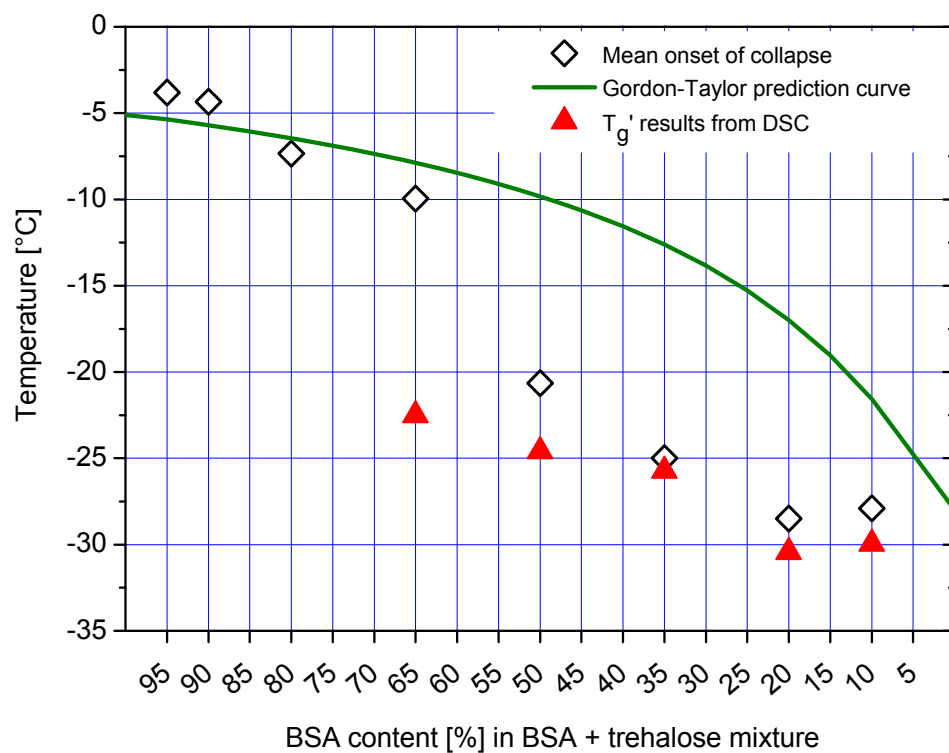


Fig. 3-38: T_{oc} , T_g' (measured by DSC) and T_g' predicted by Gordon-Taylor in dependence of the composition of various BSA + trehalose mixtures

At low protein concentrations (10-35% w/w), T_g' values measured by DSC were in excellent agreement with T_{oc} data. The BSA + sucrose mixtures temperature differences were here within $\pm 1^\circ\text{C}$. At higher protein concentrations (50 and 65% w/w), an increasing difference between T_g' and T_{oc} was observed which was up to 12°C for 65% BSA + 35% sucrose. Consequently, a prediction of T_g' for pure protein solutions by extrapolating to zero excipient concentration using T_g' values measured for binary mixtures of protein and another glass forming excipient such as sucrose over a range of excipient concentrations [7, 194] would lead to an underestimate of T_g' of the pure protein.

Calculated T_g' values (Gordon-Taylor prediction) overpredicted T_g' for mixtures with sucrose and trehalose in the composition range from 10 to 65% and underpredicted T_g' in the composition range from 90 to 95% compared to T_{oc} values or measured T_g' values, respectively. Therefore, this estimation seems to be no useful tool for the evaluation of the critical formulation temperature for primary drying of the examined systems.

3.4.2.2 Comparison of the width of collapse and glass transition

As mentioned earlier, most of the literature refers to T_{oc} when reporting FDM data. This information is often compared to T_g' values which are reported as "midpoint" temperatures. Data handling in this manner neglects the fact that the actually observed collapse event during an FDM experiment might reveal valuable information about the robustness of a structure to temperature changes. Therefore, some authors reported a glass transition/collapse temperature as a temperature region rather than a fixed temperature [148, 152], and some introduced a more complex procedure to describe the collapse phenomenon [111, 158]. Based on the detailed investigations of drying and collapse behavior of BSA/HSA + sucrose/trehalose mixtures and their T_g' values, new information on this topic could be delineated.

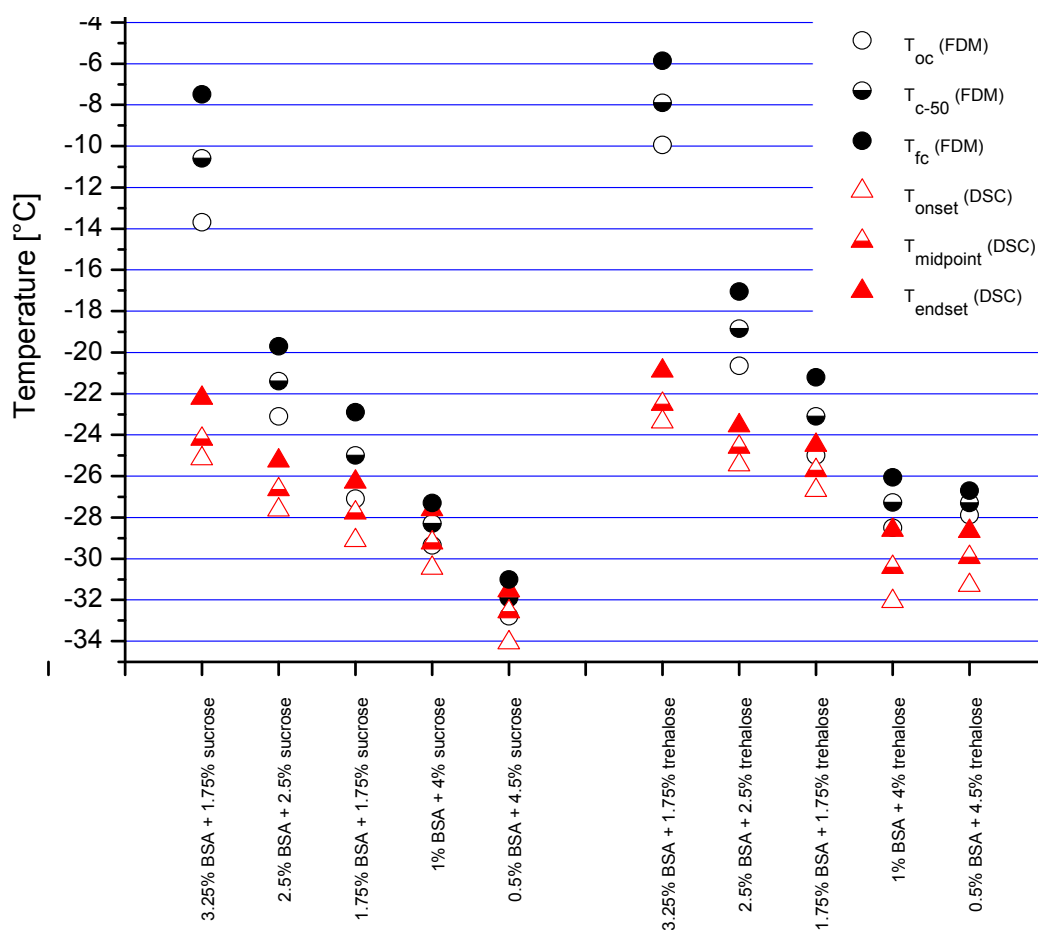


Fig. 3-39: Comparison between T_{oc} , T_{c-50} and T_{fc} obtained from FDM and T_g' (onset of T_g' , midpoint and endset of transition) by DSC for BSA + sucrose and BSA + trehalose mixtures

Fig. 3-40 shows T_{oc} , T_{c-50} and T_{fc} data obtained from FDM experiments in comparison to T_g' values from DSC measurements (onset, midpoint and endset of transition) for mixtures of BSA with sucrose or trehalose, respectively. For T_g' values, the width of the transition from onset to endset was detected to be essentially constant for both mixture types over the entire concentration range and is estimated to be approximately 2.5°C. Interestingly, ΔT between T_{oc} and T_{fc} varies for both mixture types: for solutions with very low protein content (0.5%) ΔT_c is about 0.5°C and steadily increases until it reaches a value of about 6.5°C for the BSA/sucrose solution with a high protein concentration (3.25%). For the sucrose mixtures, T_c and T_g' values were in excellent agreement for low

protein concentrations of 0.5 and 1%. In all other cases, T_g' values were found to be lower than T_c values.

The difference between corresponding onset, midpoint and endset values increased dramatically with higher protein content. This means that the protein to sugar ratio had a large impact on the width of the collapse transition and on the difference between T_g' and T_c values as well.

To compensate for the fact that the transition width is mainly constant for T_g' , and a variable for T_c , midpoint values of T_g' and of T_c (which means T_{c-50}) should be used when only single values are compared. For a better understanding of transition behavior, it is strongly recommended to report onset and endset values or the temperature interval, respectively. Especially reporting of T_{oc} and T_{fc} should help to have a first guess of robustness of a given formulation during primary freeze-drying. With regard to transferability of T_c results to freeze-drying, some runs and their results are presented in the next section, but should be objective of further detailed investigations based on the previous arguments.

3.5 Transferability of FDM results to freeze-drying cycles: preliminary experiments with sucrose

Transferability of T_c results measured by FDM to freeze-drying cycles in the laboratory is a very important aspect of the overall value of this analytical technique [130]. Even the best measurement methodology makes no sense if data are not usable or if knowledge of the scalability is insufficient.

Based on different geometrical situations (vial vs. thin, sandwich-like layer of product), a 1:1 transferability of results on collapse behavior obtained by FDM might not be expected. Tab. 3-25 lists important differences between freeze-drying in a vial, and a FDM measurement.

Tab. 3-25: Differences between freeze-drying in 20 mL vials in a freeze-dryer and a sample in a FDM stage

	20 mL vial in a freeze-dryer	Sample in a FDM stage
Sample volume	mostly 3 – 12 mL	2 μ L
Ice thickness (L_{ice})	mostly 0.5 - 2 cm	25 μ m
Product area (basis)	$\sim 6 \text{ cm}^2$	$\sim 0.5 \text{ cm}^2$
Heat transfer	mainly gas and direct conduction	almost only direct conduction
Sublimation interface	6 cm^2	$3 \cdot 10^{-3} \text{ cm}^2$

Pikal and Shah [104] argued that differences in resolution and time of observation may cause small differences between the collapse temperature measured by the microscopy method and collapse observed in vial freeze-drying. They conclude that in general, the product being freeze-dried in a vial will collapse at a slightly higher temperature. In their opinion the effect of variation of observation time, T_M , is negligible in a system of low solids content because sublimation is very rapid. To minimize the variation between FDM experiments and production behavior in lyocycles, the collapse temperature measurements by FDM should be conducted using solute concentrations comparable to the concentrations ultimately used in freeze-drying [104]. The importance of formulation composition has been proven in this thesis and leads to the previous recommendation. From the presented results on FDM methodology, problems in transferability should not be a matter of observation, but of the technical differences mentioned before. Concerning the difference in collapse temperature, further investigations were necessary since no information was provided in [104].

Comparing DSC, FDM and freeze-dryer setup, Chongprasert et al. pointed out systematic differences with respect to temperature measurement accuracy and heat transfer characteristics [101]. The best thermal contact between the sample and the heat source was found for FDM. On the one hand they expected and confirmed a relatively large difference between the freeze-dryer and the DSC of 1.0 and 1.5°C in the region of ice melting.

On the other hand they found a systematic difference between DSC and FDM of about 0.3°C in the temperature range of interest. The aluminum pan used for DSC seems to have a worse heat transfer compared to the sample in FDM experiments (glass). The authors conclude that some trial and error experimentation is required to transfer annealing temperatures from DSC or freeze-drying microscopy to the freeze-dryer.

Investigation of *Lactobacillus bulgaricus* suspensions and protective media indicated that the collapse temperature T_c , determined by FDM, can be considered as the critical formulation temperature of the product that should not be exceeded to avoid degradation of the dried structure [111].

In contrast, Colandene and co-workers [129] underline that it has become increasingly recognized that primary drying above T_g' may be acceptable in the context of protein stability [17, 24, 196]. This may be due to the relatively high viscosity of freeze-concentrated stabilizers (e.g., disaccharides), even at temperatures slightly above T_g' . In the “rubber” state, the rate of denaturation may be slowed enough to prevent protein unfolding under the time scale of freeze-drying [24]. An interesting finding from Colandene’s study was that in formulations without a crystalline bulking agent, at higher protein concentration, they were able to perform primary drying substantially above the T_g' without detrimental effects to the protein and without collapse. Further, they were able to perform primary drying at temperatures slightly above the onset temperature for collapse (as based on FDM). This was done without any apparent effect on product elegance, or stability. To explain the lack of macroscopic collapse in the sucrose-based formulation (at 80 mg/mL protein concentration) when drying well above T_g' , they hypothesize that at high protein concentrations, even though some viscous flow may occur when exceeding T_g' , the solids are packed densely enough to increase viscosity and restrict freedom of movement to effectively prevent macroscopic collapse during the time scale of freeze-drying. At lower protein concentrations, this effect was not as profound and the collapse temperature more closely matched the T_g' .

This also served as an explanation for the increasing differences between T_c and T_g' that were observed with increasing protein concentration [129]. At the same time, it was reported that proteins may show denaturation even when primary freeze-dried below T_g' which complicates the discussion [61].

3.5.1 Run data

To gain new information on transferability, T_{oc} of 2.5% and 10% (w/w) sucrose solutions were measured by FDM (standard procedure). T_{oc} of 2.5% (w/w) sucrose was found to be -34°C , T_{oc} of 10% was determined to be -30.5°C . Then, FD runs with these solutions were performed in a Lyostar II freeze-dryer with SMARTTM software installed. The setting in the software was varied so that T_p settings for the product were below T_{oc} , equivalent to T_{oc} , and above T_{oc} . As described in the materials and methods chapter, the software calculated the initial cycle recipe and optimized it during the runs, based on product temperature feedback. Thermocouples were used to measure the temperature at the bottom of the vial (T_{b-TC}) in three different center vials. MTM measurements collected data (P_{ice} , resistance) which were the basis for calculation of the product temperature at the bottom of the vial (T_{b-MTM}), and at the sublimation interface (T_{p-MTM}), respectively. Additionally, the shelf inlet temperature ($T_{s-inlet}$), the shelf surface temperature ($T_{s-surface}$) and pressure were measured. For pressure measurement, a pirani (endpoint monitoring) and capacitance manometer (control of pressure chamber) were used.

Examples of run data are given in Fig. 3-40 and Fig. 3-41. As shown, the shelf temperature was increased stepwise by the optimizing routine. Differences in T_{b-TC} between the runs in the three different center vials are clearly visible.

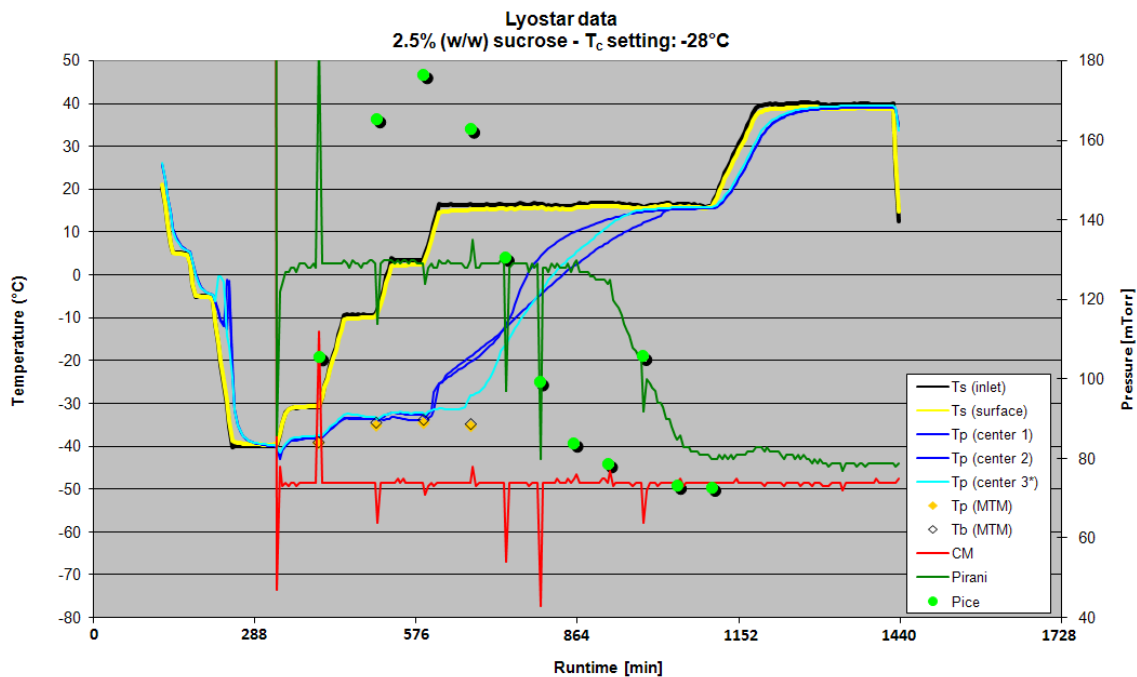


Fig. 3-40: Run data of SMART™ run with 2.5% (w/w) sucrose

21

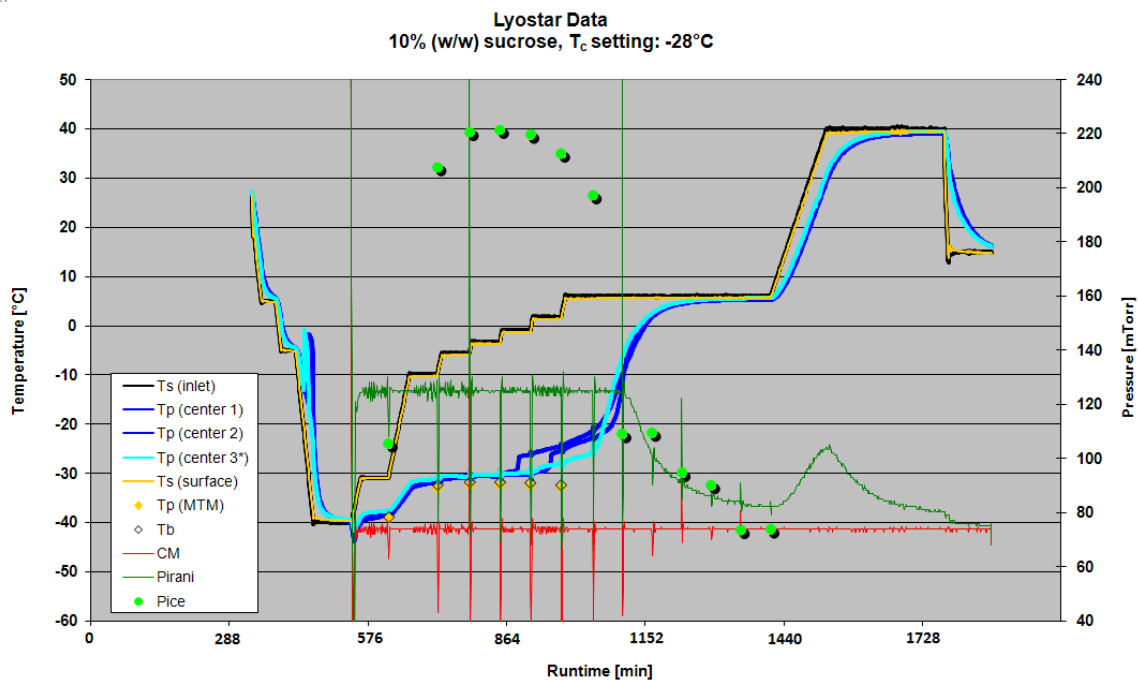


Fig. 3-41: Run data of SMART™ run with 10% (w/w) sucrose

Tab. 3-26: Data of SMART™ runs for sucrose solutions

Concentration	Critical formulation temperature setting, SMART™ [°C]	T _{oc} (FDM) [°C]	T _{b-TC} [°C]	T _{b-max} (MTM) [°C]	T _{p-max} (MTM) [°C]
2.5% (w/w)	-26	-33.6	-32.9	-33.5	-34.4
	-28	-33.6	-33.8	-33.7	-34.5
	-32	-33.6	-35.2	-35.2	-35.8
	-34	-33.6	-35.0	-35.5	-36.0
	-36	-33.6	-37.0	-37.6	-37.9
10% (w/w)	-28	-30.2	-29.9	-31.8	-32.4
	-32	-30.2	-33.7	-34.5	-34.8
	-34	-30.2	-35.1	-35.3	-35.6

Tab. 3-26 gives an overview on temperature data for the different runs. The maximum temperatures (i.e., the highest temperatures) of T_{b-TC}, T_{b-max} (MTM) and T_{p-max} (MTM) are shown for a direct comparison with T_{oc} values and settings for the critical formulation temperature in the SMART™ software. and Fig. 3-43 visualize if the border marked by T_{oc} (FDM) was passed during the single runs. In none of the runs T_{p-max} (MTM) exceeded T_{oc} (FDM). For the 2.5% sucrose solution T_{b-TC}, and T_{b-max} (MTM) were slightly above T_{oc} when drying with a temperature setting of -26°C. For 10% sucrose only T_{b-TC} exceeded T_{oc} when using -28°C as set point. Concerning the accuracy of T_{b-TC}, slight differences to T_{b-MTM} values were determined. For the 2.5% solution differences from 0°C (setting -32°C) up to 0.6°C (setting -26 and -36°C) were measured and for the 10% solution from 0.2°C (setting -34°C) up to 1.9°C. Interestingly, the safety margin built into the SMART™ software varied very strongly. For the run with a setting of -26°C with 2.5% sucrose, the setpoint was not reached (difference of 8.4°C). The temperature difference decreased continuously until reaching 1.9°C for the setting of -36°C. With the 10% solution differences were smaller (e.g., 4.4°C for a setting of -28°C, and 1.6°C for a setting of -34°C).

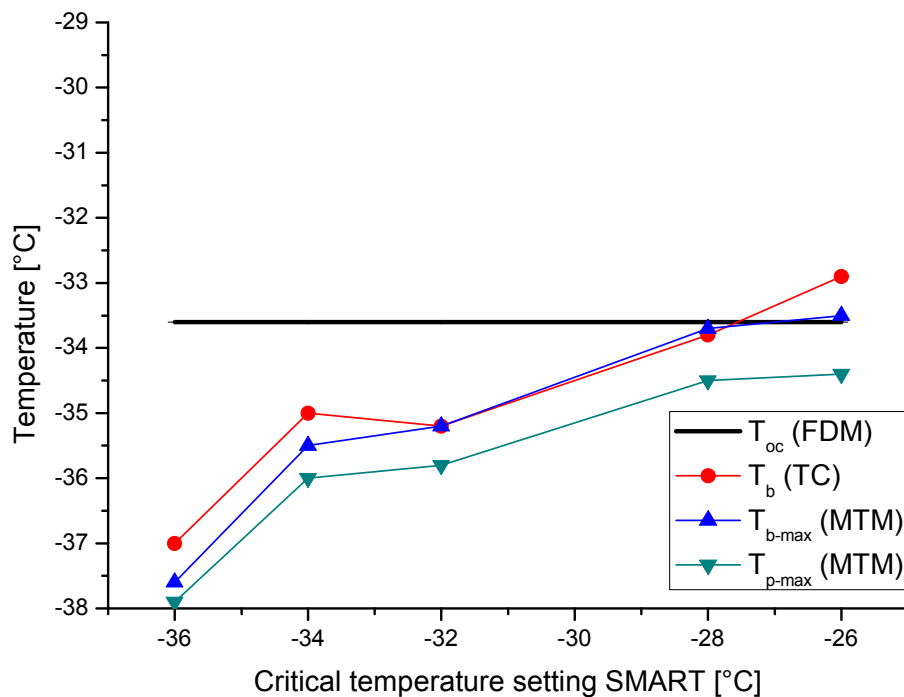


Fig. 3-42: Maximum temperature of SMARTTM run with 2.5% (w/w) sucrose in dependence of critical formulation temperature setting (scale identical to Fig. 3-43)

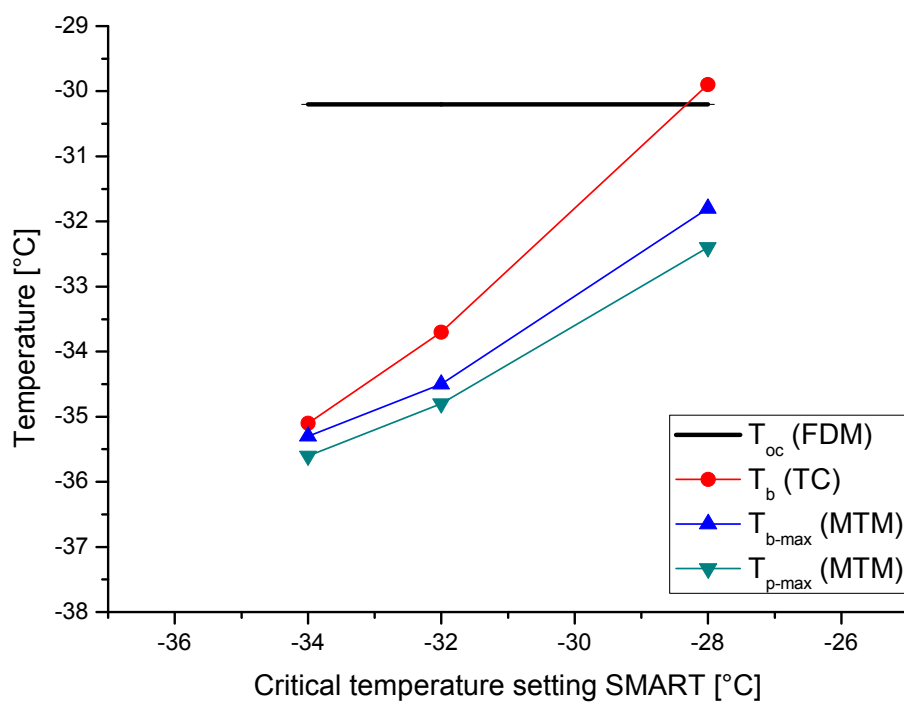


Fig. 3-43: Maximum temperature of SMARTTM run with 10% (w/w) sucrose in dependence of critical formulation temperature setting (scale identical to)

It is important to mention that the experiments described above provided preliminary data. At the time when they were performed, only an older version of the SMART™ software was available. Today, “Auto-MTM” measurements should be combined with predefined cycles to avoid the automated regulation of T_s (and pressure) described before.

In a next step, scanning electron microscopy and BET specific surface area measurements were performed to gain information on possible effects of different settings and drying temperatures on the single products.

3.5.2 SEM and SSA for evaluation of product shrinkage

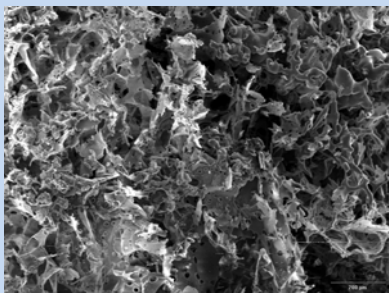
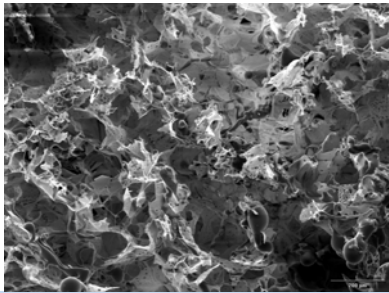
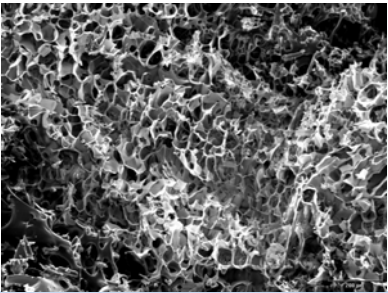
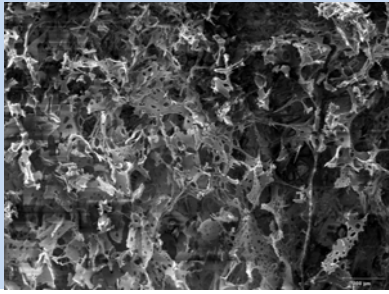
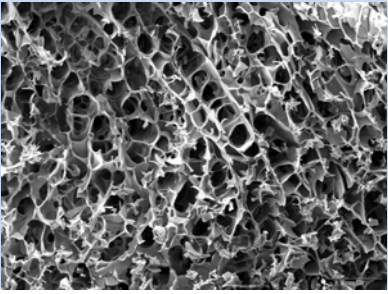
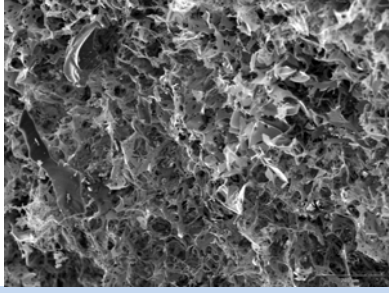
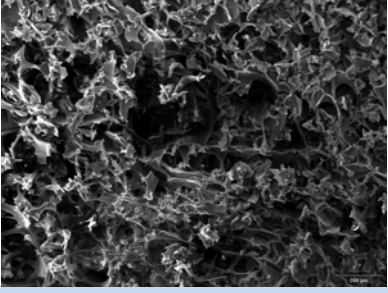
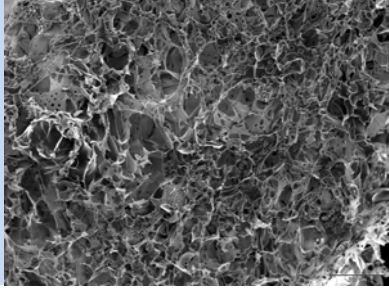
Scanning electron microscopy (SEM) is generally known as a useful technique to examine cake morphology [197]. Searles et al. [17] found based upon SEM observation that the degree of supercooling and the composition of the solution determined the ice crystal morphology. The recent work by Rambhatla et al. [21, 172] demonstrated that BET specific surface measurement is a useful method for a quantitative measurement of surface area, which characterizes the impact of the freezing step. However, Liu claims that this method should be used with caution when cakes have experienced micro- or partial collapse, since the measured surface areas in these cakes do not precisely reflect the quantity of ice crystal occupation during freezing [103].

In this study, SEM technology should help to determine possible product damages due to high product temperatures during freeze-drying. For the lyophilized cake of the 2.5% solution and settings of -32 and -34°C, cake shrinkage was measured. In literature shrinkage is described as follows: The lyophilized structure forms a cake that fails to retain the same dimensions as that of the inner dimensions of the vial and instead, experiences a loss of volume manifested as shrinkage from the inner sides of the vial [107]. During the experiments performed, 1 minus the ratio of the real volume measured with a sliding rule (height and diameter of the cake) to the theoretical volume of the frozen material was defined as shrinkage. The product with a setting of -32°C showed approximately 19-

20% of shrinkage and the one with a setting of -34°C ~ 16-18%. For the 10% sucrose solutions shrinkage appeared to be minor. In a study from 2005 it was found that sucrose shows shrinkage of about 17% regardless of the drying conditions [107]. This baseline shrinkage may be a direct result of volume change that occurs within the sucrose phase when water is removed (the sucrose freeze concentrate contains about 18% water at T_g).

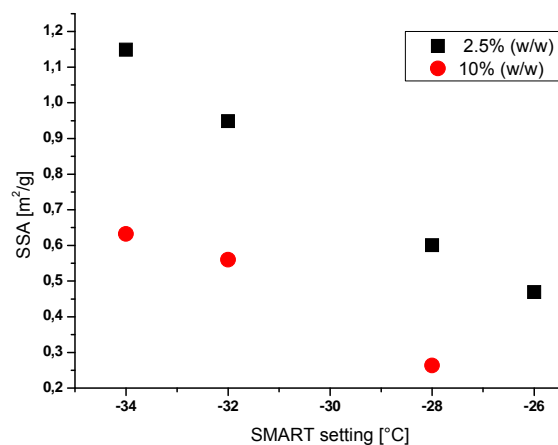
It is clear from the methodology of measuring shrinkage that these values can only serve as very rough indicators for product damage. SEM pictures shown in Tab. 3-27 provide much better information on product structure. For all products with a sucrose concentration of 2.5%, microcollapse in the structure was found, even when primary drying was conducted under very conservative conditions (setting of -36°C , $T_{p\text{-max}}$ (MTM): -37.9°C). The higher the measured $T_{p\text{-max}}$, the more droplet formation was detected by SEM. None of the products showed a full loss of structure. In contrast, the products from the 10% solution looked much more rigid although they were freeze-dried at much higher product interface temperature (-32.4°C for a setting of -28°C). No droplet formation or other indicators for viscous flow are visible in the pictures. This suggests that the result from FDM measurements, specifically a T_{oc} of -33.6 for 2.5% and of -30.2°C for 10% can be transferred, to FD cycles. The 10% solution could be dried at higher temperatures than the 2.5% solution. Additionally, $T_{b\text{-MTM}}$ and $T_{p\text{-MTM}}$ values indicate a temperature gradient within the product, where the temperature at the bottom never exceeded the collapse temperature of the 10% sucrose solution, but did exceed T_{oc} (FDM) for the low concentrated solute and a T_c setting of -26°C and -28°C , respectively. However, for collapse and shrinkage of the product, only the temperature at the sublimation interface is relevant.

Tab. 3-27: SEM pictures of different SMART™ runs with sucrose solutions (magnification all 100-fold, except 2.5% w/w sucrose at -34°C: 150-fold)

Critical formulation temperature setting SMART™ [°C]	2.5% (w/w)	10% (w/w)
-26		
-28		
-32		
-34		
-36		

These findings of different degrees of damage in the various products were confirmed by BET measurements. Using krypton as adsorptive gas and a 10-point measurement method, representative values could be obtained. Tab. 3-28 shows the results of this investigation in numbers and Fig. 3-44 as trend lines in a graph.

Total solid content of sucrose	Critical formulation temperature setting SMART™ [°C]	Specific surface area [m ² /g]
2.5% (w/w)	-26°C	0.4695
	-28°C	0.6009
	-32°C	0.9485
	-34°C	1.1486
10% (w/w)	-28°C	0.2636
	-32°C	0.5599
	-34°C	0.6326



Tab. 3-28: BET specific surface areas for 2.5 and 10% (w/w) sucrose solutions with different SMART™ settings in critical formulation temperature

Fig. 3-44: Trends in SSA depending on SMART™ critical temperature settings

For both concentrations, there is a clear dependence of SSA on product temperature during primary freeze-drying or T_c setting, respectively. Microcollapse in the products leads to a decrease of SSA which is reflected as droplets in the SEM pictures. For the 2.5 as well as for the 10% solution the SSA of the dried product is decreased by a factor of 2 when comparing the product after a T_c setting of -34°C to one of -28°C.

The results obtained in this thesis are in line with observations made before that cake shrinkage has been observed with amorphous formulations with low collapse temperatures (like sucrose and trehalose) [164]. Low collapse temperature materials are also known to cause formation of small holes in their structure after freeze-drying as observed from SEM photographs [164], thus causing a decrease in the resistance to mass transfer of the product as observed with MTM [34].

4 Summary and conclusion

Freeze-dry microscopy is the key element to determine the critical formulation temperature necessary to design rational freeze-drying cycles. Measurement theory clearly reveals that collapse temperature measurements reflect the process conditions during primary drying much better than e.g., glass transition temperature measurements by differential scanning calorimetry.

For this thesis, methodology, data interpretation and practical transferability of results measured by freeze-dry microscopy were subject to detailed investigations. Previously published research work and findings were included in the discussion and in some cases were newly interpreted.

Based on a theoretical background, experimental results led to a classification of collapse behavior in three collapse phases:

(1) Onset of collapse was defined as first structural alterations in the dried structure adjacent to the sublimation interface.

(2) At full collapse conditions, the freeze-dried structure has no interconnection to the structure at the sublimation front anymore. It undergoes structural loss right after the sublimation process resulting in dried fragments.

(3) A 50% collapse was introduced signifying a “midpoint” collapse for better comparison to “midpoint” glass transition (T_g') values and calculated as average from the temperature of the onset of collapse and of full collapse. Comparable to glass transitions, collapse is a transition within a temperature range, and onset as well as full collapse temperatures should be reported and taken into consideration for optimization purposes and formulation development.

For better theoretical and practical understanding and the explanation of recent and previous findings, a model of factors influencing freeze-dry microscopy experiments was developed in this thesis. It is based on the concept that the interaction of water molecules with the product matrix is fundamental in collapse events with water plasticizing the product matrix (containing solute and non-frozen water) [117; 79]. If influencing parameters in summary reach a critical level, the rigidity of the product matrix is critically decreased leading to viscous flow of the material into the pore which is known as “collapse”. The product matrix is characterized by its water binding affinity, the hygroscopicity of the dried solute(s), its rigidity, its specific surface area, and its resistance to water vapor flow. During freeze-dry microscopy experiments the limiting parameter of the overall balance has to be the temperature or better the heating rate used. Pressure setting should be adequate, but not limiting. Besides temperature and pressure settings, the extent of supercooling, the physical properties of solved substances and their total solid content are primary factors of collapse events.

To prove the introduced model, to investigate the importance of single parameters, and to find an optimized freeze-dry microscopy methodology, detailed studies were carried out including various experimental settings. They resulted in the following recommendations: For routine measurements a heating rate of 0.5 to 1°C/min should be used. For the evaluation of worst case collapse temperatures a more sophisticated measurement procedure with a heating rate of 0.1°C/min and 10 min holds every full degree Celsius can be carried out reflecting the situation during primary freeze-drying in some way better than standard methodology. However, the procedure prolongs experimental run time excessively, and simplifies only marginally transferability problems. For maximal reproducibility the thickness of the frozen layer must be fixed by using spacers.

Additionally, it was shown that freeze-dry microscopy is a proper tool to study the influence of different cooling rates and annealing procedures on collapse temperatures.

From correlation coefficient calculations based on values of nucleation temperature vs. corresponding concentration values for glucose, 2-(hydroxypropyl)- β -cyclodextrin, and polyvinylpyrrolidone 40 kDa no impact of nucleation temperature (or the extent of supercooling, respectively) on collapse temperatures was determined when taking all measured values into consideration. However, it is assumed that different extents of supercooling influence collapse temperature measurements (apart from random effects) reflected in relatively high standard deviations of measured collapse temperature values. Therefore, it is recommended to perform three to five independent freeze-dry microscopy measurements for each sample and to report average values to account for the described differences in the frozen structure of the maximally freeze-concentrated solution.

For sucrose, trehalose, glucose, 2-(hydroxypropyl)- β -cyclodextrin, and polyvinylpyrrolidone 10 and 40 kDa, a dependence of collapse temperatures on total solid content was found. Despite different extents and shapes of the plotted curves for the various excipients, three trends became obvious: (1) Within a given excipient class the collapse temperature increases with a higher molecular size or chain length (for polymers) and the difference between onset of collapse and full collapse decreases. (2) For all excipients an exponential correlation was investigated with low collapse temperatures for low concentrations and higher collapse temperatures for intermediate concentrations (10 to 15% w/w). (3) Hygroscopic substances show a decrease of collapse temperature values for high (about 20 to 30% w/w) total solid contents (depending on the excipient).

In general, the measurement of viscosity of the initial solutions used for freeze-dry microscopy experiments does not allow a prediction of collapse behavior relative to the total solid content. Instead, chemical structure of the substances (especially their size) and hygroscopicity of the dried solute seem to have a crucial influence on collapse behavior.

Furthermore, it was found that bovine serum albumin and human serum albumin are interchangeable from freeze-dry microscopy measurements based on their structural similarity. In addition, they might be considered as model proteins or protein substitutes in a placebo formulation. In contrast to glass transition temperature T_g' , their collapse temperatures were clearly and relatively easily detectable by freeze-dry microscopy.

Studies on binary mixtures of protein with a disaccharide revealed a high dependence of collapse temperatures (onset and full collapse) on the composition of the mixture. Differences in freeze-drying and collapse behavior were strong as well: Samples with a high concentration of protein showed structural gaps and fissures during drying well below the collapse temperature with no detectable collapse. When collapse occurred they showed an elastic behavior with characteristic filaments. In contrast, sugar-rich compositions displayed a sugar-typical collapse behavior with defined rapidly growing holes in the structure. The latter samples dried without any structural disruptions when dried below the onset of collapse. Interestingly, the difference between onset of collapse and full collapse was significantly higher for compositions with intermediate weight ratios of protein and sugar and lower for the samples with one high-concentrated compound. This finding can be explained by a surface saturation of the protein surface by disaccharide molecules.

For selected excipients and binary mixtures of protein and disaccharide the measured collapse temperatures were compared to glass transition temperatures of the maximally freeze-concentrated solutions. Due to the dependence of the collapse temperature on total solid content of the measured substance(s), differences between collapse temperatures and glass transition temperatures varied strongly for excipient solutions as well as protein/sugar mixtures. For an aqueous solution containing 3.25% (w/w) bovine serum albumin and 1.75% (w/w) sucrose, the highest difference of 12°C between the onset of collapse and the glass transition temperature was found.

The width of the collapse temperature transition (signified by the difference between the onset of collapse and full collapse) might serve as a parameter for robustness of the formulation to temperature changes during primary freeze-drying.

By freeze-dry microscopy measurements in combination with lab-scale freeze-drying runs it could be shown that obtained collapse temperature results are in general transferable to freeze-drying cycles with regard to, e.g., the difference detected for collapse temperature between different concentrations of the same excipient. Scanning electron microscopy in combination with BET specific surface area measurements clearly indicated severe damages in cakes for which primary drying was performed at higher product temperatures, even it was performed below the temperature of the onset of collapse.

In summary, freeze-dry microscopy is an extremely helpful tool for lyophilization formulation and cycle optimization. It provides a user not only with information on critical formulation temperatures for primary drying, but also on drying and collapse appearance, on collapse phases of the formulation, on its robustness to temperature changes, and e.g., on potential crystallization processes and annealing possibilities. With the described methodology, a routine usage of freeze-dry microscopy with limited experimental run times is feasible ensuring reasonable accuracy when performing three to five measurements. Transferability to freeze-drying cycles was shown exemplarily, but further investigations are necessary in order to determine an accurate transfer factor for the single excipients, APIs and formulations in general.

5 Zusammenfassung

Gefriertrocknungsmikroskopie ist die Schlüsseltechnologie schlechthin, um die kritische Temperatur der Formulierung zu bestimmen, die zum Design vernünftiger Gefriertrocknungszyklen notwendig ist. Schon der Theorie nach spiegeln Messungen der Kollaps-temperatur die Prozessverhältnisse während der Primärtrocknung besser wider als z. B. das Messen der Glasübergangstemperatur per DSC (Dynamischer Differenzieller Kalorimetrie).

Thema der vorliegenden Dissertation waren detaillierte Untersuchungen zu Methodik, Dateninterpretation und praktischer Übertragbarkeit von gefriertrocknungsmikroskopischen Messungen. Früher publizierte Arbeiten und Befunde wurden in die Diskussion integriert und in einigen Fällen neu interpretiert.

Basierend auf theoretischen Überlegungen und praktischen Erfahrungen wurde das Kollapsverhalten in drei verschiedene Kollapsphasen klassifiziert:

(1) Ein beginnender Kollaps wurde in Form von ersten strukturellen Veränderungen in der getrockneten Struktur, die an den Sublimationsbereich angrenzt, definiert.

(2) Unter den Bedingungen eines vollen Kollapses weißt die gefriergetrocknete Struktur keine Verknüpfung mehr zu der Struktur an der Sublimationsfront auf. Sie verliert gleich nach dem Sublimationsprozess ihre Struktur, was zur Bildung von getrockneten Fragmenten führt.

(3) Weiterhin wurde ein 50%-Kollaps eingeführt, der einen „Mittelpunkt“-Kollaps repräsentiert und die Vergleichbarkeit mit „Mittelpunkt“-Glasübergängen (T_g') erleichtert. Er wird als Mittelwert aus der Temperatur des beginnenden Kollapses und der des vollständigen Kollapses berechnet. Vergleichbar zu Glasübergängen wird also auch Kollaps durch einen Übergang charakterisiert, der in einem Temperaturbereich auftritt.

Deshalb sollten sowohl der beginnende als auch der vollständige Kollaps ausgewiesen und in Betracht gezogen werden, wenn es um Optimierung und Formulierungsentwicklung geht.

Um zu einem besseren theoretischen und praktischen Verständnis des Phänomens „Kollaps“ beizutragen und um Ergebnisse jüngerer und älteren Datums (besser) zu erklären, wurde im Rahmen der vorliegenden Doktorarbeit ein Modell aufgestellt, das die Faktoren, welche gefriertrocknungsmikroskopische Experimente beeinflussen, im Kontext darstellt. Es basiert auf dem Konzept, dass die Wechselwirkungen zwischen Wassermolekülen und der Produktmatrix elementar sind, was das Kollapsgeschehen betrifft, wobei Wasser als Weichmacher in der Produktmatrix, welche Substanz und ungefrorenes Wasser enthält, fungiert. Wenn die einflussnehmenden Parameter in Summe einen kritischen Level erreichen, wird die Festigkeit der Produktmatrix soweit herabgesetzt, dass es zu einem viskosen Fließen des Materials in die Pore kommt, was gemeinhin als Kollaps bezeichnet wird. Die Produktmatrix selbst wird durch ihre Wasserbindungsfähigkeit, die Hygroskopizität der getrockneten Ausgangssubstanz(en), ihre Festigkeit, ihre spezifische Oberfläche sowie ihren Strömungswiderstand gegenüber den Wassermolekülen charakterisiert. Während eines gefriertrocknungsmikroskopischen Experiments sollte der limitierende Faktor im Gesamtgleichgewicht auf Seiten der Temperatur oder - besser gesagt - der verwendeten Heizrate liegen. Die gewählten Druckeinstellungen sollten adäquat, aber nicht limitierend sein. Neben den Temperatur- und Druckbedingungen nehmen der Grad der Unterkühlung, die physikalischen Eigenschaften der gelösten Substanzen sowie ihre jeweiligen Konzentrationen primär Einfluss auf das Kollapsgeschehen.

Um das eingeführte Modell zu untermauern, die Wichtigkeit der einzelnen Parameter zu untersuchen und eine optimierte Methodik für die Gefriertrocknungsmikroskopie zu finden, wurden detaillierte Studien durchgeführt, insbesondere zu den experimentellen Einstellungsmöglichkeiten.

Diese Untersuchungen führten im Ergebnis zu folgenden Empfehlungen: Für Routinemessungen sollte eine Heizrate von 0,5 bis 1°C/min verwendet werden. Falls die minimal mögliche Kollapstemperatur in einer Art Extremwertmessung bestimmt werden soll, so kann eine komplizierte Messprozedur mit einer Heizrate von 0,1°C/min und Haltezeiten von 10 min bei jedem vollen Grad Celsius angewendet werden. Diese Methodik spiegelt die Verhältnisse, die während einer Primärtrocknung in einem Gefriertrockner herrschen, in gewisser Weise besser als die Standardmethode wider. Allerdings verlängert sie die für ein Experiment benötigte Zeit erheblich und trägt nur in geringer Weise zu einer Vereinfachung der Übertragbarkeitsproblematik bei. Für eine maximale Reproduzierbarkeit sollte die Dicke der gefrorenen Schicht mit Hilfe von Abstandshaltern fixiert werden.

Zusätzlich wurde gezeigt, dass die Gefriertrocknungsmikroskopie ein geeignetes Werkzeug ist, um den Einfluss verschiedener Kühlraten und des Temporns auf die Kollapstemperatur zu bestimmen.

Weiterhin wurden Korrelationskoeffizienten basierend auf Nukleationstemperatur und zugehörigen Konzentrationswerten für Glucose, 2-(Hydroxypropyl)- β -cyclodextrin und Polyvinylpyrrolidon 40 kDa berechnet. Hier konnte kein Einfluss der Nukleationstemperatur (bzw. des Unterkühlungsgrads) auf die Kollapstemperatur festgestellt werden, wenn alle Werte in die Untersuchung einbezogen wurden. Es wird jedoch angenommen, dass verschiedene Unterkühlungsgrade neben Zufallsereignissen die Kollapstemperaturmessung beeinflussen, was sich in den relativ hohen Standardabweichungen der gemessenen Kollapstemperaturen niederschlägt. Deshalb wird empfohlen, drei bis fünf unabhängige gefriertrocknungsmikroskopische Messungen von einer Probe durchzuführen und die Mittelwerte hieraus zu berechnen, um Unterschiede in der gefrorenen Struktur der maximal aufkonzentrierten Lösung zu relativieren.

Für Saccharose, Trehalose, Glucose, 2-(Hydroxypropyl)- β -cyclodextrin sowie Polyvinylpyrrolidon 10 kDa und 40 kDa wurde eine Abhängigkeit der Kollapstemperatur vom Feststoffgehalt der Lösung festgestellt.

Trotz der Unterschiede im Grad der Beeinflussung und trotz verschiedener Kurvenverläufe für die unterschiedlichen Hilfsstoffe, kristallisierten sich folgende tendenzielle Zusammenhänge heraus: (1) Für eine bestimmte Hilfsstoffklasse nimmt die Kollapstemperatur mit zunehmender Molekülgröße oder Kettenlänge (für Polymere) zu und die Differenz zwischen beginnendem und vollständigem Kollaps wird kleiner. (2) Für alle Hilfsstoffe wurde eine exponentielle Korrelation zwischen Konzentration und Kollapstemperatur ermittelt, wobei die Kollapstemperaturen für niedrige Konzentrationen niedrig und für mittlere Konzentrationen (10 bis 15% m/m) hoch waren. (3) Für hohe Feststoffkonzentrationen (ca. 20 bis 30% m/m) zeigen hygroskopische Substanzen eine Erniedrigung der Kollapstemperatur, deren Betrag je nach Hilfsstoff variiert.

Im Allgemeinen erlaubt es die Messung der Viskosität der Ausgangslösung, die zu gefriertrocknungsmikroskopischen Messungen herangezogen wird, nicht, Vorhersagen über das Kollapsverhalten bzw. den Einfluss der Feststoffkonzentration hierauf zu treffen. Stattdessen scheinen die chemische Struktur der Substanzen (insbesondere ihre Größe) und die Hygroskopizität des trockenen Ausgangsmaterials den ausschlaggebenden Einfluss auf das Kollapsverhalten zu haben.

Außerdem wurde gezeigt, dass bovines Serumalbumin und humanes Serumalbumin, was gefriertrocknungsmikroskopische Messungen betrifft, aufgrund ihrer strukturellen Ähnlichkeit austauschbar sind. Zusätzlich bieten sie sich für einen Einsatz als Modellproteine sowie als Proteinersatz in Placeboformulierungen an. Im Gegensatz zur Glasübergangstemperatur T_g' konnte ihre Kollapstemperatur eindeutig und relativ leicht per Gefriertrocknungsmikroskopie festgestellt werden.

Versuche mit binären Mischungen eines Proteins mit einem Disaccharid förderten eine hohe Abhängigkeit der Kollapstemperatur (des beginnenden und vollständigen Kollapses) von der Mischungszusammensetzung zu Tage.

Große Unterschiede wurden auch beim Gefriertrocknungs- und Kollapsverhalten festgestellt: Proben mit einer hohen Konzentration an Protein zeigten Risse und Spalten in der Struktur, wobei die Trocknungstemperatur weit unterhalb der Kollapstemperatur lag und kein Kollaps identifiziert werden konnte. Im Falle eines Kollapses zeigten sie ein ziemlich elastisches Verhalten unter Bildung von charakteristischen Filamenten. Im Gegensatz dazu wiesen zuckerreiche Mischungen ein zuckertypisches Kollapsverhalten mit definierten Löchern in der Struktur auf, die sich schnell vergrößerten. Die letztgenannten Proben trockneten ohne strukturelle Risse, wenn man sie unterhalb ihrer Kollapstemperatur trocknete. Interessanterweise war die Differenz zwischen beginnendem und vollständigem Kollaps signifikant höher für Mischungen mit einem ähnlichen Feststoffanteil an Protein und Zucker und geringer für die Proben mit einseitigem Mischungsverhältnis. Dieser Befund wurde durch die Oberflächenabsättigung der Proteinoberfläche durch die Disaccharidmoleküle erklärt.

Für ausgewählte Hilfsstoffe und binäre Mischungen mit Protein und Disacchariden wurden die gemessenen Kollapstemperaturen mit der Glasübergangstemperatur der maximal aufkonzentrierten Lösung verglichen. Aufgrund der Abhängigkeit der Kollapstemperatur von der Feststoffkonzentration der gemessenen Substanz(en), variierten die Differenzen zwischen der Kollapstemperatur und der Glasübergangstemperatur stark für die Hilfsstofflösungen und die Protein/Zucker-Mischungen. Die höchste Differenz zwischen dem beginnenden Kollaps und der Glasübergangstemperatur von 12°C wurde für eine wässrige Lösung gemessen, die 3,25% (m/m) bovines Serumalbumin und 1,75% (m/m) Saccharose enthielt. Die Breite des Kollapstemperaturbereiches (die durch die Differenz zwischen dem beginnendem und dem vollen Kollaps festgelegt wird) kann als Parameter dienen, um Aussagen zur Robustheit der Formulierung in Bezug auf Temperaturunterschiede während der Primärtrocknung zu treffen.

Durch gefriertrocknungsmikroskopische Messungen in Kombination mit Gefriertrocknungsläufen in einer Laboranlage konnte gezeigt werden, dass die erhaltenen Kollapstemperaturergebnisse im Allgemeinen auf Gefriertrocknungszyklen übertragbar sind, was zum Beispiel die Unterschiede in der Kollapstemperatur zwischen verschiedenen Konzentrationen eines einzelnen Hilfsstoffes betrifft. Rasterelektronenmikroskopische Aufnahmen kombiniert mit BET-Messungen der spezifischen Oberfläche wiesen eindeutig darauf hin, dass Kuchen Schäden aufwiesen, wenn sie bei höheren Produkttemperaturen während der Primärtrocknung getrocknet wurden, auch wenn diese Temperaturen unterhalb der Temperatur des beginnenden Kollapses lagen.

Zusammenfassend ist die Gefriertrocknungsmikroskopie ein äußerst hilfreiches Werkzeug zur Optimierung von Formulierungen und Gefriertrocknungszyklen. Sie stellt dem Anwender nicht nur Informationen über kritische Formulierungstemperaturen für die Primärtrocknung zur Verfügung, sondern auch zum Erscheinungsbild von Trocknung und Kollaps, zu den Kollapsphasen der Formulierung, zu ihrer Robustheit in Bezug auf Temperaturänderungen und z. B. auch zu möglichen Kristallisationsprozessen und gegebenenfalls zum Tempern. Mit der beschriebenen Methodik ist ein Routineeinsatz der Gefriertrocknungsmikroskopie mit einer begrenzten Versuchsdauer realisierbar, wobei eine vernünftige Genauigkeit erreicht wird, wenn drei bis fünf Messungen durchgeführt werden. Die Übertragbarkeit auf Gefriertrocknungszyklen wurde exemplarisch belegt, sollte aber durch weitere Untersuchungen ergänzt werden, um einen akkuraten Übertragungsfaktor für die einzelnen Hilfsstoffe, Wirkstoffe und Formulierungen im Allgemeinen zu ermitteln.

6 Suggestions for further research

As shown in the results and discussion section, the stochastic nature of nucleation and different supercooling of samples which were prepared and treated in the same way leads to high standard deviations of T_c measurements. This problem is also found in commercial freeze-drying processes where nucleation is commonly not controlled. However, new methods are available like using high pressure to assist freezing [198]. High pressure allows more extreme supercooling and nucleation induction by rapid pressure release. This leads to larger numbers of small ice crystals and vial-to-vial consistency [15]. New approaches like the mentioned one should be included in FDM stages as well. Control of supercooling and nucleation would lead to more reproducible results and better transferability, especially if ice crystal sizes obtained in vials can be imitated.

Additionally, new combinations of different analytical techniques would be helpful. Combined FDM/DSC equipment for example would allow detailed investigations on thermal behavior of formulations and would probably answer some (still) open questions on differences between T_c and T_g' . For determination of damages to APIs, a microscope with an FT-IR option and FDM observation which is available during the experiment would be of great value.

Detection problems concerning T_{oc} and T_{fc} could be solved by computer software programmed for the recognition of collapse holes and disruptions.

With regard to transferability of FDM results to runs in freeze-dryers, extensive studies are necessary. Because of the variability of the T_c dependence on total solid content of the solved substance(s), they should include various excipients and APIs. During primary drying, T_p values identical to T_c (T_{oc} , T_{fc} , or T_{c-50} respectively), below T_c and above T_c should be tested in separate runs.

Finally, product characteristics (SSA, moisture content) and their acceptability should then be compared to T_{oc} , T_{fc} , T_{c-50} , ΔT_c and T_g' values for single solutions or formulations.

7 References

1. **Verband Forschender Arzneimittelhersteller.** *Statistics 2007.* Berlin: Ruksaldruck, 2007.
2. **Roque, A.C.A., Lowe, C.R. and Taipa, M.A.** Antibodies and genetically engineered related molecules: Production and purification. *Biotechnol. Prog.* 2004, 20, pp. 639-654.
3. **Pavlou, A.K. Belsey, M.J.** The therapeutic antibodies market to 2008. *Eur. J. Pharm. Biopharm.* 2005, 59, pp. 389-396.
4. **Costantino, H.R.** Excipients for Use in Lyophilized Pharmaceutical Peptide, Protein, and other Bioproducts. In: H.R. Costantino and M.J. Pikal. *Lyophilization of Biopharmaceuticals.* Arlington VA: AAPS Press, 2004, pp. 139-228.
5. **Murgatroyd, K.** The Freeze Drying Process. In: P. Cameron. *Good pharmaceutical freeze-drying practice.* Boca Raton, Florida, USA: CRC Press LLC, 1997, pp. 1-4.
6. **Pikal, M.J.** Freeze Drying. *Encyclopedia of Pharmaceutical Technology.* Marcel Dekker, 2002, pp. 1299-1326.
7. **Pikal, M.J. and Costantino, H.R.** Lyophilization of Biopharmaceuticals. In: R.T. Borchard and C.R. Middaught. *Biotechnology: Pharmaceutical Aspects, Volume II.* Arlington, VA: AAPS Press, 2004.
8. **Carpenter, J. and Chang, B.S.** Lyophilization of protein pharmaceuticals. In: K.E. Avis, V. Wu. *Biotechnology and Biopharmaceutical Manufacturing, Processing, and Preservation.* Buffalo Grove: IL: Interpharm Press, 1996.

9. **Franks, F.** Freeze-drying of bioproducts: putting principles into practice. *Eur. J. Pharm. Biopharm.* 1998, 45, pp. 221-229.
10. **Franks, F.** Freeze drying: From empiricism to predictability. *Cryo-Letters.* 1990, 11, pp. 93-110.
11. **Nail, S.L. and Gatlin, L.A.** Freeze-drying: principles and practice. In: K.E. Avis, H.A. Lieberman and L. Lechman. *Pharmaceutical Dosage Forms: Parenteral Medications.* New York: Marcel Dekker, 1993, Vol. 2, pp. 163-233.
12. **Hussain, A.S.** Emerging Science Issues in Pharmaceutical Manufacturing: Process Analytical Technologies, FDA Science Board Meeting, 2001.
13. **FDA Guideline (2002).** Pharmaceutical cGMPs for the 21st Century - A Risk-Based Approach, accessed Sept. 2008:

<http://www.fda.gov/cder/guidance/6419fnl.pdf>.
14. **FDA Guideline (2004).** Guidance for Industry: PAT - A Framework for Innovative Pharmaceutical Development, Manufacturing and Quality Assurance, accessed Sept. 2008: <http://www.fda.gov/cder/guidance/6419fnl.pdf>.
15. **Searles, J.A.** Freezing and Annealing Phenomena in Lyophilization. In: L. Rey and J.C. May. *Freeze-Drying/Lyophilization of Pharmaceutical and Biological Products.* New York: Marcel Dekker, Inc., 2004, pp. 109-145.
16. **Bhatnagar, B.S., Bogner, R.H. and Pikal, M.J.** Protein Stability During Freezing: Separation of Stresses and Mechanisms of Protein Stabilization. *Pharm. Dev. Technol.* 2007, 12, pp. 505-523.
17. **Searles, J., Carpenter, J. and Randolph, T.** The ice nucleation temperature determines the primary drying rate of lyophilization for samples frozen on a temperature-controlled shelf. *J. Pharm. Sci.* 2001, 90, pp. 860-871.

18. **Pikal, M.J.** Freeze Drying of Proteins: Process, Formulation, and Stability. In: J.L. Cleland and R. Langer. *Formulation and Delivery of Proteins and Peptides*. Washington DC: ACS, 1994, pp. 120-133.
19. **Franks, F.** Freeze-drying: a combination of physics, chemistry, engineering, and economics. *Japanese Journal of Freezing and Drying*. 1992, 38, pp. 5-16.
20. **Kiovsky, T.E. and Pincock, R.E.** Kinetics of reactions in frozen solutions. *J. Am. Chem. Soc.* 1966, 88, pp. 7704-7710.
21. **Rambhatla, S., Ramot, R., Bhugra, C., Pikal, M.J.** Heat and mass transfer scale-up issues during freeze-drying: II. Control and characterization of the degree of supercooling. *AAPS Pharm. Sci. Tech.* 2004, 5 (4), pp. 1-8.
22. **Fennema, O., Powrie, W and Marth, E.** Low-Temperature Preservation of Foods and Living Matter. New York: Marcel Dekker, 1973.
23. **Presser, I.** Innovative Online Messverfahren zur Optimierung von Gefrier-trocknungsprozessen. München: Ph.D. thesis, 2003.
24. **Tang, X. and Pikal, M.J.** Design of Freeze-Drying Processes for Pharmaceuticals: Practical Advice. *Pharm. Res.* 2004, 21 (2), pp. 191-200.
25. **Pikal, M.J.** Freeze-drying of Proteins. Part I: Process Design. *Bio. Pharm.* 1990, 3, pp. 18-27.
26. **Pikal, M.J., Shah, S., Senior, D., Lang, J.E.** Physical chemistry of freeze-drying: measurement of sublimation rates for frozen aqueous solutions by a microbalance technique. *J. Pharm. Sci.* 1983, 72, pp. 635-650.
27. **Pikal, M.J. and Lang, J.E.** Rubber closures as a source of haze in freeze dried parenterals: test methodology for closure evaluation. *J. Parent. Drug. Assoc.* 1978, 32, pp. 162-173.

28. **Pikal, M.J., Roy, M.L. and Shah, S.** Mass and Heat Transfer in Vial Freeze-drying of Pharmaceuticals: Role of the Vial. *J. Pharm. Sci.* 1984, 73, pp. 1224-1237.
29. **Chang, B.S. and Patro, S.Y.** Freeze-drying Process Development for Protein Pharmaceuticals. In: H.R. Costantino and M.J. Pikal. *Lyophilization of Biopharmaceuticals*. Arlington VA: AAPS Press, 2004, pp. 113-138.
30. **Rambhatla, S. and Pikal, M.J.** Heat and Mass Transfer Issues in Freeze-drying Process Development. In: H.R. Costantino and M.J. Pikal. *Lyophilization of Biopharmaceuticals*. Arlington VA: AAPS Press, 2004, pp. 75-109.
31. **Gatlin, L.A. and Nail, S.L.** Protein Purification Process Engineering. Freeze-Drying: A Practical Overview. *Bioprocess. Technol.* 1994, 18, pp. 317-367.
32. **Pikal, M.J.** Use of Laboratory Data in Freeze Drying Process Design: Heat and Mass Transfer Coefficients and the Computer Simulation of Freeze Drying. *J. Parenter. Sci. Technol.* 1985, 39, pp. 115-139.
33. **Roy, M.L. and Pikal, M.J.** Process control in freeze drying: Determination of the end point of sublimation drying by an electronic moisture sensor. *J. Parenter. Sci. Technol.* 1989, pp. 60-66.
34. **Milton, N., Nail, S.L., Roy, M.L., Pikal, M.J.** Evaluation of manometric temperature measurements as a method of monitoring product temperature during lyophilization. *J. Pharm. Sci. Technol.* 1997, 51, pp. 7-16.
35. **Tang, X.C., Nail, S.L. and Pikal, M.J.** Freeze-Drying Process Design by Manometric Temperature Measurement: Design of a Smart Freeze-Dryer. *Pharm. Res.* 2005, 22, pp. 685-700.
36. **Pikal, M.J., Shah, S., Roy, M.L., Putman, R.** The secondary drying stage of freeze drying: Drying kinetics as a function of temperature and chamber pressure. *Int. J. Pharm.* 1990, 60, pp. 203-327.

37. **Abdul-Fattah, A.M., Kalonia, D.S. and Pikal, M.J.** The Challenge of Drying Method Selection for Protein Pharmaceuticals: Product Quality Implications. *J. Pharm. Sci.* 2006, pp. 1-31.
38. **Pikal, M.J. and Dellerman, K.M.** Stability testing of pharmaceuticals by high-sensitivity isothermal calorimetry at 25°C: Cephalosporins in the solid and aqueous solution states. *Int. J. Pharm.* 1989, 50, pp. 233-252.
39. **Pikal, M.J., Lukes, A.L. and Lang, J.E.** Thermal decomposition of amorphous beta-lactam antibacterials. *J. Pharm. Sci.* 1977, 66, pp. 1312-1316.
40. **Pikal, M.J., Lukes, A.L., Lang, J.E., Gaines, K.** Quantitative crystallinity determinations of Beta-lactam antibiotics by solution calorimetry: Correlations with Stability. *J. Pharm. Sci.* 1978, 67, pp. 767-773.
41. **Schwegman, J.J., Hardwick, L.M. and Akers, M.J.** Practical Formulation and Process Development of Freeze-Dried Products. *Pharm. Dev. Techn.* 2005, 10, pp. 151-173.
42. **International Pharmaceutical Excipients Council of the Americas.** Frequently Asked Questions, accessed Nov. 2008:

<http://www.ipecamericas.org/public/faqs.html#question1>.
43. **Trappler, E.** Strategies in development of lyophilized parenterals. *Am. Pharm. Rev.* 2003, 5, pp. 54-58.
44. **Abdelwahed, W., Degobert, G., Stainmesse, S., Fessi, H.** Freeze-drying of nanoparticles: Formulation, process and storage considerations. *Adv. Drug Del. Rev.* 2006, 58, pp. 1688-1713.
45. **Wang, W.** Lyophilization and development of solid protein pharmaceuticals. *Int. J. Pharm.* 2000, 203, pp. 1-60.

46. **Arakawa, T. and Timasheff, S.N.** Preferential interactions of proteins with salts in concentrated solutions. *Biochem.* 1982, 21 (25), pp. 6545-6552.
47. **Timasheff, S.N.** The Control of Protein Stability and Association by Weak Interactions with Water: How Do Solvents Affect These Processes? *Annu. Rev. Biophys. Biomol. Struct.* 1993, 22, pp. 67-97.
48. **Timasheff, S.N.** Control of protein stability and reactions by weakly interacting cosolvents: the simplicity of the complicated. *Adv. Protein Chem.* 1998, 51, pp. 355-432.
49. **Kita, Y., Arakawa, T., Lin, T.Y., Timasheff, S.N.** Contribution of the Surface Free Energy Perturbation to Protein-Solvent Interactions. *Biochem.* 1994, 33 (50), pp. 15178-15189.
50. **Arakawa, T., Bhat, R. and Timasheff, S.N.** Preferential interactions determine protein solubility in three-component solutions: the magnesium chloride system. *Biochem.* 1990, 29 (7), pp. 1914-1923.
51. **Arakawa, T. and Timasheff, S.N.** Preferential interactions of proteins with solvent components in aqueous amino acid solutions. *Arch. Biochem. Biophys.* 1983, 224 (1), pp. 169-177.
52. **Lee, J.C., Gekko, K. and Timasheff, S.N.** Measurements of preferential solvent interactions by densimetric techniques. *Methods Enzymol.* 1979, 61, pp. 26-49.
53. **Gekko, K. and Timasheff, S.N.** Thermodynamic and kinetic examination of protein stabilization by glycerol. *Biochem.* 1981, 20 (16), pp. 4677-4686.
54. **Timasheff, S.N.** Protein hydration, thermodynamic binding, and preferential hydration. *Biochem.* 2002, 41 (46), pp. 13473-13482.

55. **Bhat, R. and Timasheff, S.N.** Steric exclusion is the principal source of the preferential hydration of proteins in the presence of polyethylene glycols. *Protein Science*. 1992, 1 (9), p. 1133.
56. **Timasheff, S.N.** Water as ligand: Preferential binding and exclusion of denaturants in protein unfolding. *Biochem*. 1992, 31 (41), pp. 9857-9864.
57. **Anchordoquy, T.J. and Carpenter, J.F.** Polymers protect lactate dehydrogenase during freeze-drying by inhibiting dissociation in the frozen state. *Arch. Biochem. Biophys*. 1996, 332, pp. 231-238.
58. **Crowe, J.H. and Carpenter, J.F.** Preserving dry biomaterials: the water replacement hypothesis. *Biopharm*. 1993, 6 (2), pp. 40-42.
59. **Allison, S.D., Dong, A. and Carpenter, J.F.** Counteracting effects of thiocyanate and sucrose on chymotrypsinogen secondary structure and aggregation during freezing, drying and rehydration. *Biophys. J.* 1996, 71, pp. 2022-2032.
60. **Allison, S.D., Randolph, T.W., Manning, M.C., Middleton, K., Davis, A., Carpenter, J.F.** Effects of drying methods and additives on structure and function of actin: mechanisms of dehydration-induced damage and its inhibition. *Arch. Biochem. Biophys*. 1998, 358, pp. 171-181.
61. **Carpenter, J.F., Pikal, M.J., Chang, B.S., Randolph, T.W.** Rational Design of Stable Lyophilized Protein Formulations: Some Practical Advice. *Pharm. Res.* 1997, 14 (8), pp. 969-975.
62. **Pikal, M.J.** Freeze-drying of proteins. Part II: Formulation Selection. *Bio. Pharm.* 1990, 3, pp. 26-29.
63. **Carpenter, J.F., Crowe, J.H. and Arakawa, T.** Comparison of solute-induced protein stabilization in aqueous solution and in frozen and dried state. *J. Dairy Sci.* 1990, 73, pp. 3627-3636.

64. **Carpenter, J.F. and Crowe, J.H.** An infrared spectroscopic study of interactions of carbohydrates with dried proteins. *Biochemistry*. 1989, 28, pp. 3916-3922.
65. **Roser, B.** Trehalose drying: a novel replacement for freeze-drying. *Biopharm.* 1991, 4 (9), pp. 47-53.
66. **Hagen, S.J., Hofrichter, J. and Eaton, W.A.** Protein reaction kinetics in a room-temperature glass. *Science*. 1995, 269, pp. 959-962.
67. **Sola-Penna, M. and Meyer-Fernandes, J.R.** Stabilization against thermal inactivation promoted by sugars on enzyme structure and function: why is trehalose more effective than other sugars? *Arch. Biochem. Biophys.* 1998, 360, pp. 10-14.
68. **Andaya, J.D., Hsu, C.C. and Shire, S.J.** Mechanisms of Aggregate Formation and Carbohydrate Excipient Stabilization of Lyophilized Humanized Monoclonal Antibody Formulations. *AAPS Pharm. Sci. Tech.* 2003, 5 (2), pp. 94-104.
69. **Arakawa, T. and Timasheff, S.N.** Stabilization of protein structure by sugars. *Biochem.* 1982, 21 (25), pp. 6536-6544.
70. **Xie, G. and Timasheff, S.N.** The thermodynamic mechanism of protein stabilization by trehalose. *Biophys. Chem.* 1997, 64 (1-3), pp. 25-43.
71. **Lee, J.C. and Timasheff, S.N.** The stabilization of proteins by sucrose. *J. Biol. Chem.* 1981, 256 (14), pp. 7193-7201.
72. **Hatley, R.H.** Glass fragility and the stability of pharmaceutical preparations - excipients selection. *Pharm. Dev. Technol.* 1997, 2, pp. 257-264.
73. **Hagen, S.J., Hofrichter, J. and Eaton, W.A.** Germinate rebinding and conformational dynamics of myoglobin embedded in a glass at room temperature. *J. Phys. Chem.* 1996, 100, pp. 12008-12021.

74. **Cleland, J.L., Lam, X., Kendrick, B., Yang, T.H., Overcashier, D., Brooks, D., Hsu, C., Carpenter, J.F.** A Specific Molar Ratio of Stabilizer to Protein is Required for Storage Stability of a Lyophilized Monoclonal Antibody. *J. Pharm. Sci.* 2001, 90(3), pp. 310-321.
75. **Shire, S.J., Shahrokh, Z. and Liu, J.** Challenges in the development of high protein concentration formulations. *J. Pharm. Sci.* 2004, 93, pp. 1390-1402.
76. **Tanaka, K., Takeda, T. and Miyajima, K.** Cryoprotective effect of saccharides on denaturation of catalase by freeze-drying. *Chem. Pharm. Bull.* 1991, 39, pp. 1091-1094.
77. **Levine, H. and Slade, L.** Another view of trehalose for drying and stabilizing biological materials. *Biopharm.* 1992, pp. 36-40.
78. **Taylor, L.S. and Zografis, G.** Sugar-Polymer Hydrogen Bond Interactions in Lyophilized Amorphous Mixtures. *J. Pharm. Sci.* 1998, 87 (12), pp. 1615-1621.
79. **Librizzi, F., Vitrano, E. and Cordone, L.** Dehydration and crystallization of trehalose and sucrose glasses containing carbomonoxymyoglobin. *Biophys. J.* 1999, 76, pp. 2727-2734.
80. **Taylor, L.S. and York, P.** Characterization of the Phase Transitions of Trehalose Dihydrate on Heating and Subsequent Dehydration. *J. Pharm. Sci.* 1998, 87 (3), pp. 347-355.
81. **Dawson, P.J.** Effect of formulation and freeze-drying on long-term stability of rDNA-derived cytokines. *Dev. Biol. Stand.* 1992, 74, pp. 273-282.
82. **Nema, S. and Avis, K.E.** Freeze-thaw studies of a model protein, lactate dehydrogenase, in the presence of cryoprotectants. *J. Parenter. Sci. Technol.* 1992, 47, pp. 76-83.

83. **Physicians Desk.** Medical Economics Company Incorporation, 53rd edn. Montvale, NJ. 1999.
84. **Tarelli, E., Mire-Sluis, A., Tivnann, H.A., Bolgiano, B., Crane, D.T., Gee, C., Lemercinier, X., Athayde, M.L., Sutcliffe, N., Corran, P.H., Rafferty, B.** Recombinant human albumin as a stabilizer for biological materials and for the preparation of international reference reagents. *Biologicals*. 1998, 26, pp. 331-346.
85. **Putnam, F.W. (Ed.).** *The Plasma Proteins: Structure, Function and Genetic Control*. New York: Academic Press, 1975. pp. 141, 147.
86. **Reed, R.G. et al.** *Biochem. J.*, 1980, 191, p. 867.
87. **Hirayama, K.** BBRC, 1990, 173 (2), p. 639.
88. **Putnam, F.W. (Ed.).** *The Plasma Proteins*. 2nd Ed. New York: Academic Press, 1975. pp. 133-181.
89. **SIGMA.** Calculation based on sequence given by B. Meloun et al. 58 (1), 1975, *FEBS Letters*, p. 134.
90. **SIGMA-ALDRICH.** Certificate of Origin. 2005.
91. **Crommelin, D.J.A.** Formulation of Biotech Products, including Biopharmaceutical Considerations. In: D.J.A. Crommelin und R.D. Sindelar. *Pharmaceutical Biotechnology*. Philadelphia, PA, USA: Taylor & Francis Inc., 2007.
92. **Skrabanja, A.T., de Meere, A.L., de Ruiter, R.A., and van den Oetelaar, P.J.** Lyophilization of biotechnology products. *Pharm. Sci. Technol.* 1994, 48, pp. 311-317.

93. **Heller, M.C., Carpenter, J.F. and Randolph, T.W.** Manipulation of lyophilization-induced phase separation: implications for pharmaceutical proteins. *Biotechnol. Prog.* 1997, 13, pp. 590-596.
94. **Williams, N.A. and Dean, T.** Vial breakage by frozen mannitol solutions: Correlation with thermal characteristics and effect of stereoisomerism, additives, and vial configuration. *J. Parenter. Sci. Technol.* 1991, 45, pp. 94-100.
95. **Burger, A., Henck, J.-O., Hetz, S., Rollinger, J.M., Weissnicht, A.A., Stöttner, H.** Energy/temperature diagram and compression behavior of the polymorphs of D-mannitol. *J. Pharm. Sci.* 2000, 89 (4), pp. 457-468.
96. **Cavatur, R.K., Vemuri, N.M., Pyne, A., Chrzan, Z., Toledo-Velasquez, D., Suryanarayanan, R.** Crystallization Behavior of Mannitol in Frozen Aqueous Solutions. *Pharm. Res.* 2002, 19 (6), pp. 894-900.
97. **Cavatur, R.K. and Suryanarayanan, R.** Characterization of phase transitions during freeze drying by in situ X-ray powder diffractometry. *Pharm. Develop. and Technol.* 1998, 3, pp. 579-586.
98. **Yu, L., et al.** Existence of a mannitol hydrate during freeze drying and practical implications. *J. Pharm. Sci.* 1999, 88, pp. 196-199.
99. **Kim, A.I., Akers, M.J. and Nail, S.L.** The physical state of mannitol after freeze drying: Effects of mannitol concentration, freezing rate, and a noncrystallizing cosolute. *J. Pharm. Sci.* 1998, 87, pp. 931-935.
100. **Izutsu, K., Yoshioka, S. and Terao, T.** Effect of mannitol crystallinity on the stabilization of enzymes during freeze-drying. *Pharm. Res.* 1993, 10, pp. 1232-1237.
101. **Chongprasert, S., Knopp, S.A. and Nail, S.L.** Characterization of Frozen Solutions of Glycine. *J. Pharm. Sci.* 2001, 90 (11), pp. 1720-1728.

102. **Akers, M.J., Milton, N., Byrn, S.R., Nail, S.L.** Glycine crystallization during freezing: The effects of salt form, pH, and ionic strength. *Pharm. Res.* 1995, 12, pp. 1457-1461.
103. **Liu, J.** Physical Characterization of Pharmaceutical Formulations in Frozen and Freeze-Dried Solid States: Techniques and Applications in Freeze-Drying Development. *Pharm. Dev. Technol.* 2006, 11, pp. 3-28.
104. **Pikal, M.J. and Shah, S.** The collapse temperature in freeze drying: Dependence on measurement methodology and rate of water removal from the glassy phase. *Int. J. Pharm.* 1990, 62, pp. 165-186.
105. **MacKenzie, A.P.** Collapse During Freeze-drying: Qualitative and Quantitative Aspects. In: S.A. Goldblith and W.W. Rothmayr. *Freeze-drying and Advanced Food Technology*. New York, NY: Academic Press, 1975.
106. **Adams, G.D.J. and Ramsay, J.R.** Optimizing the lyophilization cycle and the consequences of collapse on the pharmaceutical acceptability of *Erwinia L-asparaginase*. *J. Pharm. Sci.* 1996, 85, pp. 1301-1305.
107. **Rambhatla, S., Obert, J.P., Luthra, S., Bhugra, C., Pikal, M.J.** Cake Shrinkage During Freeze Drying: A Combined Experimental and Theoretical Study. 2005, 1, pp. 33-40.
108. **Schersch, K., Betz, O., Garidel, P., Mühlau, S., Bassarab, S., Winter, G.** Effect of Collapse During Lyophilization and During Storage at Elevated Temperatures on the Stability of Pharmaceutical Protein Lyophilizates. [Proc.]. CPPR Freeze Drying of Pharmaceuticals and Biologicals Conference, Garmisch-Partenkirchen, Germany: 2006.
109. **Passot, S., Fonseca, F., Barbouche, N., Marin, M., Alarcon-Lorca, M., Rolland, D., Rapaud, M.** Effect of Product Temperature During Primary Drying

- on the Long-Term Stability of Lyophilized Proteins. *Eur. J. Pharm. Biopharm.* 2005, 60, pp. 335-348.
110. **Chang, B.S., Randall, C.S. and Lee, Y.S.** Stabilization of lyophilized porcine pancreatic elastase. *Pharm. Res.* 1993, 10, pp. 1478-1483.
111. **Fonseca, F., Passot, S., Cunin, O., Marin, M.** Collapse Temperature of Freeze-Dried *Lactobacillus bulgaricus* Suspensions and Protective Media. *Biotechnol Prog.* 2004, 20, pp. 229-238.
112. **Knopp, S.A., Chongprasert, S. and Nail, S.L.** The relationship between the TMDSC curve of frozen sucrose solutions and collapse during freeze-drying. *J. Therm. An.* 1998, 54, pp. 659-672.
113. **Bellows, R. J. and King, C. J.** Freeze-Drying of Aqueous Solutions: Maximum Allowable Operating Temperature. *Cryobiology.* 1972, 9, pp. 559-561.
114. **Kerr, W.L. and Reid, D.S.** Temperature Dependence of the Viscosity of Sugar and Maltodextrin Solutions in Coexistence with Ice. *Lebensm.-Wiss. u. -Technol.* 1994, 27, pp. 225-231.
115. **Wong, J. and Angell, C.A.** *Glass: Structure by Spectroscopy.* New York: Marcel Dekker, Inc., 1976.
116. **Williams, M.L., Landel, R.F. and Ferry, D.J.** Temperature dependence of relaxation mechanisms in amorphous polymers and other glass-forming liquids. *J. Am. Chem. Soc.* 1955, 77, pp. 3701-3706.
117. **Shamblin, S.L.** The Role of Water in Physical Transformations in Freeze-Dried Products. In: H.R. Costantino and M.J. Pikal. *Lyophilization of Biopharmaceuticals.* Arlington VA: AAPS Press, 2004, pp. 229-270.
118. **Xu, X., Jeronimidis, G. and Atkins, A.G.** On the yield stress of frozen sucrose solutions. *J. Mat. Sci.* 2003, 38, pp. 245-253.

119. **MacKenzie, A.P.** Apparatus for microscopic observations during freeze-drying. *Biodynamica*. 1964, 9, pp. 213-222.
120. **Flink, J. M. and Gejl-Hansen, F.** Two simple freeze drying microscope stages. *Rev. Sci. Instrum.* 1978, 49 (2), pp. 269-271.
121. **Freedman, M., Whittam, J.H. and Rosano, H.L.** Temperature gradient microscopy stage. *J. Food Sci.* 1972, 37, pp. 492-493.
122. **Kochs, M., Schwindke, P. and Koerber, C.** A microscope stage for the dynamic observation of freezing and freeze-drying in solutions and cell suspensions. *Cryo-Lett.* 1989, 10, pp. 401-420.
123. **Nail, S.L., Her, L.M. Proffit, C.P. and Nail, L.L.** An improved microscope stage for direct observation of freezing and freeze-drying. *Pharm. Res.* 1994, 11, pp. 1098-1100.
124. **Hsu, C.C., Walsh, A.J., Nguyen, H.M., Overcashier, D.E., Koning-Bastiaan, H., Bailey, R.C., Nail, S.L.** Design and application of a low temperature peltier-cooling microscope stage. *J. Pharm. Sci.* 1996, 85, pp. 70-74.
125. **Jiang, S. and Nail, S.L.** Effect of process conditions on recovery of protein activity after freezing and freeze-drying. *Eur. J. Pharm. Biopharm.* 1998, 45, pp. 249-257.
126. **Österberg, T., Fatouros, A. and Mikaelsson, M.** Development of a Freeze-Dried Albumin-Free Formulation of Recombinant Factor VIII SQ. *Pharm. Res.* 1997, 14 (7), pp. 892-898.
127. **Wang, D.Q., Hey, J.M. and Nail, S.L.** Effect of Collapse on the Stability of Freeze-Dried Recombinant Factor VIII and α -Amylase. *J. Pharm. Sci.* 2004, 93 (5), pp. 1253-1263.

128. **Yeo, Y. and Park, K.** Characterization of Reservoir-Type Microcapsules Made By the Solvent Exchange Method. *Pharm. Sci. Tech.* 2004, 5 (4), pp. 1-8.
129. **Colandene, J.D., Maldonado, L.M., Creagh, A.T., Vrettos, J.S., Goad, K.G., Spitznagel, T.M.** Lyophilization Cycle Development for a High-Concentration Monoclonal Antibody Formulation Lacking a Crystalline Bulging Agent. *J. Pharm. Sci.* 2007, 96 (6), pp. 1598-1608.
130. **Kramer, T., Kremer, D.M., Pikal, M.J., Petre, W.J., Shalaev, E.Y., Gatlin, L.A.** A procedure to optimize scale-up for the primary drying phase of lyophilization. *J. Pharm. Sci.* 2008, published online 27 May 2008.
131. **Skoog, D.A., Holler, F.J. and Nieman, T.A.** *Principles of instrumental analysis.* Philadelphia: Harcourt Brace, 1998.
132. **Lechuga-Ballesteros, D., Miller, D.P. and Duddu, S.P.** Thermal Analysis of Lyophilized Pharmaceutical Peptide and Protein Formulations. In: H.R. Costantino and M.J. Pikal. *Lyophilization of Biopharmaceuticals.* Arlington, VA: AAPS Press, 2004, pp. 271-335.
133. **Ablett, S., Izzard, M.J., Lillford, P.J., Arvanitoyannis, I., Blanshard, J.M.V.** Calorimetric Study of the Glass Transition Occuring in Fructose Solutions. *Carbohydrate Res.* 1993, 246, pp. 13-22.
134. **Ablett, S., Izzard, M.J. and Lillford, P.J.** Differential Scanning Calorimetric Study of Frozen Glucose and Glycerol Solutions. *J. Chem. Soc. Faraday Trans.* 1992, 88, pp. 789-794.
135. **Kawakami, K. and Pikal, M.J.** Calorimetric investigation of the structural relaxation of amorphous materials: Evaluating validity of the methodologies. *J. Pharm. Sci.* 2005, 94, pp. 948-965.
136. **Hodge, I.M.** Enthalpy relaxation and recovery in amorphous materials. *J. Non-Crystalline Solids.* 1994, 169, pp. 211-266.

137. **Hancock, B.C. and Shamblin, S.L.** Molecular mobility of amorphous pharmaceuticals determined using differential scanning calorimetry. *Thermochimica Acta*. 2001, 380, pp. 95-107.
138. **Hancock, B.C., Shamblin, S.L. and Zografi, G.** Molecular mobility of amorphous pharmaceutical solids below their glass transitions temperatures. *Pharm. Res.* 1995, 12, pp. 799-806.
139. **Bhugra, C. and Pikal, M.J.** Role of Thermodynamic, Molecular, and Kinetic Factors in Crystallization From the Amorphous State. *J. Pharm. Sci.* 2007, 97 (4), pp. 1329-1349.
140. **Masuda, K., Tabata, S., Sakata, Y., Hayase, T., Yonemochi, E., Terada, K.** Comparison of molecular mobility in the glassy state between amorphous indomethacin and salicin based on spin-lattice relaxation times. *Pharm. Res.* 2005, 22, pp. 797-805.
141. **Her, L.M., Jefferis, R.P., Gatlin, L.A., Braxton, B., Nail, S.L.** Measurement of Glass Transition Temperatures in Freeze Concentrated Solutions of Non-Electrolytes by Electrical Thermal Analysis. *Pharm. Res.* 1994, 11(7), pp. 1023-1029.
142. **Miller, D.P., de Pablo, J.J. und Corti, H.** Thermophysical Properties of Trehalose and Its Concentrated Aqueous Solutions. *Pharm. Res.* 1997, 14 (5), S. 578-590.
143. **Katayama, D.S., Carpenter, J.F., Manning, M.C., Randolph, T.W., Setlow, P., Menard, K.P.** Characterization of Amorphous Solids with Weak Glass Transitions Using High Ramp Rate Differential Scanning Calorimetry. *J. Pharm. Sci.* 2008, 97 (2), pp. 1013-1024.

144. **Slade, L.** Protein-Water Interactions: Water as a Plasticizer of Gluten and Other Protein Polymers. In: D. Phillips and J.W. Finley. *Influence of Processing on Food Proteins*. New York: Marcel Dekker, 1988.
145. **Gordon, M. and Taylor, J.S.** Ideal Copolymers and the Second-order Transitions of Synthetic Rubbers. I. Non-crystalline Copolymers. *J. Appl. Chem.* 1952, 2, pp. 493-500.
146. **Cohen, M.H. and Turnbull, D.** Molecular Transport in Liquids and Glasses. *J. Chem. Physics.* 1959, 31, pp. 1164-1169.
147. **Turnbull, D. and Cohen, M.H.** Free-volume Model for the Amorphous Phase: Glass Transition. *J. Chem. Physics.* 1961, 34, pp. 120-125.
148. **Hancock, B.C. and Zografi, G.** The Relationship Between the Glass Transition Temperature and the Water Content of Amorphous Pharmaceutical Solids. *Pharm. Res.* 1994, 11 (4), pp. 471-477.
149. **Kelley, F.N. and Bueche, F.** Viscosity and glass temperature relations for polymer diluent systems. *J. Polym. Sci.* 1961, 50, pp. 549-556.
150. **Simha, R. and Boyer, R.F.** On a General Relation Involving the Glass Temperature and Coefficients of Expansion of Polymers. *J. Chem. Physics.* 1962, 37, pp. 1003-1007.
151. **Fox, T.G.** Second order transition temperatures and related properties of polystyrene. 1. Influence of molecular weight. *J. Appl. Phys.* 1950, 21, pp. 581-591.
152. **Her, L.M. and Nail, S.L.** Measurement of glass transition temperatures of freeze-concentrated solutes by differential scanning calorimetry. *Pharm. Res.* 1994, 11, pp. 54-59.

153. **Surana, R., Pyne, A. and Suryanarayanan, R.** Effect of preparation method on physical properties of amorphous trehalose. *Pharm. Res.* 2004, 21, pp. 1167-1176.
154. **Nail, S.L., Schwegman, J.J. and Kamp, V.** Analytical tools for characterization of frozen systems in the development of freeze-dried pharmaceuticals. *Am. Pharm. Rev.* 2000, 3, pp. 17-25.
155. **Aubuchon, S.R., Thomas, L.C., Theuerl, W., Renner, H.** Investigation of the sub-ambient transitions in frozen sucrose by modulated differential scanning calorimetry (MDSC). *J. Therm. Anal.* 1998, 52, pp. 53-64.
156. **Chang, L., Milton, N., Rigsbee, D., Mishra, D.S., Tang, X., Thomas, L.C., Pikal, M.J.** Using modulated DSC to investigate the origin of multiple thermal transitions in frozen 10% sucrose solutions. *Thermochimica Acta.* 2006, 444 (2), pp. 141-147.
157. **Shalaev, E.Y. and Franks, F.** Structural glass transitions and thermophysical processes in amorphous carbohydrates and their super-saturated solutions. *J. Chem. Soc. Faraday Trans.* 1995, 91(10), pp. 1511-1517.
158. **Johnson, R.E., Ahmed, A., Hodge, C.D., Lewis, L.M.** Freeze-Drying of a Cytokine in an Amorphous Formulation above its Collapse Temperature. *Proc. AAPS Annual Meeting and Exposition, San Diego, USA.* 2007.
159. **Hancock, B.C. and Zografi, G.** Characteristics and Significance of the Amorphous State in Pharmaceutical Systems. *J. Pharm. Sci.* 1997, 86 (1), pp. 1-12.
160. **Dean, J.A.** *Lange's Handbook for Chemistry.* Thirteenth Edition. New York: McGraw-Hill, 1985. pp. 10-74.
161. **Schiffter, H.A.** Single droplet drying of proteins and protein formulations via acoustic levitation. Erlangen: Ph.D. thesis, 2006.

162. **Gardel, M.L., Shin, J.H., MacKintosh, F.C., Mahadevan, L., Matsudaira, P., Weitz, D.A.** Elastic Behavior of Cross-Linked and Bundled Actin Networks. *Science*. 2004, 304(5675), pp. 1301-1305.
163. **American Society for Testing and Materials.** Active standard: ASTM E1356-03, Standard Test Method for Assignment of the Glass Transition Temperatures by Differential Scanning Calorimetry. 2007, Book of Standards, Volume 14.02
164. **Overcashier, D.E., Patapoff, T.W. and Hsu, C.C.** Lyophilization of protein formulations in vials: investigation of the relationship between resistance to vapor flow during primary drying and small-scale product collapse. *J. Pharm. Sci.* 1999, 88, pp. 688-695.
165. **Kasraian, K., Spitznagel, T.M., Juneau, J.A., Yim, K.** Characterization of the Sucrose/Glycine/Water System by Differential Scanning Calorimetry and Freeze-Drying Microscopy. *Pharm. Dev. Techn.* 1998, 3(2), pp. 233-239.
166. **Passot, S., Fonseca, F., Alarcon-Lorca, M., Rolland, D., Marin, M.** Physical characterisation of formulations for the development of two stable freeze-dried proteins during both dried and liquid storage. *Eur. J. Pharm. Biopharm.* 2005, 60, pp. 335-348.
167. **Anderson, T.W. and Finn, J.D.** *The new statistical analysis of data*. New York: Springer-Verlag, 1996.
168. **Angell, C.A.** Viscous flow and electrical conductance in ionic liquids: Temperature and composition dependence in the light of the zero mobility concept. *J. Chem. Phys.* 1967, 46, pp. 4673-4679.
169. **Angell, C.A., Sare, E.J. and Bressel, R.D.** Concentrated electrolyte solution transport theory: Directly measured glass temperatures and vitreous ice. *J. Phys. Chem.* 1967, 71, pp. 2759-2761.

170. **Moynihan, C.T.** The temperature dependence of transport properties of ionic liquids. The conductance and viscosity of calcium nitrate tetrahydrate and sodium thiosulfate pentahydrate. *J. Phys. Chem.* 1966, 70, pp. 3399-3403.
171. **Hill, V.L., Craig, D.Q.M. and Felly, L.C.** The effects of experimental parameters and calibration on MTDSC data. *Int. J. Pharm.* 1999, 192, pp. 21-32.
172. **Pikal, M.J., Rambhatla, S. and Ramot, R.** The Impact of the freezing stage in lyophilization: Effects of the ice nucleation temperature on process design and product quality. *Amer. Pharm. Rev.* 2002, 5 (3), pp. 48-52.
173. **Goff, H.D., Verespej, E. and Jermann, D.** Glass transitions in frozen sucrose solutions are influenced by solute inclusions within ice crystals. *Thermochimica Acta.* 2003, 399, pp. 43-55.
174. **Kochs, M., Korber, C., Nunner, B., Heschel, I.** The influence of the freezing process on vapor transport during sublimation in vacuum-freeze-drying. *Int. J. Heat Mass Transfer* 1991, 34, pp. 2395-2408.
175. **Pyne, A. and Suryanarayanan.** Phase transitions of glycine in frozen aqueous solutions and during freeze-drying. *Pharm. Res.* 2001, 18, pp. 1448-1454.
176. **Nail, S.L. und Gatlin, L.A.** Freeze Drying: Principles and Practice. In: E.A. Kenneth, H.A. Lieberman und L. Lachman. *Pharmaceutical Dosage Forms: Parenteral Medications, Volume 2.* New York: Marcel Dekker, 1993.
177. **Williams, N.A., Lee, Y., Polli, G.P., Jennings, T.A.** The effects of cooling rate on solid phase transitions and associated vial breakage occurring in frozen mannitol solutions. *J. Parenter. Sci. Technol.* 1986, 40, pp. 135-141.
178. **Searles, J.A., Carpenter, J.F. and Randolph, T.W.** Annealing to optimize the primary drying rate, reduce freezing-induced drying rate heterogeneity, and determine Tg' in pharmaceutical lyophilization. *J. Pharm. Sci.* 2001, 90, pp. 872-887.

179. **Gieseler, H., Kramer, T. and Pikal, M.J.** Use of Manometric Temperature Measurement (MTM) and SMART Freeze Dryer Technology for Development of an Optimized Freeze-Drying Cycle. *J. Pharm. Sci.* 2007, 96 (12), pp. 3402-3418.
180. **Gieseler, H.** PAT for freeze drying: cycle optimization in the laboratory. *Eur. Pharm. Rev.* 2007, 1, pp. 62-67.
181. **Rice, J.A.** Mathematical Statistics and Data Analysis. Belmont, CA: Duxbury, 2007.
182. **Labrude, P., Rasolomanana, M., Vigneron, C., Thirion, C., Chaillot, B.** Protective effect of sucrose on spray drying of oxyhemoglobin. *J. Pharm. Sci.* 1988, 78 (3), pp. 223-229.
183. **Fakes, M.G., Dali, M.V., Haby, T.A., Morris, K.R., Varia, S.A., Serajuddin, A.T.M.** Moisture sorption behavior of selected bulking used in lyophilized products. *PDA J. Pharm. Sci. Techn.* 2000, 54 (2), pp. 144-149.
184. **van Drooge, D.J.** Combining the Incompatible: Inulin glass dispersions for fast dissolution, stabilization and formulation of lipophilic drugs. University of Groningen, Netherlands: Ph.D. thesis, 2006.
185. **Whittier, E.O. and Gould, S.P.** Vapor Pressures of Saturated Equilibrated Solutions of Lactose, Sucrose, Glucose, and Galactose. *Ind. Eng. Chem.* 1930, 22 (1), pp. 77-78.
186. **Docoslis, A., Giese, R.F. und van Oss, C.J.** Influence of the water-air interface on the apparent surface tension of aqueous solutions of hydrophilic solutes. *Colloids and Surfaces B: Biointerfaces.* 2000, 19, S. 147-162.
187. **Carpenter, J.F. and Crowe, J.H.** Modes of stabilization of a protein by organic solutes during desiccation. *Cryobiology.* 1988, 25, pp. 459-470.

188. **Imamura, K., Iwai, M., Ogawa, T., Sakiyama, T., Nakanishi, K.** Evaluation of Hydration States of Protein in Freeze-Dried Amorphous Sugar Matrix. *J. Pharm. Sci.* 2001, 90 (12), pp. 1955-1963.
189. **Costantino, H.R., Gurley, J.G., Wu, S., Hsu, C.C.** Water sorption of lyophilized protein-sugar systems and implications for solid-state interactions. *Int. J. Pharm.* 1998, 166, pp. 211-221.
190. **Pauling, L.** The adsorption of water by proteins. *J. Am. Chem. Soc.* 1945, 67, pp. 555-557.
191. **Green, R.W.** The adsorption of water vapor on casein. *Transactions of the Royal Society of New Zealand.* 1948, 77, pp. 313-317.
192. **Swiss-Prot Protein knowledgebase.** Accessed Nov. 2008
<http://www.expasy.ch/sprot/>.
193. **Katayama, D.S., Carpenter, J.F., Manning, M.C., Randolph, T.W., Setlow, P., Menard, K.P.** Characterization of Amorphous Solids with Weak Glass Transitions using High Ramp Rate Differential Scanning Calorimetry. *J.Pharm. Sci.* 2008, 97 (2), pp. 1013-1024.
194. **Chang, B.S. and Randall, C.S.** Use of subambient thermal analysis to optimize protein lyophilization. *Cryobiology.* 1992, 29, pp. 632-656.
195. **Levine, H. und Slade, L.** Principles of "cryostabilization" technology from structure/property relationships of carbohydrate/water systems - a review. *Cryo-Lett.* 1998, 9, pp. 21-63.
196. **Ma, X., Wang, D.Q., Bouffard, R., MacKenzie, A.** Characterization of murine monoclonal antibody to tumor necrosis factor (TNF-Mab) formulation for freeze-drying cycle development. *Pharm. Res.* 2001, 18, pp. 196-202.
197. **Jennings, T.A.** Supercooling. *Insight.* 2002, 5 (5).

198. **Sanz, P., Otero, L.C. and Carrasco, J.** Freezing processes in high-pressure domains. *Int. J. Refrig.* 1997, 20, pp. 301-307.
199. **MacKenzie, A.P.** The physico-chemical environment during the freezing and thawing of biological materials. In: R. Duckworth. *Water Relations of Foods*. London: Academic Press, 1975.
200. **Wang, W., Singh, S., Zeng, D.L., King, K., Nema, S.** Antibody Structure, Instability, and Formulation. *J. Pharm. Sci.* 96 (1), pp. 1-26.
201. **American Society for Testing and Materials.** Book of Standards, Volume 14.02. Active standard: ASTM E1356-03, Standard Test Method for Assignment of the Glass Transition Temperatures by Differential Scanning Calorimetry. 2007.
202. **Crowe, J.H., Hoekstra, F.A., and Crowe, L.M.** *Anhydrobiosis*. 1992, 54, pp. 579-599.
203. **Izutsu, K., Yoshioka, S. and Terao, T.** Decreased protein stabilizing effects of cryoprotectants due to crystallization. *Pharm. Res.* 1993, 10, pp. 1232-1237.
204. **Carpenter, J.F. and Crowe, J.H.** An infrared spectroscopic study of interactions of carbohydrates with dried proteins. *Biochemistry*. 1989, 28, pp. 3916-3922.
205. **Pikal, M.J.** Use of Laboratory Data in Freeze Drying Process Design: Heat and Mass Transfer Coefficients and the Computer Simulation of Freeze Drying. *J. Parenter. Sci. Technol.* 1995, 39(3), pp. 115-138.

Curriculum vitae

Personal data

Name	<u>Eva</u> Nicole Waltraud MEISTER
Date of birth	1 st April 1980
Place of birth	Münchberg(Germany)
Nationality	German

Education & positions held

10/2008 - present	Manager R&D Coordination Boehringer Ingelheim, Ingelheim am Rhein (Germany)
02/2005 - 09/2008	Graduate student and assistant teacher for undergraduate pharmacy students (solid dosage forms) Freeze-drying Focus Group (Dr. H. Gieseler), Department of Pharmaceutics (Prof. Dr. G. Lee), University of Erlangen-Nuremberg, Erlangen (Germany)
12/2004	Licensure as a Pharmacist
05/2004 - 10/2004	Intern: Meilwald Pharmacy, Erlangen (Germany)
11/2003 - 04/2004	Intern: Nonclinical Development: Profiling, Hoffmann La-Roche, Basel (Switzerland)
09/1999 - 10/2003	Undergraduate studies in Pharmacy University of Erlangen-Nuremberg, Erlangen (Germany)
10/1990 - 06/1999	High school Gymnasium Münchberg, Münchberg (Germany)